

Durham E-Theses

A non-perturbative study of the infra-red behaviour of QCD

Nicholas Brown

How to cite:

Brown, Nicholas (1989) A non-perturbative study of the infra-red behaviour of QCD. Doctoral thesis, Durham University.

Use policy

The full-text may be used and/or reproduced, and given to third parties in any format or medium, without prior permission or charge, for personal research or study, educational, or not-for-profit purposes provided that:

- a full bibliographic reference is made to the original source
- a <https://etheses.durham.ac.uk/id/eprint/6575/> is made to the metadata record in Durham E-Theses
- the full-text is not changed in any way

The full-text must not be sold in any format or medium without the formal permission of the copyright holders.

Please consult the [full Durham E-Theses policy](#) for further details.

**A NON-PERTURBATIVE STUDY
OF THE INFRA-RED BEHAVIOUR
OF QCD**

Nicholas Brown
Department of Physics
University of Durham

The copyright of this thesis rests with the author.
No quotation from it should be published without
his prior written consent and information derived
from it should be acknowledged.

A thesis submitted to the University of Durham
for the Degree of Doctor of Philosophy

August 1988



- 6 JUL 1989

There are more things in heaven and earth, Horatio, than are dreamt
of in your philosophy.

Hamlet, Act I, Scene V.

ABSTRACT

The non-perturbative behaviour of the non-Abelian gauge theory of strong interactions, namely QCD, is investigated using the Schwinger-Dyson equations. Using an approximation based on solving the Slavnov-Taylor identities, we derive a closed integral equation for the full gluon propagator. We numerically solve this equation, finding a consistent solution which is as singular as $1/p^4$ as the momentum $p^2 \rightarrow 0$, whilst at large momenta the gluon propagates like a free particle.

This infra-red behaviour can be seen as a signal for the confinement of quarks and gluons, implying, for example, that the Wilson loop operator behaves an 'area law'.

We then derive an equation for the full massless quark propagator. Using our solution for the gluon, we find the quark propagator to be suppressed at low momentum, to such an extent that the physical particle pole is removed, and free quarks cannot propagate. This is just what we might expect of a confining theory.

The inclusion of quarks means we must study their dynamical effects via closed fermion loops in the gluon propagator equation. This couples the two equations together. We solve the two equations simultaneously, finding that the previous infra-red behaviour still holds. As we introduce more flavours of fermions, however, the infra-red enhancement of the gluon propagator is diminished, and this in turn means that the quark propagator is less suppressed. This exhibits the dynamical importance of quarks.

These physically realistic results demonstrate the importance and validity of the Schwinger-Dyson equations as a valuable tool for investigating the non-perturbative features of gauge theories.

ACKNOWLEDGEMENTS

This thesis owes its existence to many people. First and foremost of these is my supervisor Mike Pennington, who has helped above and beyond the call of duty. He has been teacher, collaborator, banker, foster parent, car salesman, reprimander (usually justified), p.r. man, employment adviser, and most of all a friend. He has shown every confidence in me (not always justified), and is to him that any complaints should be addressed. Thanks Mike, and may the SERC triple your salary!

I must also thank Alan Martin and Kaoru Hagiwara, who both showed great patience in helping me take my first tentative steps.

Five months of my time were spent at Brookhaven National Laboratory, New York, U.S.A. It is a pleasure to thank Bill Marciano and the rest of the theory group there for their hospitality. Whilst admitting that I learnt much scientifically, I would like to take this opportunity to warn young single people who are even remotely sociable against staying there. It is appropriate to take a quote from Jeremy Bernstein's autobiographical 'The life it brings':

'It was (and is) a wonderful place scientifically, but for me, after my year in France, it caused a *drastic culture shock*'. (My italics).

Special thanks to Patti Pennington for her kindness and hospitality, and for the best eating house on Long Island.

Then we come to those electronic machines, which would have remained an enigma to me, were it not for Stuart Grayson, who showed me how to switch them on, and to Mike Whalley, who is ever ready to answer the most stupid of questions.

Particular mention must go to the fellow occupants of room 303: Simon Webb, Yanos Michopoulos, Mohammed Nobary and Mohammed Hussein. They not only had to suffer my continuous chatter, but also had the same addiction to caffeine as myself. What can I say? 5-a-side, home brew, Greek holidays,

siestas, naughty postcards, the Vic. on a Friday night. How could one have survived three years in Durham without them? May the Mykonos philosophy live (or is it sleep) on.

Special commendation goes to those in the group who rarely discuss physics: Nigel Glover (mentioned in dispatches for outstanding cynicism), Anthony Allan, Tony Peacock, Martin Carter, Jenny Nicholls, Ahmed Bawa, David Pentney, James Stirling, Dominic Walsh and Michael Wade. No disrespect of course to those who did occasionally talk shop, after all we shouldn't forget our purpose in life: Peter Collins, Chris Maxwell and not least, Peter Harri-man. On the subject of physicists, I must also thank Ed Witten for his letter of encouragement.

A cosmologist or two for luck: Laurence Jones who must also be mentioned for much hospitality when the beer had taken effect, and for taking pity on the homeless; also Duncan Hale-Sutton. Without the sterling efforts of these two young gentlemen the publicans of Durham would be much the poorer.

These last three years would lie heavier on me than otherwise were it not for the gentler sex, who made the place look (and occasionally feel) prettier. In alphabetical order: Ann, Ann, Clare, Coral, Kate, Mandy, Margaret, Sally, Sara and Sue. Special mention to Vicky Augustyneck for forcing various and collected Italian dishes down my throat. Most of all though, thanks and much love to Helen.

Last, and by no means least, I must thank my parents for their support and love. If I have not always done as they would have wished, they have never criticised.

Princeton University

Department of Physics: Joseph Henry Laboratories
Jadwin Hall
Post Office Box 708
Princeton, New Jersey 08544

Dear Messrs. Webb, Brown, and
Tuchopoulos,

Best wishes for success
in all your endeavors!

Sincerely,

Edward Witten

To Mum, Dad, and Helen

DECLARATION

I declare that no material in this thesis has previously been submitted for a degree at this or any other university.

The research described in chapters three, four, five and six has been carried out in collaboration with Dr. M.R. Pennington and has been published as follows:

- (i) 'Preludes to Confinement: Infra-red Properties of the Gluon Propagator in the Landau gauge'
N. Brown and M.R. Pennington, *Phys. Lett.* **106B** (1988) 133
- (ii) 'Studies of Confinement: How Quarks and Gluons Propagate'
N. Brown and M.R. Pennington, Brookhaven preprint BNL-41101, to be published in *Phys. Rev. D* (1988)

The copyright of this thesis rests with the author. No quotation from it should be published without prior written consent and any information derived from it should be acknowledged.

Other published work by the author:

- (i) 'Scalar Electron and Zino Production on and Beyond the Z Resonance in e^+e^- Annihilation'
A.R. Allan, N. Brown and A.D. Martin, *Z. Phys.* **C31** (1986) 479
- (ii) 'Polarization Amplitudes and Predictions for $e^+e^- \rightarrow n\gamma$ '
N. Brown, K. Hagiwara and A.D. Martin, *Nucl. Phys.* **B288** (1987) 783

- (iii) 'Parisi Multijet Shape Variables in e^+e^- Annihilation in terms of Partonic Energy-Momentum Fractions'
N. Brown, Y. Michopoulos and M.R. Pennington, *J. Phys. G* **14** (1988) 519
- (iv) 'An Improved Presentation of a Novel Perturbative Scheme in Field Theory'
N. Brown, *Phys. Rev. D* **38** (1988) 723
- (v) 'Perturbative QCD Algorithms for Transverse Momentum Distributions in e^+e^- Annihilation'
Y. Michopoulos, N. Brown and M.R. Pennington, *J. Phys. G* **14** (1988) 1027

TABLE OF CONTENTS

CHAPTER ONE STRONG INTERACTIONS

| | | |
|-----|------------------------|----|
| 1.1 | Introduction | 1 |
| 1.2 | Historical Background | 2 |
| 1.3 | Local Gauge Invariance | 11 |
| 1.4 | Perturbative QCD | 15 |
| 1.5 | Confinement | 20 |

CHAPTER TWO THE SCHWINGER-DYSON EQUATIONS

| | | |
|-----|---|----|
| 2.1 | Path Integrals and Functional Methods in Field Theory | 24 |
| 2.2 | The Schwinger-Dyson Equations for Scalar Field Theory | 30 |
| 2.3 | Fermions and Path Integrals | 33 |
| 2.4 | The Schwinger-Dyson Equations for QCD | 34 |
| 2.5 | The Slavnov-Taylor/Ward-Takahashi Identities | 41 |
| 2.6 | The Perturbative Gluon and Quark Propagators | 50 |

CHAPTER THREE THE GLUON EQUATION

| | | |
|-----|---|----|
| 3.1 | Derivation of the Equation for $\mathcal{G}(p)$ | 54 |
| 3.2 | The Gluon Loop | 57 |
| 3.3 | Renormalisation | 62 |
| 3.4 | Consistent Asymptotic Behaviour of $\mathcal{G}_R(p)$ | 67 |
| 3.5 | Technical Details | 70 |
| 3.6 | The Solution | 81 |

CHAPTER FOUR THE MANDELSTAM APPROXIMATION

| | | |
|-----|--------------|----|
| 4.1 | Introduction | 84 |
|-----|--------------|----|

| | | |
|--|---|-----|
| 4.2 | The Calculation and Renormalisation | 85 |
| 4.3 | The Solution | 90 |
| 4.4 | How Good is the Mandelstam Approximation? | 94 |
| 4.5 | Confinement and a $1/p^4$ Gluon Propagator | 97 |
| | | |
| CHAPTER FIVE THE FERMION EQUATION | | |
| 5.1 | Introduction | 110 |
| 5.2 | The Ward Identity and the Equation for $\mathcal{F}(p)$ | 111 |
| 5.3 | Renormalisation | 115 |
| 5.4 | The Solution for $\mathcal{F}_R(p)$ | 123 |
| | | |
| CHAPTER SIX QUARK LOOPS | | |
| 6.1 | Introduction | 128 |
| 6.2 | The Quark Loop Diagram | 130 |
| 6.3 | The Gluon Equation with Quarks | 135 |
| | | |
| CHAPTER SEVEN A NON-PERTURBATIVE STUDY OF QCD | | |
| 7.1 | Propagation of Quarks and Gluons | 149 |
| 7.2 | Ultraviolet Problems | 151 |
| 7.3 | Infra-red Problems | 156 |
| 7.4 | Approximations and Improvements | 161 |
| 7.5 | Comments on the Solutions | 164 |
| | | |
| APPENDIX A INTEGRALS | | 167 |
| | | |
| REFERENCES | | 177 |

CHAPTER ONE

STRONG INTERACTIONS

1.1 Introduction

The modern study of particles and their interactions has provided us with the great successes of non-Abelian gauge theories, which in their second quantised form provide us with an extremely accurate description of the weak and electromagnetic forces. These two interactions are seen to be different manifestations of a more fundamental 'electroweak' force. This was experimentally confirmed by the discovery of the W and Z bosons[1.1], which along with the photon constitute the carriers of this force. It also appears that another non-Abelian gauge theory, that of Quantum Chromodynamics (QCD), may well provide us with a dynamical theory of the strong nuclear force. Unfortunately, despite many successful predictions at collider energies, we do not yet understand the most important manifestation of this strong interaction, namely the plethora of low energy bound states we call hadrons; their masses, lifetimes, decay modes and interactions. Nevertheless, a great many theoretical physicists accept this 'standard model' of relatively low energy physics as proven, and cast their research efforts towards 'loftier' goals.

The most important of these is to try and understand how the eligible bachelor of general relativity can be married to the unwilling bride of quantum theory. It is hoped that the offspring of such a match would be a full quantum description of gravity, the attainment of which has been one of the outstanding aims of physics for over fifty years. Unfortunately it is unlikely that we shall find any experimental evidence to guide us below energies of the Planck mass ($\sim 10^{19}$ GeV), a scale totally inaccessible to the earth bound scientist for the foreseeable future. Indeed, experiment has yet to give us any real clues about physics beyond the standard model, despite the belief of most physicists that



there is much more to learn.

In the absence of experimental clues, much research is guided less by physical intuition and more by a desire for mathematical elegance, an avenue which has not always proven the most fruitful. The most recent craze is for 'superstring' theories, which are held to promise the unification of all known (and unknown) forces. Here the fundamental objects are not particles, but one dimensional 'strings', living in some higher dimensional space-time. As a growing band of physicists flock to the superstring banner, it is worthwhile to consider that we have still to understand the existence of many 'everyday' particles such as the proton and neutron, the building blocks of nearly all matter in the universe!

This study is an examination of the proposed theory of strong interactions, namely QCD, at the low energies where hadrons dominate. If QCD is the theory of strong interactions then there are some fundamental questions which must be answered. Here we describe a framework which may well provide these answers and we make some first steps towards them, obtaining results which qualitatively at least, are physically realistic, and bode well for future studies. We shall, however, try to highlight various shortcomings and problems which will hopefully be addressed in future studies.

1.2 Historical Background

The earliest manifestation of strong interactions is now known to be the production of α -rays in the nuclear decays of uranium. The radiation from uranium was first observed by Becquerel in 1896. At the time however, the nucleus was yet to be discovered and these so called 'Becquerel rays' remained unexplained.

It was 1911 before Rutherford proposed the nuclear model of the atom to explain the large angle scattering of α -rays off a gold foil target as observed by

Geiger and Marsden. Subsequent experiments confirmed Rutherford's scattering formula and the atomic nucleus came into existence.

In many ways Rutherford was fortunate that the energy of his α -rays (~ 5 MeV) was too low to penetrate the Coulomb barrier of the relatively heavy nuclei, such as gold, used in the target. After the first world war the experiment was repeated but this time with light nuclei, particularly Hydrogen, in the target, for which the coulomb repulsion was less. For the first time induced nuclear reactions were observed[1.2] as massive deviations from the electromagnetic coulomb repulsion, the first signal of a new force.

Despite the success of the nuclear model, the problem remained of atomic mass and it was not until 1930 that Bothe and Bekke observed a new penetrating form of radiation. Chadwick was then able to show that this was due to a new, electrically neutral particle with the same mass as the proton. With this new particle, the neutron (n), and the already discovered electron (e) and proton (p), the family of subatomic particles seemed complete. The atom was held to be a small central nucleus consisting of protons and neutrons, around which the electrons orbited.

The question remained as to how the nucleus was held together against the electrostatic Coulomb repulsion of the protons. Experiment showed that the $n - n$, $p - p$, and $n - p$ nuclear forces were similar in strength, leading to the conclusion that the nuclear force was independent of the electrical charge of the particle involved. This was made into a more sophisticated statement by considering the neutron and proton as two different aspects of one particle, the nucleon (N), similar in concept to the two different spin states of any spin- $\frac{1}{2}$ particle. More exactly, the nucleon was a doublet of isotopic spin or isospin, $I = \frac{1}{2}$. The proton was assigned $I_3 = +\frac{1}{2}$ and the neutron $I_3 = -\frac{1}{2}$, where I_3 is the third component of the isospin vector. The nuclear forces were invariant under the isospin rotations of the group $SU(2)$.

On a more dynamical level, Yukawa proposed that this force would be carried by a particle called the pi-meson or pion (π), by analogy with how the photon carried the electromagnetic force. Because of the short range of the nuclear forces, this pion would have to be massive, of the order of 100 Mev. A particle of this mass was indeed observed in cosmic rays and naturally identified as the pion. Unfortunately it had all the wrong properties and was later realised to be a more massive copy of the electron, which became known as the muon (μ). The pion itself was discovered just after the second world war, and had all the properties expected.

These early advances went hand in hand with the development of quantum theory, and particularly quantum field theory, in which particles were created and annihilated in interactions. Unfortunately quantum field theories are plagued with infinities in any calculations beyond the lowest order in perturbation theory, the only known consistent method for performing calculations. These occur in momentum (loop) integrals which are divergent at large, or 'ultraviolet' momenta. One of the major theoretical successes of the thirties and forties was to show that for quantum electrodynamics (QED) the theory of electromagnetism, that these infinities could be absorbed into infinite renormalisations of the fields, masses and coupling constants. Any quantity was then finite when expressed in terms of these renormalised quantities. This program of renormalisation has allowed calculations to be performed in QED in which we can obtain the finest agreement known between theory and experiment.

At the same time people tried to develop a quantum field theory of the strong (and weak) nuclear forces. Perturbation theory expresses quantities as a power series in the coupling constant. For QED the relevant quantity is the fine structure constant $\alpha \approx \frac{1}{137}$. Since this is a small number, we might expect the first few terms of such a series to give accurate answers. The same quantity for strong interactions was estimated to be of the order of 10. A power series in

this was likely to be meaningless, without addressing the problem of finding a theory which could be made finite by renormalisation. Perhaps the situation is best summed up in a conversation between Dirac and Feynman when they first met in 1961[1.3]:

- F. I am Feynman.
 D. I am Dirac. (Silence.)
 F. It must be wonderful to be the discoverer of that equation.
 D. That was a long time ago. (Pause.)
 D. What are you working on?
 F. Mesons.
 D. Are you trying to find an equation for them?
 F. It is very hard.
 D. One must try.

In 1947 the situation was further complicated by the discovery of new particles in cosmic rays by Rochester and Butler[1.4]. These were called V-particles because of the tracks they made in the bubble chambers. Soon new particles were being copiously produced in accelerators. It was noticed that these new particles were always produced in pairs, and this led to the idea of 'associated production', or conservation of a new quantum number known as strangeness (S). The known particles, the proton, neutron and pion were assigned zero strangeness, i.e $S=0$. So, for example, in the reaction



the new particles K^+ and Λ were assigned strangeness $S= +1$ and $S= -1$ respectively, and strangeness is seen to be conserved in this allowed reaction. This concept also helped to explain the relatively long lifetimes of these strange particles ($\sim 10^{-9}$ s compared to the usual strong interaction scale of $\sim 10^{-23}$ s).

Since strong interactions conserved strangeness, these particles could only decay via the weak nuclear force which was seen to violate strangeness conservation, but was very much weaker than the strong force, leading to long lifetimes.

The way forward was by an extension of the isospin $SU(2)$ symmetry. The three pions (π^+ , π^0 , π^-) fitted into this symmetry as an $I=1$ triplet of isospin. With the discovery of strange particles, similar assignments were looked for. Gell-Mann and others[1.5] realised that the particles could be fitted into representations of the larger group $SU(3)$, which contained the isospin $SU(2)$ as a subgroup. $SU(3)$ has eight generators compared to three for $SU(2)$. Some of these $SU(3)$ multiplet assignments are shown in fig. 1.1.

If this $SU(3)$ symmetry were exact, then all particles in the same multiplet would have the same mass. Deviations from this were larger than those seen within isospin multiplets. By assuming that isospin is an exact symmetry, and that the mass term breaking the $SU(3)$ symmetry transforms like the eighth generator of $SU(3)$ it was possible to derive a formula relating the masses of the different particles in the multiplets. This is the famous Gell-Mann – Okubo mass formula for the octet, which states that

$$M_N + M_{\Xi} = \frac{1}{2}(M_{\Lambda} + 3M_{\Sigma})$$

with $M_N = 940$ MeV, $M_{\Xi} = 1320$ MeV, $M_{\Lambda} = 1115$ MeV and $M_{\Sigma} = 1190$ MeV, this formula is seen to hold to a good approximation. More importantly, at the time the Ω^- was missing from the decuplet in fig. 1.1. Gell-Mann was able to predict its mass of 1680 MeV and its electric charge. When in 1964 such a particle was discovered with the correct mass and charge at Brookhaven, $SU(3)$ symmetry was in!

Despite its apparent simplicity, it seemed that nature did not want to use the simplest representations of $SU(3)$, namely a triplet $\mathbf{3}$, and its conjugate representation $\bar{\mathbf{3}}$. It is possible to build up all the higher representations by

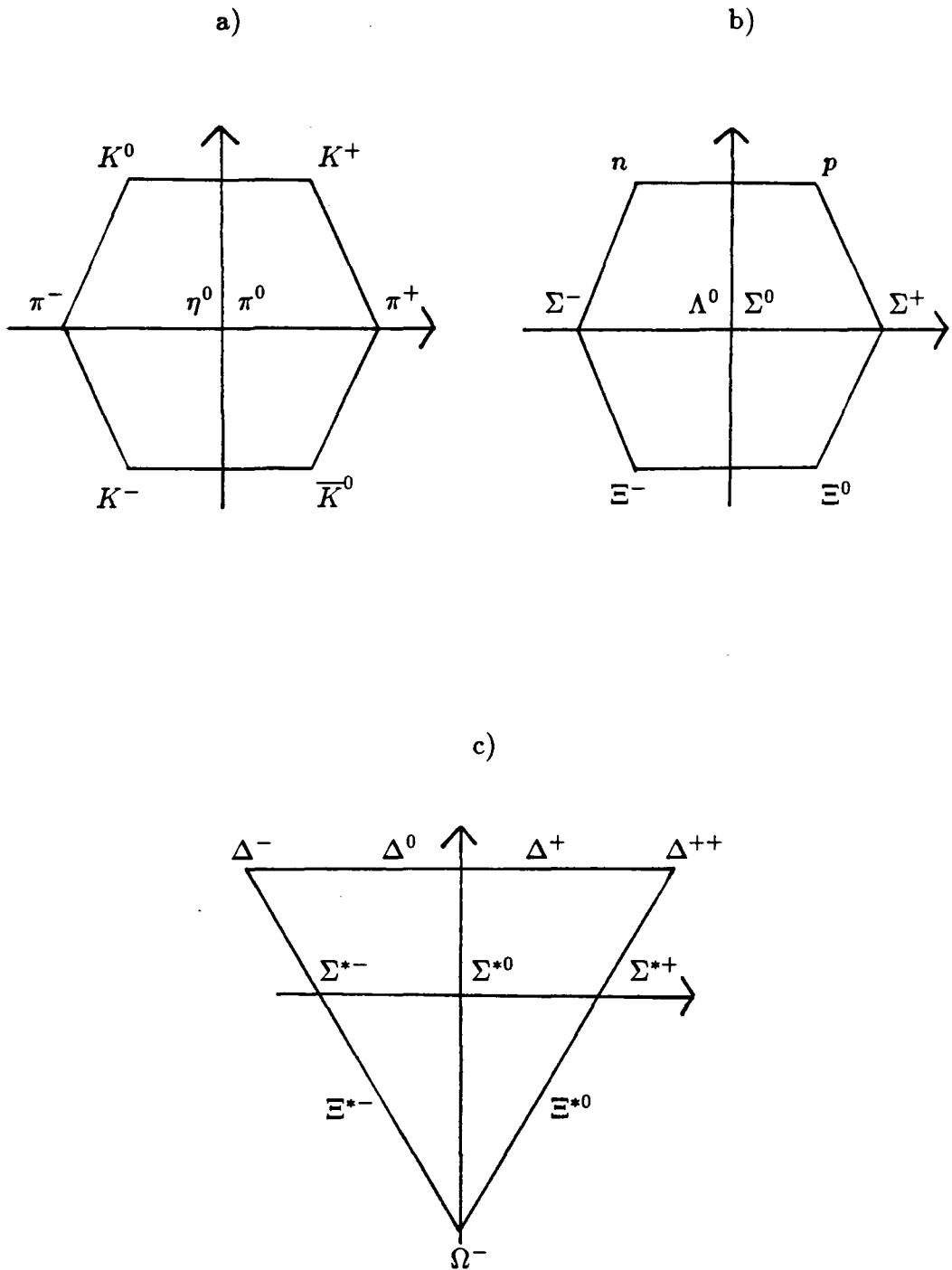


Fig. 1.1: SU(3) particle multiplets: a) $J^P = 0^-$ meson octet, b) $J^P = \frac{1}{2}^+$ baryon octet, c) $J^P = \frac{3}{2}^+$ baryon decuplet. Horizontal axis denotes I_3 , vertical axis denotes Hypercharge $Y = S + B$, where B is baryon number.

taking tensor products of these fundamental representations. For example we have:

$$3 \otimes \bar{3} = 1 \oplus 8$$

$$3 \otimes 3 \otimes 3 = 10 \oplus 8 \oplus 8 \oplus 1$$

Those hadrons with integer spin, known as mesons, e.g. the pions, appeared in multiplets from the first of these decompositions, those with half integer spin, known as the baryons, from the second. It was as though there were three fundamental particles with spin- $\frac{1}{2}$ in the 3 representation called quarks (q). The mesons appeared to be made from $q\bar{q}$ pairs, and the baryons from qqq combinations. This quark triplet is shown in fig 1.2. It consists of an up (u) quark of charge $+\frac{2}{3}$ and a down (d) and strange (s) quark both of charge $-\frac{1}{3}$. If the masses of the up and down quarks were the same, with the strange quark heavier, then this would give rise to the correct mass formula which was seen to hold to a good approximation. By assigning $I_3 = +\frac{1}{2}, -\frac{1}{2}, 0$ and $S = 0, 0, -1$ to the u,d,s quarks respectively, the correct quantum numbers for the hadrons were obtained. The u,d,s labels have become known as different 'flavours' of quarks.

It should be stressed that at this stage quarks were purely mathematical objects, and their fractional electric charge in particular made it difficult for them to be thought of as real particles.

The situation changed dramatically in what has become known as the Deep Inelastic Scattering experiments performed at SLAC during the sixties. Here high energy electrons were scattered onto protons. The latter broke up to create a shower of hadrons. As far as we know an electron is a truly fundamental particle, It therefore survives the impact and can be detected in the final state to 'tag' the collision. The process is depicted diagrammatically in fig. 1.3. If the

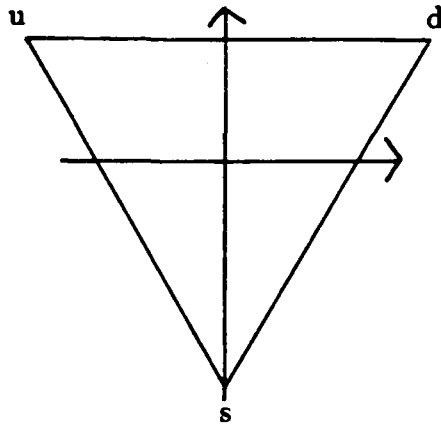


Fig 1.2: fundamental quark triplet of SU(3).

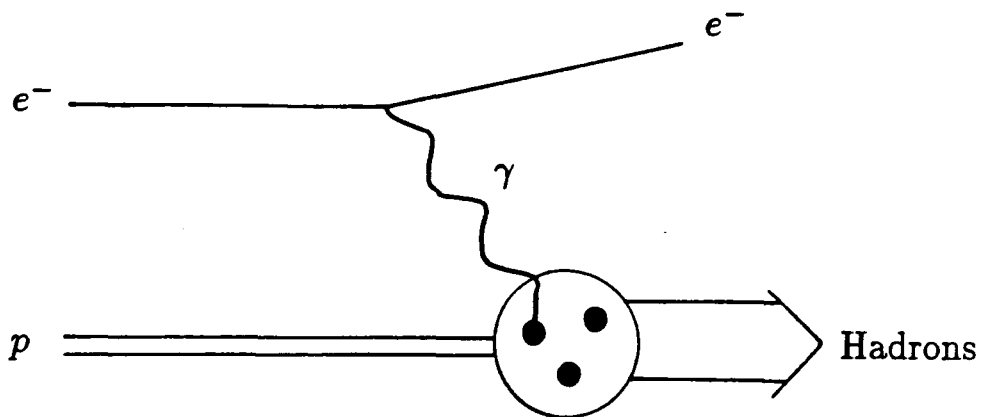


Fig 1.3: Deep Inelastic Scattering. A high energy virtual photon scatters off a parton inside the proton.

virtual photon produced has a high enough energy, and hence a short enough wavelength, then it will probe the internal structure of the proton, if any exists.

It was found[1.2], that by analogy with Rutherford's famous experiments of fifty years earlier, that a significant number of high energy events involved the electron being scattered through a large angle. The analysis revealed that this was consistent with the virtual photon scattering off free, spin- $\frac{1}{2}$, point-like objects *within* the proton. It was natural to identify these 'partons', as they were called, with the quarks. The 'parton model' of Feynman assumed that

these quarks were essentially free inside the proton, and that they interacted instantaneously with the incident photon. It was on a much larger time scale that the subsequent break-up and hadronisation of the proton into the final state particles occurred. This model had much success in phenomenological studies of hadrons. Quarks had arrived as real particles! Despite these successes, problems still remained:

(i) Why were free quarks not observed in nature, and only $q\bar{q}$, qqq combinations seen.

(ii) Quarks must have spin- $\frac{1}{2}$ to explain the observed hadrons. The Δ^{++} with third component of spin $S_3 = +\frac{3}{2}$ must therefore be made up from three up quarks all with $S_3 = +\frac{1}{2}$ and therefore have a symmetric wave function with respect to interchange of any two of these identical quarks. This was a violation of Fermi-Dirac statistics.

The most satisfactory solution to this second problem is to suppose that the quarks have an additional quantum number, which we shall call colour, and that the colour wave function is antisymmetric with respect to interchange of quarks. Thus it is postulated that all observable hadrons are singlets with respect to the colour degree of freedom.

How many colours are there? This can be answered by experiment. For example the ratio

$$R = \frac{\sigma(e^+e^- \rightarrow \text{hadrons})}{\sigma(e^+e^- \rightarrow \mu^+\mu^-)}$$

is naively expected to be constant and equal to the sum of the squares of the quark charges. For three flavours (and later four and five) this ratio was found to be a factor of three too small when compared with experiment. By proposing three colours, each flavour of quark is counted three times and we can obtain

agreement. This was supported by a similar argument in calculating the width for the decay $\pi^0 \rightarrow \gamma\gamma$, which was found to be about nine times too small when compared with experiment, and was expected to be proportional to the number of colours squared.

Progress was being made, but there was still no *dynamical* theory of strong interactions, and such a theory would have to explain the non-observation of free quarks, despite the fact that in high energy collisions they behaved as almost free particles!

1.3 Local Gauge Invariance

The way forward to a dynamical theory of strong interactions was by the principle of local gauge invariance, which had provided us with the successful theory of electromagnetism, QED. The non-Abelian extension of this was to provide us with a candidate theory for the unified electroweak interactions, and since gauge theories were playing such a crucial role in nature, it was sensible to attempt to extend the idea to strong interactions.

Symmetries play an important role in both classical and quantum physics. In quantum field theory we usually think of a symmetry as a group of transformations on the fields, which leave the Lagrangian invariant. Consider the Lagrangian for a free Dirac fermion:

$$\mathcal{L}_0 = \bar{\Psi}(x)(i\gamma^\mu \partial_\mu - m)\Psi(x) \quad (1.1)$$

This is invariant under a constant change of phase

$$\begin{aligned} \Psi(x) &\rightarrow \Psi'(x) = e^{i\alpha}\Psi(x) \\ \bar{\Psi}(x) &\rightarrow \bar{\Psi}'(x) = \bar{\Psi}(x)e^{-i\alpha} \end{aligned} \quad (1.2)$$

This is not the case if we let α be space-time dependent, because of the derivative in Eq. 1.1. We can restore invariance by introducing a new field $A_\mu(x)$, and defining a covariant derivative D_μ , such that

$$D_\mu \Psi(x) = (\partial_\mu + igA_\mu)\Psi(x) \quad (1.3)$$

where g is a free parameter.

Consider the new Lagrangian:

$$\mathcal{L} = \bar{\Psi}(x)(i\gamma^\mu D_\mu - m)\Psi(x) \quad (1.4)$$

This is invariant under the phase transformations in Eq. 1.1 with α now $\alpha(x)$, a function of space-time x , if we let the field A_μ transform as:

$$A_\mu(x) \rightarrow A'_\mu(x) = A_\mu(x) - \frac{1}{g}\partial_\mu\alpha(x) \quad (1.5)$$

As yet the new gauge field A_μ has no kinetic term, and so we add the simplest term quadratic in $A_\mu(x)$ and invariant under the transformation of Eq. 1.5, to obtain the well known Lagrangian:

$$\mathcal{L}_{QED} = \bar{\Psi}(x)(iD_\mu\gamma^\mu - m)\Psi(x) - \frac{1}{4}F^{\mu\nu}F_{\mu\nu} \quad (1.6)$$

where

$$F_{\mu\nu}(x) = \partial_\mu A_\nu(x) - \partial_\nu A_\mu(x) \quad (1.7)$$

This is the Lagrangian for QED, where we identify $A_\mu(x)$ as the photon field. Its interaction with the electron field $\Psi(x)$ is uniquely defined by demanding invariance under local phase, or gauge transformations. Composition of these phase transformations forms the Abelian group $U(1)$.

We expect the quark field to have three components because of the three degrees of colour:

$$\Psi \equiv \begin{pmatrix} \psi_{red} \\ \psi_{blue} \\ \psi_{green} \end{pmatrix}$$

where we use the labels red, blue and green to denote the three colours.

Thus our free Lagrangian for one flavour of quark will be:

$$\mathcal{L}_0 = \bar{\Psi}(x)(i\partial - m)\Psi(x) \quad (1.8)$$

but where the $\Psi(x)$ are three component quantities.

This is invariant under the transformations of the larger non-Abelian group SU(3) (not to be confused with the flavour SU(3) invariance above):

$$\Psi(x) \rightarrow \Psi'(x) = e^{i\theta^a \lambda^a / 2} \Psi(x) \quad (1.9)$$

where the eight quantities $\lambda^a/2$ are the Gell-Mann 3×3 matrices which generate the group SU(3). The θ^a are eight phase parameters. The λ^a satisfy the well known commutation relations:

$$\left[\frac{\lambda^a}{2}, \frac{\lambda^b}{2} \right] = if_{abc} \frac{\lambda^c}{2} \quad (1.10)$$

where the f_{abc} are called the structure constants of the group

Following the same procedure as that for QED, we would like to derive a Lagrangian which is invariant when the θ^a become the space-time dependent functions $\theta^a(x)$. This time we have to introduce eight gauge fields $A_\mu^a(x)$, one for each generator of the group. Introducing the matrix function $U(x) = e^{i\theta^a(x)\lambda^a/2}$, we define the covariant derivative in a similar way to before:

$$D_\mu \Psi(x) = \left(\partial_\mu + ig \frac{\lambda^a}{2} A_\mu^a(x) \right) \Psi(x) \quad (1.11)$$

where it is to be stressed that D_μ is a 3×3 matrix, and we will write $A_\mu(x)$ for the matrix $A_\mu^a(x)\lambda^a/2$.

We can obtain invariance under local SU(3) transformations provided $A_\mu(x)$ transforms as:

$$A_\mu(x) \rightarrow A'_\mu = U(x)A_\mu U^\dagger(x) - \frac{i}{g}U(x)\partial_\mu U^\dagger(x) \quad (1.12)$$

The covariant derivative has the transformation property:

$$D_\mu(x) \rightarrow D'_\mu(x) = U(x)D_\mu(x)U^\dagger(x) \quad (1.13)$$

And so the quantity $F_{\mu\nu}^a = -i/g[D_\mu, D_\nu]$ transforms in the same way.

Explicit calculation yields:

$$F_{\mu\nu} = \partial_\mu A_\nu - \partial_\nu A_\mu + ig[A_\mu, A_\nu] \quad (1.14)$$

Using the commutation relations in Eq. 1.10, and writing the matrix $F_{\mu\nu}$ as $F_{\mu\nu}^a \lambda^a/2$ we obtain:

$$F_{\mu\nu}^a = \partial_\mu A_\nu^a - \partial_\nu A_\mu^a - gf_{abc}A_\mu^b A_\nu^c \quad (1.15)$$

This is the non Abelian extension of Eq. 1.7. Thus our gauge invariant Lagrangian will now read:

$$\mathcal{L}_{QCD} = \bar{\Psi}(x)(iD_\mu \gamma^\mu - m)\Psi(x) - \frac{1}{4}F_{\mu\nu}^a F_a^{\mu\nu} \quad (1.16)$$

This is the classical Lagrangian from which the quantum field theory known as QCD is obtained. In other words QCD is the theory of gauged SU(3) colour transformations, specifying how the coloured quarks interact with the non-Abelian gauge fields we call gluons (g). Unlike QED it should be noted that the gluons themselves carry the colour charge, and so can interact with other gluons, a feature of essential importance.

Finally it should be mentioned that gauge theories are renormalisable, and in fact are the only possible theories of spin-1 particles in which we can consistently eliminate the ultraviolet divergences of field theory.

1.4 Perturbative QCD

As mentioned earlier, perturbation theory in powers of the coupling constant is the only way we know of consistently calculating most quantities in field theory. Although the pion-nucleon coupling is large, since it was observed that quarks behave like almost free particles inside a proton, the QCD coupling between these partons may well be small, allowing us to perform a perturbative calculation. This is indeed the case, and we briefly mention some of the successes of perturbative QCD[1.6].

For the process $e^+e^- \rightarrow q\bar{q}$, contributing to the ratio R already mentioned, we can consider the QCD correction, where one of the produced quarks can radiate a gluon. If the parton hypothesis is correct, then this process will occur on an extremely short time scale compared to the subsequent hadronisation. Thus if all three final state particles are sufficiently energetic, we might expect to see three reasonably well-defined streams or 'jets' of hadrons.

This was indeed seen to occur with exactly the correct distribution as expected from QCD. It was possible to show that the process involved a spin-1 particle in the final state, i.e the gluon. Indeed processes with more partons in the final state have now been seen, for example, 'four-jet' events from the processes $e^+e^- \rightarrow q\bar{q}gg$, $e^+e^- \rightarrow qq\bar{q}\bar{q}$ have been seen, with final state distributions conforming to the predictions of QCD.

More importantly, since QCD is a renormalisable field theory, higher order calculations have been carried out with testable experimental predictions. For example, the distribution of quarks inside the proton is described in terms of two structure functions. The naive parton model implies that these are related, and that certain quantities are independent of the energy of the virtual photon. Essentially this is a consequence of the quarks being considered as free particles, and is known as 'scaling'. The QCD higher order interactions can be calculated to cause deviations from this scaling, and these QCD predictions have been

experimentally confirmed. There are many other confirmations that at high energies at least, QCD correctly describes the interactions of quarks and gluons.

An extremely important consequence of higher order calculations in field theory is that the coupling strength becomes momentum dependent. For example, keeping the dominant (leading) logarithm terms only, the effective quark-gluon coupling becomes:

$$\bar{g}(q) = g - \beta_0 \frac{g^3}{32\pi^2} \ln\left(\frac{q^2}{\kappa^2}\right) + O(g^5) \quad (1.17)$$

where g is the lowest order ('bare') coupling appearing in Eq. 1.11, q is the incoming gluon momentum, and κ is a large (ultraviolet) momentum cutoff, which is needed to make the higher order corrections finite. β_0 is equal to $(11/3)N_c - (2/3)n_f$, where N_c is the number of colours, and n_f is the number of quark flavours. For $N_c = 3$, and with six quark flavours, as is commonly supposed, this quantity is positive. We work with the quantity $\alpha_s = g^2/4\pi$, and so squaring Eq. 1.17 gives us:

$$\alpha_s(q) = \alpha_s - \alpha_s^2 \frac{\beta_0}{4\pi} \ln\left(\frac{q^2}{\kappa^2}\right) + O(\alpha_s^3) \quad (1.18)$$

If we evaluate this equation at another scale $q^2 = \mu^2$ we obtain:

$$\alpha_s(\mu) = \alpha_s - \alpha_s^2 \frac{\beta_0}{4\pi} \ln\left(\frac{\mu^2}{\kappa^2}\right) + O(\alpha_s^3) \quad (1.19)$$

It is possible to eliminate α_s and κ^2 between these two equations to obtain:

$$\alpha_s(q) = \alpha_s(\mu) - \alpha_s^2(\mu) \frac{\beta_0}{4\pi} \ln\left(\frac{q^2}{\mu^2}\right) + O(\alpha_s^3(\mu)) \quad (1.20)$$

This can be verified by substituting Eq. 1.19 into Eq. 1.18 and working to $O(\alpha_s^2(\mu))$. Here we have expressed the coupling at one scale q^2 in terms of the coupling at another scale μ^2 , and in doing so have eliminated the dependence

on the bare coupling as well as the ultraviolet cutoff. This is an example of renormalisation.

Unfortunately even if $\alpha_s(\mu) \ll 1$, the perturbative series will break down at large momenta, because of the logarithm. In Eq. 1.20, however, the scale μ is arbitrary, and so the value of the coupling at q should not depend on the choice of the scale μ . This means that the higher terms in the series must all be related, so that the series sums to an answer *independent* of μ . In fact the series is summed by solving a differential equation, but here we merely note that to this order we can rewrite Eq. 1.20 as:

$$\alpha_s(q) = \frac{\alpha_s(\mu)}{1 + \alpha_s(\mu)(\beta_0/4\pi)\ln(q^2/\mu^2)} \quad (1.21)$$

That this is independent of μ can be seen by taking the reciprocal of this equation to get:

$$\frac{1}{\alpha_s(q)} - \frac{\beta_0}{4\pi}\ln q^2 = \frac{1}{\alpha_s(\mu)} - \frac{\beta_0}{4\pi}\ln \mu^2 \quad (1.22)$$

The left hand side of this equation is independent of μ , whilst the right hand side is independent of q . Thus both sides must be equal to a constant which we write as $(\beta_0/4\pi)\ln \Lambda^2$. Thus we obtain:

$$\alpha_s(q) = \frac{4\pi}{\beta_0 \ln(q^2/\Lambda^2)} \quad (1.23)$$

Here Λ is a scale introduced in the theory because of the requirements of renormalisation. It is not specified, and must be deduced from experiment. The important thing to note is that at large momenta, $q^2 \gg \Lambda^2$, $\alpha_s(q)$ becomes smaller and smaller. Thus as $q^2 \rightarrow \infty$ we find that $\alpha_s(q) \rightarrow 0$. This property is known as 'asymptotic freedom'. At small momenta however, the coupling becomes large, and indeed from Eq. 1.23 becomes infinite at $q^2 = \Lambda^2$. Before we reached this scale though, the fact that the coupling is large would mean that

we could no longer rely on perturbation theory, and the derivation of Eq. 1.23 would break down.

The conclusion to be drawn from this is that at larger momentum scales, perturbative QCD becomes more reliable, and is self-consistent. At low momenta perturbation theory is no longer valid and we require a non-perturbative treatment if we are to test QCD in this crucial region.

For QED exactly the opposite happens. The quantity β_0 is negative, and hence it is at low momenta that perturbative QED is reliable and self-consistent. Although perturbation theory will break down at large momenta, this is expected to occur at a scale many orders of magnitude larger than that achieved in any experiment.

What is the physical meaning of this momentum dependence of the coupling? If we consider an electron, we can measure its electric charge by placing a test particle in its Coulomb field and measuring the force. In field theory, however, we cannot just consider an electron on its own, but we must take into account the emission of photons, which can produce e^+e^- pairs. These can exist for a tiny fraction of a second before annihilating into a photon, to be subsequently reabsorbed by the electron. Because opposite charges attract, the positrons will be preferentially closer to the initial electron, thus 'screening' its charge. The closer the test particle approaches the electron, the more it penetrates this cloud of surrounding positrons, and thus it will 'see' a larger charge.

For QCD we expect the same screening to occur, but this time we must not only take into account $q\bar{q}$ pairs, but must also include the effect of the gluons, since they carry the colour charge, unlike QED where the photon is electrically neutral. It turns out that the effect of the gluons is to preferentially surround a 'blue' quark with other blue charges. As our test particle is moved closer to our initial quark, it is the effect of the gluons which dominate, and so we

will now see less blue charge, and consequently the coupling measured will be smaller. We say that QCD produces ‘anti-screening’. Since the distance probed is inversely proportional to the momentum scale, we have a heuristic explanation for Eq. 1.22 and its equivalent in QED. The smallness of the coupling at large momenta helps to explain the observation that a high energy probe sees almost free quarks inside a proton. Presumably the coupling becomes large at low momenta, prohibiting the quarks from escaping to become free particles, but until we can perform a calculation in this non-perturbative region, we have no way of knowing whether this is true, or indeed of knowing how the coupling really behaves at low energies.

Returning to Eq. 1.21, this independence of the result of the arbitrary scale μ is called ‘renormalisation group’ invariance[1.6], a subject of important study in its own right. It leads to equations that allow the potentially large logarithms which can appear in field theory to be summed to give an answer independent of μ . An example occurs in the QCD corrections to the ratio R mentioned in section 1.2. Higher order corrections give to leading logarithmic order:

$$R = N \sum_q e_q^2 \left[1 + \frac{\alpha_s}{\pi} - \frac{\beta_0}{4\pi^2} \alpha_s^2 \ln\left(\frac{W^2}{\kappa^2}\right) \right] \quad (1.24)$$

where the sum is over the different quark flavours and the e_q are the electric charges of the quarks. Here W^2 is the centre of mass energy squared of the e^+e^- pair. Substituting the renormalised coupling $\alpha_s(\mu)$ from Eq. 1.18 gives, to the same order in $\alpha_s(\mu)$:

$$R = N \sum_q e_q^2 \left[1 + \frac{\alpha_s(\mu)}{\pi} - \frac{\beta_0}{4\pi^2} \alpha_s^2(\mu) \ln\left(\frac{W^2}{\mu^2}\right) \right] \quad (1.25)$$

R must be independent of μ , and we recognise the last two terms as the start of the series in Eq. 1.20. Thus we obtain

$$R = N \sum_q e_q^2 \left[1 + \frac{\alpha_s(W)}{\pi} + O(\alpha_s^2(W)) \right] \quad (1.26)$$

In principle, an all orders calculation would sum all logarithms into a power series in $\alpha_s(W)$ with non-logarithmic coefficients.

1.5 Confinement

At high energies perturbative QCD is seen to be theoretically self-consistent. Higher order calculations have been performed for many processes, and good agreement has been found with experiment. The quarks and gluons which we suppose to be true elementary particles, however, are not seen as free particles in nature unlike the electron and photon of QED. Instead we see the host of colourless particles and resonances we call the hadrons with masses of the order of 1 GeV. We interpret these hadrons as bound states of quarks and gluons, although we do not yet understand the mechanism which confines them[1.7].

If we are to accept that QCD really is the theory of strong interactions, as seems to be the case at high energies, then we must try to understand how the quarks are trapped inside the hadrons. Even if we cannot calculate the exact quantitative nature of confinement, we should at least expect to understand how its qualitative features follow from a non-Abelian gauge theory.

One of the main problems has been to formulate a framework in which these questions can be answered. As we have seen, our best calculational tool in field theory, namely perturbation theory, is not applicable. This thesis describes an attempt to formulate a non-perturbative framework in which, qualitatively at least, the nature of low energy QCD can be studied.

Despite not being able to use perturbation theory, we might expect that some aspect of confinement might be apparent even at high energies, and that some evidence of this might appear in a perturbative calculation. Below we

shall give an argument which suggests that this is not so, and that confinement will *only* be understood if we can go beyond perturbation theory. We shall then briefly describe one of the most promising avenues of non-perturbative calculations to date, that of lattice gauge theories.

Within perturbation theory in both QED and QCD we do not just find the ultraviolet divergences removed by renormalisation, but we also find infra-red divergences which occur at zero momenta in the loop integrals. These arise because of the masslessness of the gauge particles, the photon and the gluon. When calculating, for example, the elastic scattering of an electron off an external potential, the higher order corrections are infra-red divergent. These can be removed by having a fictitious mass λ for the photon, and we obtain terms proportional to $\ln(\lambda)$. It can be shown that in perturbation theory we generate a series which sums to be proportional to $\exp(\ln\lambda)$. Thus by letting $\lambda \rightarrow 0$ this exponential damping factor makes the cross-section vanish. Thus purely elastic scattering is forbidden. Because of the masslessness of the photon, it is kinematically possible to emit an infinite number of very low energy (soft) photons, and elastic scattering has zero probability.

To overcome this, physicists use the Bloch-Nordsieck treatment, where we calculate only *physically observable* cross-sections. Since any experiment must have a finite energy resolution, in our scattering experiment we must also include processes which involve emission of undetectable soft photons. In perturbation theory the infra-red divergences will cancel between the higher order corrections to the elastic process (virtual corrections) and the soft photon emission processes (real corrections) *order by order*[1.8].

In QCD the infra-red divergences are more severe because of the self-coupling of the gluon. However, it has been shown that here they also produce exponential factors damping elastic scattering processes. The question remains as to whether we can define physically observable cross-sections as in QED. It is

found that the Bloch-Nordsieck treatment works in QCD, as long as we sum over the colour degree of freedom of the initial and final states (even this condition is not always required). Thus for a detector with a finite energy resolution, and which is 'colour blind', we can calculate finite cross-sections involving the fundamental constituents of QCD, namely the quarks and gluons.

This result implies that asymptotic states with quark quantum numbers (e.g. fractional electric charge) can exist in perturbation theory. Since they are not observed in nature, we deduce that quark confinement is a truly non-perturbative phenomenon.

Nevertheless it is argued[1.9] that the severe infra-red behaviour of QCD does provide a possible mechanism for confinement. Support for this is drawn from two dimensional QED and QCD whose infra-red behaviour are extremely severe. The simplicity of these models enables us to examine their spectrum. In two dimensional massless QED, the theory is exactly solvable. The fermion and photon field which appear in the Lagrangian disappear from the physical spectrum, leaving a free massive scalar particle. With a fermion mass the theory is no longer exactly solvable, but we still find only scalar particles in the physical spectrum. In two dimensional QCD, an expansion based on having a large number of colours N , and letting $1/N$ being an expansion parameter, similarly finds that the quark and gluon are absent from the spectrum, leaving only scalar particles. Although suggestive, it is not possible to extend the analysis from these relatively simple models to the more realistic but far more complicated four dimensional ones. Nevertheless it is argued by some that in QCD for scattering involving external coloured particles, we have the possibility that the soft gluon emission processes themselves sum to a finite answer, although they are individually infra-red divergent. This leaves the cross-section damped by the exponential factor from the virtual corrections, and therefore vanishing when the gluon mass $\lambda \rightarrow 0$. It has not yet been possible to show that this

is indeed the case, and it seems difficult to relate it to the view of many, that confinement is intimately related to the QCD coupling becoming large at low momenta, and thus binding the quarks and gluons together so strongly that they cannot exist as free particles.

Probably the most important development in non-perturbative field theory has been that of lattice gauge theories[1.10]. Treating space-time as a finite four dimensional lattice, it was shown how to formulate a gauge theory on this discrete space. It was also shown how to perform these lattice calculations using computers. Theoretically it should be possible to calculate the properties of bound states (if they exist) such as masses. Unfortunately the present lattice sizes of about 24^4 sites are probably too small to give believable results, although progress is being made. The use of larger lattices is limited by the size of computers available, although this should increase in future. To obtain results which apply to real physical space-time, it is necessary to take the 'continuum' limit of lattice calculations, where the lattice spacing is to be taken to zero. It is not clear that the continuum limit of a lattice theory is necessarily related to the continuum theory itself. Nevertheless this area will remain an important testing ground for gauge theories.

It would be desirable then, to have a non-perturbative, continuum analysis of QCD, which, even if it could not accurately calculate the proton mass or other quantitative details, would at least allow us to understand the qualitative mechanism whereby quarks and gluons are confined.

CHAPTER TWO

THE SCHWINGER-DYSON EQUATIONS

2.1 Path Integrals and Functional Methods in Field Theory

Our approach to a non-perturbative study of QCD will be to examine certain integral equations which in general form are obeyed by all quantum field theories. Before we do this however, we must first set up a framework in which to define various quantities in field theory, and then to derive these equations.

The starting point for the functional approach to field theory is the generating functional[2.1]:

$$Z[J] = \int [D\phi] \exp \left(iS + i \int d^4x \phi(x) J(x) \right) \quad (2.1)$$

where here we are looking at a scalar field theory. The symbol $[D\phi]$ denotes a functional integral over all possible field configurations $\phi(x)$, and S is the classical action. In field theory we generally want to calculate the Green's functions, which are defined by

$$G_n(x_1, \dots, x_n) = \int [D\phi] \phi(x_1) \dots \phi(x_n) e^{iS} / \int [D\phi] e^{iS} \quad (2.2)$$

In general we can relate the n-point Green's function to the n-particle scattering amplitude[2.2]. These Green's functions can be obtained from the generating functional via functional differentiation:

$$G_n(x_1, \dots, x_n) = \left\{ \frac{1}{Z[J]} \frac{\delta^n Z[J]}{i\delta J(x_1) \dots i\delta J(x_n)} \right\} \Big|_{J=0} \quad (2.3)$$

We define a related quantity $W[J]$ by

$$Z[J] = \exp W[J] \quad (2.4)$$

We call $W[J]$ the generator of connected Green's functions $G_n^c(x_1, \dots, x_n)$. Using the definition of Eq. 2.4 we can easily derive:

$$\frac{1}{Z[J]} \frac{\delta Z[J]}{i\delta J(x)} = \frac{\delta W[J]}{i\delta J(x)} \quad (2.5)$$

further differentiation yields:

$$\begin{aligned} G_1(x_1) &= G_1^c(x_1) \\ G_2(x_1, x_2) &= G_2^c(x_1, x_2) + G_1^c(x_1)G_1^c(x_2) \\ G_3(x_1, x_2, x_3) &= G_3^c(x_1, x_2, x_3) + G_2^c(x_1, x_2)G_1^c(x_3) \\ &\quad + G_2^c(x_2, x_3)G_1^c(x_1) + G_2^c(x_3, x_1)G_1^c(x_2) \\ &\quad + G_1^c(x_1)G_1^c(x_2)G_1^c(x_3) \\ G_4(x_1, x_2, x_3, x_4) &= G_4^c(x_1, x_2, x_3, x_4) \\ &\quad + G_3^c(x_1, x_2, x_3)G_1^c(x_4) + \text{cyclic permutations} \\ &\quad + G_2^c(x_1, x_2)G_2^c(x_3, x_4) + \text{cyclic permutations} \\ &\quad + G_1^c(x_1)G_1^c(x_2)G_1^c(x_3)G_1^c(x_4) \end{aligned} \quad (2.6)$$

These equations and higher ones give the relation between the full Green's function generated by $Z[J]$ and the connected ones generated by $W[J]$. The connected two point function $G_2^c(x, y)$ is called the propagator, and is denoted $i\Delta(x - y)$. For theories such as $\lambda\phi^4$ theory, where the action is symmetric under $\phi \rightarrow -\phi$, then when we set $J = 0$, the odd Green's functions will vanish. For this case, we depict the last of Eq. 2.6 in fig. 2.1.

For a free field theory, where S contains only kinetic and mass terms, then the functional integral can be performed[2.1] to give

$$Z_0[J] = Z[0] \exp \frac{1}{2} \left(\int d^4x_1 d^4x_2 iJ(x_1) i\Delta_0(x_1 - x_2) iJ(x_2) \right) \quad (2.7)$$

where $i\Delta_0(x - y)$ is the usual free scalar field propagator.

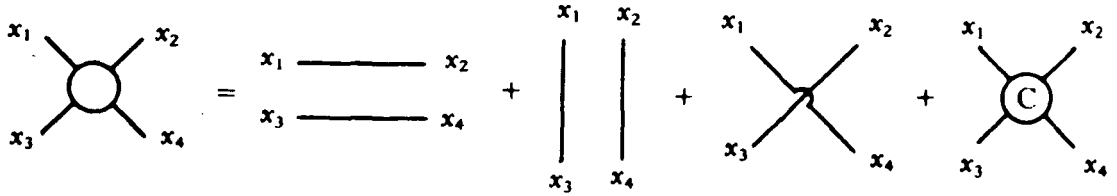


fig. 2.1: The relation between full and connected Green's functions. Here a long line represents a full propagator, a circle denotes a full Green's function, and a C inside a circle denotes a connected Green's function. Taken from Nash, ref. [2.1].

The final quantity we need is the effective action $\Gamma[\phi]$, defined via the functional Legendre transform:

$$W[J] = i\Gamma[\phi] + i \int d^4x J(x)\phi(x) \quad (2.8)$$

Here we think of W as a function of J alone, and Γ as a function of ϕ alone. $\phi(x)$ is usually referred to as the classical field, and is not to be confused with the functional integration variable in Eq. 2.1. From Eq. 2.8 we have the definitions

$$\phi(x) = \frac{\delta W}{i\delta J(x)} \quad J(x) = -\frac{\delta \Gamma}{\delta \phi(x)} \quad (2.9)$$

We can functionally expand $\Gamma[\phi]$ as:

$$\Gamma[\phi] = \sum_{n=0}^{\infty} \frac{1}{n!} \int \left(\prod_{i=0}^n dx_i \right) \Gamma_n(x_1, \dots, x_n) \phi(x_1) \cdots \phi(x_n) \quad (2.10)$$

where the $\Gamma_n(x_1, \dots, x_n)$ are called the proper vertices and can be related to scattering amplitudes[2.2]. Thus we have:

$$\Gamma_n(x_1, \dots, x_n) = \left. \frac{\delta^n \Gamma[\phi]}{\delta \phi(x_1) \cdots \delta \phi(x_n)} \right|_{\phi=0} \quad (2.11)$$

The following equation is a functional identity:

$$\int d^4z \frac{\delta\phi(x)}{i\delta J(z)} \frac{i\delta J(z)}{\delta\phi(y)} = \delta(x-y) \quad (2.12)$$

where $\delta(x)$ denotes a four dimensional delta function. Using the definitions in Eq. 2.9 we obtain the relation:

$$\int d^4z \frac{\delta^2 W}{i\delta J(z)i\delta J(x)} \frac{-i\delta^2 \Gamma}{\delta\phi(y)\delta\phi(z)} = \delta(x-y) \quad (2.13)$$

from which we see that $-i\delta^2 \Gamma/\delta\phi\delta\phi$ is the inverse propagator. Taking the derivative of Eq. 2.13 with respect to $i\delta J(w)$ and using Eq. 2.9 gives:

$$\begin{aligned} & \int d^4z \frac{\delta^3 W}{i\delta J(z)i\delta J(x)i\delta J(w)} \frac{-i\delta^2 \Gamma}{\delta\phi(y)\delta\phi(z)} \\ & + \int d^4z d^4v \frac{\delta^2 W}{i\delta J(z)i\delta J(x)} \frac{-i\delta^3 \Gamma}{\delta\phi(y)\delta\phi(z)\delta\phi(v)} \frac{\delta^2 W}{i\delta J(v)i\delta J(w)} = 0 \end{aligned} \quad (2.14)$$

multiplying this expression by $\delta^2 W/i\delta J(y)i\delta J(u)$, integrating over d^4y and using the relation in Eq. 2.13 gives us:

$$\frac{\delta^3 W}{i\delta J(u)i\delta J(x)i\delta J(w)} = \frac{i\delta^3 \Gamma}{\delta\phi(y)\delta\phi(z)\delta\phi(v)} i\Delta(z-x)i\Delta(v-w)i\Delta(y-u) \quad (2.15)$$

Here we have introduced a convention whereby a repeated space-time variable is to be integrated over. This equation is depicted diagrammatically in fig. 2.2. We call $i\delta\Gamma/\delta\phi\delta\phi\delta\phi$ the one particle irreducible Green's functions. Because the propagators on the external legs have been removed, we cannot split this Green's function into two pieces by 'cutting' one propagator. This is the meaning of 'one-particle irreducible'. Taking the derivative of Eq. 2.15 with respect to $i\delta J(t)$ we obtain:

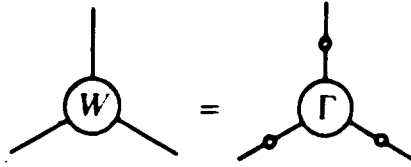


fig. 2.2: The relation between the connected and one particle irreducible three point function. A W in a circle denotes a connected Green's function, a Γ in a circle denotes one particle irreducible Green's function. A line with a circle on it represents a full propagator. Taken from Nash, ref. [2.1].

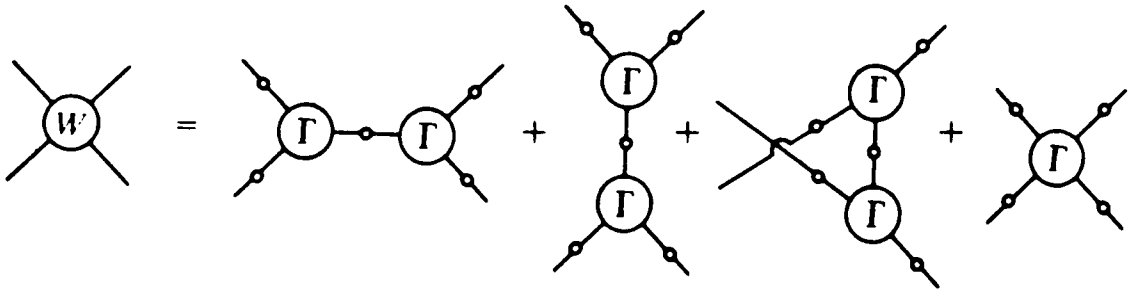


fig. 2.3: The relation between the connected four point Green's function, and the one particle irreducible Green's functions. Taken from Nash, ref. [2.1].

$$\begin{aligned}
 \frac{\delta^4 W}{i\delta J(t)i\delta J(u)i\delta J(x)i\delta J(w)} &= \frac{i\delta^4 \Gamma}{\delta\phi(s)\delta\phi(y)\delta\phi(z)\delta\phi(v)} \times \\
 &\quad \times i\Delta(s-t)i\Delta(z-x)i\Delta(v-w)i\Delta(y-u) \\
 &\quad + \frac{i\delta^3 \Gamma}{\delta\phi(y)\delta\phi(z)\delta\phi(v)} \frac{i\delta^3 \Gamma}{\delta\phi(x')\delta\phi(z')\delta\phi(v')} \times \\
 &\quad \times i\Delta(v-w)i\Delta(y-u)i\Delta(x-x')i\Delta(t-v')i\Delta(z-z') \\
 &\quad + \text{cyclic permutations}
 \end{aligned} \tag{2.16}$$

For the last terms, we have used the fact that one derivative of $i\Delta$ with respect to $i\delta J$ is equal to $\delta^3 W/i\delta J i\delta J i\delta J$ and used Eq. 2.15. Eq. 2.16 is depicted diagrammatically in fig. 2.3. Again we see that $\Gamma[\phi]$ generates the one particle

irreducible Green's functions. Taking higher functional derivatives of Eq. 2.16 will reveal the same structure for the higher Green's functions, the general proof going by induction.

We are now in a position to perform a perturbative expansion. First we write

$$S = S_0 + S_I \quad (2.17)$$

where S_0 is the free action, and S_I contains any interaction terms. The free action is quadratic in ϕ , and we write it as

$$S_0 = \frac{1}{2} \int d^4x d^4y \phi(x) S_2(x, y) \phi(y) \quad (2.18)$$

S_I will in general be a polynomial in ϕ where we call each term a vertex.

For a vertex of order N , we can write its contribution to S_I as:

$$\frac{1}{N!} \int \left(\prod_{i=1}^N d^4x_i \right) S_N(x_1, \dots, x_N) \phi(x_1) \cdots \phi(x_N) \quad (2.19)$$

The perturbative series is generated by using the expansion

$$e^{iS_I} = \sum_{n=0}^{\infty} \frac{(iS_I)^n}{n!} \quad (2.20)$$

then any factors of $\phi(x)$ which appear in Eq. 2.20 can be written as $\delta/i\delta J(x)$, and taken outside the functional integral. Thus the perturbative solution for a Green's function $G_n(x_1, \dots, x_n)$ is

$$G_n(x_1, \dots, x_n) = \left\{ \left(\sum_{m=0}^{\infty} \frac{1}{m!} \left(iS_I \left(\frac{\delta}{i\delta J} \right) \right)^m \right) \left(\prod_{i=1}^n \frac{\delta}{i\delta J(x_i)} \right) \frac{Z_0[J]}{Z[0]} \right\} \Bigg|_{J=0} \quad (2.21)$$

where $Z_0[J]$ is the free field generating functional, Eq. 2.7. Here the functional derivatives act on $Z_0[J]$ to bring down free field propagator factors. These are

connected together by the vertices, such as that in Eq. 2.19. The lowest non-trivial contribution to the Green's function $G_N(x_1, \dots, x_N)$ for this vertex is therefore seen to be:

$$\int \left(\prod_{k=1}^N d^4 y_k \right) \left(\prod_{i=1}^N \frac{\delta}{i \delta J(x_i)} \right) \left(\prod_{j=1}^N \frac{\delta}{i \delta J(y_j)} \frac{i}{N!} \right) S_N(y_1, \dots, y_N) \frac{Z_0[J]}{Z[0]} \quad (2.22)$$

For a connected Green's function, the free field propagators must connect one x -variable to one y -variable in Eq. 2.22. This can be done in $N!$ different ways, so we can simply read off the Feynman rule for this vertex as $i \int (\prod_{k=1}^N d^4 y_k) S_N(y_1, \dots, y_N)$. In momentum space, we simply take the Fourier transform. For example, in $\lambda \phi^4$ theory we have:

$$\begin{aligned} S_I &= -\frac{\lambda}{4!} \int d^4 x \phi^4(x) \\ &= -\frac{\lambda}{4!} \int \left(\prod_{k=1}^4 dx_k \right) \delta(x_1 - x_2) \delta(x_1 - x_3) \delta(x_1 - x_4) \phi(x_1) \phi(x_2) \phi(x_3) \phi(x_4) \end{aligned} \quad (2.23)$$

From this we can read off the Feynman rule in momentum space to be $-i\lambda$, as usual.

Having set up the machinery, we are now in a position to derive our equations, which relate the various Green's functions of the theory.

2.2 The Schwinger-Dyson Equations for Scalar Field Theory

The Schwinger-Dyson equations are derived from $Z[J]$ by using the fact that the functional integral of a derivative vanishes:

$$\int [D\phi] \frac{\delta}{\delta \phi(x)} \exp \left(iS + i \int d^4 y \phi(y) J(y) \right) = 0 \quad (2.24)$$

which gives us the functional equation

$$\int [D\phi] \left(\frac{\delta S}{\delta \phi(x)} + J(x) \right) \exp \left(iS + i \int d^4 y \phi(y) J(y) \right) = 0 \quad (2.25)$$

Note the similarity of Eq. 2.25 to the classical equations of motion in the presence of a source term:

$$\frac{\delta S}{\delta \phi(x)} + J(x) = 0 \quad (2.26)$$

In this sense Eq. 2.25, and the equations we shall derive from it can be seen as the equations of motion of a quantum field theory. If we use the symbol $\langle H(x) \rangle$ to denote the path integral of $H(x)$ weighted by the exponential of $iS + i \int d^4 y \phi(y) J(y)$, all divided by $Z[0]$, then Eq. 2.25 can be written

$$\left\langle \frac{\delta S}{\delta \phi(x)} \right\rangle + J(x) = \left\langle \frac{\delta S_0}{\delta \phi(x)} \right\rangle + \left\langle \frac{\delta S_I}{\delta \phi(x)} \right\rangle + J(x) = 0 \quad (2.27)$$

Let us find the contribution to this equation of our vertex of Eq. 2.19.

We have from Eq. 2.27:

$$\begin{aligned} -J(x_1) &= S_2(x_1, y) \frac{\delta}{i\delta J(y)} \frac{Z[J]}{Z[0]} \\ &+ \frac{1}{(N-1)!} S_N(x_1, y_1, \dots, y_{N-1}) \prod_{j=1}^{N-1} \frac{\delta}{i\delta J(y_j)} \frac{Z[J]}{Z[0]} \end{aligned} \quad (2.28)$$

where once again we have replaced $\phi(y_i)$ by $\delta/i\delta J(y_i)$, and a repeated space-time index is to be integrated over. Taking the derivative with respect to the classical field $\phi(x_2)$, Eq. 2.9, and using its definitions we obtain:

$$\begin{aligned} \frac{\delta^2 \Gamma}{\delta \phi(x_1) \delta \phi(x_2)} &= S_2(x_1, x_2) \\ &+ \frac{1}{(N-1)!} S_N(x_1, y_1, \dots, y_{N-1}) \frac{i\delta J(y_N)}{\delta \phi(x_2)} \left(\prod_{j=1}^N \frac{\delta}{i\delta J(y_j)} \right) \frac{Z[J]}{Z[0]} \end{aligned} \quad (2.29)$$

where we have used the functional chain rule for differentiation in the second term. Recognising $-iS_2(x_1, x_2)$ as the inverse free propagator, and setting the source term J equal to zero gives us the equation:

$$(i\Delta(x_1 - x_2))^{-1} = (i\Delta_0(x_1 - x_2))^{-1} - \frac{1}{(N-1)!} iS_N(x_1, y_1, \dots, y_{N-1}) G_n(y_1, \dots, y_N) (i\Delta(y_N - x_2))^{-1} \quad (2.30)$$

We can represent this equation diagrammatically by noting that it states that the full inverse propagator is equal to the free inverse propagator minus a term which contracts the lowest order vertex iS_N , with the full N -point Green's function with the propagator on one external leg removed. For $\lambda\phi^4$ theory, we use the form of the vertex in Eq. 2.23. Using the relations between the full and connected Green's functions, Eq. 2.6, and then using the relations between the connected and the one particle irreducible Green's functions, Eqs. 2.15 and 2.16., we obtain the equation depicted diagrammatically in fig. 2.4.

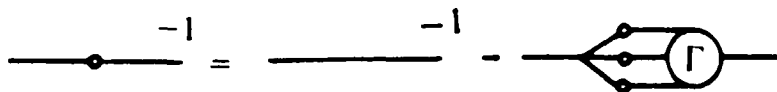


fig. 2.4: The Schwinger-Dyson equation for the inverse propagator in $\lambda\phi^4$ theory. Taken from Nash, ref. [2.1].

This is the Schwinger-Dyson equation for the full inverse propagator in $\lambda\phi^4$ theory. It is an integral equation, which relates the full two and four point functions of the theory. Higher equations are simply derived by taking more functional derivatives of Eq. 2.29. The resulting equation for the four point function in $\lambda\phi^4$ theory is depicted in fig. 2.5. Here we can see that, in general, the equation for the n -point function involves contributions from up to the $(n+2)$ -point function.

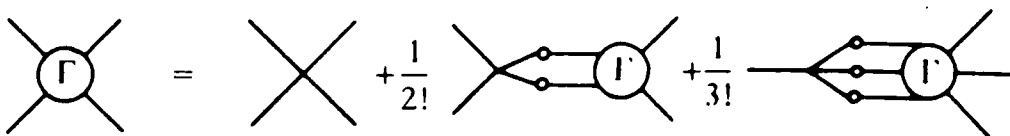


fig 2.5: The Schwinger-Dyson equation for the four point function in $\lambda\phi^4$ theory.

Taken from Nash, ref. [2.1].

The form of Eq. 2.30 arises naturally in perturbation theory. Consider a lowest order correction $\Sigma(p)$ which contributes to the self energy of the propagator in momentum space. Then the full perturbation series for the propagator will contain the terms:

$$\begin{aligned}
 i\Delta(p) &= i\Delta_0(p) + i\Delta_0(p)\Sigma(p)i\Delta_0(p) + i\Delta_0(p)\Sigma(p)i\Delta_0(p)\Sigma(p)i\Delta_0(p) + \dots \\
 &= i\Delta_0(p) \left(1 + i\Delta_0(p)\Sigma(p) + (i\Delta_0(p)\Sigma(p))^2 + \dots \right) \\
 &= \frac{i\Delta_0(p)}{1 - i\Delta_0(p)\Sigma(p)}
 \end{aligned} \tag{2.31}$$

simply inverting this expression gives:

$$(i\Delta(p))^{-1} = (i\Delta_0(p))^{-1} - \Sigma(p) \tag{2.32}$$

which is identical in structure to Eq. 2.30.

2.3 Fermions and Path Integrals

A slightly different procedure is needed to deal with fermions, requiring us to perform the functional integral over anticommuting, or Grassmann fields, see ref. [2.1] for more details. In general though, for each fermion we introduce two fields $\bar{\psi}$, ψ and two anticommuting sources $\bar{\eta}$, η . The fermionic part of the path integral is then:

$$Z[\bar{\eta}, \eta] = \int [D\bar{\psi}][D\psi] \exp \left(iS + i \int d^4x (\bar{\eta}(x)\psi(x) + \bar{\psi}(x)\eta(x)) \right) \quad (2.33)$$

The general n-point Green's functions are defined by:

$$G_{2n}(x_1, \dots, x_n, y_1, \dots, y_n) = \left. \left\{ \frac{1}{Z[\bar{\eta}, \eta]} \frac{\delta}{\delta \bar{\eta}(x_1)} \dots \frac{\delta}{\bar{\eta}(x_n)} \frac{\delta}{\eta(y_1)} \dots \frac{\delta}{\delta \eta(y_n)} Z[\bar{\eta}, \eta] \right\} \right|_{\bar{\eta}=0, \eta=0} \quad (2.34)$$

In a similar way to before, we define $W[\bar{\eta}, \eta]$ and $\Gamma[\bar{\psi}, \psi]$. This time because of the anticommuting nature of the fields we have as the parallel of Eq. 2.9:

$$\begin{aligned} \psi(x) &= \frac{\delta W}{i\delta \bar{\eta}(x)} \\ \bar{\psi}(x) &= \frac{\delta W}{-i\delta \eta(x)} \\ \eta(x) &= -\frac{\delta \Gamma}{\delta \bar{\psi}(x)} \\ \bar{\eta}(x) &= \frac{\delta \Gamma}{\delta \psi(x)} \end{aligned} \quad (2.35)$$

Thus the fermion propagator is defined as:

$$iS_{F\alpha\beta}(x, y) = \frac{\delta^2 W}{\delta \bar{\eta}_\alpha(x) \delta \eta_\beta(y)} = -\frac{\delta^2 W}{\delta \eta_\beta(y) \delta \bar{\eta}_\alpha(x)} \quad (2.36)$$

where α and β are spinor indices, which we shall in general suppress. It can easily be verified that $i\delta^2 \Gamma / \delta \bar{\psi}(x) \delta \psi(y)$ is the inverse fermion propagator. Similar relations hold between the connected and the one-particle irreducible Green's functions as for the scalar case.

2.4 The Schwinger-Dyson Equations for QCD

The path integral formulation of non-Abelian gauge theories has proved to be the most intuitive way of formulating the full quantum field theory[2.3]. It is an elegant way of imposing the constraints of quantising a massless spin-1

field, which has only the two transverse degrees of freedom as dynamical fields. Because the path integration should really be over only gauge inequivalent fields, we need to introduce a ‘gauge fixing term’. This procedure also involves the introduction of the so-called ‘ghost’ fields, which are anti-commuting. In an Abelian theory, or in axial gauges for a non-abelian theory, these ghost fields decouple. In covariant gauges however, they are an essential feature, preserving the unitarity of scattering amplitudes, and the transversality of the gauge field. This path integral formulation of a gauge theory is a well understood procedure, and here we will merely write down the full QCD Lagrangian:

$$\mathcal{L} = \mathcal{L}_{\text{gauge}} + \mathcal{L}_{\text{gauge-fix}} + \mathcal{L}_{\text{ghost}} + \mathcal{L}_{\text{quark}} \quad (2.37)$$

where

$$\begin{aligned} \mathcal{L}_{\text{gauge}} &= -\frac{1}{4} F^{\mu\nu a} F_{\mu\nu a} \\ \mathcal{L}_{\text{gauge-fix}} &= -\frac{1}{2\xi} \left(\partial_\mu A^{\mu a} \right)^2 \\ \mathcal{L}_{\text{ghost}} &= - \left(\partial_\mu \bar{C}^a \right) D_{ab}^\mu C^b \\ &= - \partial_\mu \bar{C}^a \partial^\mu C^a - g \partial_\mu \bar{C}^a f^{abc} C^b A^{\mu c} \end{aligned} \quad (2.38)$$

$$\begin{aligned} \mathcal{L}_{\text{quark}} &= \bar{\psi}_i (iD_{ij}^\mu \gamma_\mu - m) \psi_j \\ &= \bar{\psi}_i (i\not{\partial} - m) \psi + g T_{ij}^a A^{\mu a} \bar{\psi}_i \gamma_\mu \psi_j \end{aligned}$$

where $T_{ij}^a = \lambda_{ij}^a/2$ and C^a, \bar{C}^a are the ghost and anti-ghost fields respectively. ξ is a parameter which fixes the gauge, where for example $\xi = 0$ is the Landau gauge and $\xi = 1$ is the Feynman gauge. All the other quantities are defined in section 1.3. The action is defined as:

$$S = \int d^4x \mathcal{L}(x) \quad (2.39)$$

We can therefore write the pure gauge part of the action as:

$$\begin{aligned} S_{\text{gauge}} + S_{\text{gauge-fix}} &= \frac{1}{2} \int d^4x_1 A_\mu^a(x_1) \left(\square g^{\mu\nu} - (1 - 1/\xi) \partial^\mu \partial^\nu \right) A_\nu^b(x_1) \delta_{ab} \\ &+ \frac{g}{3!} \Gamma_{0\mu\nu\sigma}^{abc}(x_1, x_2, x_3) A_\mu^a(x_1) A_\nu^b(x_2) A_\sigma^c(x_3) \\ &+ \frac{g^2}{4!} \Gamma_{0\mu\nu\sigma\tau}^{abcd}(x_1, x_2, x_3, x_4) A_\mu^a(x_1) A_\nu^b(x_2) A_\sigma^c(x_3) A_\tau^d(x_4) \end{aligned} \quad (2.40)$$

where:

$$\begin{aligned} \Gamma_{0\mu\nu\sigma}^{abc} &= -f^{abc} \left\{ \delta_{\mu\nu} \left(\frac{\partial}{\partial x_1} - \frac{\partial}{\partial x_2} \right)_\sigma \delta(x_1 - x_3) \delta(x_2 - x_3) \right. \\ &+ \delta_{\sigma\nu} \left(\frac{\partial}{\partial x_2} - \frac{\partial}{\partial x_3} \right)_\mu \delta(x_2 - x_1) \delta(x_3 - x_1) \\ &\left. + \delta_{\mu\sigma} \left(\frac{\partial}{\partial x_3} - \frac{\partial}{\partial x_1} \right)_\nu \delta(x_3 - x_1) \delta(x_1 - x_1) \right\} \end{aligned}$$

$$\begin{aligned} \Gamma_{0\mu\nu\sigma\tau}^{abcd} &= \left(f^{abe} f^{cde} \left[\delta_{\mu\sigma} \delta_{\nu\tau} - \delta_{\nu\sigma} \delta_{\mu\tau} \right] \right. \\ &+ f^{bce} f^{dae} \left[\delta_{\mu\sigma} \delta_{\nu\tau} - \delta_{\sigma\tau} \delta_{\mu\nu} \right] \\ &\left. + f^{bde} f^{cae} \left[\delta_{\nu\sigma} \delta_{\mu\tau} - \delta_{\mu\nu} \delta_{\sigma\tau} \right] \right) \delta(x_1 - x_2) \delta(x_3 - x_4) \delta(x_2 - x_3) \end{aligned} \quad (2.41)$$

Once again it is implicit that repeated space-time variables are to be integrated over. Here we recognise $ig\Gamma_{0\mu\nu\sigma}^{abc}$, $ig^2\Gamma_{0\mu\nu\sigma\tau}^{abcd}$ as the bare triple and quartic gluon couplings respectively[2.1]. Next we have:

$$\begin{aligned}
 S_{\text{ghost}} &= \int d^4x_1 \bar{C}^a(x_1) \square C^a \\
 &+ g \Gamma_{0\mu}^{abc}(x_1, x_2, x_3) A^{\mu c}(x_1) \bar{C}^a(x_2) C^b(x_3)
 \end{aligned} \tag{2.42}$$

where

$$\Gamma_{g\mu}^{abc} = f^{abc} \frac{\partial}{\partial x_2^\nu} \delta(x_2 - x_3) \delta(x_3 - x_1) \delta^{\mu\nu} \tag{2.43}$$

is the bare ghost-gluon coupling. Finally we have:

$$\begin{aligned}
 S_{\text{quark}} &= \int d^4x_1 \bar{\psi}_i(x_1) (i\not{\partial} - m) \psi_i(x_1) \\
 &+ g \Lambda_{0\alpha\beta ij}^{\mu a}(x_1, x_2, x_3) A_\mu^a(x_1) \bar{\psi}_{\alpha i}(x_2) \psi_{\beta j}(x_3)
 \end{aligned} \tag{2.44}$$

where α and β are spinor indices, and

$$\Lambda_{0\alpha\beta ij}^{\mu a}(x_1, x_2, x_3) = T_{ij}^a \gamma_{\alpha\beta}^\mu \delta(x_1 - x_2) \delta(x_2 - x_3) \tag{2.45}$$

Following the form of Eq. 2.26, the Schwinger-Dyson equation for the gluon field reads

$$\left\langle \frac{\delta S}{\delta A_\mu^a(x)} \right\rangle = -J_\mu^a \tag{2.46}$$

Thus we obtain:

$$\begin{aligned}
 \frac{\delta \Gamma}{\delta A_\mu^a(x)} &= (\square g^{\mu\nu} - (1 - 1/\xi) \partial^\mu \partial^\nu) \langle A_\nu^a(x) \rangle \\
 &+ g/2! \Gamma_{0\mu\sigma\tau}^{acd}(x, x_1, x_2) \langle A^{\sigma c}(x_1) A^{\tau d}(x_2) \rangle \\
 &+ g^2/3! \Gamma_{0\mu\sigma\tau\rho}^{acde}(x, x_1, x_2, x_3) \langle A^{\sigma c}(x_1) A^{\tau d}(x_2) A^{\rho e}(x_3) \rangle \\
 &- g \Gamma_{0\mu}^{acd}(x, x_1, x_2) \langle C^d(x_2) \bar{C}^c(x_1) \rangle \\
 &- g \Lambda_{0\alpha\beta ij}^{\mu a}(x, x_1, x_2) \langle \psi_{\beta j}(x_2) \bar{\psi}_{\alpha i}(x_1) \rangle
 \end{aligned} \tag{2.47}$$

where the minus signs in the last two terms come from interchanging the order of anticommuting fields. In terms of the classical field A_μ^a , and the connected Green's functions we have:

$$\begin{aligned}
 \frac{\delta\Gamma}{\delta A_a^\mu(x)} &= \left(\square g^{\mu\nu} - (1 - 1/\xi)\partial^\mu\partial^\nu \right) A_a^\nu(x) \\
 &+ g/2! \Gamma_{0\mu\sigma\tau}^{acd}(x, x_1, x_2) \left(\frac{\delta^2 W}{i\delta J_\sigma^c(x_1) i\delta J_\tau^d(x_2)} + A^{\sigma c}(x_1) A^{\tau d}(x_2) \right) \\
 &+ g/3! \Gamma_{0\mu\sigma\tau\rho}^{acde}(x, x_1, x_2, x_3) \left(\frac{\delta^3 W}{i\delta J_\sigma^c(x_1) i\delta J_\tau^d(x_2) i\delta J_\rho^e(x_3)} \right. \\
 &\quad \left. + 3 \frac{\delta^2 W}{i\delta J_\sigma^c(x_1) i\delta J_\tau^d(x_2)} A^{\rho e}(x_3) + A^{\sigma c}(x_1) A^{\tau d}(x_2) A^{\rho e}(x_3) \right) \\
 &- g\Gamma_0^{\mu acd}(x, x_1, x_2) \left(\frac{\delta^2 W}{\delta\bar{\omega}^d(x_2)\delta\omega^c(x_1)} + C^d(x_1)\bar{C}^c(x_2) \right) \\
 &- g\Lambda_{0\alpha\beta ij}^{\mu a}(x, x_1, x_2) \left(\frac{\delta^2 W}{\delta\bar{\eta}_j^\beta(x_2)\delta\eta_i^\alpha(x_1)} + \psi_j^\beta(x_2)\bar{\psi}_j^\alpha(x_1) \right)
 \end{aligned} \tag{2.48}$$

where $\bar{\omega}, \omega$ are the sources for the ghost fields. Taking a further derivative with respect to $A_b^\nu(y)$ and setting $J = A = 0$ we obtain:

$$\begin{aligned}
 \frac{\delta\Gamma}{\delta A_a^\mu A_b^\nu(y)} &= \left(\square g^{\mu\nu} - (1 - 1/\xi)\partial^\mu\partial^\nu \right) \delta(x - y) \\
 &+ g/2! \Gamma_{0\mu\sigma\tau}^{acd}(x, x_1, x_2) \frac{\delta^3 W}{i\delta J_{\nu'}^{b'}(y') i\delta J_\sigma^c(x_1) i\delta J_\tau^d(x_2)} \frac{-i\delta^2\Gamma}{\delta A_{b'}^{\nu'}(y') \delta A_b^\nu(y)} \\
 &+ g/3! \Gamma_{0\mu\sigma\tau\rho}^{acde}(x, x_1, x_2, x_3) \frac{\delta^4 W}{i\delta J_{\nu'}^{b'}(y') i\delta J_\sigma^c(x_1) i\delta J_\tau^d(x_2) i\delta J_\rho^e(x_3)} \times \\
 &\quad \times \frac{-i\delta^2\Gamma}{\delta A_{b'}^{\nu'}(y') \delta A_b^\nu(y)} \\
 &+ g/2! \Gamma_{0\mu\sigma\tau\rho}^{acde}(x, x_1, x_2, y) \frac{\delta^2 W}{i\delta J_\sigma^c(x_1) i\delta J_\tau^d(x_2)} \\
 &- g\Gamma_0^{\mu acd}(x, x_1, x_2) \frac{\delta^3 W}{i\delta J_{\nu'}^{b'}(y') \delta\bar{\omega}^d(x_2)\delta\omega^c(x_1)} \frac{-i\delta^2\Gamma}{\delta A_{b'}^{\nu'}(y') \delta A_b^\nu(y)} \\
 &- g\Lambda_{0\alpha\beta ij}^{\mu a}(x, x_1, x_2) \left(\frac{\delta^3 W}{i\delta J_{\nu'}^{b'}(y') \delta\bar{\eta}_j^\beta(x_2)\delta\eta_i^\alpha(x_1)} \frac{-i\delta^2\Gamma}{\delta A_{b'}^{\nu'}(y') \delta A_b^\nu(y)} \right)
 \end{aligned} \tag{2.49}$$

On multiplying by $-i$, and using Eqs. 2.13-2.16 which hold in identical form for the gluon field, we obtain the Schwinger-Dyson equation for the inverse gluon propagator, first derived in ref. [2.4], and depicted diagrammatically in fig. 2.6. The relative minus sign of the last two terms in Eq. 3.49 can be ascribed to

closed loops of anti-commuting fields.

Equations can similarly be derived for the ghost and quark propagators. The equation for the quark propagator will be derived in chapter five. Until then we consider a pure gauge theory, in which quark fields are absent.

Equations for the higher point Green's functions can also be derived, by taking more functional derivatives of Eq. 2.48. It is easy to see from this that the equation for the n -point gluon Green's function will involve contributions from the $2, 3, \dots, n, n+1, n+2$ point functions. Our equation for the propagator, or two point function, is the first example of this, involving contributions from the full 2, 3 and 4-point functions.

Since the Schwinger-Dyson equations are exactly satisfied by the full Green's functions of the theory, by solving them we would hope to obtain information on the non-perturbative features of QCD, particularly that of confinement. Because there are infinitely many of these equations, one for each Green's function, and all of them coupled, it is obviously an impossible task to solve them exactly. Nevertheless we might hope to solve some truncated version of them. This is in fact nothing more than we having been doing all along in perturbation theory. The simplest truncation possible of the Schwinger-Dyson equations is to ignore all terms involving loops. We are left with equations which state that the 2,3 and 4-point functions are equal to the corresponding bare ones appearing in the classical Lagrangian, with the higher Green's functions all vanishing. We can then take these solutions and substitute them in the right hand side of the Schwinger-Dyson equations. Thus Eq. 2.49, for example, will generate the first few terms of the perturbative expansion of the inverse gluon propagator. More exactly, perturbation theory is nothing else than the solution to the Schwinger-Dyson equations based on a truncation in successive powers of the coupling constant. Of course, perturbation theory is a very special truncation, in that it satisfies the requirements of renormalisability and unitarity, i.e. it

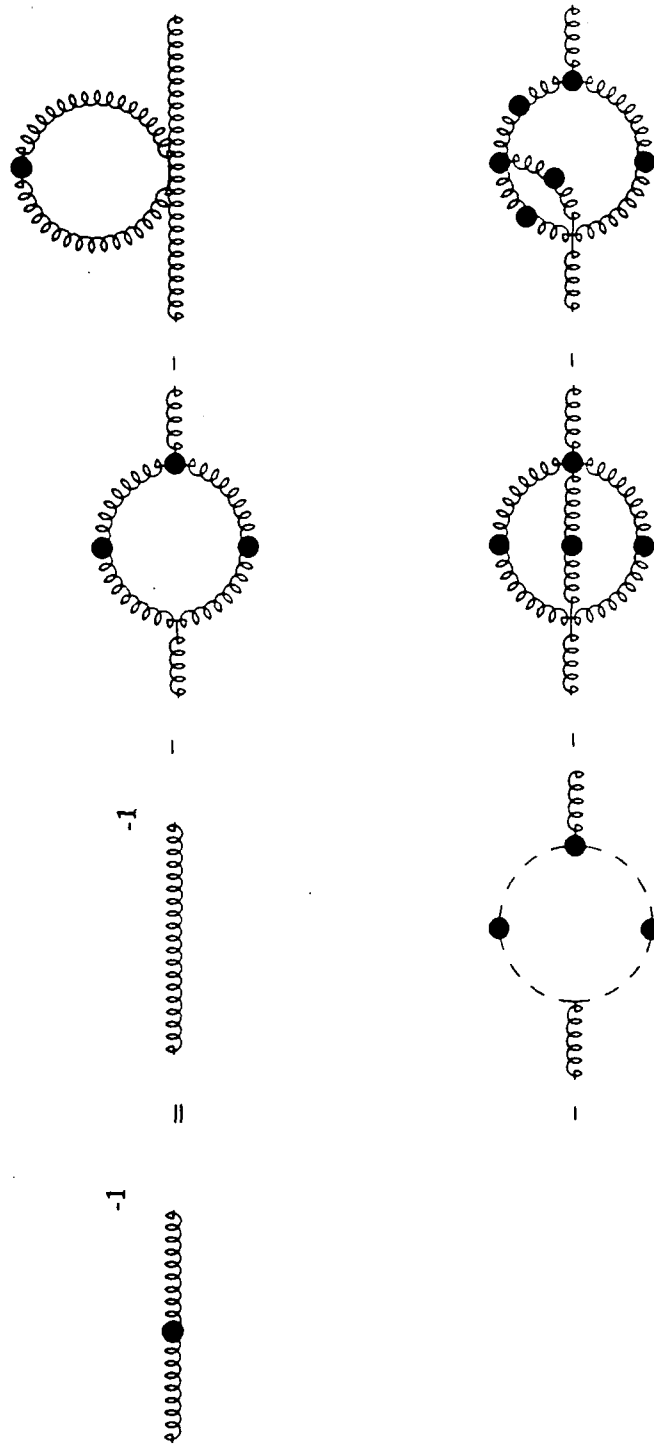


fig 2.6: The Schwinger-Dyson equation for the gluon propagator in QCD. The curly lines represent gluons, the dotted lines ghosts. A dark circle on a line represents a full propagator, a dark circle on a vertex represents a full one particle irreducible vertex. We have not included the fermion contribution, for this see chapter six.

allows a systematic removal of the ultraviolet infinities, to give answers in which quantum mechanical probabilities are conserved. These are essential features in the calculation of physical quantities.

This thesis details an entirely different truncation of the Schwinger-Dyson equations, in which quantities are not truncated at some particular order in the coupling constant, and so contain some information to all orders in g . In this way we might hope to attack the non-perturbative region of QCD. That this truncation has yet to be made entirely consistent in the way perturbation theory is, should not deter us. At the best, we may eventually discover a fully consistent non-perturbative treatment of QCD. At the worst, we might still expect to divine some of the salient features of the theory.

2.5 The Slavnov-Taylor/Ward-Takahashi Identities

The importance of a gauge theory lies in the constraints of gauge invariance which are essential in ensuring renormalisability and unitarity in perturbation theory. At the quantum level, this gauge symmetry is manifested in the Slavnov-Taylor identities for a non-Abelian theory[2.5], the generalisations of the Ward-Takahashi identities for QED[2.6]. These identities are relations between the full Green's functions of the theory. The generic form for these identities in momentum space is

$$p_1^\mu \Gamma_n^{\mu \dots}(p_1, \dots) = \Phi_n[\Gamma_{n-1}, \Gamma_{n-2}, \dots, \Gamma_2] \quad (2.50)$$

where p_1^μ is an external boson momentum contracted with the appropriate Lorentz index of a Green's function. The Slavnov-Taylor identities equate this contraction to a combination of lower Green's functions, denoted symbolically here by Φ_n . The most well known example arises in QED:

$$q^\mu \Gamma_\mu(q, p, p') = S_F^{-1}(p') - S_f^{-1}(p) \quad (2.51)$$

where $\Gamma^\mu(q, p, p')$ is the full electron-photon three point irreducible Green's function, q is the incoming photon momentum, equal to $p' - p$, and S_F is the full electron propagator. This identity holds for the full Green's functions, but also holds order by order in perturbation theory. Thus to lowest order $\Gamma_\mu = -i\gamma^\mu$, $S_F = i/\not{p}$, and Eq. 2.51 holds trivially.

In general we can divide such a vertex into a longitudinal and a transverse piece[2.7], where the transverse piece is defined by the property that it vanishes when contracted with any external boson momenta. i.e.

$$\Gamma^{\mu_1 \cdots \mu_n}(p_1, \cdots, p_n) = \Gamma_L^{\mu_1 \cdots \mu_n}(p_1, \cdots, p_n) + \Gamma_T^{\mu_1 \cdots \mu_n}(p_1, \cdots, p_n) \quad (2.52)$$

where we have

$$p_i^{\mu_i} \Gamma_T^{\mu_1 \cdots \mu_i \cdots \mu_n}(p_1, \cdots, p_i, \cdots, p_n) = 0, \quad \forall i \quad (2.53)$$

The transverse part is obviously unconstrained by the Ward identities. Moreover, this split is not unique because we can always add an arbitrary amount of the transverse part to the longitudinal part. We can ensure uniqueness, however, by demanding that Γ_L be free of kinematic singularities. Since the complete vertex must also be free of kinematic singularities, then the transverse part must be as well. The important point about this condition, is that in general it allows us to 'solve' the Ward identity for the longitudinal vertex in terms of the lower Green's functions in a unique way. The best way of demonstrating this is to give an example.

In scalar electrodynamics, we have a three-point vertex describing the interaction of the photon with a charged scalar particle. The Ward identity for this vertex reads[2.7]:

$$q^\mu \Gamma_\mu(q, p, p') = D^{-1}(p') - D^{-1}(p) \quad (2.54)$$

where $D(p)$ is the full scalar propagator. Since momentum is conserved at the vertex we can write

$$\Gamma_\mu = Ap_\mu + Bp'_\mu \quad (2.55)$$

where A, B are scalar functions of the momenta. The Ward identity Eq. 2.54 gives us the following condition on A and B :

$$p \cdot qA + p' \cdot qB = D^{-1}(p') - D^{-1}(p) \quad (2.56)$$

Thus we can eliminate B to obtain:

$$\Gamma_\mu = \left(D^{-1}(p') - D^{-1}(p) \right) \frac{p'_\mu}{p' \cdot q} + A \left(p_\mu - \frac{p \cdot q}{p' \cdot q} p'_\mu \right) \quad (2.57)$$

The first term has a kinematic singularity at $p' \cdot q = 0$ which must be cancelled by a similar singularity in the second term. Evidently A satisfies:

$$\lim_{p' \cdot q \rightarrow 0} (p \cdot qA) = D^{-1}(p') - D^{-1}(p) \quad (2.58)$$

As $p' \cdot q \rightarrow 0$ then $p \cdot q \rightarrow (p'^2 - p^2)$, so we have:

$$A = \frac{D^{-1}(p') - D^{-1}(p)}{p'^2 - p^2} + p' \cdot qA' \quad (2.59)$$

with A' unconstrained. Thus for our vertex we obtain:

$$\Gamma_\mu = \frac{D^{-1}(p') - D^{-1}(p)}{p'^2 - p^2} (p'_\mu + p_\mu) + A' (p' \cdot qp_\mu - p \cdot qp'_\mu) \quad (2.60)$$

The first term is the longitudinal part of the vertex which is free of kinematic singularities, the second is transverse to q^μ and is unconstrained.

An important consequence of this unique division into a longitudinal and a transverse piece, using absence of kinematic singularities, can be determined from Eq. 2.53. Taking the derivative of this equation with respect to p'_μ gives:

$$\Gamma_T^{\mu_1 \dots \nu \dots \mu_n} + p_i^{\mu_i} \frac{\partial}{\partial p_i^\nu} \Gamma_T^{\mu_1 \dots \mu_i \dots \mu_n} = 0 \quad (2.61)$$

From our previous discussion we have obtained a Γ_T which is itself free from kinematic singularities. Thus as $p_i \rightarrow 0$ the second term must vanish. From Eq. 2.61 we therefore deduce that Γ_T itself vanishes in this limit that the external momenta go to zero. In other words by splitting the vertex as we have done, the low momentum behaviour is given entirely by the longitudinal part, precisely the piece we can determine from the Ward identity. This result is of much importance in a non-Abelian theory, in which it is the low momentum behaviour of Green's functions which cannot be determined in perturbation theory, and which we wish to investigate.

We are now in a position to outline the approach we will take to solve the Schwinger-Dyson equations[2.8]. We can write the full hierarchy of equations symbolically as follows:

$$\begin{aligned} \Gamma_2 &= \Omega_2 [\Gamma_2, \Gamma_3, \Gamma_4] \\ \Gamma_3 &= \Omega_3 [\Gamma_2, \Gamma_3, \Gamma_4, \Gamma_5] \\ &\cdot \\ &\cdot \\ \Gamma_n &= \Omega_n [\Gamma_2, \dots, \Gamma_n, \Gamma_{n+1}, \Gamma_{n+2}] \end{aligned} \quad (2.62)$$

Here Γ_n represents the n -point gluon Green's function, and Ω_n the relevant combination of Green's functions. The first thing we do is to truncate the equations at, say, the equation for Γ_n . If we first set $\Gamma_{n+2} \equiv 0$, and then set Γ_{n+1} equal to its longitudinal part in the expression for Ω_n , then we will have a closed set of equations which we can think about solving. Since the longitudinal part of Γ_{n+1} gives the exact behaviour in the zero momentum limit, we should expect this to be a valid approximation in which to study the low momentum

behaviour of Green's functions. The neglecting of the terms involving Γ_{n+2} can also be justified (see section 3.1). The procedure is to solve this truncated version of the equations for $n = 2$. We would then repeat the procedure for $n = 3$ and higher until the solutions for the lower Green's functions remain stable as we increase n .

The first step then, is to consider the equation for the gluon propagator, Eq. 2.49. In practice it will probably not be possible to go beyond this first equation, because of the increasing complexity of the problem, which in general, requires numerical techniques to find a solution. Moreover, the Schwinger-Dyson equation for the n -point function is in general a multitude of tensor equations. The equation for three point triple gluon vertex for example, can be divided into 14 coupled equations[2.7], and so attempting to treat this equation will need an extraordinary amount of computing power. Nevertheless, by considering this first equation, we might hope to extract some indication as to the low momentum behaviour of the gluon propagator. This in turn may help us understand the non-perturbative aspects of gluons.

Before we do this, however, we must consider the Slavnov-Taylor identities for QCD. These have the same general features as in Eq 2.50, although the situation is complicated by ghost terms. Also, from now on we work in Euclidean space. This is partly because quantum field theories are really only defined in Euclidean space[2.1], with a Wick rotation to Minkowski space to be performed at the end of a calculation. Moreover, in perturbation theory, in order to perform the integrals that arise in higher order corrections, and to isolate their divergent parts, we usually use the technique of 'dimensional regularisation', which again, is really only defined in Euclidean space. The use of Euclidean space also eases the numerical integrations we shall perform in later chapters.

First of all we introduce the full gluon propagator in a covariant gauge:

$$\Delta_{ab}^{\mu\nu} = \left(\frac{\mathcal{G}(p)}{p^2} (\delta^{\mu\nu} - p^\mu p^\nu) + \xi \frac{p^\mu p^\nu}{p^4} \right) \delta_{ab} \quad (2.63)$$

where ξ is our gauge parameter. Here we are working in momentum space. The tensor structure of Eq. 2.63 is determined by the Slavnov-Taylor identity for the gluon propagator which ignoring colour indices reads:

$$p_\mu \Pi^{\mu\nu} = (1/\xi) p^\nu p^2 \quad (2.64)$$

where $\Pi^{\mu\nu}$ is the inverse gluon propagator. This means that the longitudinal part of the full gluon propagator is equal to that of the free propagator, so that the full propagator is an undetermined transverse piece plus the free longitudinal part, as in Eq. 2.63. The full non-perturbative content of the propagator is contained in the gluon renormalisation function $\mathcal{G}(p)$.

The full ghost propagator is simply a scalar function of p^2 :

$$\Delta_{ab}(p) = \delta_{ab} \frac{H(p)}{p^2} \quad (2.65)$$

Finally we decompose the ghost gluon vertex as:

$$\Gamma_{abc}^\mu(p, q, r) = f_{abc} r^\nu \Gamma^{\mu\nu}(p, q, r) \quad (2.66)$$

where r^ν is the anti-ghost incoming momentum, and p is the incoming gluon momentum.

We write the full triple gluon vertex as $\Gamma_{abc}^{\mu\nu\sigma}(p, q, r) = f_{abc} \Gamma^{\mu\nu\sigma}(p, q, r)$. In terms of these quantities the Slavnov-Taylor identity for the full triple gluon vertex reads:

$$q^\nu \Gamma_{\mu\nu\sigma}(p, q, r) = H(q) \left\{ -\frac{1}{\mathcal{G}(r)} (\delta^{\tau\sigma} r^2 - r^\tau r^\sigma) \Gamma_{\tau\mu}(p, q, r) \right. \\ \left. + \frac{1}{\mathcal{G}(p)} (\delta^{\mu\tau} p^2 - p^\mu p^\tau) \Gamma_{\tau\sigma}(r, q, p) \right\} \quad (2.67)$$

This can be solved [2.7] to determine the longitudinal part of $\Gamma_{\mu\nu\sigma}(p, q, r)$ which is free of kinematic singularities, in terms of the ghost-gluon vertex, and the ghost and gluon propagators. From Eq. 2.67 we see that:

$$p^\mu q^\nu \Gamma_{\mu\nu\sigma}(p, q, r) = 0 \quad (2.68)$$

and this, with its cyclic permutations, provides further constraints on the vertex.

Further simplifying approximations can be used if we work in the Landau gauge ($\xi = 0$) [2.9, 1.6]. We can write the full ghost-gluon vertex diagrammatically as in fig. 2.7. This is essentially the Schwinger-Dyson equation for this vertex. It says the full ghost-gluon vertex is equal to the bare one, plus a ghost-gluon scattering kernel. This kernel is proportional to r^μ from the external anti-ghost line, and contains a term $l^\rho \Delta^{\nu\rho}(q-l) = q^\rho \Delta^{\nu\rho}(q-l)$, by using the fact that the gluon propagator is transverse in this gauge. Thus this kernel is proportional to $r^\mu q^\nu$ and so vanishes when one of these external momenta goes to zero. In this limit the full ghost-gluon vertex is equal to the bare one, and we have $\Gamma_{\mu\nu} = \delta_{\mu\nu}$. This considerably simplifies the Slavnov-Taylor identity Eq. 2.67. Again since it is the low momentum behaviour of the theory we wish to determine, we can use this simplification.

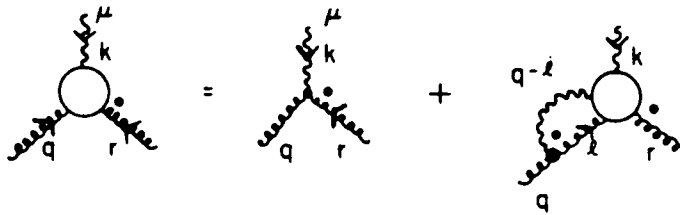


fig. 2.7: Equation for the full ghost-gluon vertex. A wavy line denotes a gluon, a curly line denotes a ghost. The black dots denote an anti-ghost line. The momenta are labelled. Taken from Marciano and Pagels, ref. [1.6].

If we now consider:

$$p^\mu q^\nu \Gamma_{\mu\nu\sigma}(p, q, r) \quad (2.69)$$

we can perform the two contractions in either order. Performing the q^ν contraction first and using the simplified Slavnov-Taylor identity of Eq. 2.67 we obtain the expression:

$$-H(q) \frac{p^\mu}{\mathcal{G}(r)} (r^2 \delta^{\sigma\mu} - r^\mu r^\sigma) \quad (2.70)$$

On the other hand, if we perform them the other way round we obtain the expression:

$$H(p) \frac{q^\nu}{\mathcal{G}(r)} (r^2 \delta^{\sigma\nu} - r^\nu r^\sigma) \quad (2.71)$$

and these two expressions must be equal. Since $p+q+r=0$, we have $p=-q-r$. The tensors in Eqs. 2.70 and 2.71 are transverse, and vanish when contracted with r . Thus the tensor parts are equal, and hence we deduce that $H(p)=H(q)$. Thus the ghost propagator function H is a constant which we set equal to one, its bare value. We therefore obtain the final version of the Slavnov-Taylor identity for the triple gluon vertex:

$$q^\mu \Gamma_{\mu\nu\sigma}(p, q, r) = \frac{1}{\mathcal{G}(p)} (p^2 \delta^{\mu\sigma} - p^\mu p^\sigma) - \frac{1}{\mathcal{G}(r)} (r^2 \delta^{\mu\sigma} - r^\mu r^\sigma) \quad (2.72)$$

This can be ‘solved’ for the longitudinal part of the triple gluon vertex[2.7] to give:

$$\begin{aligned}
 \Gamma_{\mu\nu\sigma}^L(p, q, r) &= \delta_{\mu\nu} \left(\frac{p_\sigma}{\mathcal{G}(p)} - \frac{q_\sigma}{\mathcal{G}(q)} \right) \\
 &+ \delta_{\nu\sigma} \left(\frac{q_\mu}{\mathcal{G}(q)} - \frac{r_\mu}{\mathcal{G}(r)} \right) \\
 &+ \delta_{\sigma\mu} \left(\frac{r_\nu}{\mathcal{G}(r)} - \frac{p_\nu}{\mathcal{G}(p)} \right) \\
 &+ \frac{1}{p^2 - q^2} \left(\frac{1}{\mathcal{G}(p)} - \frac{1}{\mathcal{G}(q)} \right) (p_\nu q_\mu - \delta_{\mu\nu} p \cdot q) (p_\sigma - q_\sigma) \\
 &+ \frac{1}{q^2 - r^2} \left(\frac{1}{\mathcal{G}(q)} - \frac{1}{\mathcal{G}(r)} \right) (q_\sigma r_\nu - \delta_{\nu\sigma} q \cdot r) (q_\mu - r_\mu) \\
 &+ \frac{1}{r^2 - p^2} \left(\frac{1}{\mathcal{G}(r)} - \frac{1}{\mathcal{G}(p)} \right) (r_\mu p_\sigma - \delta_{\mu\sigma} r \cdot p) (r_\nu - p_\nu)
 \end{aligned} \tag{2.73}$$

We shall use this form of the triple gluon vertex in the next chapter.

For completeness we give the Slavnov-Taylor identity for the quark-gluon vertex $\Gamma_{ij}^{\mu a}(q, p, p')$ [2.7]:

$$q^\mu \Gamma_{ij}^{\mu a}(q, p, p') = H(q) \left(\Lambda_{ij}^a(q, p, p') S_F^{-1}(p') - S_F^{-1}(p) \Lambda_{ij}^a(q, p, p') \right) \tag{2.74}$$

where $\Lambda_{ij}^a(q, p, p')$ is a ghost-quark scattering kernel, similar in form to the ghost-gluon scattering kernel in fig. 2.7. As before, it can be shown that as the external momenta go to zero, that $\Lambda_{ij}^a(q, p, p')$ behaves like T_{ij}^a , the bare kernel[2.9]. This is simply the colour matrix of $\Gamma_{ij}^{\mu a} = T_{ij}^a \Gamma^\mu$, and so using this low momentum approximation the Slavnov-Taylor identity of Eq. 2.74 reduces to an Abelian-like Ward identity to give:

$$q_\mu \Gamma^\mu(q, p, p') = S_F^{-1}(p') - S_F^{-1}(p) \tag{2.75}$$

For massless quarks we have $S_F(p) = \mathcal{F}(p)/\not{p}$, and the identity of Eq. 2.75 can be solved for the longitudinal part of the vertex[2.7], to give:

$$\begin{aligned} \Gamma_L^\mu(q, p, p') &= \frac{1}{2} \left(\frac{1}{\mathcal{F}(p)} + \frac{1}{\mathcal{F}(p')} \right) \gamma^\mu \\ &+ \frac{1}{2} (\not{p} + \not{p}') (p'^\mu + p^\mu) \left(\frac{1}{\mathcal{F}(p)} - \frac{1}{\mathcal{F}(p')} \right) \frac{1}{p^2 - p'^2} \end{aligned} \quad (2.76)$$

This form of the quark-gluon vertex will be used in chapters five and six.

2.6 The Perturbative Gluon and Quark Propagators

Our first study will be to examine the Schwinger-Dyson equation for the gluon propagator. This will constitute the work of the next two chapters. Before we do this, we give the one-loop perturbative calculation of the gluon propagator.

In perturbation theory it is usual to perform the calculation in $n = 4 - 2\epsilon$ space-time dimensions. The divergences which occur at the large momentum end of the loop integrals, now appear as poles in ϵ , diverging when $\epsilon \rightarrow 0$, or $n \rightarrow 4$.

For the pure gauge theory there are the same one-loop diagrams as those fig. 2.6, but now with all propagators and vertices being bare. In n dimensions the ‘tadpole’ diagram vanishes, and we are left with just the ghost and gluon loops.

Here we just give the results of this calculation[1.6,2.1]. The gluon loops contribute a self-energy correction:

$$\begin{aligned} \Sigma_{\text{gluon}}^{\mu\nu} &= \frac{g^2(\mu)C_A}{32\pi^2} \left(\left(\frac{25}{6} - \xi \right) \left(\frac{1}{\epsilon} - \gamma_E + \ln \frac{4\pi\mu^2}{p^2} \right) + \frac{89}{18} + \xi + \frac{\xi^2}{2} \right) p^2 \delta^{\mu\nu} \\ &- \frac{g^2(\mu)C_A}{32\pi^2} \left(\left(\frac{14}{3} - \xi \right) \left(\frac{1}{\epsilon} - \gamma_E + \ln \frac{4\pi\mu^2}{p^2} \right) + \frac{107}{18} + \xi + \frac{\xi^2}{2} \right) p^\mu p^\nu \end{aligned} \quad (2.77)$$

where C_A is the relevant group Casimir, equal to N for an $SU(N)$ gauge theory, γ_E is the Euler-Mascheroni constant and μ^2 is an arbitrary momentum scale needed to define the integrals in n dimensions. $g(\mu)$ is the running coupling introduced in section 1.4. From the ghost loop we get a correction:

$$\begin{aligned}\Sigma_{\text{ghost}}^{\mu\nu} &= \frac{g^2(\mu)C_A}{32\pi^2} \left(\frac{1}{6} \left(\frac{1}{\varepsilon} - \gamma_E + \ln \frac{4\pi\mu^2}{p^2} \right) + \frac{4}{9} \right) p^2 \delta^{\mu\nu} \\ &+ \frac{g^2(\mu)C_A}{32\pi^2} \left(\frac{1}{3} \left(\frac{1}{\varepsilon} - \gamma_E + \ln \frac{4\pi\mu^2}{p^2} \right) + \frac{5}{9} \right) p^\mu p^\nu\end{aligned}\quad (2.78)$$

Adding these together gives

$$\Sigma^{\mu\nu} = \frac{g^2(\mu)C_A}{32\pi^2} \left(\left(\frac{13}{3} - \xi \right) \left(\frac{1}{\varepsilon} - \gamma_E + \ln \frac{4\pi\mu^2}{p^2} \right) + \frac{97}{18} + \xi + \frac{\xi^2}{2} \right) (p^2 \delta^{\mu\nu} - p^\mu p^\nu)\quad (2.79)$$

Note that this correction is transverse, and so the Slavnov-Taylor identity for the gluon propagator Eq. 2.64 holds. Essentially this identity states that the longitudinal part will not get renormalised by higher order corrections, and we see that this is indeed the case.

Although the ghost corrections are essential in preserving the transversality of the higher order corrections to the propagator, we see that for ‘sensible’ gauges, such as $\xi = 0$, they make a *numerically* small contribution of less than 10%. This provides further support for our neglect of the ghost terms in section 2.5.

Renormalisation consists of subtracting the poles in ε . We use the $\overline{\text{MS}}$ scheme which also subtracts the γ_E and $\ln 4\pi$ factors, to give the renormalised self-energy

$$\Sigma^{\mu\nu}(p) = \frac{g^2 C_A}{32\pi^2} \left(\left(\frac{13}{3} - \xi \right) \ln \frac{\mu^2}{p^2} + \frac{97}{18} + \xi + \frac{\xi^2}{2} \right)\quad (2.80)$$

Since we have:

$$\Delta^{\mu\nu}(p) = \Delta_0^{\mu\nu}(p) - \Sigma^{\mu\nu}\quad (2.81)$$

we can invert this to extract:

$$\mathcal{G}(p) = 1 + \frac{g^2(\mu)C_A}{32\pi^2} \left(\left(\frac{13}{3} - \xi \right) \ln \frac{\mu^2}{p^2} + \frac{97}{18} + \xi + \frac{\xi^2}{2} \right) \quad (2.82)$$

For large p^2 we must use the renormalisation group techniques detailed in section 1.4 to eliminate the large logarithms of Eq. 2.82 and obtain for large momenta:

$$\mathcal{G}(p) \approx \mathcal{G}(\mu) \left(\frac{g^2(p)}{g^2(\mu)} \right)^{\gamma_0/\beta_0} \approx \left(\frac{1}{1 + \frac{g^2(\mu)\beta_0}{16\pi} \ln p^2/\mu^2} \right)^{\gamma_0/\beta_0} \quad (2.83)$$

where $g(p)$ is the renormalised running coupling of Eq. 1.22, and $\beta_0 = (11/3)C_A$. Here γ_0 is extracted from Eq. 2.82 and is equal to $(13/6 - \xi/2)C_A$. To define our renormalisation completely, we choose a value for μ^2 and specify the value of $\mathcal{G}(\mu)$

For large momenta, we see from Eq. 2.83 that $\mathcal{G}(p)$ is only logarithmically different from 1, and so the propagator behaves as if the gluon were almost 'free'. This is what we observe in high energy collisions. In the next two chapters we will see that in the non-perturbative regime at low momenta, we find a startlingly different behaviour for $\mathcal{G}(p)$.

Once again, for completeness we give the one-loop perturbative results for the quark propagator, where in the same $\overline{\text{MS}}$ scheme the fermion propagator function $\mathcal{F}(p)$ is given by:

$$\mathcal{F}(p) = 1 + \frac{g^2(\mu)C_F}{16\pi^2} \xi \left(\ln \frac{\mu^2}{p^2} + 2 - \frac{1}{\xi} \right) \quad (2.84)$$

where C_F is the quark Casimir, equal to $(N^2 - 1)/2N$. Once again these potentially large logarithms can be summed for large p^2 to give:

$$\mathcal{F}(p) = \mathcal{F}(\mu) \left(\frac{g^2(p)}{g^2(\mu)} \right)^{\gamma_0^f/\beta_0} \quad (2.85)$$

where $\gamma_0^g = \xi C_F$.

The introduction of quarks introduces a closed fermion loop in the calculation for the gluon propagator. This merely changes the form of γ_0 to $(13/6 - \xi/2)C_A - (4/3)n_f T_F$, and changes β_0 to $(11/3)C_A - (4/3)n_f T_F$ in Eq. 2.83. Here T_F is a colour trace, with $T_F = 1/2$ for QCD.

We now return to a world without quarks, and attempt to solve the truncated Schwinger-Dyson equation for the gluon propagator, using the approximations outlined in section 2.5.

CHAPTER THREE

THE GLUON EQUATION

3.1 Derivation of the Equation for $\mathcal{G}(p)$

We now proceed to derive a closed equation for the gluon renormalisation function $\mathcal{G}(p)$, following the procedure outlined in section 2.5[3.1]. The complete Schwinger-Dyson equation for the inverse gluon propagator, depicted in fig. 2.6 involves the unknown triple and quartic gluon vertices, as well as the ghost contributions. In order to derive a closed equation for the gluon renormalisation function we must make some approximations.

The first step is to ignore those diagrams which involve quartic gluon couplings, (see section 2.5). This can be seen as a first step in an iterative procedure to solve the entire hierarchy of the Schwinger-Dyson equations. Perhaps more realistically, we note that these diagrams contain an explicit factor of α_0^2 , where $\alpha_0 = g_0^2/4\pi$ is the bare coupling. When we come to renormalise our equation (see section 3.3), we will do this at some scale μ^2 , which we will choose to be in the perturbative regime. The bare couplings which appear in the unrenormalised equation will be replaced by the renormalised running coupling $\alpha(\mu)$, which, since μ^2 is in the perturbative region, will be a small number. Hence these diagrams involving the quartic couplings will be suppressed by a factor $\alpha(\mu)$ relative to the remaining terms. Of course, the value of the loop integral could swamp this suppression, but it seems natural to believe that the triple gluon vertex already contains the seeds, if not all the details, of a confining mechanism.

Next we consider the ghost diagram. Since we choose to work in the Landau gauge, then as was seen in section 2.5, it is believed that the ghost kernels which appear in the Slavnov-Taylor identities for both the triple gluon vertex, and the quark-gluon vertex, will vanish as one of the external momenta

goes to zero. Although the ghost contributions are essential in preserving the transversality of the inverse gluon propagator, it is to be hoped that they will not play a significant role in the analytic behaviour of $\mathcal{G}(p)$. This is supported by the fact that in a one-loop perturbative calculation, the ghost loop (see section 2.6) makes a *numerically* small contribution to $\mathcal{G}(p)$, at least for the Landau, and other ‘sensible’ gauges.

Our equation still involves the full triple gluon vertex. In the light of the above comments on the infra-red vanishing of the ghost kernels, by setting them identically to zero, we can ‘solve’ the Slavnov-Taylor identity for this vertex entirely in terms of $\mathcal{G}(p)$. This was done in section 2.5. This allows us to completely determine the longitudinal part of the vertex; the Slavnov-Taylor identity does not constrain any transverse part. Fortunately it can be shown, Eq. 2.61, that as one of the external momenta of the vertex goes to zero, then the transverse part vanishes. In QCD it is precisely the low momentum behaviour which cannot be determined by perturbation theory, and it is in this region that our various approximations made are likely to be valid. Thus we set the full triple gluon vertex equal to its longitudinal part, determined in terms of \mathcal{G} from the Slavnov-Taylor identity in the absence of ghosts.

At this stage we do not include the contributions of quarks, which would contribute a quark loop diagram to our equation. If this were included, we would have to consider the Schwinger-Dyson equation for the fermions as well. This problem is addressed in chapters five and six. For the moment we consider only the pure gauge theory, as we expect that it is the non-Abelian nature of the gauge part of the theory which is responsible for confinement.

After all these approximations, we have managed to derive a closed equation for the gluon function $\mathcal{G}(p)$:

$$\Pi_{ab}^{\mu\nu} = \Pi_{0ab}^{\mu\nu} - \Sigma_{ab}^{\mu\nu} \quad (3.1)$$

Here Π represents the full inverse gluon propagator, Π_0 the bare one, and Σ is the contribution to the gluon self-energy from the equation depicted diagrammatically in fig. 2.6, neglecting the ghost and two-loop terms. The colour indices of Eq. 3.1 are given on both sides by δ^{ab} , and we factor this out. We project with the tensor

$$P^{\mu\nu} = \frac{1}{3p^2} \left(4p^\mu p^\nu - p^2 \delta^{\mu\nu} \right) \quad (3.2)$$

to give a scalar equation. This tensor gives zero when contracted with $\delta^{\mu\nu}$, and gives 1 when contracted with $p^\mu p^\nu$. The contribution of the tadpole diagram in fig. 2.6 is as usual proportional to $\delta^{\mu\nu}$ and so this contribution vanishes. Thus the only diagram contributing to the self-energy is the gluon loop diagram shown in fig. 3.1 which we now calculate.

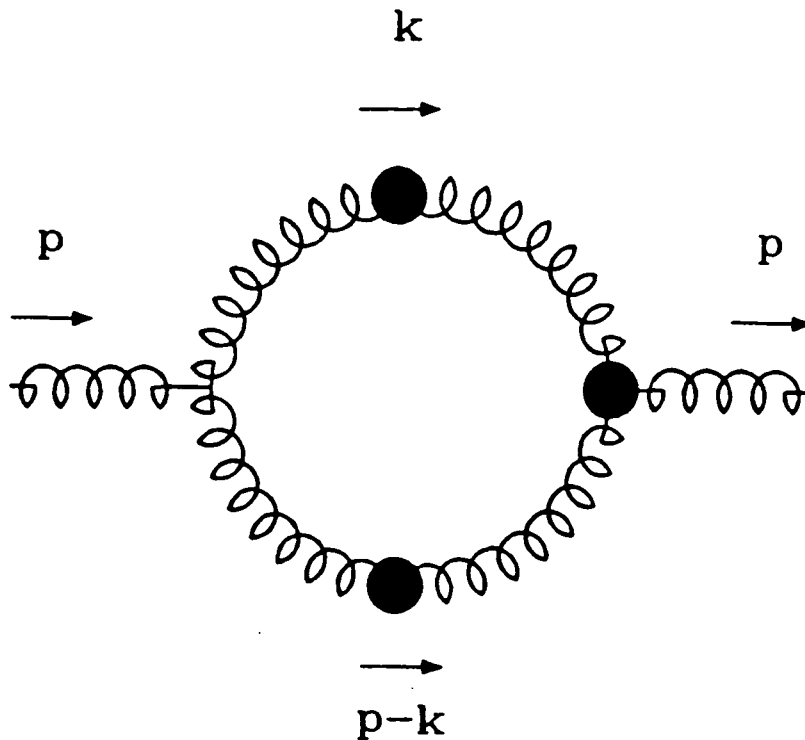


fig. 3.1: The gluon loop contributing to the truncated Schwinger-Dyson equation for the inverse gluon propagator.

3.2 The Gluon Loop

We can write out our equation as:

$$\frac{1}{\mathcal{G}(p)} = 1 + \frac{g_0^2 C_A}{32\pi^4 p^2} P_{\mu\nu} \int d^4 k \Gamma_0^{\mu\alpha\delta}(-p, k, q) \Delta_{\alpha\beta}(k) \Delta_{\gamma\delta}(q) \Gamma_L^{\beta\nu\gamma}(-k, p, -q) \quad (3.3)$$

where $\Gamma_0^{\mu\alpha\delta}(-p, k, q)$ is the bare triple gluon vertex, and $\Gamma_L^{\beta\nu\gamma}(-k, p, -q)$ is the longitudinal part of the full triple gluon vertex, which we take to be given by Eq. 2.73. The momenta are as labelled in fig. 3.1. Working in the Landau gauge, the full gluon propagator is given by:

$$\Delta^{\mu\nu} = \frac{\mathcal{G}(p)}{p^2} \left(\frac{p^2 \delta^{\mu\nu} - p^\mu p^\nu}{p^2} \right) \quad (3.4)$$

We write the integrand in Eq. 3.3 as $\mathcal{G}(k)\mathcal{G}(q)I^{\mu\nu}/k^2q^2$, with:

$$I^{\mu\nu} = I_1^{\mu\nu} - \frac{I_2^{\mu\nu}}{k^2} - \frac{I_3^{\mu\nu}}{q^2} + \frac{I_4^{\mu\nu}}{k^2q^2} \quad (3.5)$$

where:

$$\begin{aligned} I_1^{\mu\nu} &= \Gamma_0^{\mu\alpha\delta}(-p, k, q) \delta_{\alpha\beta} \delta_{\gamma\delta} \Gamma_L^{\beta\nu\gamma}(-k, p, -q) \\ I_2^{\mu\nu} &= \Gamma_0^{\mu\alpha\delta}(-p, k, q) k_\alpha k_\beta \delta_{\gamma\delta} \Gamma_L^{\beta\nu\gamma}(-k, p, -q) \\ I_3^{\mu\nu} &= \Gamma_0^{\mu\alpha\delta}(-p, k, q) \delta_{\alpha\beta} q_\gamma q_\delta \Gamma_L^{\beta\nu\gamma}(-k, p, -q) \\ I_4^{\mu\nu} &= \Gamma_0^{\mu\alpha\delta}(-p, k, q) k_\alpha k_\beta q_\gamma q_\delta \Gamma_L^{\beta\nu\gamma}(-k, p, -q) \end{aligned} \quad (3.6)$$

We can now use the Slavnov-Taylor identities in the absence of ghost contributions:

$$\begin{aligned} q_\nu \Gamma_0^{\mu\nu\sigma}(p, q, r) &= (p^2 \delta^{\mu\nu} - p^\mu p^\nu) - (r^2 \delta^{\mu\nu} - r^\mu r^\nu) \\ q_\nu \Gamma_L^{\mu\nu\sigma}(p, q, r) &= \frac{(p^2 \delta^{\mu\nu} - p^\mu p^\nu)}{\mathcal{G}(p)} - \frac{(r^2 \delta^{\mu\nu} - r^\mu r^\nu)}{\mathcal{G}(r)} \end{aligned} \quad (3.7)$$

which are satisfied by the vertices in Eq. 3.3 (see Eq. 2.72), to simplify some of the expressions in Eq. 3.6. Some easy tensor algebra gives:

$$\begin{aligned}
 I_2^{\mu\nu} &= \frac{1}{\mathcal{G}(q)} q^2 (q^2 \delta^{\mu\nu} - q^\mu q^\nu) + \frac{1}{\mathcal{G}(p)} p^2 (p^2 \delta^{\mu\nu} - p^\mu p^\nu) \\
 &\quad - \frac{1}{\mathcal{G}(q)} (p^2 q^2 \delta^{\mu\nu} - p^2 q^\mu q^\nu - q^2 p^\mu p^\nu + p \cdot q p^\mu q^\nu) \\
 &\quad - \frac{1}{\mathcal{G}(p)} (p^2 q^2 \delta^{\mu\nu} - p^2 q^\mu q^\nu - q^2 p^\mu p^\nu + p \cdot q p^\nu q^\mu)
 \end{aligned} \tag{3.8}$$

$I_3^{\mu\nu}$ is identical to $I_2^{\mu\nu}$, but with k and q interchanged. We also have:

$$I_4^{\mu\nu} = \frac{1}{\mathcal{G}(p)} (p^4 k^\mu k^\nu - p^2 p \cdot k (p^\mu k^\nu + k^\mu p^\nu) + (p \cdot k)^2 p^\mu p^\nu) \tag{3.9}$$

$I_1^{\mu\nu}$ is more complicated. After performing the Lorentz contractions in Eq. 3.6 it is equal to $\Gamma_{0\beta\gamma}^\mu(-p, k, q) \Gamma_L^{\beta\nu\gamma}(-k, p, -q)$, which from Eqs. 2.73 and 2.41 we write as:

$$\begin{aligned}
 &\left((-p-k)_\gamma \delta^\mu_\beta + (2k-p)^\mu \delta_{\beta\gamma} + (2p-k)_\beta \delta^\mu_\gamma \right) \times \\
 &\left[\frac{1}{\mathcal{G}(k)} (k^\nu \delta^{\beta\gamma} - k^\gamma \delta^{\beta\nu}) + \frac{1}{\mathcal{G}(p)} (p^\beta \delta^{\nu\gamma} - p^\gamma \delta^{\nu\beta}) \right. \\
 &\quad \left. + \frac{1}{\mathcal{G}(q)} (q^\beta \delta^{\nu\gamma} - q^\nu \delta^{\beta\gamma}) \right. \\
 &\quad \left. + (p \cdot k \delta^{\beta\nu} - p^\beta k^\nu) (-p-k)^\gamma \frac{1}{k^2 - p^2} \left(\frac{1}{\mathcal{G}(k)} - \frac{1}{\mathcal{G}(p)} \right) \right. \\
 &\quad \left. + (p \cdot q \delta^{\nu\gamma} - p^\gamma q^\nu) (p+q)^\beta \frac{1}{p^2 - q^2} \left(\frac{1}{\mathcal{G}(p)} - \frac{1}{\mathcal{G}(q)} \right) \right. \\
 &\quad \left. + (k \cdot q \delta^{\beta\gamma} - k^\gamma q^\beta) (k-q)^\nu \frac{1}{q^2 - k^2} \left(\frac{1}{\mathcal{G}(q)} - \frac{1}{\mathcal{G}(k)} \right) \right]
 \end{aligned} \tag{3.10}$$

After performing the Lorentz contractions we obtain:

$$\begin{aligned}
 I_1^{\mu\nu} &= \frac{3}{\mathcal{G}(p)}(p^2\delta^{\mu\nu} - p^\mu p^\nu) \\
 &+ \frac{1}{\mathcal{G}(k)}\left((k^2 + p \cdot k)\delta^{\mu\nu} - 2p^\mu k^\nu - 2k^\mu p^\nu + 5k^\mu k^\nu\right) \\
 &+ \frac{1}{\mathcal{G}(q)}\left((q^2 + p \cdot q)\delta^{\mu\nu} - 2p^\mu q^\nu - 2q^\mu p^\nu + 5q^\mu q^\nu\right) \\
 &+ \frac{1}{k^2 - p^2}\left(\frac{1}{\mathcal{G}(k)} - \frac{1}{\mathcal{G}(p)}\right)\left(\delta^{\mu\nu}(p+k)^2 p \cdot k + 4p^2 k^\mu k^\nu \right. \\
 &\quad \left. - p \cdot k p^\mu p^\nu - (k^2 + 2p \cdot k)p^\mu k^\nu - 4p \cdot k k^\mu p^\nu\right) \\
 &+ \frac{1}{p^2 - q^2}\left(\frac{1}{\mathcal{G}(p)} - \frac{1}{\mathcal{G}(q)}\right)\left(\delta^{\mu\nu}(p+q)^2 p \cdot q + 4p^2 q^\mu q^\nu \right. \\
 &\quad \left. - p \cdot q p^\mu p^\nu - (q^2 + 2p \cdot q)p^\mu q^\nu - 4p \cdot q q^\mu p^\nu\right) \\
 &+ \frac{1}{q^2 - k^2}\left(\frac{1}{\mathcal{G}(q)} - \frac{1}{\mathcal{G}(k)}\right)(k-q)^\nu\left((2q^2 - k \cdot q)k^\mu + (k \cdot q - 2k^2)q^\mu\right)
 \end{aligned} \tag{3.11}$$

Note that the integrand is symmetric between k and q , as it should be. Using this symmetry, we can replace $I_3^{\mu\nu}/q^2$ with $I_2^{\mu\nu}/k^2$, and we can also simplify $I_1^{\mu\nu}$, writing it as:

$$\begin{aligned}
 I_1^{\mu\nu} &= \frac{3}{\mathcal{G}(p)}(p^2\delta^{\mu\nu} - p^\mu p^\nu) \\
 &+ \frac{2}{\mathcal{G}(q)}\left((q^2 + p \cdot q)\delta^{\mu\nu} - 2p^\mu q^\nu - 2q^\mu p^\nu + 5q^\mu q^\nu\right) \\
 &+ \frac{2}{p^2 - q^2}\left(\frac{1}{\mathcal{G}(p)} - \frac{1}{\mathcal{G}(q)}\right)\left(\delta^{\mu\nu}(p+q)^2 p \cdot q + 4p^2 q^\mu q^\nu \right. \\
 &\quad \left. - p \cdot q p^\mu p^\nu - (q^2 + 2p \cdot q)p^\mu q^\nu - 4p \cdot q q^\mu p^\nu\right) \\
 &+ \frac{1}{q^2 - k^2}\left(\frac{1}{\mathcal{G}(q)} - \frac{1}{\mathcal{G}(k)}\right)(k-q)^\nu\left((2q^2 - k \cdot q)k^\mu + (k \cdot q - 2k^2)q^\mu\right)
 \end{aligned} \tag{3.12}$$

Projecting with the tensor $P^{\mu\nu}$, Eq. 3.2, we obtain:

$$I_4^{\mu\nu} P_{\mu\nu} = \frac{1}{3\mathcal{G}(p)}(p^2(p \cdot k)^2 - k^2 p^4) \tag{3.13}$$

Next we have:

$$\begin{aligned}
 I_2^{\mu\nu} P_{\mu\nu} &= \frac{4}{3\mathcal{G}(q)} \frac{q^2}{p^2} (q^2 p^2 - (p \cdot q)^2) - \frac{q^4}{\mathcal{G}(q)} - \frac{p^4}{\mathcal{G}(p)} \\
 &+ \frac{1}{3\mathcal{G}(q)} (2p^2 q^2 + (p \cdot q)^2) + \frac{1}{3\mathcal{G}(p)} (2p^2 q^2 + (p \cdot q)^2) \\
 &= \frac{1}{3\mathcal{G}(p)} (2p^2 k^2 - 6p^2 p \cdot k + (p \cdot k)^2) \\
 &+ \frac{1}{3\mathcal{G}(q)} \frac{1}{p^2} (8(p \cdot k)^3 - 3p^2 (p \cdot k)^2 - 4k^2 (k \cdot p)^2 + p^2 k^4 - 2p^2 k^2 p \cdot k)
 \end{aligned} \tag{3.14}$$

Finally we split $I_1^{\mu\nu}$ into four terms:

$$P_{\mu\nu} \frac{3}{\mathcal{G}(p)} (p^2 \delta^{\mu\nu} - p^\mu p^\nu) = -\frac{3p^2}{\mathcal{G}(p)}$$

$$\begin{aligned}
 P_{\mu\nu} \frac{2}{\mathcal{G}(q)} &\left((q^2 + p \cdot q) \delta^{\mu\nu} - 2p^\mu q^\nu - 2q^\mu p^\nu + 5q^\mu q^\nu \right) \\
 &= \frac{2}{3\mathcal{G}(q)} \left(-12p \cdot q + 20 \frac{(p \cdot q)^2}{p^2} - 5q^2 \right) \\
 &= \frac{2}{3\mathcal{G}(q)} \left(3p^2 - 18p \cdot k + 20 \frac{(p \cdot k)^2}{p^2} - 5k^2 \right)
 \end{aligned}$$

$$\begin{aligned}
 P_{\mu\nu} \frac{2}{p^2 - q^2} &\left(\frac{1}{\mathcal{G}(p)} - \frac{1}{\mathcal{G}(q)} \right) \left(\delta^{\mu\nu} (p+q)^2 p \cdot q + 4p^2 q^\mu q^\nu \right. \\
 &\left. - p \cdot q p^\mu p^\nu - (q^2 + 2p \cdot q) p^\mu q^\nu - 4p \cdot q q^\mu p^\nu \right) \\
 &= \frac{2}{p^2 - q^2} \left(\frac{1}{\mathcal{G}(p)} - \frac{1}{\mathcal{G}(q)} \right) \frac{1}{3} \left(-2(p \cdot q)^2 - 3q^2 p \cdot q - 3p^2 p \cdot q - 4p^2 q^2 \right) \\
 &= \frac{2}{3} \frac{1}{p^2 - q^2} \left(\frac{1}{\mathcal{G}(p)} - \frac{1}{\mathcal{G}(q)} \right) \left(-12p^4 + 24p^2 p \cdot k + 3k^2 p \cdot k \right. \\
 &\quad \left. - 7k^2 p^2 - 8(p \cdot k)^2 \right)
 \end{aligned}$$

$$\begin{aligned}
 P_{\mu\nu} & \frac{1}{q^2 - k^2} \left(\frac{1}{\mathcal{G}(q)} - \frac{1}{\mathcal{G}(k)} \right) (k - q)^\nu \left((2q^2 - k \cdot q)k^\mu + (k \cdot q - 2k^2)q^\mu \right) \\
 & = \frac{1}{q^2 - k^2} \left(\frac{1}{\mathcal{G}(q)} - \frac{1}{\mathcal{G}(k)} \right) \frac{1}{3} \left[(2q^2 - k \cdot q) \times \right. \\
 & \quad \left(\frac{4(p \cdot k)^2}{p^2} - k^2 - \frac{4(p \cdot k)(p \cdot q)}{p^2} + k \cdot q \right) \\
 & \quad \left. + (k \cdot q - 2k^2) \left(\frac{4(p \cdot k)(p \cdot q)}{p^2} - k \cdot q - \frac{4(p \cdot q)^2}{p^2} + q^2 \right) \right] \\
 & = \frac{1}{q^2 - k^2} \left(\frac{1}{\mathcal{G}(q)} - \frac{1}{\mathcal{G}(k)} \right) \frac{1}{3} \left(48 \frac{k^2(p \cdot k)^2}{p^2} - 24k^2 p \cdot k \right. \\
 & \quad \left. - 48 \frac{(p \cdot k)^3}{p^2} + 40(p \cdot k)^2 - 12k^4 - 9p^2 p \cdot k + 5k^2 p^2 \right)
 \end{aligned} \tag{3.15}$$

Putting all this together allows us to write the equation for $\mathcal{G}(p)$ as follows:

$$\begin{aligned}
 \frac{1}{\mathcal{G}(p)} & = 1 + \frac{C_A g_0^2}{96\pi^4 p^2} \int d^4 k \left(\frac{\mathcal{G}(k)A(k, p)}{k^4 q^2 p^2} + \frac{\mathcal{G}(k)\mathcal{G}(q) B(k, p)}{\mathcal{G}(p) k^4 q^4} \right. \\
 & \quad \left. + \frac{\mathcal{G}(q) - \mathcal{G}(p)}{q^2 - p^2} \frac{C(k, p)}{k^2 q^2} \frac{\mathcal{G}(k)}{\mathcal{G}(p)} + \frac{\mathcal{G}(q) - \mathcal{G}(k)}{q^2 - k^2} \frac{D(k, p)}{k^2 q^2 p^2} \right)
 \end{aligned} \tag{3.16}$$

where

$$\begin{aligned}
 A(k, p) & = 48k^2(p \cdot k)^2 - 32k^2 p^2 p \cdot k - 16(p \cdot k)^3 - 12k^4 p^2 \\
 & \quad + 6k^2 p^4 + 6p^2(p \cdot k)^2 \\
 B(k, p) & = 38k^2 p^2 p \cdot k - 25p^2(p \cdot k)^2 - 14k^2 p^4 + 12p^4 p \cdot k \\
 & \quad - 13k^4 p^2 - 2k^2(p \cdot k)^2 + 4(p \cdot k)^3 \\
 C(k, p) & = 24p^4 + 14k^2 p^2 + 16(p \cdot k)^2 - 48p^2 p \cdot k - 6k^2 p \cdot k \\
 D(k, p) & = 12k^4 p^2 - 48k^2(p \cdot k)^2 + 48(p \cdot k)^3 + 24k^2 p^2 p \cdot k \\
 & \quad - 5k^2 p^4 - 40p^2(p \cdot k)^2 + 9p^4 p \cdot k
 \end{aligned} \tag{3.17}$$

This is the equation we have to solve. As it stands, however, the integrals have ultraviolet logarithmic divergences, as well as potential infra-red divergences. These must be dealt with to give us a finite renormalised equation.

3.3 Renormalisation

As we shall later argue, the only possible consistent behaviour for $\mathcal{G}(p)$ as $p^2 \rightarrow 0$ is $\mathcal{G}(p) \sim 1/p^2$. If $\mathcal{G}(p)$ is this singular, however, the integrals in Eq. 3.16 are potentially infra-red divergent. In a related study in the axial gauge[3.2], such divergences are avoided by assuming that: (i) the full axial gauge propagator has the same tensor structure as the bare one, and (ii) that the coefficient of such an infra-red enhanced term is independent of the choice of axial gauge. It is possible that if we could solve the complete Schwinger-Dyson equation with no approximations or truncations, then such a term would not give rise to divergences. Nevertheless, as they do appear in our truncation, we must deal with them. We choose to treat them by defining $\mathcal{G}(p)$ by a ‘plus’ prescription, which we define later in section 3.5. Of course, this prescription is not determined by the theory, but put in ‘by hand’. In chapter five, and in other work[3.3], different treatments are used, but the justification here will lie in the physically meaningful results we obtain. One of the long term goals of any analysis based upon the Schwinger-Dyson equations will be to eliminate these infra-red divergences in a self-consistent way, entirely within the context of the theory. A fuller discussion of this and other infra-red problems appears in chapter seven.

Even when we have dealt with these divergences, we still obtain contributions violating the masslessness of the gluon, a condition demanded by gauge invariance. If $\mathcal{G}(p)$ has such an infra-red singular term, on dimensional grounds it must be $A\mu^2/p^2$. Even after integration, the dimensionful quantity μ^2 must be balanced, and the only quantity available is p^2 . Thus we get contributions

to the right hand side of Eq. 3.16 which behave like $1/p^2$. The condition for masslessness is:

$$\lim_{p^2 \rightarrow 0} p^2 \Pi^{\mu\nu} = 0 \quad (3.18)$$

where $\Pi^{\mu\nu}$ is the full inverse gluon propagator. Since the bare inverse gluon propagator obeys the condition Eq. 3.18, then all our integrals on the right hand side of Eq. 3.16, must obey this as well. This is clearly not true of some of the terms which arise from integration of the infra-red enhanced term. We must perform a subtraction to remove these terms. Formally, we may imagine some appropriate counter-terms in the bare Lagrangian to achieve this

The easiest way to preserve masslessness is to write $\mathcal{G}(p) = A\mu^2/p^2 + \mathcal{G}_1(p)$, where $p^2\mathcal{G}_1(p) \rightarrow 0$ as $p^2 \rightarrow 0$. The entire contribution to the mass term comes from the enhanced term $A\mu^2/p^2$. Thus if in the right hand side of Eq. 3.16 we set $\mathcal{G}(p) \equiv A\mu^2/p^2$ and subtract this from Eq. 3.16, then no mass term will arise. Note that if the mass term should be equal to zero, then the term subtracted will vanish as well. This mass renormalisation, and the ‘plus’ prescription treatment of the infra-red divergences do not prejudge that $\mathcal{G}(p)$ does possess such an infra-red enhanced term, as we allow the possibility that the coefficient of this term can vanish. Finally, any terms on the right hand side of Eq. 3.16 which are linear in \mathcal{G} will have the entire contribution of the enhanced term subtracted by this mass renormalisation. In these terms we can effectively set $\mathcal{G} \equiv \mathcal{G}_1$.

We still have the usual logarithmic ultraviolet divergences, which arise from the momentum loop integral at large k^2 . To handle these we cast Eq. 3.16 into the form:

$$\frac{1}{\mathcal{G}(p)} = \frac{C_{A\alpha_0}}{24\pi^3} \int d^4k \mathcal{K}(k, p) + \frac{C_{A\alpha_0}}{24\pi^3 \mathcal{G}(p)} \int d^4k \mathcal{G}(k) \mathcal{L}(k, p) \quad (3.19)$$

where:

$$\begin{aligned}\mathcal{K}(k,p) &= \frac{\mathcal{G}(k)A(k,p)}{k^4 q^2 p^4} + \frac{\mathcal{G}(q) - \mathcal{G}(k)}{q^2 - k^2} \frac{D(k,p)}{k^2 q^2 p^4} - \frac{\mathcal{G}(k)C(k,p)}{(q^2 + \mu^2)k^2 q^2 p^2} \\ \mathcal{L}(k,p) &= \frac{\mathcal{G}(q)B(k,p)}{k^4 q^4 p^2} + \frac{C(k,p)}{q^2 - p^2} \left[\mathcal{G}(q) - \mathcal{G}(p) \left(\frac{p^2 + \mu^2}{q^2 + \mu^2} \right) \right] \frac{1}{k^2 q^2 p^2}\end{aligned}\tag{3.20}$$

Here $\mathcal{K}(k,p)$ contains those terms which are linear in \mathcal{G} , whereas $\mathcal{L}(k,p)$ contains those terms which are quadratic in \mathcal{G} in the numerator, with an explicit $1/\mathcal{G}(p)$ in the denominator.

In splitting the integral into these two terms, there is a slight technicality over the term proportional to $C(k,p)$, which involves the factor $(\mathcal{G}(k)/\mathcal{G}(p))(\mathcal{G}(q) - \mathcal{G}(p))/(q^2 - p^2)$. This term contains a part which belongs to $\mathcal{K}(k,p)$ and a part belonging to $\mathcal{L}(k,p)$. These will be renormalised differently, and so we must be careful not to introduce any singularities from the $q^2 - p^2$ term in the denominator. This is done by writing:

$$\begin{aligned}\frac{\mathcal{G}(k)}{\mathcal{G}(p)} \frac{\mathcal{G}(q) - \mathcal{G}(p)}{q^2 - p^2} &= \frac{\mathcal{G}(k)}{\mathcal{G}(p)} \frac{\mathcal{G}(q)}{q^2 - p^2} \left(1 - \frac{\mathcal{G}(p)}{\mathcal{G}(q)} \frac{p^2 + \mu^2}{q^2 + \mu^2} \right) \\ &\quad - \frac{\mathcal{G}(k)}{\mathcal{G}(p)} \frac{\mathcal{G}(p)}{q^2 - p^2} \left(1 - \frac{p^2 + \mu^2}{q^2 + \mu^2} \right) \\ &= \frac{1}{q^2 - p^2} \frac{\mathcal{G}(k)}{\mathcal{G}(p)} \left(\mathcal{G}(q) - \mathcal{G}(p) \frac{p^2 + \mu^2}{q^2 + \mu^2} \right) - \frac{\mathcal{G}(k)}{q^2 + \mu^2}\end{aligned}\tag{3.21}$$

Here we call the first term part of $\mathcal{L}(k,p)$ and the second term part of $\mathcal{K}(k,p)$. All we have done is to add and subtract a term which ensures both parts are individually finite at $p^2 = q^2$. This term is obviously arbitrary, but we have chosen it so that it does not introduce any extra ultraviolet divergences, being finite by power counting. The momentum μ^2 in Eq. 3.21 is also arbitrary, but for convenience we choose it equal to our renormalisation scale.

Returning to Eq. 3.20, we define a renormalised gluon function $\mathcal{G}_R(p)$ via:

$$\mathcal{G}(p) = Z(\kappa/\mu)\mathcal{G}_R(p) \quad (3.22)$$

for convenience we also use $\mathcal{K}_R(k, p), \mathcal{L}_R(k, p)$; which are equal to $\mathcal{K}(k, p)$ and $\mathcal{L}(k, p)$ respectively but with \mathcal{G} replaced by \mathcal{G}_R . Here κ is an ultraviolet cutoff which serves to make the integrals finite. We now define a renormalised running coupling constant by:

$$g^2(\mu) = \frac{g_0^2 Z(\kappa/\mu)}{1 + \frac{g_0^2 C_A}{96\pi^4} \int d^4k \mathcal{K}_R(k, \mu)} \quad (3.23)$$

Using Eq. 3.19 we can also rewrite this as:

$$g^2(\mu) = \frac{g_0^2 Z^2(\kappa/\mu)\mathcal{G}_R(\mu)}{1 - \frac{g_0^2 C_A}{96\pi^4} Z^2(\kappa/\mu) \int d^4k \mathcal{G}_R(k)\mathcal{L}_R(k, \mu)} \quad (3.24)$$

Inverting these two equations in terms of the bare coupling g_0^2 gives us:

$$g_0^2 Z(\kappa/\mu) = \frac{g^2(\mu)}{1 - \frac{g^2(\mu)C_A}{96\pi^4} \int d^4k \mathcal{K}_R(k, \mu)} \quad (3.25)$$

$$g_0^2 Z^2(\kappa/\mu) = \frac{g^2(\mu)}{\mathcal{G}_R(\mu) + \frac{g^2(\mu)C_A}{96\pi^4} \int d^4k \mathcal{G}_R(k)\mathcal{L}_R(k, \mu)}$$

Substituting these expressions in Eq. 3.25 into Eq 3.19, and using the definition of Eq. 3.22 gives, after a little rearranging:

$$\begin{aligned} & \frac{1}{\mathcal{G}(p)} \left[\mathcal{G}_R(\mu) + \frac{g^2(\mu)}{96\pi^4} \int d^4k \mathcal{G}_R(k) \left(\mathcal{L}_R(k, \mu) - \mathcal{L}_R(k, p) \right) \right] \\ &= \left[1 + \frac{g^2(\mu)C_A}{96\pi^4} \int d^4k \left(\mathcal{K}_R(k, p) - \mathcal{K}_R(k, \mu) \right) \right] \times \\ & \quad \times \frac{\mathcal{G}_R(\mu) + \frac{g^2(\mu)C_A}{96\pi^4} \int d^4k \mathcal{G}_R(k)\mathcal{L}_R(k, \mu)}{1 - \frac{g^2(\mu)C_A}{96\pi^4} \int d^4k \mathcal{K}_R(k, \mu)} \end{aligned} \quad (3.26)$$

The quotient in the third line of Eq. 3.26 is seen to be simply $1/Z(\kappa/\mu)$ from Eq. 3.25. This can be used to renormalise the factor of $1/\mathcal{G}(p)$ on the left hand side of Eq. 3.26 to give us the renormalised equation in which all integrals will be ultraviolet finite:

$$\begin{aligned} \frac{\mathcal{G}_R(\mu)}{\mathcal{G}_R(p)} &= 1 + \frac{\alpha(\mu)C_A}{24\pi^3} \int d^4k \left(\mathcal{K}_R(k, p) - \mathcal{K}_R(k, \mu) \right) \\ &\quad + \frac{\alpha(\mu)C_A}{\mathcal{G}_R(p)24\pi^3} \int d^4k \mathcal{G}_R(k) \left(\mathcal{L}_R(k, p) - \mathcal{L}_R(k, \mu) \right) \end{aligned} \quad (3.27)$$

In the next section, we will need a more explicit form for the running coupling, in order to determine the behaviour of $\mathcal{G}_R(p)$ at large p^2 . We first invert Eq. 3.23 to give:

$$\frac{Z(\kappa/\mu)}{g^2(\mu)} = \frac{1}{g_0^2} + \frac{C_A}{96\pi^4} \int d^4k \mathcal{K}(k, \mu) \quad (3.28)$$

subtracting Eq. 3.28, from the same equation evaluated at p gives:

$$\frac{Z(\kappa/p)}{g^2(p)} = \frac{Z(\kappa/\mu)}{g^2(\mu)} + Z(\kappa/\mu) \frac{C_A}{96\pi^4} \int d^4k \left(\mathcal{K}_R(k, p) - \mathcal{K}_R(k, \mu) \right) \quad (3.29)$$

If we take the definition of Eq. 3.22, and instead renormalise at p^2 we would have:

$$\mathcal{G}(p) = Z(\kappa/p)\mathcal{G}_{R_p}(p) \quad (3.30)$$

where for clarity we have written the subscript R_p to denote that p^2 is our renormalisation scale. However we must have $\mathcal{G}_{R_p}(p) = \mathcal{G}_{R_\mu}(\mu)$, and we rewrite Eq. 3.30 as:

$$\mathcal{G}(p) = Z(\kappa/p)\mathcal{G}_{R_\mu}(\mu) \quad (3.31)$$

Then the equality of Eqs. 3.22 and Eq. 3.31 allows us to write:

$$\frac{Z(\kappa/p)}{Z(\kappa/\mu)} = \frac{\mathcal{G}_R(p)}{\mathcal{G}_R(\mu)} \quad (3.32)$$

where all quantities are renormalised at the scale μ^2 . This allows us to simply rewrite Eq. 3.29 as:

$$\frac{1}{g^2(p)} = \frac{\mathcal{G}_R(\mu)}{\mathcal{G}_R(p)} \left[\frac{1}{g^2(\mu)} + \frac{C_A}{96\pi^4} \int d^4k \left(\mathcal{K}_R(k, p) - \mathcal{K}_R(k, \mu) \right) \right] \quad (3.33)$$

as an equation for the renormalised running coupling constant. We have given the derivation of Eq. 3.33 in some detail, as the same sort of arguments will be used to define the other running couplings which will appear in our study.

3.4 Consistent Asymptotic Behaviour of $\mathcal{G}_R(p)$

Because of the complicated structure of our equation for the gluon renormalisation function $\mathcal{G}_R(p)$, Eq. 3.27, an analytic solution is not possible, and we attempt a numerical study. Before we do this, we investigate the possible asymptotic behaviour for both small and large p^2 that we should build into our numerical solution. In general we will take a trial input function $\mathcal{G}_{in}(p)$, and substitute this into the right hand side of our equation, Eq. 3.27. After performing the integrals we obtain an output function $1/\mathcal{G}_{out}(p)$, to be compared to the reciprocal of the input function. We allow our trial function to depend on a number of parameters, and we vary these until we find good agreement between input and output over a suitable range of p^2 .

All of the integrals in Eq. 3.27 give rise to dimensionless quantities, and all contain the factor $1/k^2 q^2$ in their denominator. This allows us to derive the following general results

a) If $\mathcal{G}_{in}(p) \rightarrow \text{constant}$, as $p^2 \rightarrow 0$, then the output of the right hand side of Eq. 3.27 is easily seen to give:

$$\frac{1}{\mathcal{G}_{out}} = 1 + (\text{constant}) \ln(p^2/\mu^2)$$

b) If $\mathcal{G}_{in}(p) \sim \ln p^2$ as $p^2 \rightarrow 0$, then the right hand side gives:

$$\frac{1}{\mathcal{G}_{out}} = 1 + \text{constant} \ln^2(p^2/\mu^2)$$

c) These logarithms may sum to a power. If we let $\mathcal{G}_{in}(p) \rightarrow (\mu^2/p^2)^\alpha$ as $p^2 \rightarrow 0$ with $\alpha < 1$, then all the integrals are infra-red finite, and we would obtain:

$$\frac{1}{\mathcal{G}_{out}} = 1 + \text{constant} \left(\frac{\mu^2}{p^2}\right)^\alpha$$

where this is purely on dimensional grounds, to balance the dimensionful quantity μ^2 .

In all of these cases it is not possible to obtain agreement between input and output. If, however, we consider the case $\mathcal{G}_{in} \rightarrow \mu^2/p^2$, and we use some regularisation technique to deal with the infra-red divergences, then we would find by the same dimensional arguments that

$$\frac{1}{\mathcal{G}_{out}} = 1 + C\mu^2/p^2$$

where C is a constant. Unlike the terms in c) above, this will violate our masslessness condition, and so must be subtracted. Then if the higher order terms in p^2 of $\mathcal{G}(p)$ generate a contribution to the right hand side of which cancels the explicit factor of 1, then the right hand side of the equation would vanish as $p^2 \rightarrow 0$. This is exactly the behavior of the left hand side, and we have the possibility of finding agreement. If the next order p^2 corrections to $\mathcal{G}_{in}(p)$ behaved like a constant, a logarithm, or a power as in c) above, but with $0 < \alpha < 1$, then this would give rise to inconsistent behaviour, as the left hand side of Eq. 3.27, i.e the reciprocal of the input function *vanishes* at small p^2 . We therefore will attempt to find solutions which behave like:

$$\mathcal{G}_{in} = A\mu^2/p^2 + B(p^2/\mu^2)^\nu, \quad \nu > 0$$

as $p^2 \rightarrow 0$.

We can now use Eqs. 3.27 and 3.33 to determine the asymptotic form of our equation for large p^2 . By writing $\mathcal{G}_R = 1 + O(\alpha(\mu))$ then if we only work to $O(\alpha(\mu))$, we can simply set $\mathcal{G}_R = 1$ on the right hand side of Eq. 3.27. However, if we set $\mathcal{G}_R = 1$ in our ansatz for the full triple gluon vertex Eq. 2.73, it reduces to the bare vertex. Thus the leading term from this diagram is simply that of perturbation theory (see section 2.6), and we have:

$$\frac{1}{\mathcal{G}_R(p)} = 1 + \frac{\alpha(\mu)}{4\pi} \gamma_0 \ln\left(\frac{p^2}{\mu^2}\right) \quad (3.34)$$

where from Eq. 2.77 we have $\gamma_0 = \frac{7}{3}C_A$. This can also be verified using the integrals of Appendix A, Eq. A.32. We also need to know the leading behaviour of the renormalised running coupling Eq. 3.33. We extract the leading term of $\int d^4k \left[\mathcal{K}_R(k, p) - \mathcal{K}_R(k, \mu) \right]$ by using $\mathcal{G}_R = 1$ in Eq. 3.23. We therefore must work out the leading contribution of

$$\int d^4k \left(\frac{A(k, p)}{k^4 q^2 p^4} - \frac{C(k, p)}{(q^2 + \mu^2) k^2 q^2 p^2} \right) \quad (3.35)$$

using Eq 3.21 and Eq. A.32 in Appendix A, we obtain the leading behaviour of Eq. 3.35 as:

$$\begin{aligned} & \left(12 - \frac{32}{2} - \frac{16}{4} + 6 + \frac{6}{4} - 14 - \frac{16}{4} + 6 \right) \ln\left(\frac{p^2}{\mu^2}\right) \\ & = \left(-\frac{1}{2} - 12 \right) \ln\left(\frac{p^2}{\mu^2}\right) = -\frac{25}{2} \ln\left(\frac{p^2}{\mu^2}\right) \end{aligned} \quad (3.36)$$

Thus from Eq 3.36 we obtain from Eq. 3.33:

$$\frac{1}{\alpha(p)} = \frac{\mathcal{G}_R(\mu)}{\mathcal{G}_R(p)} \left(\frac{1}{\alpha(\mu)} + \frac{25C_A}{48\pi} \ln\left(\frac{p^2}{\mu^2}\right) \right) \quad (3.37)$$

Using Eq. 3.34 to expand $\mathcal{G}_R(p)$, we obtain:

$$\frac{1}{\alpha(p)} = \frac{1}{\alpha(\mu)} + \frac{\beta_0}{4\pi} \ln\left(\frac{p^2}{\mu^2}\right) \quad (3.38)$$

where $\beta_0 = \frac{53}{12}C_A$. This is to be compared with the usual β_0 of perturbation theory being $\frac{11}{3}C_A$. In the usual way (see section 1.4), we can eliminate the arbitrary momentum μ^2 , by rewriting Eq. 3.38 as:

$$\alpha(p) = \frac{4\pi}{\beta_0 \ln(p^2/\Lambda^2)} \quad (3.39)$$

The usual renormalisation group argument allows us to rewrite the asymptotic form for $\mathcal{G}_R(p)$ as:

$$\mathcal{G}_R(p) \sim \mathcal{G}_R(\mu) \left(\frac{\alpha(p)}{\alpha(\mu)} \right)^{\gamma_0/\beta_0} \sim \left(\ln(p^2/\mu^2) \right)^{-\gamma_0/\beta_0} \quad (3.40)$$

We have given this derivation of the asymptotic form in some detail, as we shall use similar arguments throughout this study. From now on though, we shall merely give the answer. The arithmetic can easily be checked with the integrals in Eq. A.32.

We have therefore deduced the possible analytic behaviour of $\mathcal{G}_R(p)$ for both small and large p^2 . Before we proceed with our numerical study, however, there are some technical details to be dealt with.

3.5 Technical Details

In order to calculate the numerical integrals in Eq. 3.27, there are a number of technical details which we give here. The most important of these is the definition and implementation of the ‘plus’ prescription, which we use to make our potentially infra-red divergent integrals finite. The basic definition is as follows:

$$\int_0^\infty dk^2 \left(\frac{A\mu^2}{k^2} \right)_+ S(k,p) = \int_0^{p^2} dk^2 \left(\frac{A\mu^2}{k^2} \right) (S(k,p) - S(0,p)) + \int_{p^2}^\infty dk^2 \left(\frac{A\mu^2}{k^2} \right) S(k,p) \quad (3.41)$$

where the subtraction in the first integral removes any pole at $k^2 = 0$ leaving us with a finite answer. For those integrals in which the angular integrals can be performed analytically, the implementation of this prescription is easy. Unfortunately for many of the integrals we have to deal with, namely the $\mathcal{L}(k, p)$ terms, the angular integrals cannot all be performed analytically, and must be done numerically. Thus writing:

$$S(k, p) = \int_0^\pi \sin^2 \psi \, d\psi \, s(k, p, \cos \psi) \quad (3.42)$$

we define

$$S(0, p) = \lim_{k^2 \rightarrow 0} \int_0^\pi \sin^2 \psi \, d\psi \, s(k, p, \cos \psi) \quad (3.43)$$

For many of these terms the limit and the integral sign in Eq. 3.43 can be interchanged to give us $s(0, p, \cos \psi)$, for other terms more work remains to be done. We illustrate this and other problems by means of some examples.

First of all, some of the terms are infra-red finite, and for these, the subtraction detailed in Eq. 3.41 does not occur, $S(0, p)$ being zero. This includes all terms with $S(k, p) = O(k)$ or higher. For the higher powers, finiteness is obvious. For those terms with $S(k, p) = O(k)$, since the integration measure is dk^2 , we have an integrable singularity at $k^2 = 0$. This can be removed by writing $dk^2 = 2k \, dk$.

In general the terms from $\mathcal{L}(k, p)$ are proportional to $\mathcal{G}(k)\mathcal{G}(q)$, and either of these two can be infra-red enhanced, the contribution where both are enhanced being subtracted by our mass renormalisation (see section 3.3). By transforming integration variables $k \rightarrow q$ we can always make the enhanced term $A\mu^2/k^2$.

From Eq. 3.20 we deal with the terms from $B(k, p)$. From Eq. 3.17 and its transform when $k \leftrightarrow q$, we can read off the kind of terms we have to

deal with. The measure d^4k gives us a factor of $k^2 dk^2$, so terms in $B(k, p)$ with three powers of k or higher in the numerator are explicitly infra-red finite. This leaves us with infra-red divergent terms having:

$$s(k, p) \sim \frac{p^2 k \cdot p}{q^2 k^2} \mathcal{G}_1(q), \frac{(k \cdot p)^2}{q^4 k^2} \mathcal{G}_1(q), \frac{p^2}{q^4} \mathcal{G}_1(q) \quad (3.44)$$

where \mathcal{G}_1 is the non enhanced part of \mathcal{G} . The second two of these are relatively easy to deal with giving rise to:

$$s(0, p, \cos\psi) \sim \frac{\cos^2\psi}{p^2} \mathcal{G}_1(p), \frac{1}{p^2} \mathcal{G}_1(p) \quad (3.45)$$

To calculate the actual value of the integrand at $k^2 = 0$, we can Taylor expand $s(k, p, \cos\psi)$, subtracting the leading term $s(0, p, \cos\psi)$. Thus for the second of the terms in Eq. 3.44 we obtain:

$$s(k, p) = \frac{\cos^2\psi}{p^2} \left(\mathcal{G}_1(p) + (k^2 - 2k \cdot p) \mathcal{G}'_1(p) + 2(k \cdot p)^2 \mathcal{G}''_1(p) \right) \times \quad (3.446)$$

$$\times \left(1 - 2\frac{k^2}{p^2} + 4\frac{k \cdot p}{p^2} + \frac{12(k \cdot p)^2}{p^4} \right) + O(k^3)$$

where a prime denotes differentiation with respect to p^2 . Here we can expand the brackets, subtract the leading term (Eq. 3.45), and use the fact that terms odd in $\cos\psi$ will integrate to zero over ψ .

We perform our numerical integrations by a Simpson's rule method, increasing the number of integration points until the answer is stable to within 0.1 %, as well as demanding similar numerical agreement with the analytically calculable answer when $\mathcal{G}_1 \equiv 1$. To implement our plus prescription, Eq. 3.41, numerically, the integral from 0 to p^2 is split into two regions: 0 to ϵp^2 , and ϵp^2 to p^2 . Over the second region, away from $k^2 = 0$ we simply use $s(k, p) - s(0, p)$ in our integrand. Over the first region we use the Taylor expansion to $O(k^2)$, subtracting the leading term. By using $\epsilon = 10^{-4}$ we maintain our numerical accuracy.

The first of the terms in Eq. 3.44 is a little more difficult, itself appearing divergent as $k^2 \rightarrow 0$, leaving $s(0, p)$ apparently undefined. In this case the limit and integral sign in Eq. 3.43 cannot be naively interchanged. Taylor expanding $s(k, p)$ we obtain:

$$\begin{aligned} s(k, p) &= \frac{p^2 k \cdot p}{q^4 k^2} \mathcal{G}_1(q) \\ &= \frac{p^2 k \cdot p}{p^4 k^2} \left(\mathcal{G}_1(p) + (k^2 - 2k \cdot p) \mathcal{G}'_1(p) \right) \left(1 - 2 \frac{k^2 - 2k \cdot p}{p^2} \right) + O(k) \end{aligned} \quad (3.47)$$

The potentially divergent leading term is odd in $\cos\psi$ and so will vanish on performing the ψ integration. Thus from Eq. 3.47 we obtain:

$$s(0, p) = \cos^2\psi \left(4 \frac{\mathcal{G}_1(p)}{p^2} - 2\mathcal{G}'_1(p) \right) \quad (3.48)$$

Once again we can split the 0 to p^2 integration into two regions, using the Taylor expansion with the leading term Eq. 3.47 subtracted for $0 < k^2 < \epsilon p^2$, and with the full $s(k, p) - s(0, p)$ for $\epsilon p^2 < k^2 < p^2$.

We are left with the terms from $C(k, p)$ in Eq. 3.20. With $\mathcal{G}(k)$ enhanced, all the terms are finite by counting powers of k except for the term proportional to p^4 for which

$$s(k, p) = \frac{24p^4}{q^2 p^2} \left(\mathcal{G}_1(q) - \frac{p^2 + \mu^2}{q^2 + \mu^2} \mathcal{G}_1(p) \right) \frac{1}{q^2 - p^2} \quad (3.49)$$

By Taylor expanding we can easily obtain:

$$s(0, p) = 24 \left(\frac{\mathcal{G}_1(p)}{p^2 + \mu^2} + \mathcal{G}'_1(p) \right) \quad (3.50)$$

and we use the same treatment of the numerical integrals as outlined above. For the case where $\mathcal{G}(q)$ is enhanced, we can transform variables $k \leftrightarrow q$ for the $C(k, p)$ terms. It can easily be checked that $C(k, p)$ transforms to the following quantity:

$$8k^2 p^2 + 4(k \cdot p)^2 + 6k^2 k \cdot p + 6p^2 k \cdot p \quad (3.51)$$

and all terms are explicitly infra-red finite because of sufficient powers of k in the numerator. This completes our discussion of the plus prescription and its implementation.

We now turn to the ultraviolet region of our integrals, where we must implement the renormalisation procedure outlined in section 3.3. As we have mentioned our numerical integrations are performed using a Simpson's rule technique. This allows us to integrate over a finite region, and so we must transform variables from the infinite momentum region of the loop integral. We split the k^2 integration into two regions, the first from 0 to p^2 , and the second from p^2 to infinity. In the first region we implement the Simpson's rule on the integrals as they stand. For the second region we change variables, using $w^2 = 1/k^2$ to transform to a finite integration region. For those integrals which are ultraviolet finite, this is sufficient. For those which diverge, however, we must make sure our renormalisation procedure cancels these divergences *before* we perform our numerical integrations. The terms involving the enhanced infra-red behaviour for \mathcal{G} are all ultraviolet finite by power counting, because of the extra power of k^2 in the denominator from this term. Thus we are left to deal with the terms where $\mathcal{G} \equiv \mathcal{G}_1$.

Turning to Eq. 3.17, we first look at the $A(k, p)$ terms. Some of these appear quadratically divergent by power counting, but this divergence will cancel between compensating terms leaving only a logarithmic divergence. Other terms appear linearly divergent, but here the angular integrations will make them only logarithmically divergent again. Since the term proportional to $A(k, p)$ is linear in \mathcal{G} , we can analytically perform the angular integrals. Using Eq. A.28 from Appendix A we obtain:

$$\begin{aligned}
 \int d^4 k \frac{\mathcal{G}_1(k)A(k,p)}{k^4 q^2 p^4} &= 2\pi^2 \int_0^{p^2} dk^2 \frac{\mathcal{G}_1(k)}{k^2 p^4} \left\{ \frac{48(p^2 + k^2)k^4 p^2}{8p^4} - \frac{32k^4 p^3}{4p^3} - \frac{16p^3 k^6}{16p^5} \right. \\
 &\quad \left. - \frac{16p^3 k^4}{8p^3} - \frac{12k^4 p^2}{2p^2} + \frac{6k^2 p^4}{2p^2} + \frac{6p^4 k^2 (p^2 + k^2)}{8p^4} \right\} \\
 &\quad + 2\pi^2 \int_{p^2}^{\kappa^2} dk^2 \frac{\mathcal{G}_1(k)}{k^2 p^4} \left\{ \frac{48(p^2 + k^2)k^4 p^2}{8k^4} - \frac{32k^3 p^4}{4k^3} - \frac{16p^6 k^3}{16k^5} \right. \\
 &\quad \left. - \frac{16p^4 k^3}{8k^3} - \frac{12k^4 p^2}{2k^2} + \frac{6k^2 p^4}{2k^2} + \frac{6p^4 k^2 (p^2 + k^2)}{8k^4} \right\} \\
 &= 2\pi^2 \int_0^{p^2} dk^2 \frac{\mathcal{G}_1(k)}{k^2 p^4} \left\{ \frac{5k^6}{p^2} - \frac{37k^4}{4} + \frac{15k^2 p^2}{4} \right\} \\
 &\quad + 2\pi^2 \int_{p^2}^{\kappa^2} dk^2 \frac{\mathcal{G}_1(k)}{k^2 p^4} \left\{ -\frac{p^4}{4} - \frac{p^6}{4k^2} \right\}
 \end{aligned} \tag{3.52}$$

here we can see the explicit cancellation of the quadratically divergent terms, and the absence of linearly divergent terms. We are left with a logarithmically divergent integral, where for the moment we have retained the ultraviolet cutoff κ^2 . The renormalisation procedure essentially consists of subtracting Eq. 3.52 evaluated at $p^2 = \mu^2$, from itself, (see Eq. 3.27). The logarithmically divergent term in the second of the integrals of Eq. 3.52 is independent of p^2 , and so will cancel in this subtraction, leaving us with a finite integral. For the finite terms in Eq. 3.52, our renormalisation consists of a finite subtraction. The integrals in Eq. 3.52 are the easiest case to consider, because we have been able to perform the angular integrals explicitly.

We now turn to the $B(k,p)$ terms in Eq. 3.17. There are eight powers of k in the denominator, so that with the four powers of k from the integration measure $d^4 k$, the only divergent terms are those proportional to $-13k^4 - 2k^2(k \cdot p)^2/p^2$. After our ultraviolet subtraction we must calculate the following integral:

$$\int d^4k \mathcal{G}_1(k) (-13 - 2\cos^2\psi) \left(\frac{\mathcal{G}_1(q)}{q^4} - \frac{\mathcal{G}_1(q_\mu)}{q_\mu^4} \right) \quad (3.53)$$

where $q_m = k^2 + \mu^2 - 2k \cdot \mu$. Here μ is a Euclidean 4-vector in the direction of p , with $\mu \cdot \mu = \mu^2$. We can add and subtract a term proportional to $\mathcal{G}_1(q)/q_m^4$ to give:

$$2\pi \int \sin^2\psi d\psi dk^2 \mathcal{G}_1(k) (-13 - 2\cos^2\psi) \left(\frac{\mathcal{G}_1(q)}{q^4 q_m^4} (q_m^4 - q^4) + \frac{1}{q_m^4} (\mathcal{G}_1(q) - \mathcal{G}_1(q_\mu)) \right) \quad (3.54)$$

In the first term the highest power of k^2 cancels in the $q_m^4 - q^4$ term, leaving us with a finite integral. The second term is still divergent by power counting. We integrate this term up to some large momentum R , with $R^2 \gg \mu^2, p^2$. Then we can expand:

$$\begin{aligned} \mathcal{G}_1(q) &= \mathcal{G}_1(k) + (q^2 - k^2)\mathcal{G}'_1(k) + \frac{1}{2}(q^2 - k^2)^2\mathcal{G}''_1(k) + O(1/k^3) \\ &= \mathcal{G}_1(k) + (p^2 - 2k \cdot p)\mathcal{G}'_1(k) + 2(k \cdot p)^2\mathcal{G}''_1(k) + O(1/k^3) \end{aligned} \quad (3.55)$$

A similar expansion for $\mathcal{G}_1(q_m)$ allows us to write $\mathcal{G}_1(q) - \mathcal{G}_1(q_m)$ as:

$$(p^2 - \mu^2 + 2k \cdot \mu - 2k \cdot p)\mathcal{G}'_1(k) + 2((k \cdot p)^2 - (k \cdot \mu)^2)\mathcal{G}''_1(k) + O(1/k^3) \quad (3.56)$$

Since we will choose an explicit parameterisation for \mathcal{G}_1 , its derivatives can be calculated, and the extra powers of k^2 in the denominator coming from these make the integral finite. These powers can be explicitly extracted to enable us to perform the numerical integration (see Eq. 3.74). For R^2 sufficiently large, the errors introduced by ignoring higher terms in the expansion are small. We usually choose $R^2 = 10^3 \max(p^2, \mu^2)$.

We now move on to the $C(k, p)$ terms in Eq. 3.20. These are of two types, those that contribute to $\mathcal{K}(k, p)$, and those that contribute to $\mathcal{L}(k, p)$. For

the former we can count six powers of k^2 in the denominator, and so the divergent terms can be read off as those proportional to $14k^2p^2 + 16(k \cdot p)^2 - 6k^2k \cdot p$. The last term here appears linearly divergent, but if we could perform the angular integrals the divergence would be only logarithmic. To deal with this we write the contribution of this last term as:

$$\int d^4k \left(\frac{6k^2k \cdot p}{(q^2 + \mu^2)k^2q^2p^2} - \frac{6k^2k \cdot p}{(k^2 + \mu^2)k^4p^2} \right) \mathcal{G}_1(k) \quad (3.57)$$

where the term we have subtracted is equal to zero because its numerator is odd in $\cos\psi$, and there is no other ψ dependence. We can rewrite Eq. 3.57 as:

$$\int d^4k \frac{6\mathcal{G}_1(k)k \cdot p}{p^2} \left(\frac{k^2(k^2 + \mu^2) - q^2(q^2 + \mu^2)}{(q^2 + \mu^2)(k^2 + \mu^2)k^2q^2} \right) \quad (3.58)$$

we can see that the highest power of k will cancel in the numerator, leaving us with a logarithmically divergent integral. We can extract this divergent piece, finding it to be:

$$24 \int d^4k \mathcal{G}_1(k) \frac{(k \cdot p)^2}{(q^2 + \mu^2)(k^2 + \mu^2)q^2p^2} \quad (3.59)$$

After renormalisation, this becomes:

$$24 \int d^4k \frac{\mathcal{G}_1(k)k^2 \cos^2\psi}{k^2 + \mu^2} \left(\frac{1}{q^2(q^2 + \mu^2)} - \frac{1}{q_m^2(q_m^2 + \mu^2)} \right) \quad (3.60)$$

The term in brackets from Eq. 3.60 can be written over a common denominator, with a numerator equal to $\mu^2(q_m^2 - q^2) + q_m^4 - q^4$. It is obvious that the highest power of k^2 cancels, and again we are left with a finite integral. The remaining divergent terms from $C(k, p)$ are dealt with in a similar manner to this.

For the $C(k, p)$ terms contributing to $\mathcal{L}(k, p)$ we split the k^2 integral into two regions, from 0 to $4\max(p^2, \mu^2)$, and from $4\max(p^2, \mu^2)$ to infinity. In this second region we are well away from the points where $q^2 = p^2$ or $q_m^2 = \mu^2$.

Then from the factor $\mathcal{G}_1(q) - \mathcal{G}_1(p)(p^2 + \mu^2)/(q^2 + \mu^2)$ in Eq. 3.20, we see that the second term carries an extra power of k^2 in the denominator, and this makes all the integrals involving this term ultraviolet finite by power counting. The logarithmically divergent terms proportional to $\mathcal{G}_1(q)$ can be dealt with in exactly the same way as the terms from $B(k, p)$, see Eqs 3.53-3.56. The only difficult term is that proportional to:

$$\int d^4k \frac{\mathcal{G}_1(k)\mathcal{G}_1(q)}{k^2 q^2 p^2} \frac{k^2 k \cdot p}{q^2 - p^2} \left(1 - \frac{\mathcal{G}_1(p)}{\mathcal{G}_1(q)} \left(\frac{p^2 + \mu^2}{q^2 + \mu^2} \right) \right) \quad (3.61)$$

which appears linearly divergent. This time we cannot perform the angular integrals analytically, nor can we perform an easy subtraction as in Eq. 3.57.

We deal with this term by writing it as:

$$I = \int d^4k \left\{ \frac{\mathcal{G}_1(k)\mathcal{G}_1(q)}{k^2 q^2 p^2 (q^2 - p^2)(k^2 - p^2)} \right\} (k^2 - p^2) k^2 k \cdot p \left(1 - \frac{\mathcal{G}_1(p)}{\mathcal{G}_1(q)} \left(\frac{p^2 + \mu^2}{q^2 + \mu^2} \right) \right) \quad (3.62)$$

We have introduced a term $(k^2 - p^2)/(k^2 - p^2)$ so that the term in brackets in eq. 3.62 is $q \leftrightarrow k$ symmetric. By changing variables $q \leftrightarrow k$, and relabelling the momenta we obtain:

$$I = \int d^4k \left\{ \frac{\mathcal{G}_1(k)\mathcal{G}_1(q)}{k^2 q^2 p^2 (q^2 - p^2)(k^2 - p^2)} \right\} (q^2 - p^2) (W(k, p) - k^2 k \cdot p) \times \left(1 - \frac{\mathcal{G}_1(p)}{\mathcal{G}_1(k)} \left(\frac{p^2 + \mu^2}{k^2 + \mu^2} \right) \right) \quad (3.63)$$

where for convenience we have introduced $W(k, p) = k^2 p^2 - 3p^2 k \cdot p + 2(k \cdot p)^2 + p^4$. Both Eq. 3.62 and Eq. 3.63 are finite at $k^2 = p^2$ and $q^2 = p^2$. Using the fact that I is equal to half the sum of Eqs. 3.62 and 3.63, we can simply apply Simpson's rule for the k^2 integral for $0 < k^2 < 4\max(p^2, \mu^2)$. For k^2 greater than this, we can split the integrand, isolating the divergent terms which we read off as:

$$\int d^4 k \frac{\mathcal{G}_1(k)\mathcal{G}_1(q)}{k^2 q^2 p^2 (k^2 - p^2)(q^2 - p^2)} \left((k^2 - p^2)k^2 k \cdot p + (q^2 - p^2)(W(k, p) - k^2 k \cdot p) \right) \quad (3.64)$$

Writing $q^2 - p^2 = (k^2 - p^2) + (p^2 - 2k \cdot p)$ we can rewrite the bracketed term in the numerator of Eq. 3.64 as:

$$(q^2 - p^2)W(k, p) - (p^2 - 2k \cdot p)k^2 k \cdot p \quad (3.65)$$

We are left with terms which are only logarithmically divergent, which we deal with in exactly the same way as in Eqs. 3.53-3.56.

Finally we turn to the $D(k, p)$ terms in Eq. 3.20. This contains apparent quadratic divergences, which we will show to be absent because of the angular integrations. First of all, however, we deal with the apparent linearly divergent terms in $D(k, p)$ proportional to $(k \cdot p)^3$ and $k^2 p^2 k \cdot p$. We write:

$$\begin{aligned} I_1 &= \int d^4 k \frac{\mathcal{G}_1(q) - \mathcal{G}_1(k)}{q^2 - k^2} \frac{k^2 k \cdot p}{k^2 q^2 p^2} \\ I_2 &= \int d^4 k \frac{\mathcal{G}_1(q) - \mathcal{G}_1(k)}{q^2 - k^2} \frac{(k \cdot p)^3}{k^2 q^2 p^4} \end{aligned} \quad (3.66)$$

Once again we transform variables $k \leftrightarrow q$, and relabel the momenta. We find that I_1 is equal to

$$\begin{aligned} I_1 &= \int d^4 k \frac{\mathcal{G}_1(q) - \mathcal{G}_1(k)}{q^2 - k^2} \frac{1}{k^2 q^2 p^2} (-k^2 k \cdot p + p^2 k^2 + p^4 - 3p^2 k \cdot p + 2(k \cdot p)^2) \\ &= -I_1 + \int d^4 k \frac{\mathcal{G}_1(q) - \mathcal{G}_1(k)}{q^2 - k^2} \frac{1}{k^2 q^2 p^2} (p^2 k^2 + p^4 - 3p^2 k \cdot p + 2(k \cdot p)^2) \end{aligned} \quad (3.67)$$

Thus we obtain:

$$I_1 = \frac{1}{2} \int d^4 k \frac{\mathcal{G}_1(q) - \mathcal{G}_1(k)}{q^2 - k^2} \frac{1}{k^2 q^2 p^2} (p^2 k^2 + p^4 - 3p^2 k \cdot p + 2(k \cdot p)^2) \quad (3.68)$$

In exactly the same way we can compute:

$$I_2 = \frac{1}{2} \int d^4 k \frac{\mathcal{G}_1(q) - \mathcal{G}_1(k)}{q^2 - k^2} \frac{1}{k^2 q^2 p^4} (p^6 - 3p^4 k \cdot p + 3p^2 (k \cdot p)^2) \quad (3.69)$$

and both Eq. 3.68 and Eq. 3.69 are only logarithmically divergent.

We now turn to the quadratically divergent terms, proportional to

$$\int d^4 k \frac{\mathcal{G}_1(q) - \mathcal{G}_1(k)}{q^2 - k^2} \frac{1}{k^2 q^2 p^4} (12k^4 p^2 - 48k^4 p^2 \cos^2 \psi) \quad (3.69)$$

As before we integrate this up to $k^2 = R^2 = 10^3 \max(p^2, \mu^2)$ as it stands. For $k^2 > R^2$ we Taylor expand the integrand, giving us

$$\frac{\mathcal{G}_1(q) - \mathcal{G}_1(k)}{q^2 - k^2} = \mathcal{G}'_1(k) + O(1/k^3) \quad (3.70)$$

It is this first term in this expansion which is potentially quadratically divergent.

We can now perform the angular integrals using Eq. A.28 for $k^2 > p^2$, from Appendix A to find the high momentum contribution of this term:

$$\begin{aligned} & 2\pi^2 \int_{R^2}^{\kappa^2} dk^2 \mathcal{G}'_1(k) \frac{12k^4}{p^2} \left(\frac{1}{2k^2} - \frac{4(k^2 + p^2)}{8k^4} \right) \\ &= 24\pi^2 \int_{R^2}^{\kappa^2} dk^2 \mathcal{G}'_1(k) \left(-\frac{1}{2} \right) \end{aligned} \quad (3.72)$$

Since $\mathcal{G}'(k) = O(1/k^2)$, we see that the quadratic divergences have cancelled. This procedure can be continued to isolate the other logarithmically divergent pieces, and the leading order finite pieces. By expanding $1/q^2$ in powers of p^2/k^2 as well, we can perform the angular integrals term by term. Since the integrals give a dimensionless answer, the logarithmically divergent terms must be simply proportional to dk^2/k^2 , and so independent of p^2 . Thus just as in Eq. 3.52 the renormalisation will explicitly cancel these terms, leaving us with the leading order finite terms for $k^2 > R^2$, and hence convergent integrals.

This completes our discussion of the technical details of the calculation. We have mentioned them in some detail since the calculations of this chapter

are somewhat more complicated than those we will meet in later chapters. Thus from now on we will not dwell at length on the technical details needed to compute the numerical integrals.

3.6 The Solution

We choose a parameterisation for $\mathcal{G}_R(p)$ consistent with the expected infra-red enhancement, and the asymptotic behaviour of Eq. 3.40. We introduce:

$$\mathcal{G}_\infty(p) = \left(1 + \frac{\beta_0 \alpha_s(\mu)}{4\pi} \ln \left(1 + \frac{p^2}{\mu^2} \right) \right)^{-\gamma_0/\beta_0} \quad (3.73)$$

which is well behaved at all values of p^2 . Here $\gamma_0/\beta_0 = 28/53$ We choose to parameterise $\mathcal{G}_R(p)$ by:

$$\mathcal{G}_R(p) = \frac{A\mu^2}{p^2} + \mathcal{G}_\infty(p) \sum_{n=1}^N a_n \left(\frac{p^2}{p^2 + p_0^2} \right)^{nb} \quad (3.74)$$

Here the parameters A, p_0, a_n, b are to be determined by self-consistency of Eq. 3.27. We substitute this form into Eq. 3.27, treating the enhanced infra-red term by our plus prescription, and performing the numerical integrals, the details of which are given in section 3.5. Where needed the derivatives of Eq. 3.74 are easily calculated.

We then vary these parameters until good agreement is obtained over a range of values of p^2 , between the right and left hand sides of Eq. 3.27. Because of the extreme length of time needed to perform these two dimensional integrals numerically, we set $p_0^2 = 0.3 \text{ GeV}^2$ and $b = 0.3$, values for which we obtained approximate agreement 'by hand'. Since these are the only parameters on which the dependence of Eq. 3.74 is non-linear, the integrals of Eq. 3.27 can be performed once, and the output stored. We then allow A and the a_n to vary within the numerical minimisation program MINUIT.

We choose our range of momentum to be $0.01 < p^2 < 100 \text{ GeV}^2$, with the renormalisation scale $\mu^2 = 10 \text{ GeV}^2$ a scale we know from experiment to be in

the perturbative regime. We set $\mathcal{G}_R(\mu) = 1$, and choose a value for $\alpha_s(\mu)$. With $N = 4$ in Eq. 3.74 we find this matching is achieved to impressive numerical accuracy, over the whole momentum range, from the deep infra-red to the deep ultraviolet. Using the form of Eq. 3.38 for the running coupling, we detail the solutions obtained for $\Lambda = 200$ and $\Lambda = 500\text{MeV}$ i.e. $\alpha_s(\mu) = 0.172$ and 0.257 respectively (see Eq. 3.39). The results are plotted in fig. 3.2, and the parameters are detailed in Table 3.1.

| Λ (MeV) | 200 | 500 |
|-----------------------------|----------|----------|
| $\alpha_s(\mu)$ | 0.172 | 0.257 |
| A | 0.01934 | 0.07363 |
| b | 0.3 | 0.3 |
| q_0^2 (GeV ²) | 0.3 | 0.3 |
| a_1 | 2.637 | 1.469 |
| a_2 | 0.009379 | -0.09048 |
| a_3 | -0.4407 | 0.2547 |
| a_4 | -1.180 | -0.6274 |

Table 1 : parameters for $\mathcal{G}(q)$, Eq. 3.72, for solutions shown in fig. 3.2

We find that the solution to this truncated Schwinger-Dyson equation for the gluon propagator does indeed possess a solution in which the function $\mathcal{G}_R(p) \sim 1/p^2$ as $p^2 \rightarrow 0$. Thus the propagator itself will behave like $1/p^4$ in this limit. Before we go on to discuss the importance of this result, and its relevance to confinement physics in section 4.5, we first detail a far simpler approximation to this gluon equation, which nevertheless possesses the same qualitative solutions as those we have obtained here.

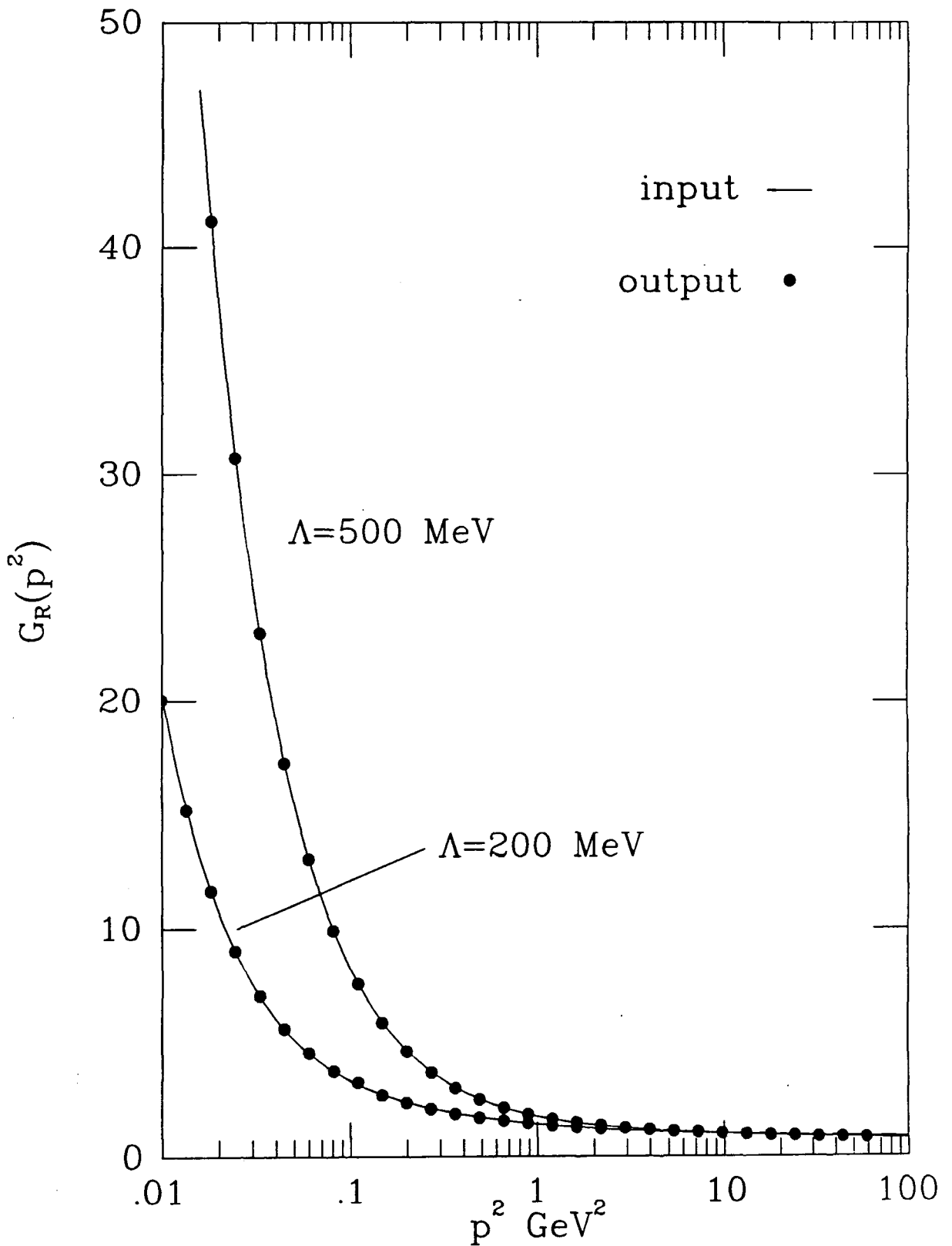


fig. 3.2: The gluon renormalisation function $\mathcal{G}_R(p)$ as a function of p^2 for $\Lambda = 200, 500$ MeV.

CHAPTER FOUR

THE MANDELSTAM APPROXIMATION

4.1 Introduction

In this chapter we consider again the Schwinger-Dyson equation for the inverse gluon propagator, but this time in a simpler approximation first proposed by Mandelstam [4.1]. We shall demonstrate, qualitatively at least, that the solutions using this approximation have the same features as those obtained in chapter three, and discuss why this is so. Because of the simplicity of this so called ‘Mandelstam approximation’ we use it as a basis for the calculations of chapters five and six.

In solving the Slavnov-Taylor identity for the triple gluon vertex in terms of the gluon renormalisation function $\mathcal{G}(p)$, Eq. 2.72, we see that the determined longitudinal part of the vertex, Eq. 2.73, always involves terms proportional to $1/\mathcal{G}$, with arguments p, k, q . The two gluon propagators in the gluon loop of fig. 3.1, give a contribution of $\mathcal{G}(k)\mathcal{G}(q)$, partially cancelling some of these $1/\mathcal{G}$ terms. Mandelstam has suggested an approximation which assumes this cancellation to be complete, where we simply write the full triple gluon vertex as $1/\mathcal{G}(q)$ times the bare vertex. This reduces the diagram of fig. 3.1 to that of fig. 4.1.

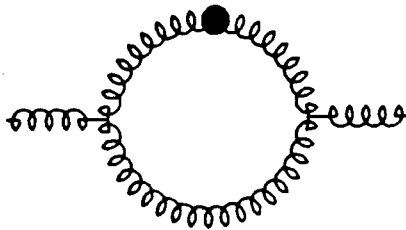


fig. 4.1: The gluon loop diagram in the Mandelstam approximation.

This approximation has also been studied by others [3.3], but as it is the basis of our later calculations, we give it in some detail, as our approach differs in some respects, particularly in the renormalisation of the equation in section 4.2.

As in chapter three we still neglect the ghost contributions and the diagrams involving quartic gluon couplings. This allows our simplified equation to be written diagrammatically as in fig. 4.2, giving us the following mathematical equation for the inverse gluon propagator:

$$\Pi_{ab}^{\mu\nu} = \Pi_{0ab}^{\mu\nu} + \delta_{ab} \frac{C_A g_0^2}{32\pi^4} \int d^4k \Gamma_0^{\mu\alpha\delta}(-p, k, q) \Delta_{\alpha\beta}(k) \Delta_{\gamma\delta}(q) \frac{\Gamma_0^{\beta\nu\gamma}(-k, p, -q)}{\mathcal{G}(q)} \quad (4.1)$$

where all the quantities are defined in sections 2.4 and 2.5, and once again we work in the Landau gauge.

4.2 The Calculation and Renormalisation

Following Eq. 3.4 we write the integrand in Eq. 4.1 as $\mathcal{G}(k)N^{\mu\nu}/k^2q^2$, where we have explicitly extracted the simple functional dependence on \mathcal{G} and $N^{\mu\nu}$ is defined as:

$$N^{\mu\nu} = N_1^{\mu\nu} - \frac{N_2^{\mu\nu}}{k^2} - \frac{N_3^{\mu\nu}}{q^2} + \frac{N_4^{\mu\nu}}{k^2q^2} \quad (4.2)$$

where:

$$\begin{aligned} N_1^{\mu\nu} &= \Gamma_0^{\mu\alpha\delta}(-p, k, q) \delta_{\alpha\beta} \delta_{\gamma\delta} \Gamma_0^{\beta\nu\gamma}(-k, p, -q) \\ N_2^{\mu\nu} &= \Gamma_0^{\mu\alpha\delta}(-p, k, q) k_\alpha k_\beta \delta_{\gamma\delta} \Gamma_0^{\beta\nu\gamma}(-k, p, -q) \\ N_3^{\mu\nu} &= \Gamma_0^{\mu\alpha\delta}(-p, k, q) \delta_{\alpha\beta} q_\gamma q_\delta \Gamma_0^{\beta\nu\gamma}(-k, p, -q) \\ N_4^{\mu\nu} &= \Gamma_0^{\mu\alpha\delta}(-p, k, q) k_\alpha k_\beta q_\gamma q_\delta \Gamma_0^{\beta\nu\gamma}(-k, p, -q) \end{aligned} \quad (4.3)$$

Using the form of the bare triple gluon vertex, as used in Eq. 3.10, some simple tensor algebra gives:

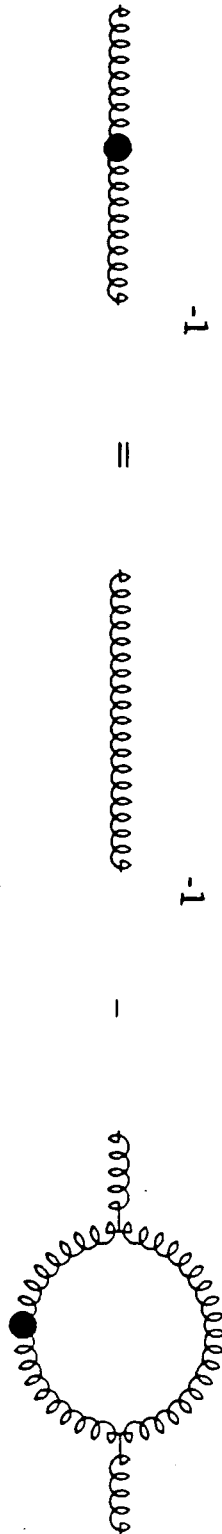


fig. 4.2: The Schwinger-Dyson equation for the inverse gluon propagator using the Mandelstam approximation.

$$\begin{aligned}
 N_1^{\mu\nu} &= \delta^{\mu\nu}(5p^2 - 2p \cdot k + 2k^2) - 2p^\mu p^\nu + 10k^\mu k^\nu - 5(k^\mu p^\nu + p^\mu k^\nu) \\
 N_2^{\mu\nu} &= \delta^{\mu\nu}(p^4 + q^4 - 2q^2 p^2) + k^2 p^\mu p^\nu + k^\mu k^\nu (p^2 + 2p \cdot k - k^2) \\
 &+ (k^\mu p^\nu + p^\mu k^\nu)(k^2 - 3k \cdot p) \\
 N_3^{\mu\nu} &= \delta^{\mu\nu}(p^4 + k^4 - 2k^2 p^2) + (2k^2 - p^2)p^\mu p^\nu + (2p^2 - k^2)k^\mu k^\nu \\
 &- p \cdot k(k^\mu p^\nu + p^\mu k^\nu) \\
 N_4^{\mu\nu} &= p^4 k^\mu k^\nu - p^2 p \cdot k(p^\mu k^\nu + p^\nu k^\mu) + (p \cdot k)^2 p^\mu p^\nu
 \end{aligned} \tag{4.4}$$

Projecting with the tensor $P^{\mu\nu}$, Eq. 3.2, and denoting $N_i = N_i^{\mu\nu} P_{\mu\nu}$ we obtain:

$$\begin{aligned}
 N_1 &= -2p^2 + \frac{40}{3} \frac{(k \cdot p)^2}{p^2} - \frac{10}{3} k^2 - 10k \cdot p \\
 N_2 &= \frac{2}{3} k^2 p^2 - \frac{14}{3} (k \cdot p)^2 + \frac{k^4}{3} + \frac{4}{3} k^2 k \cdot p \\
 &+ \frac{8}{3} \frac{(k \cdot p)^3}{p^2} - \frac{4}{3} \frac{k^2 (k \cdot p)^2}{p^2} \\
 N_3 &= \frac{4}{3} p^2 k^2 - p^4 + \frac{k^4}{3} - \frac{4}{3} \frac{k^2 (k \cdot p)^2}{p^2} \\
 &+ \frac{2}{3} (k \cdot p)^2 \\
 N_4 &= \frac{1}{3} ((k \cdot p)^2 p^2 - p^4 k^2)
 \end{aligned} \tag{4.5}$$

We can now use the results of Appendix A to perform the angular integrals to obtain:

$$\begin{aligned}
 \int \frac{d^4 k}{k^2 q^2} N_1 \mathcal{G}(k) &= \frac{1}{2} \int_0^{p^2} dk^2 \mathcal{G}(k) \left(-4 - 10 \frac{k^2}{p^2} + \frac{20 k^4}{3 p^4} \right) \\
 &\quad + \frac{1}{2} \int_{p^2}^{\kappa^2} dk^2 \mathcal{G}(k) \left(\frac{-22 p^2}{3 k^2} \right) \\
 \int \frac{d^4 k}{k^2 q^2} \frac{N_2}{k^2} \mathcal{G}(k) &= \frac{1}{2} \int_0^{p^2} dk^2 \mathcal{G}(k) \left(-1 + \frac{1 k^2}{3 p^2} \right) \\
 &\quad + \frac{1}{2} \int_{p^2}^{\kappa^2} dk^2 \mathcal{G}(k) \left(\frac{p^2}{k^2} - \frac{5 p^4}{3 k^4} \right) \\
 \int \frac{d^4 k}{k^2 q^2} \frac{N_3}{q^2} \mathcal{G}(k) &= \frac{1}{2} \int_0^{p^2} dk^2 \mathcal{G}(k) \left(-2 + \frac{k^2}{p^2} + 2 \frac{k^4}{p^4} \right) \\
 &\quad + \frac{1}{2} \int_{p^2}^{\kappa^2} dk^2 \mathcal{G}(k) \left(\frac{p^2}{k^2} \right) \\
 \int \frac{d^4 k}{k^2 q^2} \frac{N_4}{k^2 q^2} \mathcal{G}(k) &= \frac{1}{2} \int_0^{p^2} dk^2 \mathcal{G}(k) \left(-\frac{1}{2} \right) \\
 &\quad + \frac{1}{2} \int_{p^2}^{\kappa^2} dk^2 \mathcal{G}(k) \left(-\frac{1 p^4}{2 k^4} \right)
 \end{aligned} \tag{4.6}$$

where we have introduced an ultraviolet cutoff κ^2 making all the integrals in Eq. 4.6 finite. Putting all this together, dividing by p^2 , and factoring out the colour matrix δ^{ab} , we obtain the following equation:

$$\begin{aligned}
 \frac{1}{\mathcal{G}(p)} &= 1 + \frac{C_A g_0^2}{16\pi^2 p^2} \left\{ \int_0^{p^2} dk^2 \mathcal{G}(k) \left[\frac{7k^4}{6p^4} - \frac{17k^2}{6p^2} - \frac{3}{8} \right] \right. \\
 &\quad \left. + \int_{p^2}^{\kappa^2} dk^2 \mathcal{G}(k) \left[-\frac{7p^2}{3k^2} + \frac{7p^4}{24k^4} \right] \right\}
 \end{aligned} \tag{4.7}$$

The beauty of this Mandelstam approximation is that it allows all the angular integrals to be performed analytically, leaving us with just the momentum integration to do. This is to be compared to the far more complicated situation in chapter three. Thus Eq. 4.7 is a far easier equation to deal with numerically,

a feature which will be of essential importance when we come to consider the coupled gluon and quark system in chapter six.

Because of the presence of the ultraviolet cutoff, we have really only defined $\mathcal{G}(p, \kappa)$. As in chapter three we define a renormalised gluon renormalisation function by:

$$Z_G(\kappa/\mu)\mathcal{G}_R(p) = \mathcal{G}(p, \kappa) \quad (4.8)$$

To obtain an equation independent of the cutoff κ^2 , we first evaluate Eq. 4.7 at $p^2 = \mu^2$, where once again μ^2 is some arbitrary momentum. We then subtract this from Eq. 4.7, and use the definition in Eq. 4.8 to obtain a renormalised equation:

$$\frac{1}{\mathcal{G}_R(p)} = \frac{1}{\mathcal{G}_R(\mu)} + \frac{C_A\alpha_1(\mu)}{4\pi} \int_0^{\kappa^2} dk^2 [\mathcal{J}(k, p) - \mathcal{J}(k, \mu)] \mathcal{G}_R(k) \quad (4.9)$$

where the kernel $\mathcal{J}(k, p)$ is simply read off from Eq. 4.7. Here the renormalised running coupling is given as:

$$g^2(\mu) = Z_G(\kappa/\mu)^2 g_0^2 \quad (4.11)$$

and as usual $\alpha_1(\mu) = g^2(\mu)/4\pi$. The subscript on the coupling $\alpha_1(\mu)$ is to distinguish it from the couplings $\alpha_2(\mu), \alpha_3(\mu)$ defined from the quark-gluon vertex which we will meet later in chapters five and six. The consistent renormalisation of the Schwinger-Dyson equations is a highly non-trivial problem, which we discuss further in chapter seven.

We must also mention the gluon mass renormalisation as in section 3.3. A term violating $p^2/\mathcal{G}(p) \rightarrow 0$, as $p^2 \rightarrow 0$ will arise from terms where $\mathcal{G}(p) \sim A\mu^2/p^2$ on the right hand side of Eq. 4.9. This is equivalent to a gluon mass term and must be subtracted. As in the previous chapter, the easiest way to

deal with such mass terms is to subtract the contribution where $\mathcal{G}(p) = A\mu^2/p^2$. Since the right hand side of Eq. 4.9 is linear in $\mathcal{G}(k)$, the effect of this is to completely cancel the contribution of such an infra-red enhanced term to the integrals in Eq. 4.9. Such an enhanced term will, in general, give rise to infra-red divergent integrals (see section 3.3). However, because of the gluon mass renormalisation this term does not appear on the right hand side of Eq. 4.9, and thus no infra-red divergences arise. Thus if we write $\mathcal{G}_R(p) = A\mu^2/p^2 + \mathcal{G}_1(p)$, it is only the term \mathcal{G}_1 which will appear within our integrals.

4.3 The Solution

As in chapter three, it has not proved possible to find an analytic solution to Eq. 4.9, and again we attempt a numerical solution. The analysis of the possible low momentum behaviour of $\mathcal{G}_R(p)$ is similar to the dimensional analysis of section 3.4, so again we look for a solution with the enhanced infra-red term, bearing in mind that the gluon mass renormalisation above means that this term does not contribute to the integrals we must perform. As in section 3.4 we can also extract the asymptotic form of $\mathcal{G}_R(p)$ for large p^2 . By expanding $\mathcal{G}_R = 1 + O(\alpha_1(\mu))$, we easily obtain for the leading behaviour:

$$\frac{1}{\mathcal{G}_R(p)} = \frac{1}{\mathcal{G}_R(\mu)} + \frac{\gamma'_0 \alpha_1(\mu)}{4\pi} \ln \frac{p^2}{\mu^2} \quad (4.11)$$

where the final momentum integral can easily be performed to give $\gamma'_0 = \frac{7}{3}C_A$. Using Eq. 3.33, we can recast our definition of the running coupling in the form:

$$\alpha_1(p) = \alpha_1(\mu) \left(\frac{\mathcal{G}_R(p)}{\mathcal{G}_R(\mu)} \right)^2 \quad (4.12)$$

Again expanding in powers of $\alpha_1(\mu)$, and using Eq. 4.11 we obtain:

$$\frac{1}{\alpha_1(p)} = \frac{1}{\alpha_1(\mu)} + \frac{\beta'_0}{4\pi} \ln \frac{p^2}{\mu^2} \quad (4.13)$$

where we easily see that $\beta'_0 = 2\gamma'_0 = \frac{14}{3}C_A$ from the simple form of Eq. 4.12.

The standard renormalisation group argument yields:

$$\mathcal{G}_R(p) = \mathcal{G}_R(\mu) \left(\frac{\alpha_1(p)}{\alpha_1(\mu)} \right)^{\gamma'_0/\beta'_0} \quad (4.14)$$

Since $\gamma'_0/\beta'_0 = 1/2$, we can use the usual one-loop asymptotic form for the coupling arising from Eq. 4.13, to give us the asymptotic form for $\mathcal{G}_R(p)$ as:

$$\mathcal{G}_R(p) \sim \frac{1}{\left(\ln\left(\frac{p^2}{\mu^2}\right) \right)^{\frac{1}{2}}} \quad (4.15)$$

Again we choose a parameterisation for $\mathcal{G}_R(p)$ which reproduces this asymptotic form, so we first introduce:

$$\mathcal{G}_\infty(p) = \left[1 + \frac{\beta'_0 \alpha_1(\mu)}{4\pi} \ln\left(\frac{p^2}{\mu^2} + 1\right) \right]^{-\gamma'_0/\beta'_0} \quad (4.16)$$

allowing us to parameterise $\mathcal{G}_R(p)$ by:

$$\mathcal{G}_R(p) = \frac{A\mu^2}{p^2} + \mathcal{G}_\infty(p) \left\{ \sum_{n=1}^M a_n \left(\frac{p^2}{p^2 + p_n^2} \right)^{b_n} + \sum_{n=1}^N c_n \left(\frac{p^2 \mu^2}{p^4 + q_n^4} \right)^{d_n} \right\} \quad (4.17)$$

where the parameters $A, a_n, b_n, c_n, d_n, p_n$ and q_n are allowed to vary. Since all the angular integrals have been performed, we can allow the dimensionful parameters p_n, q_n to vary numerically. This is unlike the situation in chapter three, where the corresponding dimensionful parameters were chosen by trial and error. This was because of the large amount of computing time needed when the parameters are allowed to vary under the integral sign, where only one of the angular integrals can be performed numerically. Also, we expect a non-zero value for the coefficient of the infra-red enhanced term A , but again we do not prejudice this result, by allowing the possibility that this parameter can be zero.

As before, we set $\mathcal{G}_R(\mu) = 1$ and choose $\mu^2 = 10 \text{ GeV}^2$. We demand consistent numerical agreement between input and output for the range $0.01 < p^2 < 100 \text{ GeV}^2$, with $\alpha_1(\mu) = 0.15, 0.2, 0.25, 0.3$, i.e $\Lambda_1 = 159, 335, 525, 708 \text{ MeV}$ respectively, where Λ_1 is calculated using Eq. 1.23 with $\beta_0 = \frac{14}{3} C_A$. In fact the equation Eq. 4.9 has a momentum scale dependence which is wholly specified by μ , and by the value of the running coupling $\alpha_1(p)$ at $p^2 = \mu^2$. As usual though, this scale can be defined in terms of an intrinsic parameter of the theory, namely Λ_1 . We find good agreement (to within 1%) with $N, M = 1$ in Eq. 4.17. We plot our results in fig. 4.3, and give the parameters obtained in table 4.1.

| $\alpha(\mu)$ | 0.15 | 0.2 | 0.25 | 0.3 |
|---------------|----------|---------|---------|---------|
| A | 0.004207 | 0.01533 | 0.03254 | 0.05263 |
| a_1 | 0.9313 | 0.9352 | 0.9744 | 1.006 |
| p_0 (GeV) | 0.1794 | 0.3037 | 0.4501 | 0.6121 |
| b_1 | 1.055 | 0.9394 | 1.198 | 1.527 |
| c_1 | 0.1308 | 0.1386 | 0.1079 | 0.09592 |
| q_0 (GeV) | 0.1443 | 0.2636 | 0.3870 | 0.4867 |
| d_1 | 0.4379 | 0.4918 | 0.6605 | 0.8051 |

Table 4.1 : Parameters for $\mathcal{G}_R(p)$, Eq. 4.9, for solutions shown in figs. 4.3.

Once again we obtain solutions which possess the infra-red enhancement we saw in chapter three. Note that the size of this enhanced term rises with Λ_1 exactly as we would expect if Λ_1 is the intrinsic momentum scale of the theory. We discuss this further in chapter seven. In section 4.5 we will discuss the physical implications of this enhancement of $\mathcal{G}_R(p)$ and hence the gluon propagator, and see how it is related to confinement. Before this we first discuss

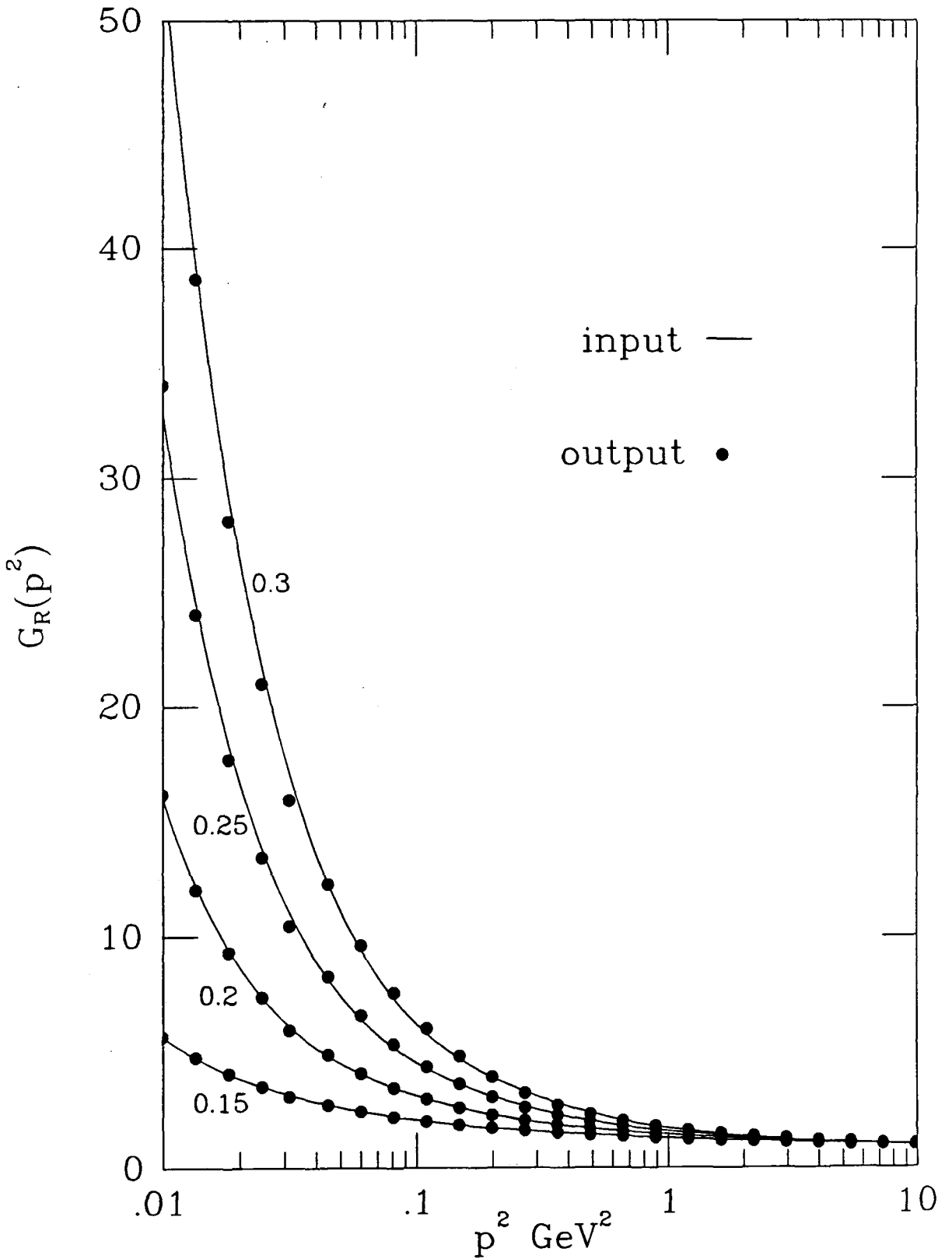


fig 4.3: The gluon renormalisation function $\mathcal{G}_R(p)$ in the Mandelstam approximation, as a function of p^2 , for $\alpha_1(\mu) = 0.15, 0.2, 0.25, 0.3$.

the relationship between the Mandelstam approximation, and the full vertex approximation of chapter three.

4.4 How Good is the Mandelstam Approximation?

In this and the preceding chapter, we have used two different approximation schemes to solve the Schwinger-Dyson equation for the gluon propagator. In both cases we have obtained solutions for the gluon renormalisation function $\mathcal{G}_R(p)$ which has an infra-red enhanced term $A\mu^2/p^2$, which we believe to be indicative of confinement. In chapter three we solved the Slavnov-Taylor identity for the triple gluon vertex in the absence of ghost contributions. This allows us to write the longitudinal part of this vertex in terms of \mathcal{G} , where we drop the subscript R for the discussion of this section. The solution for this longitudinal part is proportional to $1/\mathcal{G}$ with arguments p, k and q . The propagators in the gluon loop of fig. 3.1 contain a factor $\mathcal{G}(k)\mathcal{G}(q)$, and so we obtain three generic terms, proportional to

$$\frac{\mathcal{G}(k)\mathcal{G}(q)}{\mathcal{G}(p)}, \mathcal{G}(k) \text{ and } \mathcal{G}(q) \quad (4.18)$$

The last type can be made equal to the second type by the change of variable $k \rightarrow q, q \rightarrow k$ within the loop integral. The first term we denoted by $\mathcal{L}(k, p)$, the second and third by $\mathcal{K}(k, p)$, see Eq. 3.20. The Mandelstam approximation assumes that the cancellation which occurs for the second and third terms in Eq. 4.18 occurs for the entire vertex.

An essential feature of both our calculations is the gluon mass renormalisation, which subtracts off those terms on the right hand side of Eqs. 3.27 and 4.9, which do not vanish when we multiply by p^2 and let $p^2 \rightarrow 0$. Such contributions only arise from the infra-red enhanced term, so we write $\mathcal{G}(p) = A\mu^2/p^2 + \mathcal{G}_1(p)$, and subtract from these equations the contribution where any \mathcal{G} which appears in the numerator is put *equal* to its infra-red en-

hanced term only. This means that such singular terms do not contribute to the right hand side of the Mandelstam approximation at all, and similarly not in the $\mathcal{K}(k, p)$ terms of the full vertex approximation. After this subtraction the only singular terms which contribute to the $\mathcal{L}(k, p)$ are those where one of the factors of \mathcal{G} in the numerator is equal to $A\mu^2/k^2$, and the other is equal to \mathcal{G}_1 . For example:

$$\frac{(A\mu^2/k^2)\mathcal{G}_1(q)}{\mathcal{G}(p)} \tag{4.19}$$

where the other contribution can be put in a similar form by a change of integration variable. In section 3.5 we define the divergent contributions arising from such a term by means of a plus prescription and the technical details are described there. On dimensional grounds though, the integration must provide a dimensionful quantity to balance the factor of μ^2 . Since the only variable available to us is p^2 , after integrating such a quantity as in Eq. 4.19 we get a contribution proportional to:

$$\frac{(A\mu^2/p^2)W(p)}{\mathcal{G}(p)} \tag{4.20}$$

where $W(p)$ is some function arising from the integration which is well behaved as $p^2 \rightarrow 0$. In this limit the factor in the denominator also behaves like $A\mu^2/p^2$ and cancels with the term in the numerator. Thus the cancellation which occurs completely in the Mandelstam equation, and partially for the $\mathcal{K}(k, p)$ term in the full vertex approximation *before* integration, is seen in a sense, to occur in the infra-red limit of the equation for the $\mathcal{L}(k, p)$ term *after* integration. Since it is in this $p^2 \rightarrow 0$ limit in which using only the longitudinal part of the vertex, and neglecting the transverse part is valid, we might expect that the simpler Mandelstam equation will work. Of course the arguments above concern only the qualitative analytic behaviour, and there is no reason why the Mandelstam

equation should not give quantitatively different results. By comparing fig. 4.3 with fig. 3.2 we see that this is indeed the case. However, as was mentioned in ref. [3.2], although neglecting the transverse part of the triple gluon vertex will not affect the existence of infra-red enhanced solutions, it will affect the coefficient of such a term, and so we should not therefore worry about any further quantitative difference induced by using the Mandelstam approximation.

Another difference between the two approximations lies in the different renormalisations, and hence the different running couplings, Eq. 3.33 and Eq. 4.12. The important fact though, is the dependence of the running coupling on $\mathcal{G}(p)$, and in both cases we have:

$$\alpha(p) \sim \alpha(\mu) \left(\frac{\mathcal{G}(p)}{\mathcal{G}(\mu)} \right)^n \quad (4.21)$$

where $n = 1$ for the full vertex approximation and $n = 2$ for the Mandelstam approximation. Although different, both couplings become strongly enhanced at low p^2 , because of the factor of $\mathcal{G}(p)$ in the numerator. This is exactly what we would expect of the coupling in a confining theory, and in both cases this enhancement is by a power law. In chapter seven we discuss other differences between these couplings, and a later one which we shall meet in the inclusion of quark loops in the gluon equation.

In summary, the cancellation of factors of \mathcal{G} used in the Mandelstam equation is seen to arise in the full vertex approximation, partially before integration, and partially after. The much simpler Mandelstam equation gives rise to qualitatively similar solutions, both for the gluon renormalisation function $\mathcal{G}(p)$ and for the running coupling. Since the Mandelstam equation is far simpler to use, both analytically, and more importantly, numerically, it is this approximation that we shall use in our studies of fermions in a non-Abelian gauge theory in the subsequent chapters.

4.5 Confinement and a $1/p^4$ Gluon Propagator

In the studies of the Schwinger-Dyson equation for the gluon propagator in this and the preceding chapter, we have demonstrated solutions for the gluon renormalisation function $\mathcal{G}(p)$ which are as singular as $1/p^2$ as $p^2 \rightarrow 0$. This in turn means that the gluon propagator is as singular as $1/p^4$. This same behaviour has been found by others[3.2,3.3,4.2] in various different approximations and truncations of these equations. It seems likely then, that this does reflect the true behaviour of the gluon. Before we go on to study the inclusion of coloured fermions in the theory, we first discuss ways in which this infra-red enhanced gluon propagator is related to confinement.

Since we do not 'see' the gluon as a physical particle in the real world, unlike the electron or photon, we cannot immediately translate this low energy, or long distance, enhancement of its propagator directly into physical statements. Indeed, since the gluon propagator itself is not a gauge invariant quantity we should not expect this. Nevertheless, there is good reason to suggest that this enhancement is physically meaningful, and related to the confinement of colour. Here we shall discuss three ways in which to translate the behaviour we have obtained for the propagator into statements about confinement. This is not meant to be an exhaustive study of the implications of our solutions, but they do contain good evidence that the infra-red behaviour we have obtained is indeed a signal of confinement.

(i) The Static Colour Potential

In QED the long range force between two static electric charges is directly related to the photon propagator[2.1]. By virtue of gauge invariance this guarantees the Coulomb $1/r^2$ force law. The connection is based on considering a 'one photon exchange' approximation, which for an Abelian theory correctly gives the large distance limit. For QCD, because of the self coupling of the

gluon, this approximation breaks down[4.3], and we have to consider ‘multi-gluon’ exchanges between static colour charges as well. Nevertheless we present here the ‘one-gluon’ exchange contribution to the large distance behaviour of QCD, which gives us an intuitive feeling for the meaning of a propagator which is as infra-red singular as $1/p^4$. Here we calculate a contribution to the large distance potential between static colour charges. Because the gluon is a vector particle, this one gluon exchange generates a vector contribution to the potential. The multi-gluon exchanges we neglect will generate a scalar component to the potential, and this is expected to play an important role[4.3].

The potential arising from one gluon exchange for a colour singlet state is related to the propagator via:

$$V(\mathbf{r}) = -C_F g^2 \int_{-\infty}^{\infty} dt \Delta_{00}(\mathbf{r}, t) \quad (4.22)$$

where Δ_{00} is the time-time component of the full gluon propagator in configuration space. Using its Fourier transform we obtain:

$$V(\mathbf{r}) = -C_F g^2 \int_{-\infty}^{\infty} dt \int \frac{d^4 k}{(2\pi)^4} \Delta_{00}(k^2) e^{-ik \cdot x} \quad (4.23)$$

where $x = (t, \mathbf{r})$ is the space-time variable. The t integral can be performed to give a delta function of k_0 , allowing the k_0 integral to be performed trivially, giving us:

$$V(\mathbf{r}) = -C_F g^2 \int \frac{d^3 \mathbf{k}}{(2\pi)^3} \Delta_{00}(\mathbf{k}^2) e^{-i\mathbf{k} \cdot \mathbf{r}} \quad (4.24)$$

where \mathbf{k}, \mathbf{r} are three-vectors. Using spherical polar coordinates we obtain:

$$V(\mathbf{r}) = -\frac{C_F \alpha_s}{2\pi^2} \int_0^{\infty} k^2 dk \int_{-1}^1 dz \int_0^{2\pi} d\phi \Delta_{00}(\mathbf{k}^2) e^{-i\mathbf{k} \cdot \mathbf{r} z} \quad (4.25)$$

where $z = \cos\theta$. We perform the ϕ and z integrals to give:

$$V(r) = -\frac{2C_F\alpha_s}{\pi r^3} \int_0^\infty \omega d\omega \sin\omega \Delta_{00}(\omega/r) \quad (4.26)$$

where $\omega = kr$.

Evaluating the gluon propagator at $k_0 = 0$ gives us

$$\Delta_{00}(\mathbf{k}^2) = \frac{\mathcal{G}(\mathbf{k}^2)}{\mathbf{k}^2} \quad (4.27)$$

and so our form for this one gluon exchange potential is:

$$V(r) = -\frac{2C_F\alpha_s}{\pi r} \int_0^\infty d\omega \sin\omega \frac{\mathcal{G}(\omega/r)}{\omega} \quad (4.28)$$

For QED we expect the photon renormalisation function to be approximately one. The potential can be easily calculated to be:

$$\begin{aligned} V_{QED}(r) &= \frac{e_1 e_2}{2\pi^2 r} \int_0^\infty \frac{d\omega}{\omega} \sin\omega \\ &= \frac{e_1 e_2}{4\pi r} \end{aligned} \quad (4.29)$$

where e_1, e_2 are the electric charges of the two particles. This is the usual Coulomb potential. For QCD, however, we have obtained a very different behaviour for $\mathcal{G}(k)$, which we parameterise as $A\mu^2/k^2 + \mathcal{G}_1(k)$. The infra-red enhanced term gives a contribution to the potential

$$V_{IR}(r) = -\frac{2C_F\alpha_s r}{\pi} A\mu^2 \int_{\lambda r}^\infty \frac{d\omega}{\omega^3} \sin\omega \quad (4.30)$$

where we have introduced a small momentum cutoff λ to make the integral finite. Using integration by parts twice, we can write the integral in Eq. 4.30 as:

$$\frac{\sin(\lambda r)}{2(\lambda r)^2} + \frac{\cos(\lambda r)}{2\lambda r} - \frac{1}{2} \int_{\lambda r}^\infty \frac{d\omega}{\omega} \sin\omega \quad (4.31)$$

The integral in Eq. 4.31 is well behaved as $\lambda \rightarrow 0$, so we can expand Eq. 4.31 in powers of λ giving:

$$\int_{\lambda r}^{\infty} \frac{d\omega}{\omega^3} \sin\omega = \frac{1}{\lambda r} - \frac{\pi}{4} \quad (4.32)$$

The first term here gives a contribution to the potential which has no r dependence. Although it diverges in the limit $\lambda \rightarrow 0$ we can always subtract a constant term from a potential, and so we remove this infinite constant, giving us the enhanced contribution to the potential:

$$V_{IR}(r) = \frac{C_F \alpha_s}{2} A \mu^2 r \quad (4.33)$$

Thus our $1/p^4$ propagator generates a linear term to the static colour potential. This linear potential is a good signal for confinement. In a Coulomb potential the flux lines spread out radially to give a $1/r^2$ force law, for a linear potential, they must be squeezed into a narrow 'flux tube' between the colour charges. The energy needed to separate these charges grows linearly with their separation. Eventually it will be energetically more favourable to create a $q\bar{q}$ pair from the vacuum to shorten these stretched lines of flux. This process can be repeated, until the momenta of the created quarks is low enough that they form the bound states we call hadrons.

The $\mathcal{G}_1(\mathbf{k}^2)$ contribution to the potential can be calculated numerically, and the result for $\alpha_s(\mu) = 0.25$ is plotted in fig. 4.4. For comparison we plot it against the phenomenological potential of Quigg and Rosner[4.4], which has been successful in describing the properties of heavy $q\bar{q}$ states, and is simply parameterised as a sum of a linear term and a Coulomb $1/r$ term. From the nature of our solution for \mathcal{G} , we see that this form for the potential arises naturally.

(ii) The Wilson Loop Operator

As we mentioned previously, this naive treatment of the propagator to obtain the static colour potential does not give the whole answer for QCD. Thus we cannot yet conclude that this potential does rise linearly with distance

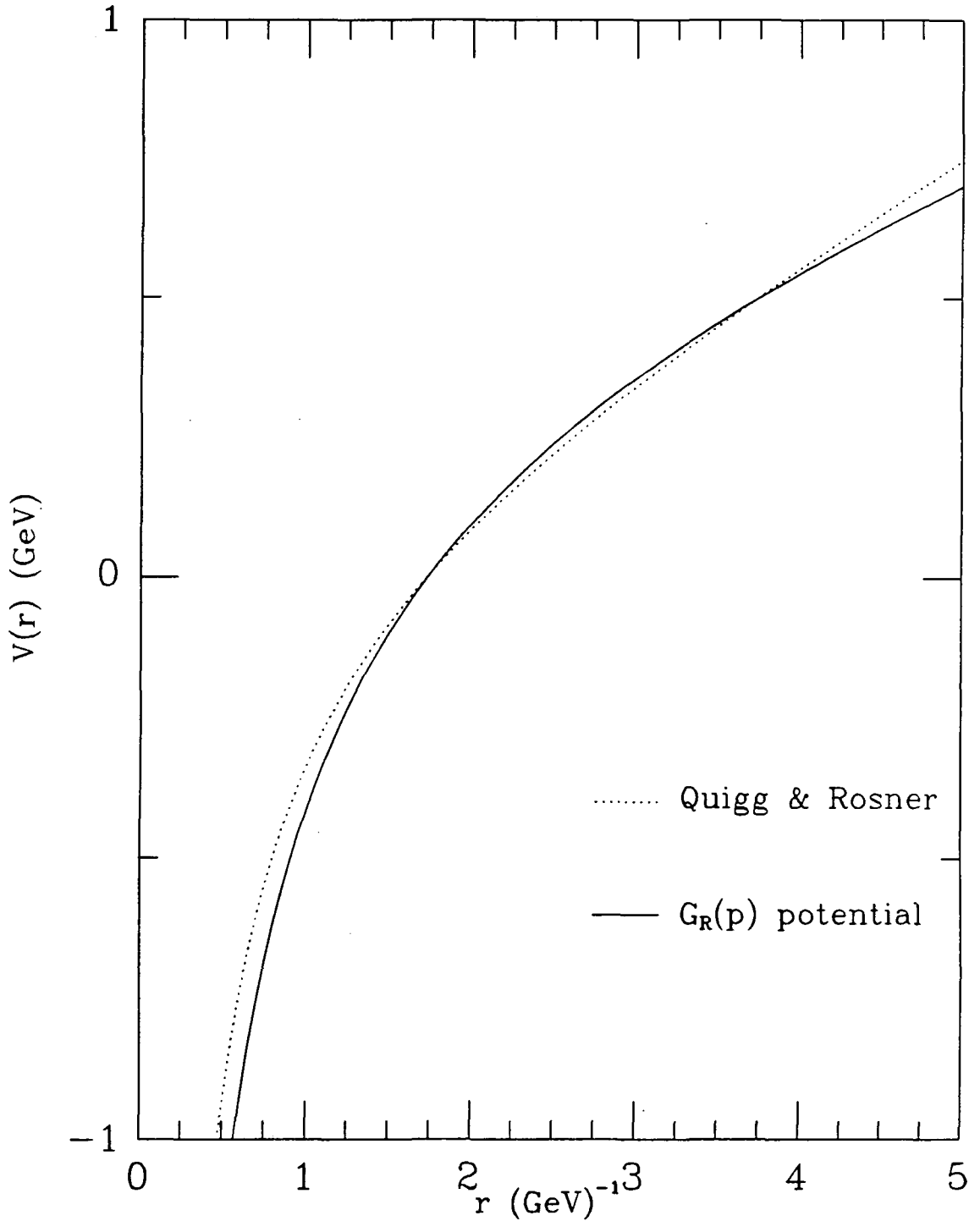


fig. 4.4: The static colour potential $V(r)$ as a function of r , derived from our gluon function $G_R(p)$ with $\alpha_1(\mu) = 0.25$. We have chosen the renormalisation constant to maximise the agreement with a phenomenological potential of Quigg and Rosner in the region probed by $c\bar{c}$ and $b\bar{b}$ spectra.



for large separations. Indeed since the gluon propagator itself is not a gauge invariant quantity, we should not expect to immediately be able to translate its properties into physical statements. A quantity which is gauge invariant, however, is the Wilson loop operator $W(L)$ [1.10], defined by:

$$W(L) = \int [DA] w(L) e^{-S} / \int [DA] e^{-S} \quad (4.34)$$

where $[DA]$ denotes a functional integral over the gauge field, where we are working in Euclidean space. Here we need the quantity $w(L)$ defined by:

$$w(L) = P \exp \left(ig \oint_L dx^\mu A_\mu^a \lambda^a \right) \quad (4.35)$$

which is the integral of the gauge field around a closed loop L in space-time. Here the symbol P denotes the path ordering of the λ^a matrices around the loop, which were introduced in section 1.3. For rectangular loops, in which the time distance is very long compared to the space distance, then the Wilson loop operator is related to the static colour potential[1.7] via:

$$W(L) = \exp \left(-TV(r) \right) \quad (4.36)$$

where T is the length of the time interval. For QCD to confine, it is supposed that $V(r)$ must behave linearly with r for large distances. Writing $V(r) = \kappa r$, where we call κ the string tension, we would find in this case that

$$W(L) = \exp \left(-\kappa A_L \right) \quad (4.37)$$

where A_L is the area enclosed by the loop. This result generalises to any shape of contour. Thus a possible criterion for confinement which is gauge invariant would be that the Wilson loop obeyed a so-called 'area law' for large loops, i.e. that this operator was exponentially damped, with the damping proportional to the area enclosed by the loop. For a non-confining theory such as QED, we

expect the potential to be constant at large distances, and thus the Wilson loop will be exponentially damped only proportional to the perimeter length of the loop.

The Wilson loop is a quantity that can be calculated on a space-time lattice[1.10], and indeed Creutz has shown an area law at least for a lattice SU(2) theory in the strong coupling limit. It is hoped that lattice simulations of QCD will themselves reveal an area law, which will still hold in the continuum limit of these lattice theories (see section 1.5).

An important result by West[4.5] relates the Wilson loop operator to the full gluon propagator. The result states that if in *any* gauge, the full gluon propagator is as singular as $1/p^4$ as $p^2 \rightarrow 0$, then the Wilson loop obeys an area law. This is the result we need, relating our gauge variant propagator to a gauge invariant quantity, which itself is related to the static potential. Some comments are needed here. First of all, since we had to truncate the Schwinger-Dyson equations in order to obtain a closed equation, we cannot yet prove that the enhanced infra-red behaviour we have found is indeed the behaviour of the exact propagator. Nevertheless, the link with our results and a linear confining potential is suggestive. If we could show that this enhanced behaviour does hold for the exact propagator, then it will have essentially been demonstrated that QCD can indeed confine coloured objects. This would provide impressive support for the perturbative successes of QCD.

There have been previous studies of the Schwinger-Dyson equation for the gluon propagator, and it is appropriate here to mention the most important of these, by Baker, Ball and Zachariasen[3.2]. Their study is in many ways similar to our own, but with the crucial difference that they work in an axial gauge instead of a covariant one. This has the bonus that all the ghost terms are absent, greatly simplifying the equations themselves, as well as the Slavnov-Taylor identities. The propagator itself, however, is more complicated, depending on

two scalar functions instead of just the one, namely \mathcal{G} , in our calculation. They employ an approximation in which they assume that the dominant infra-red behaviour is given by only one of these functions, so that their full propagator has the tensor structure of the free one. They also assume that the coefficient of any infra-red enhanced term is independent of the gauge chosen. Under these assumptions the integrals involved in the truncated Schwinger-Dyson equation for the propagator are infra-red finite, even in the presence of the enhanced term. Unfortunately these approximations are put in somewhat by hand, and as usual in axial gauges, there is still the problem of dealing with the spurious singularities when one of the momenta in the problem becomes orthogonal to the vector defining the particular axial gauge. A prescription for dealing with these has also to be introduced 'by hand', and there is still controversy over how to deal with them properly[4.6], even in perturbation theory.

The most compelling reason, however, for choosing to work in a covariant gauge is because of another important result by West[4.7]. Here he shows that because all the particles appearing in axial gauges are physical ones (i.e. no ghosts), that the spectral functions obey certain positivity conditions. The important conclusion from this is that he finds it impossible for the full axial gauge propagator have an infra-red behaviour more singular than $1/p^2$. Note that this does not contradict the results of Baker, Ball and Zachariasen, in that they only considered one of the two scalar functions appearing in the axial gauge propagator. This may well indeed be as infra-red singular as $1/p^4$ even though the full propagator is not. Presumably this enhanced infra-red behaviour would cancel between the two functions. This does, however, call into question their approximation of only considering one of the functions. More importantly, we must relate whatever behaviour we find for the propagator to physical, and hence gauge invariant quantities. The conclusion of this 'no-go' theorem of West's, is that it will be impossible to prove confinement via the Wilson loop in axial

gauges.

Fortunately this theorem does not hold in a covariant gauge, and does not in anyway constrain the possible infra-red behaviour of the covariant gauge propagator. In the light of the problems arising in axial gauges, this is a compelling reason for studying the Schwinger-Dyson equations in a covariant gauge.

(iii) The QCD Vacuum and Dual Chromomagnetic Superconductivity

A different approach to the link between confinement and a $1/p^4$ propagator is related to the ideas of superconductivity[4.8] and electromagnetic duality. This duality is the invariance of Maxwell's equations under the transformations:

$$\mathbf{E} \rightarrow \mathbf{B} \quad \mathbf{B} \rightarrow -\mathbf{E} \quad \rho_e \rightarrow \rho_g \quad \rho_g \rightarrow \rho_e \quad (4.38)$$

Here ρ_e, ρ_g are the electric and magnetic charge densities respectively, and \mathbf{E} and \mathbf{B} are the electric and magnetic field vectors.

First we consider the electromagnetic action in a source-free, translationally invariant medium:

$$S = -\frac{1}{4} \int d^4x d^4y F_{\mu\nu}(x) \epsilon(x-y) F^{\mu\nu}(y) \quad (4.39)$$

as usual $F_{\mu\nu} = \partial_\mu A_\nu - \partial_\nu A_\mu$, and $\epsilon(x-y)$ is the dielectric constant describing the polarisation properties of the medium. For a free theory we have $\epsilon(x-y) = \delta(x-y)$ and Eq. 4.39 reduces to the usual Maxwell action. The action of Eq. 4.39 leads to the equations:

$$\partial_\mu \tilde{G}_{\mu\nu} = 0 \quad \partial_\mu \tilde{F}_{\mu\nu} = 0 \quad (4.40)$$

where:

$$\begin{aligned}\tilde{G}_{\mu\nu}(x) &= \int d^4y \epsilon(x-y) F_{\mu\nu}(y) \\ \tilde{F}_{\mu\nu}(x) &= \frac{1}{2} \epsilon_{\mu\nu\rho\sigma} F^{\rho\sigma}(x)\end{aligned}\tag{4.41}$$

The first of the equations of Eq. 4.40 is the equation of motion, whilst the second is the Bianchi identity.

It is equally possible to formulate this theory in terms of magnetic, or dual potentials B_μ . We introduce $G_{\mu\nu} = \partial_\mu B_\nu - \partial_\nu B_\mu$. Then the action, Eq. 4.39, can be written:

$$S = -\frac{1}{4} \int d^4x d^4y G_{\mu\nu}(x) \mu(x-y) G^{\mu\nu}(y)\tag{4.42}$$

where we call $\mu(x-y)$ the magnetic permeability, which satisfies:

$$\int d^4y \epsilon(x-y) \mu(y-z) = \delta(x-z)\tag{4.43}$$

Using this new action Eq. 4.42, we have the equations:

$$\partial_\mu \tilde{G}_{\mu\nu} = 0 \quad \partial_\mu \tilde{F}_{\mu\nu} = 0\tag{4.44}$$

where

$$\begin{aligned}\tilde{F}_{\mu\nu}(x) &= \int d^4y \mu(x-y) G_{\mu\nu}(y) \\ \tilde{G}_{\mu\nu}(x) &= \frac{1}{2} \epsilon_{\mu\nu\rho\sigma} G^{\rho\sigma}(x)\end{aligned}\tag{4.45}$$

where this time the second of Eq. 4.44 is the equation of motion and the first is the Bianchi identity. The statement of duality, is the invariance of physics under the transformation $F_{\mu\nu} \leftrightarrow G_{\mu\nu}$.

An electric source is best treated by adding a term $J_\nu^E A^\nu$ to Eq. 4.39, changing the first of Eq. 4.40 to $\partial_\mu \tilde{G}_{\mu\nu} = J_\nu^E$. For a magnetic source we can add a term $J_\nu^M B^\nu$ to Eq. 4.42 to change the second of Eq. 4.44 to $\partial_\mu \tilde{F}_{\mu\nu} = J_\nu^M$

The formulation preferred depends on the sources present and the properties of the medium.

We can form the current:

$$\frac{\delta S}{\delta A^\nu(y)} = \partial_\mu \int d^4x F_{\mu\nu}(x) \epsilon(x-y) \quad (4.46)$$

and the current correlation

$$\langle J_\mu(x)^E J_\nu^E(y) \rangle = (\square \delta_{\mu\nu} - \partial_\mu \partial_\nu) \epsilon(x-y) \quad (4.47)$$

Similarly we have the magnetic current correlation:

$$\langle J_\mu(x)^M J_\nu^M(y) \rangle = (\square \delta_{\mu\nu} - \partial_\mu \partial_\nu) \mu(x-y) \quad (4.48)$$

These correlations are nothing more than inverse propagators. In momentum space, the relation Eq. 4.43 between ϵ and μ becomes $\epsilon(k^2)\mu(k^2) = 1$, with both equal to unity for a free theory. Perturbatively we can write:

$$\epsilon(k^2) = 1 + \chi(k^2) \iff \mu(k^2) = 1 - \chi(k^2) \quad (4.49)$$

Since we know that electrically charged particles produce screening for the A_μ potential (i.e. QED), they must produce anti-screening for the B_μ potentials. The opposite will hold for magnetically charged particles or magnetic monopoles. Thus the anti-screening observed in QCD can be ascribed to a 'monopole-like' behaviour, and indeed this can be made somewhat more rigorous[4.9].

We now turn to a consideration of electrical superconductivity. This is a fully non-perturbative phenomenon, with ϵ and μ very different from unity. The most important manifestation of superconductivity is the exclusion of magnetic fields from inside the superconducting medium, suggesting $\mu(k^2) = 0$. In fact we know that magnetic fields penetrate up to the London penetration depth λ_L . So for a finite λ_L we would have at small k^2 that $\mu(k^2) = k^2/m_L^2$, where $m_L = 1/\lambda_L$.

Using the fact that $\epsilon\mu = 1$ we have that for small k^2 that $\epsilon(k^2) = m_L^2/k^2$. Thus for small momenta, using Eq. 4.47 the inverse photon propagator becomes proportional to:

$$(\delta_{\mu\nu} - k_\mu k_\nu/k^2)m_L^2 \quad (4.50)$$

Thus the propagator behaves like $1/m_L^2$ for small momenta, and we see that the photon has acquired a mass. It therefore only propagates over distances comparable to the London length λ_L . On the other hand the inverse propagator for the 'dual' photon, derived from the B_μ potentials, has a small momentum behaviour given by:

$$(\delta_{\mu\nu} - k_\mu k_\nu/k^2)k^4/m_L^2 \quad (4.51)$$

Thus the dual photon propagator is as singular as $1/k^4$ in this limit.

Consider then the theoretical possibility of a 'magnetic superconductor', where exactly the reverse happens. We would now have a massive dual photon, with the photon itself as singular as $1/k^4$ at small momenta.

This result is suggestive, as this is precisely the momentum behaviour we have found for the gluon at small momenta. For QCD though, this analysis is complicated by the non-Abelian nature of the theory. Nevertheless, it is still possible to define dual non-Abelian potentials[4.10], and it is expected that the correlation between the behaviour of the gluon propagator and its dual holds. Thus our result that the gluon propagator is as singular as $1/k^4$ at small momenta can be interpreted as a signal that the QCD vacuum is behaving like an infinite chromo-magnetic, or dual superconductor.

It is interesting to consider what would happen when we put magnetic monopoles inside our ordinary electrical superconductor. Because of the Meissner effect, a single monopole would not be able to exist, as it would take

infinite energy to place it inside our superconductor. With more than one monopole, however, we would have the possibility of forming monopole-anti-monopole bound states, where the two particles would have a separation of the order of the London penetration length or less. In a type I superconductor the magnetic flux would be essentially contained within a small volume, whereas for a type II superconductor the magnetic flux would be squeezed into a small tube, with the monopole and the anti-monopole at the ends.

With a dual or magnetic superconductor, it would be electric monopoles which could not exist singly, but could form bound states with other electric charges.

Thus we can now formulate a physically intuitive, albeit heuristic picture of confinement. The QCD vacuum behaves like a chromo-magnetic superconductor. Colour electric monopoles, such as quarks, cannot exist singly within the vacuum but can form bound states with other quarks. There has been speculation as to whether a type I chromo-magnetic superconductor corresponds to a bag model of hadrons, whereas the type II version would correspond to flux-tube solutions. Indeed in a closer study of the dual formulation of QCD[4.10] explicit flux-tube solutions have been constructed, displaying much of the behaviour we might expect. A signal for this picture of confinement might well be the $1/k^4$ propagator that our investigation of the Schwinger-Dyson equations has suggested.

CHAPTER FIVE

THE FERMION EQUATION

5.1 Introduction

We now turn to the Schwinger-Dyson equation for the inverse fermion propagator in a non-Abelian gauge theory. In a similar manner to the derivation of the gluon equation in section 2.4 we can derive an integral equation for the quark propagator. Again we use the fact that the functional integral of a derivative vanishes to obtain:

$$\left\langle \frac{\delta S}{\delta \bar{\psi}(x)} \right\rangle + \eta(x) = 0 \quad (5.1)$$

Using Eq. 2.35 and the QCD Lagrangian Eq. 2.38, we obtain:

$$\frac{\delta \Gamma}{\delta \bar{\psi}_{\alpha i}(x)} = (i\not{D} - m)\psi_{\alpha i} + g\Lambda_{0\alpha\beta ij}^{\mu a}(x_1, x, x_2) \langle A^{a\mu}(x_1)\psi_{\beta j}(x_2) \rangle \quad (5.2)$$

In terms of classical fields and connected Green's functions, we can write this as:

$$\begin{aligned} \frac{\delta \Gamma}{\delta \bar{\psi}_{\alpha i}(x)} &= (i\not{D} - m)\psi_{\alpha i} + g\Lambda_{0\alpha\beta ij}^{\mu a}(x_1, x, x_2) \times \\ &\times \left(\frac{\delta^2 W}{i\delta J^{\mu a}(x_1) i\delta \bar{\eta}_{\beta j}(x_2)} + A^{a\mu}(x_1)\psi_{\beta j}(x_2) \right) \end{aligned} \quad (5.3)$$

Taking the derivative of Eq. 5.3 with respect to $\psi_{\beta j}(y)$ and setting the source terms and the classical fields to zero gives us:

$$\begin{aligned} -\frac{\delta^2 \Gamma}{\delta \bar{\psi}_{\alpha i}(x) \delta \psi_{\beta j}(y)} &= (i\not{D} - m)\delta(x - y) + g\Lambda_{0\alpha\beta ij}^{\mu a}(x_1, x, x_2) \times \\ &\times \left(\frac{-\delta^3 W}{i\delta J^{\mu a}(x_1) i\delta \bar{\eta}_{\beta j}(x_2) i\delta \eta_{\beta' j'}(y')} \frac{i\delta \eta_{\beta' j'}(y')}{\delta \psi_{\beta j}(y)} \right) \end{aligned} \quad (5.4)$$

Now $i\delta\eta/\delta\psi$ is equal to the inverse quark propagator from Eq. 2.35, and so we obtain the equation depicted in fig. 5.1.

Our aim is to solve this equation for the fermion renormalisation function $\mathcal{F}(p)$, see ref. [5.1] for previous studies of this equation. Of course, once we have fermions in our theory we must include their effects in the pure gauge sector, by considering closed fermion loops, which occur, for example, in the gluon equation. As a first approximation, however, we can neglect these terms in the so-called ‘quenched’ approximation. In this limit, the equation for the inverse gluon propagator is that of a pure gauge theory. Thus we can take our solution for $\mathcal{G}(p)$ and use it whenever it occurs in the fermion equation.

The real world of course, contains the fermions we call quarks which do couple to the gluons. In chapter six we will consider the equations for the gluon and quark as a coupled system, fully including the dynamical effects of the fermions in the gluon equation. As a first step towards this, the ‘quenched’ approximation serves to outline the type of solutions we might expect in the full theory, as well as setting up the machinery for the more involved study later.

5.2 The Ward Identity and the Equation for $\mathcal{F}(p)$

As in the discussion before Eq. 2.76, we write the full fermion propagator as:

$$S_F(p) = \frac{\mathcal{F}(p)}{\not{p}} \quad (5.5)$$

Using this we can write the diagrammatic equation depicted in fig. 5.1 as:

$$S_F^{-1}(p) = S_{0F}^{-1}(p) - \frac{g_0^2 C_F}{16\pi^4} \int d^4k \gamma^\mu S_F(q) \Gamma^\nu(k, q, p) \Delta_{\mu\nu}(k) \quad (5.6)$$

Here S_{0F} is the bare fermion propagator, i.e. Eq. (5.5) with $\mathcal{F}(p) \equiv 1$, C_F the appropriate color factor, $(N_C^2 - 1)/2N_C$, and $\Gamma^\nu(k, q, p)$ is the full quark-gluon vertex. As before $q = p - k$.

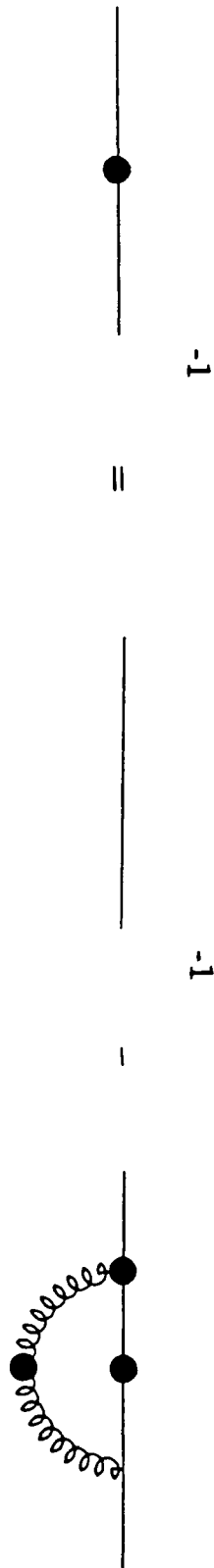


fig. 5.1: The Schwinger-Dyson equation for the inverse fermion propagator in a gauge theory.

Once again it is the infra-red or low momentum behaviour we are interested in, and as demonstrated in section 2.3, it is the longitudinal part of the vertex function Γ_μ^L which determines this. Once again we can use the Slavnov-Taylor identity for the quark-gluon vertex [2.7] to determine this longitudinal part. Neglecting ghost contributions as before, this reduces to the Ward identity of an Abelian theory, Eq. 2.75, which we solve for the longitudinal part, give in Eq. 2.76. Using this, and the solution we obtained for the gluon function $\mathcal{G}(p)$ in chapter four, we can now derive a closed integral equation for the fermion renormalisation function $\mathcal{F}(p)$,

$$\frac{\not{p}}{\mathcal{F}(p)} = \not{p} - \frac{g_0^2 C_F}{16\pi^4} \int d^4 k \frac{\gamma_\mu \not{k} \Gamma_\nu^L}{q^2 k^4} (k^2 \delta^{\mu\nu} - k^\mu k^\nu) \mathcal{G}(k) \mathcal{F}(q) \quad (5.7)$$

As an aside, we note that we have only included massless fermions. In general, the mass is also a dynamical function of p^2 , and its contribution to the Ward identity of Eq. 2.75 can be determined [2.7]. Formally, however, a solution to the Schwinger-Dyson equation in which this dynamical mass is identically zero always exists, at least for vertex functions of the form of Eq. 2.76. However, there is the possibility of addressing the important question of chiral symmetry breaking through these equations, and there have been some studies in toy models [5.2], and in more realistic calculations [5.3]. Nevertheless, to a good approximation, the non-generation of a dynamical mass should be a valid approximation, at least for the first generation of quarks.

Returning to Eq. 5.7, we take its trace having first multiplied by $\not{p}/4$ to obtain:

$$\frac{1}{\mathcal{F}(p)} = 1 - \frac{g_0^2 C_F}{16\pi^4} \int d^4 k \frac{\text{Tr}[\not{p} \gamma_\mu \not{k} \Gamma_\nu^L]}{4p^2 q^2 k^4} (k^2 \delta^{\mu\nu} - k^\mu k^\nu) \mathcal{G}(k) \mathcal{F}(q) \quad (5.8)$$

To perform the algebra, we write $\Gamma_\nu^L = \Gamma_\nu^1 + \Gamma_\nu^2$, where:

$$\begin{aligned}\Gamma_\nu^1 &= \frac{1}{2} \left[\frac{1}{\mathcal{F}(q)} + \frac{1}{\mathcal{F}(p)} \right] \gamma_\nu \\ \Gamma_\nu^2 &= \frac{1}{2} \left[\frac{1}{\mathcal{F}(q)} - \frac{1}{\mathcal{F}(p)} \right] \frac{(\not{q} + \not{p})}{q^2 - p^2} (q + p)_\nu\end{aligned}\quad (5.9)$$

Defining:

$$2I_1(k, p) = \frac{1}{4} \text{Tr}[\not{p} \gamma_\mu \not{q} \gamma_\nu] (k^2 \delta^{\mu\nu} - k^\mu k^\nu) \quad (5.10)$$

Using the usual manipulations of spin algebra we first work out

$$\begin{aligned}\gamma_\mu \not{q} \gamma_\nu (k^2 \delta^{\mu\nu} - k^\mu k^\nu) &= k^2 \gamma^\mu \not{q} \gamma_\mu - \not{k} \not{q} \not{k} \\ &= -2k^2 \not{q} - 2k \cdot q \not{k} + \not{q} k^2 \\ &= -\not{q} k^2 - 2k \cdot q \not{k}\end{aligned}\quad (5.11)$$

Multiplying by $\not{p}/4$ and taking the trace gives:

$$\begin{aligned}I_1(k, p) &= \frac{1}{2} (-q \cdot p k^2 - 2k \cdot q k \cdot p) \\ &= \frac{1}{2} (-p^2 k^2 + k \cdot p k^2 - 2(k \cdot p)^2 + 2k^2 k \cdot p) \\ &= \frac{1}{2} (3k^2 k \cdot p - p^2 k^2 - 2(k \cdot p)^2)\end{aligned}\quad (5.12)$$

Next, defining

$$2I_2(k, p) = \frac{1}{4} \text{Tr}[\not{p} \gamma^\mu \not{q} (\not{q} + \not{p})] (q + p)^\nu (k^2 \delta^{\mu\nu} - k^\mu k^\nu) \quad (5.13)$$

we first work out

$$\begin{aligned}&\gamma^\mu \not{q} (\not{q} + \not{p}) (q + p)^\nu (k^2 \delta^{\mu\nu} - k^\mu k^\nu) \\ &= (\not{q} + \not{p}) \not{q} (\not{q} + \not{p}) k^2 - \not{k} \not{q} (\not{q} + \not{p}) (k \cdot q + k \cdot p) \\ &= 2(q + p) \cdot q k^2 (\not{q} + \not{p}) - (q + p)^2 k^2 \not{q} - \not{k} q^2 (k \cdot q + k \cdot p) \\ &\quad - \not{k} p^2 (k \cdot q + k \cdot p) + k^2 \not{p} (k \cdot q + k \cdot p)\end{aligned}\quad (5.14)$$

Once again we multiply by $\not{p}/4$ and take the trace to obtain:

$$\begin{aligned}
 I_2(k, p) &= \frac{1}{2} [2(2p^2 + k^2 - 3k \cdot p)k^2(2p^2 - k \cdot p) - (2p - k)^2 k^2 (p^2 - k \cdot p) \\
 &\quad + (2k \cdot p - k^2)(k^2 p^2 - 2p^2 k \cdot p - k^2 k \cdot p + 2(k \cdot p)^2)] \\
 &= k^4 p^2 - k^2 (k \cdot p)^2 - 2k^2 p^2 (k \cdot p) + 2(k \cdot p)^3 - 2p^2 (k \cdot p)^2 + 2p^4 k^2
 \end{aligned} \tag{5.15}$$

A useful way of writing $I_2(k, p)$ can easily be verified to be:

$$\begin{aligned}
 I_2(k, p) &= (k^2 p^2 - (k \cdot p)^2)(k^2 - 2k \cdot p + 2p^2) \\
 &= (k^2 p^2 - (k \cdot p)^2)(q^2 + p^2)
 \end{aligned} \tag{5.16}$$

This allows us to write the equation for $\mathcal{F}(p)$ as:

$$\begin{aligned}
 \frac{1}{\mathcal{F}(p)} &= 1 - \frac{g_0^2 C_F}{16\pi^4} \int d^4 k \frac{\mathcal{G}(k)\mathcal{F}(q)}{p^2 q^2 k^4} \left[I_1(k, p) \left(\frac{1}{\mathcal{F}(p)} + \frac{1}{\mathcal{F}(q)} \right) \right. \\
 &\quad \left. + I_2(k, p) \left(\frac{1}{\mathcal{F}(q)} - \frac{1}{\mathcal{F}(p)} \right) \frac{1}{q^2 - p^2} \right]
 \end{aligned} \tag{5.17}$$

where $I_1(k, p)$ and $I_2(k, p)$ are given in Eqs. 5.12 and 5.16 respectively. This equation, however, is in terms of bare quantities and contains divergences which need to be renormalised, which we now proceed to do.

5.3 Renormalisation

As it stands Eq. 5.17 contains the usual logarithmic ultraviolet divergences as well as being potentially infra-red divergent as a result of the enhanced low momentum behaviour of $\mathcal{G}(p)$ we have discovered in the preceding chapters. This equation is somewhat more complicated than that for the gluon we considered in chapter four, as it involves both \mathcal{F} and \mathcal{G} . As usual, we make the equation ultraviolet finite by introducing a running coupling. Before we do this, however, we note the similarity of the structure of Eq. 5.17 to that of the gluon equation,

Eq. 3.27, we considered in chapter three. Generically we have two types of terms, one set proportional to $\mathcal{G}(k)$, the other proportional to $\mathcal{G}(k)\mathcal{F}(q)/\mathcal{F}(p)$. As in section 3.3, there is a slight technicality with the terms in $I_2(k, p)$ because of the factor $1/(q^2 - p^2)$. To deal with these we write $I_2(k, p)$ in the following way:

$$\begin{aligned} I_2(k, p) &= (q^2 + p^2)(k^2 p^2 - (k \cdot p)^2) \\ &= (q^2 - p^2)(k^2 p^2 - (k \cdot p)^2) + 2p^2(k^2 p^2 - (k \cdot p)^2) \end{aligned} \quad (5.18)$$

In the first term the factor $q^2 - p^2$ cancels between the denominator and the numerator. As in section 3.3 this split is by no means unique, but once again, the term we have added and subtracted contains less powers of k^2 in the numerator and so is ultraviolet convergent.

We can now cast Eq. 5.18 in the following form:

$$\frac{1}{\mathcal{F}(p)} = 1 - \frac{g_0^2 C_F}{16\pi^4} \int d^4 k \mathcal{G}(k) \mathcal{K}(k, p) - \frac{g_0^2 C_F}{16\pi^4} \frac{1}{\mathcal{F}(p)} \int d^4 k \mathcal{G}(k) \mathcal{L}(k, p) \quad (5.19)$$

where

$$\begin{aligned} \mathcal{K}(k, p) &= \frac{1}{k^4 q^2 p^2} [I_1(k, p) + k^2 p^2 - (k \cdot p)^2] \\ \mathcal{L}(k, p) &= \frac{1}{k^4 q^2 p^2} \left(\mathcal{F}(q) [I_1(k, p) - k^2 p^2 + (k \cdot p)^2] \right. \\ &\quad \left. + 2p^2 (k^2 p^2 - (k \cdot p)^2) \left[\frac{\mathcal{F}(p) - \mathcal{F}(q)}{q^2 - p^2} \right] \right) \end{aligned} \quad (5.20)$$

At this stage, $\mathcal{F}(p)$ is formally $\mathcal{F}(p, \kappa, \lambda)$, where λ, κ are infra-red and ultraviolet cutoffs respectively, introduced to make the integrals in Eq. 5.19 finite. Infra-red divergences arise only from the enhanced $1/k^2$ term in $\mathcal{G}(k)$, and as we shall later show, only in the second integral of Eq. 5.19 involving $\mathcal{L}(k, p)$, the other being infra-red finite.

To deal with the ultraviolet divergences, we introduce a running coupling defined by:

$$g^2(\mu) = \frac{g_0^2 Z_G(\kappa/\mu)}{1 - \frac{g_0^2 C_F}{16\pi^4} \int d^4 k \mathcal{K}(k, \mu) \mathcal{G}(k, \kappa)} \quad (5.21)$$

where we introduce the renormalised functions \mathcal{G}_R (as in section 4.2) and \mathcal{F}_r specified by:

$$Z_G(\kappa/\mu) \mathcal{G}_R(p) = \mathcal{G}(p, \kappa) \quad (5.22)$$

$$Z_F(\kappa/\mu, \lambda/\mu) \mathcal{F}_r(p, \lambda) = \mathcal{F}(p, \lambda, \kappa)$$

Note that since this definition only involves the \mathcal{K} term, all the quantities in in Eq. 5.21 are infra-red finite, and this coupling is well defined when $\lambda \rightarrow 0$.

Using Eq. 5.19 we can also write this coupling as:

$$g^2(\mu) = \frac{g_0^2 Z_G(\kappa/\mu) Z_F(\kappa/\mu, \lambda/\mu) \mathcal{F}_r(\mu, \lambda)}{1 + \frac{g_0^2 C_F}{16\pi^4} \int d^4 k \mathcal{L}_r(k, \mu) \mathcal{G}(k, \kappa)} \quad (5.23)$$

where $\mathcal{L}_r(k, \mu)$ is the same as $\mathcal{L}(k, \mu)$, but with \mathcal{F} replaced by \mathcal{F}_r in Eq. 5.17.

Inverting Eq. 5.21 gives:

$$\frac{Z_G(\kappa/\mu)}{g^2(\mu)} = \frac{1}{g_0^2} - \frac{C_F}{16\pi^4} \int d^4 k \mathcal{K}(k, \mu) \mathcal{G}(k, \kappa) \quad (5.24)$$

Following the same procedure we used in Eqs. 3.28-3.33, we subtract Eq. 5.21 from itself evaluated at p , which gives:

$$\frac{Z_G(\kappa/p)}{g^2(p)} = \frac{Z_G(\kappa/\mu)}{g^2(\mu)} - \frac{C_F Z_G(\kappa/\mu)}{16\pi^4} \int d^4 k \mathcal{G}_R(k) [\mathcal{K}(k, p) - \mathcal{K}(k, \mu)] \quad (5.25)$$

We now use Eq. 3.32, which simply derives from the definitions in Eq. 5.22 to give:

$$\frac{1}{g^2(p)} = \frac{\mathcal{G}_R(\mu)}{\mathcal{G}_R(p)} \left(\frac{1}{g^2(\mu)} - \frac{C_F}{4\pi^3} \int d^4 k \mathcal{G}_R(k) (\mathcal{K}(k, p) - \mathcal{K}(k, \mu)) \right). \quad (5.26)$$

Introducing $\alpha_2(\mu) = g^2(\mu)/4\pi$, we can expand Eq. 5.26 in powers of $\alpha_2(\mu)$ to give:

$$\frac{1}{\alpha_2(p)} = \frac{1}{\alpha_2(\mu)} + \frac{\beta_0''}{4\pi} \ln \frac{p^2}{\mu^2} \quad (5.27)$$

where $\beta_0'' = \frac{7}{3}C_A + \frac{3}{4}C_F$. The C_A term comes from expanding the $1/\mathcal{G}_R(p)$, using the result of Eq. 4.10. The C_F term comes from the integral in Eq. 5.26 with $\mathcal{G}_R(k) = 1 + O(\alpha_2)$, see Appendix A for the simple integrals needed to calculate this. It is important to note that this coupling differs from $\alpha_1(\mu)$ defined in chapter four. We postpone a discussion of this, and the consistency of the renormalisations we have used until chapter seven.

Again we follow the manipulations of section 3.3, inverting Eqs. 5.21 and 5.23 in terms of the bare coupling g_0 to give:

$$g_0^2 Z_G(\kappa/\mu) = \frac{g^2(\mu)}{1 + \frac{C_F g^2(\mu)}{16\pi^4} \int d^4k \mathcal{G}_R(k) \mathcal{K}(k, \mu)} \quad (5.28)$$

$$g_0^2 Z_G(\kappa/\mu) Z_F(\kappa/\mu, \lambda/\mu) = \frac{g^2(\mu)}{\mathcal{F}_r(\mu, \lambda) - \frac{C_F g^2(\mu)}{16\pi^4} \int d^4k \mathcal{G}_R(k) \mathcal{L}_r(k, \mu)}$$

Substituting these expressions in Eq. 5.19 gives after the usual rearrangement the ultraviolet renormalised equation:

$$\frac{\mathcal{F}_r(\mu, \lambda)}{\mathcal{F}_r(p, \lambda)} = 1 - \frac{\alpha_2(\mu) C_F}{4\pi^3} \left[\int d^4k \mathcal{G}_R(k) (\mathcal{K}(k, p) - \mathcal{K}(k, \mu)) + \int d^4k \mathcal{G}_R(k) (\mathcal{L}_r(k, p) - \mathcal{L}_r(k, \mu)) \right] \quad (5.29)$$

Before we proceed further, we must deal with the infra-red divergences which arise from the enhanced $A\mu^2/k^2$ term in the gluon renormalisation function $\mathcal{G}_R(k)$. First of all, we determine the form of these divergences by setting $\mathcal{G}_R(k) = A\mu^2/k^2$ in Eq. 5.26. The \mathcal{K} -term gives rise to an integral:

$$\begin{aligned} & \int d^4k \frac{A\mu^2}{k^2} \left(\frac{I_1(k, p) + k^2 p^2 - (k \cdot p)^2}{k^4 q^2} \right) \\ &= \int d^4k \frac{A\mu^2}{k^2} \left(\frac{\frac{3}{2} k^2 k \cdot p - 2(k \cdot p)^2 + \frac{1}{2} k^2 p^2}{k^4 q^2} \right) \end{aligned} \quad (5.30)$$

Using the angular integrals in Appendix A, Eq. A.28, we find that this is equal to:

$$\begin{aligned} & \frac{A\pi^2}{2} \int_{\lambda^2}^{p^2} \frac{dk^2}{k^4} \left[\frac{3k^4}{2p^2} - k^2 + \frac{k^4}{p^2} + k^2 \right] \\ & + \frac{A\pi^2}{2} \int_{p^2}^{\kappa^2} \frac{dk^2}{k^4} \left[\frac{3p^4}{2k^2} - \frac{p^4}{k^2} - p^2 + p^2 \right] \end{aligned} \quad (5.31)$$

This explicitly demonstrates that the infra-red divergent terms in the first of these integrals cancel, leaving us with a finite contribution, as we mentioned earlier. The \mathcal{L}_r -term involves the following integral:

$$\begin{aligned} & \int \frac{d^4 k}{k^4 q^2} \frac{A\mu^2}{k^2} \left[(I_1(k, p) - k^2 p^2 + (k \cdot p)^2) \mathcal{F}_r(q, \lambda) \right. \\ & \left. + 2p^2 (k^2 p^2 - (k \cdot p)^2) \frac{\mathcal{F}_r(p, \lambda) - \mathcal{F}_r(q, \lambda)}{q^2 - p^2} \right] \end{aligned} \quad (5.32)$$

We split the range of integration into two regions (i) $\lambda^2 < k^2 < p^2$ and (ii) $p^2 < k^2$. The infra-red divergences occur in the first of these regions, and we extract the divergent terms explicitly by writing the term in square brackets in Eq. 5.32 as:

$$\begin{aligned} & [I_1(k, p) - k^2 p^2 + (k \cdot p)^2] (\mathcal{F}_r(q, \lambda) - \mathcal{F}_r(p, \lambda)) \\ & + [I_1(k, p) - k^2 p^2 + (k \cdot p)^2] \mathcal{F}_r(p, \lambda) \\ & + 2p^2 (k^2 p^2 - (k \cdot p)^2) \left[\frac{\mathcal{F}_r(p, \lambda) - \mathcal{F}_r(q, \lambda)}{q^2 - p^2} + \mathcal{F}'_r(p, \lambda) \right] \\ & - 2p^2 (k^2 p^2 - (k \cdot p)^2) \mathcal{F}'_r(p, \lambda) \end{aligned} \quad (5.33)$$

Here the prime denotes a derivative with respect to p^2 . Essentially all we have done is to add and subtract a term which cancels with the integrand in the limit $k^2 \rightarrow 0$, using the first term in a Taylor expansion of \mathcal{F}_r . Thus the first and third of the terms in Eq. 5.33 are infra-red finite, leaving us with the divergent integral:

$$\int_{\lambda^2 < k^2 < p^2} \frac{d^4 k}{k^4 q^2} \frac{A\mu^2}{k^2} \left[(I_1(k, p) - k^2 p^2 + (k \cdot p)^2) \mathcal{F}_r(p, \lambda) - 2p^2 (k^2 p^2 - (k \cdot p)^2) \mathcal{F}'_r(p, \lambda) \right] \quad (5.34)$$

Since the argument of \mathcal{F}_r in Eq. 5.36 is p , the angular integrals can be performed (see Appendix A) to give us:

$$\frac{\pi^2}{2} \int_{\lambda^2}^{p^2} dk^2 \frac{A\mu^2}{k^2} \frac{1}{k^2} \left[\left(\frac{3}{2} \frac{k^4}{p^2} - 3k^2 \right) \mathcal{F}_r(p, \lambda) - 2p^2 \mathcal{F}'_r(p, \lambda) \left(2k^2 - \frac{1}{2} \frac{k^4}{p^2} - \frac{1}{2} k^2 \right) \right] \quad (5.35)$$

The terms with a factor of k^4 in the numerator are obviously finite, so we read off the divergent terms as:

$$\begin{aligned} \frac{\pi^2}{2} \int_{\lambda^2}^{p^2} dk^2 \frac{A\mu^2}{k^2} [-3k^2 \mathcal{F}_r(p, \lambda) - 3k^2 p^2 \mathcal{F}'_r(p, \lambda)] \\ = - \frac{3\pi^2 A\mu^2}{2} \left(\mathcal{F}_r(p, \lambda) + p^2 \mathcal{F}'_r(p, \lambda) \right) \ln \frac{p^2}{\lambda^2} \end{aligned} \quad (5.36)$$

We can therefore write Eq. 5.29 in the symbolic form:

$$\frac{\mathcal{F}_r(\mu, \lambda)}{\mathcal{F}_r(p, \lambda)} = 1 + A(p, \mu) + \frac{1}{\mathcal{F}_r(p, \lambda)} \left[B(p, \mu) + C(p, \mu) \ln \frac{\lambda}{\mu} \right] \quad (5.37)$$

Here the $A(p, \mu)$ term comes from the \mathcal{K} -term which was infra-red finite. The \mathcal{L} -term is divided into a finite piece $B(p, \mu)$ and a divergent piece, being $\ln(\lambda/\mu)$ times $C(p, \mu)$. The form of $C(p, \mu)$ is easily read off from Eqs. 5.37 and Eq. 5.29 to be:

$$C(p, \mu) = - \frac{3\alpha_2(\mu) C_F}{4\pi} \left[\frac{\mathcal{F}_r(p, \lambda)}{p^2} + \mathcal{F}'_r(p, \lambda) - \frac{\mathcal{F}_r(\mu, \lambda)}{\mu^2} - \mathcal{F}'_r(\mu, \lambda) \right] \quad (5.38)$$

Note we have used the identity $\ln(p^2/\lambda^2) = \ln(p^2/\mu^2) - 2\ln(\lambda/\mu)$ in going from Eq. 5.36 to Eq. 5.38, and included the $\ln p^2/\mu^2$ term in $B(p, \mu)$. We have also

included the infra-red finite terms from Eqs. 5.33 and 5.35 in $B(p, \mu)$. Both $A(p, \mu)$ and $B(p, \mu)$ also include the contributions where we have used $\mathcal{G}_1(k)$ for the gluon function, where as before we use $\mathcal{G}_R(p) = A\mu^2/p^2 + \mathcal{G}_1(p)$. This term has no infra-red enhancement, and so all the integrals will converge as $\lambda \rightarrow 0$. Unlike the expression for $C(p, \mu)$, Eq. 5.38, no easy analytic form exists for $A(p, \mu)$ and $B(p, \mu)$, and they are evaluated numerically on a computer.

Before we do this, however, we must make our equation infra-red finite by eliminating the dependence on λ . To do this we take Eq. 5.37 and evaluate it at $p^2 = \mu'^2$. λ can then be simply eliminated between the two equations to give:

$$\begin{aligned} \frac{1}{C(p, \mu)} \left(\mathcal{F}_r(\mu, \lambda) - B(p, \mu) - \mathcal{F}_r(p, \lambda)(1 + A(p, \mu)) \right) \\ = \frac{1}{C(\mu', \mu)} \left(\mathcal{F}_r(\mu, \lambda) - B(\mu', \mu) - \mathcal{F}_r(\mu', \lambda)(1 + A(\mu', \mu)) \right) \end{aligned} \quad (5.39)$$

The term $B(p, \mu)$ contains a factor \mathcal{F}_r in its integral definition from Eq. 5.29. Thus the numerator of Eq. 5.39 is linear in \mathcal{F}_r , as is the denominator from Eq. 5.38. Thus we define a factor $Z_{IR}(\lambda/\mu)$ such that:

$$\mathcal{F}_r(p, \lambda) = Z_{IR}(\lambda/\mu) \mathcal{F}_R(p) \quad (5.40)$$

where $\mathcal{F}_R(p)$ is the ultraviolet and infra-red finite fermion renormalisation function. The factor $Z_{IR}(\lambda/\mu)$ cancels between numerator and denominator, and we can rewrite our renormalised equation as:

$$\begin{aligned} \frac{\mathcal{F}_R(\mu)}{\mathcal{F}_R(p)} = 1 + A(p, \mu) + \frac{B(p, \mu)}{\mathcal{F}_R(p)} + \frac{C(p, \mu)}{C(\mu', \mu)} \frac{1}{\mathcal{F}_R(p)} \left[\mathcal{F}_R(\mu) - \mathcal{F}_R(\mu') \right] \\ - \frac{C(p, \mu)}{C(\mu', \mu)} \frac{\mathcal{F}_R(\mu')}{\mathcal{F}_R(p)} \left[A(\mu', \mu) + \frac{B(\mu', \mu)}{\mathcal{F}_R(\mu')} \right] \end{aligned} \quad (5.41)$$

It is important to mention that this way of dealing with the infra-red divergences is different to the method employed in chapter three, where we defined finite quantities by means of a ‘plus’ prescription. A fuller discussion of this, and other features of the infra-red problems of these equations appears in chapter seven. There is no contradiction with the calculations of chapter three, however, since it is the gluon function determined by the Mandelstam approximation in chapter four that we have used here. There any infra-red divergences were removed by the gluon mass renormalisation, and the problem did not arise.

Eq. 5.41 is a complicated equation to solve, but it is possible to simplify it. Since the equation is invariant when we multiply \mathcal{F}_R by a constant (this is easiest seen from the form of the unrenormalised equation Eq. 5.19), we can essentially see it as an equation for $\mathcal{F}_R(p)/\mathcal{F}_R(\mu)$. Thus the value of $\mathcal{F}_R(\mu)$ is not determined and we will later set it equal to 1. We can now rewrite Eq. 5.41, returning to the form of Eq. 5.38, but this time as an equation for the finite function $\mathcal{F}_R(p)$. The left hand side of this equation is a function of p and independent of μ' , whereas the right hand side is a function of μ' independent of p . Hence each side must be equal to a constant which we write as $\ln\delta/\mu$. Thus $\mathcal{F}_R(p)$ satisfies:

$$\frac{\mathcal{F}_R(\mu)}{\mathcal{F}_R(p)} = 1 + A(p, \mu) + \frac{1}{\mathcal{F}_R(p)} [B(p, \mu) + C(p, \mu) \ln \frac{\delta}{\mu}] \quad (5.42)$$

This is of course symbolically the same as Eq. 5.37, but with the important distinction that all quantities are well-defined when we let $\lambda \rightarrow 0$.

In Eq. 5.41, $\mathcal{F}_R(\mu')$ is not an arbitrary number, in the sense that whilst we are free to choose the momentum μ' , the functional dependence of $\mathcal{F}_R(\mu')$ on μ' is determined by the fact it is to be a solution of the Schwinger-Dyson equation. Thus, in Eq. 5.42, δ is a parameter to be determined. This was demonstrated explicitly by choosing a parameterisation for \mathcal{F}_R (see section 5.4) and

first solving Eq. 5.41 by varying the parameters until good numerical agreement is obtained between the right and left hand sides. Then, taking our solution for $\mathcal{F}_R(p)$ we can determine δ through Eq. 5.42 for *all* values of p^2 for which we numerically solved the equation. Over the range $0.01 < p^2 < 100 \text{ GeV}^2$, we found that $\ln\delta$ was constant within the numerical accuracy to which we worked. Solving Eq. 5.42 directly, with $\ln\delta$ as a parameter is more efficient numerically, since we determine δ directly, rather than implicitly through Eq. 5.41. Of course, once we have obtained a solution for $\mathcal{F}_R(p)$ the two approaches are identical.

Since we allow δ to be determined, it can be seen as a dynamically generated infra-red cut-off whose value, a priori, could be anything. Remarkably we found δ to be of the order of a few MeV. This is a momentum scale which does arise in strong interactions and we discuss this further in chapter seven. That the value is physically sensible, seems to justify the rather involved procedure outlined above which makes the equation for the fermion function $\mathcal{F}_R(p)$ infra-red finite.

5.4 The Solution for $\mathcal{F}_R(p)$

Just as in chapters three and four, an analytic solution to this equation Eq. 5.42 is not possible, and again we attempt a numerical study. Before we do this, we investigate the possible analytic form our parameterisation should take.

(i) If $\mathcal{F}_R(p) \sim \mu^2/p^2$ as $p^2 \rightarrow 0$, then the left hand side behaves like p^2/μ^2 in this limit. The small momentum behaviour of the right hand side is dominated by the enhanced μ^2/k^2 term in $\mathcal{G}_R(k)$. On dimensional grounds we must balance the μ^2 in the numerator by a p^2 in the denominator, and we see that agreement is not possible.

(ii) If $\mathcal{F}_R(p) \sim \text{constant}$ as $p^2 \rightarrow 0$, then the left hand side will also behave like a constant. As in (i) above, the right hand side gives a μ^2/p^2 behaviour, and

again consistency is not possible.

(iii) Finally, if $\mathcal{F}_R(p) \sim p^2/\mu^2$ as $p^2 \rightarrow 0$, then the left hand side of Eq. 5.17 behaves like μ^2/p^2 , the same behavior we expect on dimensional grounds from the right hand side. Thus in this case there is the possibility of a consistent solution.

This rough analysis reveals the possibility of a solution for $\mathcal{F}_R(p)$ which vanishes as $p^2 \rightarrow 0$. Note that we have not proven that the fermion equation Eq. 5.42 does indeed demand this behaviour. It might be that it is impossible to obtain a consistent solution over a range of values of p^2 away from zero. In order to demonstrate that this behaviour is indeed realised, we must investigate the equation numerically.

In the asymptotic region for large p^2 , we can expand $\mathcal{F}_R(p) = 1 + O(\alpha_2)$, $\mathcal{G}_R(p) = 1 + O(\alpha_2)$. As in the usual one-loop perturbative calculation of the fermion self energy, \mathcal{F}_R is finite. The $I_2(k, p)$ term vanishes to this order because of the $\mathcal{F}_R(p) - \mathcal{F}_R(q)$ factor (see Eq. 5.17), and the only contribution comes from the $I_1(k, p)$ term, Eq. 5.12, which with $\mathcal{F} = 1$ is identical to the one-loop perturbative term (see section 2.6). Thus to $O(\alpha_2)$ we have:

$$\mathcal{F}_R \rightarrow \text{constant} \tag{5.43}$$

asymptotically. We therefore choose a parameterisation for $\mathcal{F}_R(p)$ which not only vanishes as $p^2 \rightarrow 0$ but also reproduces the simple asymptotic form Eq. 5.43. We use

$$\mathcal{F}_R(p) = \sum_{n=1}^N \frac{f_n p^2}{p^2 + r_n^2} \tag{5.44}$$

where f_n, r_n are parameters to be determined.

The use of such a form as in Eq. 5.44 seems to have prejudged the vanishing of $\mathcal{F}_R(p)$ as $p^2 \rightarrow 0$. We argued above that this was the only possible

behaviour for small p^2 . It is fairly trivial to add a constant term f_0 to Eq. 5.44, and whilst it will then be impossible to find consistent agreement in the exact limit $p^2 \rightarrow 0$, if we *numerically* solve the equation down to a small but finite value of p^2 , self-consistency of the solution may not demand that $f_0 = 0$, but only that it be small. Indeed, in an earlier study [3.3], the value of such a constant term was found to be $O(10^{-2})$. Justified by this numerically small value we explicitly set $f_0 = 0$ in keeping with the analytic arguments above. Once again we choose $\mu^2 = 10 \text{ GeV}^2$, a momentum scale in the perturbative regime, and set $\mathcal{F}_R(\mu) = 1$. We vary the parameters in Eq. 5.42 until we obtain good numerical agreement over the usual range of $0.01 < p^2 < 100 \text{ GeV}^2$. Because of the simple asymptotics in the Landau gauge, Eq. 5.43, we find agreement to within 1% for $N = 1$ in Eq. 5.46. We solve the equation for $\alpha_2(\mu) = 0.15, 0.2, 0.25, 0.3$, the same values as in chapter four. The results are plotted in fig. 5.2 and the parameters are listed in Table 5.1.

| $\alpha(\mu)$ | 0.15 | 0.2 | 0.25 | 0.3 |
|----------------------|--------|--------|--------|--------|
| f_1 | 0.9985 | 1.004 | 1.021 | 1.046 |
| r_1 | 0.1034 | 0.2130 | 0.4049 | 0.6410 |
| $\delta(\text{MeV})$ | 4.422 | 13.22 | 8.861 | 5.087 |

Table 5.1 : Parameters for $\mathcal{F}_R(p)$, Eq. 5.42, for solutions shown in fig. 5.2.

These results show numerically that the truncated Schwinger-Dyson equation for the fermion renormalisation function $\mathcal{F}_R(p)$ does have a solution which vanishes as $p^2 \rightarrow 0$. This behaviour is a direct result of the infra-red enhancement of the gluon propagator, derived in chapters three and four. This suppression occurs at a scale Λ which will be related to the usual scale of QCD.

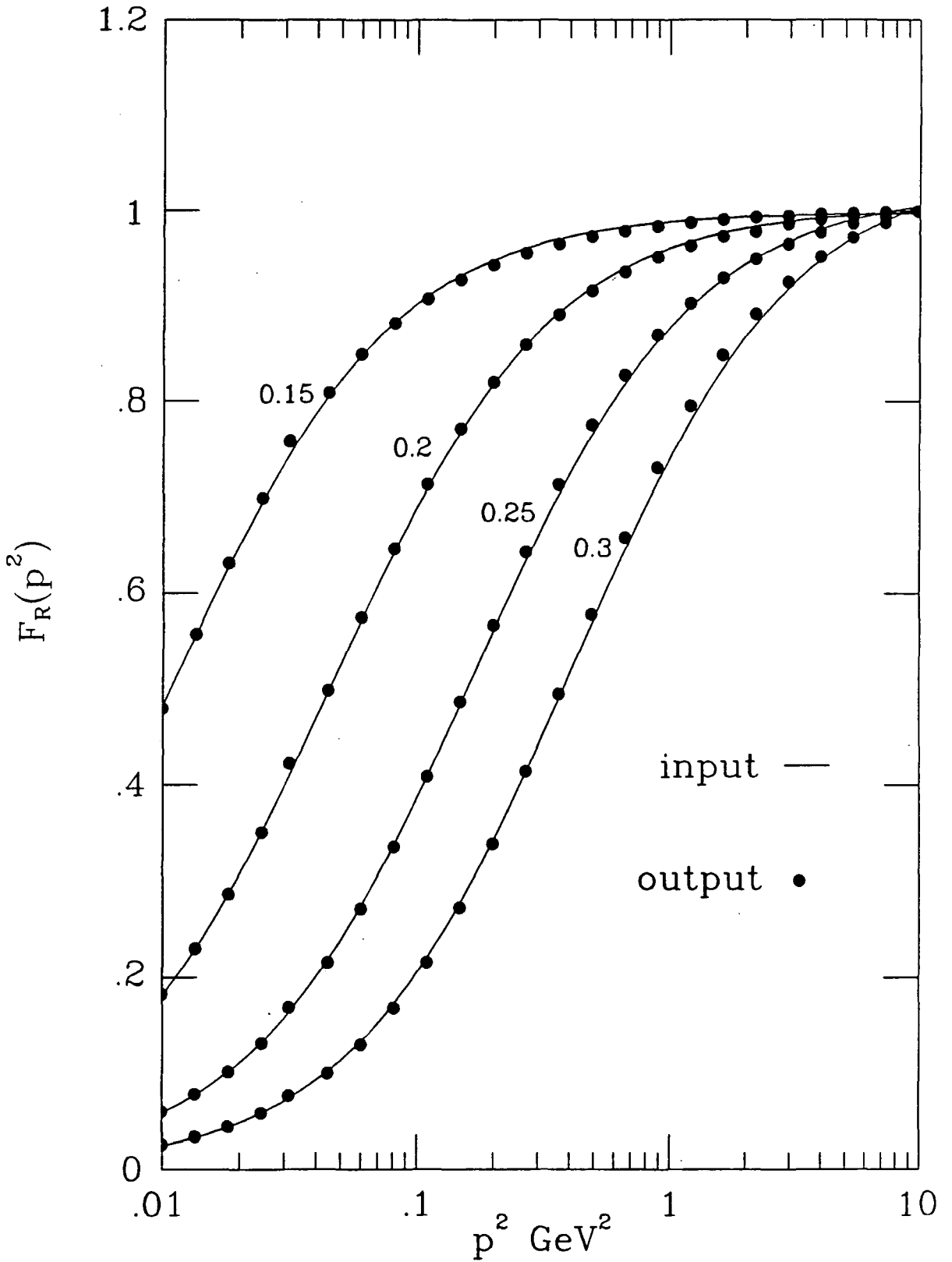


fig. 5.2: The quark renormalisation function $\mathcal{F}_R(p)$ as a function of p^2 , for $\alpha_2(\mu) = 0.15, 0.2, 0.25, 0.3$.

For larger $\alpha_2(\mu)$ we see that the suppression scale rises exactly as we would expect from the dependence of the coupling on the intrinsic scale of the theory (see sections 1.4 and chapter seven). For large p^2 , $\mathcal{F}_R(p) \sim 1$ as in perturbation theory, and the full fermion propagator behaves essentially like the bare one. If this is taken as a model of the behaviour of the full quark propagator, we would deduce that at large momenta they propagate as almost free particles, just as we see in high energy scattering, and as we would expect from the arguments of ‘asymptotic freedom’. At low momenta, however, the propagation is suppressed, and as $p^2 \rightarrow 0$ the suppression is sufficient that the quark propagator would vanish, removing the particle pole on mass-shell at $p^2 = 0$. This surely models the features of a confining theory, answering the paradox of ‘asymptotic freedom’ and ‘infra-red slavery’. A more detailed discussion of all our results appears in chapter seven.

CHAPTER SIX

QUARK LOOPS

6.1 Introduction

In the previous chapters we have obtained solutions for the quark and gluon renormalisation functions $\mathcal{F}_R(p)$, $\mathcal{G}_R(p)$, which realistically model the qualitative features we would expect of a confining theory. To date, however, we have neglected the contribution of dynamical quarks by suppressing closed fermion loops in the Schwinger-Dyson equation for the gluon. The relevant diagram is depicted in fig. 6.1 with momentum labels. By neglecting this term in the so-called ‘quenched’ approximation, the equation for the gluon decouples and can be solved separately. The solution obtained can then be substituted in the fermion equation. By including the contribution of closed fermion loops, there is no decoupling, and we must try to solve the two equations simultaneously[6.1]. The validity of the ‘quenched’ approximation is based on the assumption that the contribution of the added quark loop is small, and this would seem to be borne out by the results of perturbation theory, where, for example the one-loop beta function gives us:

$$\beta_0 = \frac{11}{3}N_c - \frac{2}{3}n_f \quad (6.1)$$

where N_C is the number of colours and n_f the number of light quark flavours. The naive counting given by this expression suggests that the effect of quarks will be small.

There is other evidence [1.7], however, that in the non-perturbative region quark loops play an important role. Indeed in a preliminary study of the Schwinger-Dyson equations[6.2] the inclusion of quark loops has a marked effect on the gluon renormalisation function. In that study, the contribution of quark loops was calculated using the solutions obtained in the ‘quenched’

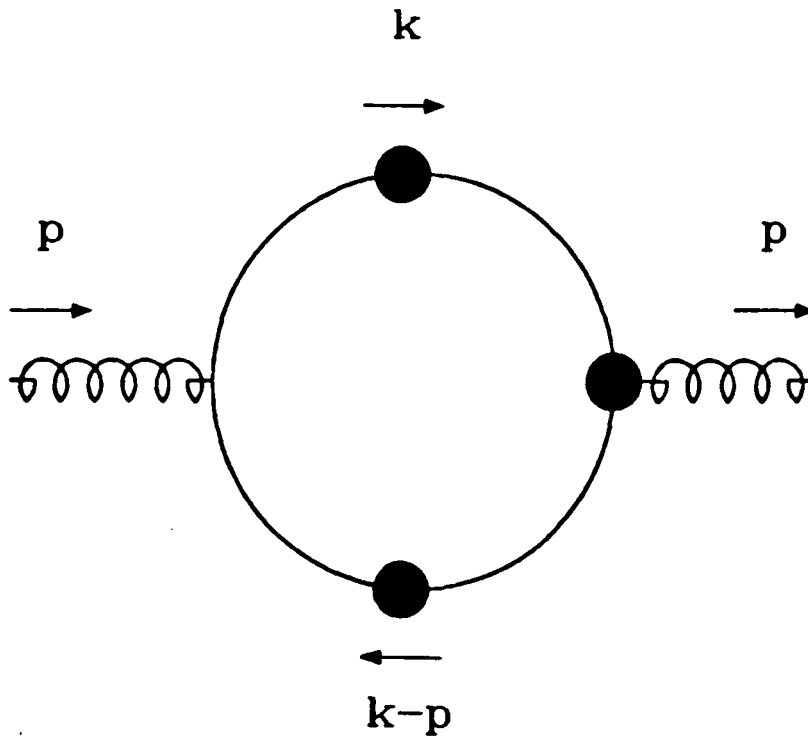


fig. 6.1: The closed fermion loop contribution to the Schwinger-Dyson equation for the inverse gluon propagator, Eq. 4.7 depicted diagrammatically in fig. 4.2.

approximation. Although this result motivates us to investigate the effect of these contributions, until the two equations have been consistently solved as a coupled system, the effect of quark loops remains unclear.

Solving two coupled non-linear integral equations is, however, an extremely non-trivial exercise. In particular, as we are attempting to solve the equations numerically, the computing time needed to solve the two equations simultaneously is dramatically increased. To simplify matters as much as possible, we adopt the Mandelstam approximation for the gluon equation, which, as was mentioned in chapter four, allows us to perform all the angular integrals, reducing the computing time required. As we stressed there, this approximation satisfactorily models the behaviour of the more exact equation considered in chapter three. The solutions obtained possessed the same qualitative features, namely the infra-red enhancement, which we believe to be a signal of confine-

ment. Since both equations derived involve truncations and approximations, we cannot hope to investigate quantitatively the low momentum properties of QCD, but we can at least *model* its infra-red behaviour, and it is in this sense, that it is valid to use the Mandelstam approximation.

6.2 The Quark Loop diagram

The first step in this study is to calculate the contribution of the diagram shown in fig. 6.1, for one flavour of massless quark. We write its contribution as:

$$\Pi_F^{\mu\nu} = \Pi_F(\delta^{\mu\nu} p^2 - p^\mu p^\nu) = -\frac{g_0^2 T_F}{16\pi^4} \int d^4 k \frac{\text{Tr}[\gamma^\mu S_F(k) \Gamma_L^\nu(-p, k, q) S_F(q)]}{k^2 q^2} \quad (6.2)$$

As usual, the colour matrix δ^{ab} has been factored out. T_F is the appropriate colour trace, and we have a minus sign arising from the Feynman rules for closed fermion loops. Note that since the fermion momenta are directed, we have $q = k - p$. The other quantities are defined in chapters four and five. In line with the calculation for the fermion equation in chapter five, we have replaced the quark-gluon vertex with its longitudinal part, using the form Eq. 2.76 for this, based on solving its Slavnov-Taylor identity in the absence of ghost contributions, Eq. 2.75.

As defined in Eq. 5.9 we write $\Gamma_L^\nu = \Gamma_1^\nu + \Gamma_2^\nu$. We therefore need to evaluate two spin traces:

$$\text{Tr}[\gamma^\mu \not{k} \gamma^\nu \not{q}] = 4(k^\mu q^\nu + k^\nu q^\mu - k \cdot q \delta^{\mu\nu}) \quad (6.3)$$

and

$$\begin{aligned} \text{Tr}[\gamma^\mu \not{k} (\not{k} + \not{q}) \not{q}] &= \text{Tr}[\gamma^\mu k^2 \not{q} + \gamma^\nu \not{k} q^2] \\ &= 4k^2 q^\mu + 4q^2 k^\mu \end{aligned} \quad (6.4)$$

We now contract this with the projection tensor $P^{\mu\nu}$, Eq. 3.2, giving the contribution of Γ_1^ν as:

$$\frac{g_0^2 T_F}{16\pi^4} \int \frac{d^4 k}{k^2 q^2} \frac{2}{3} (\mathcal{F}(k) + \mathcal{F}(q)) \left[\frac{8(k \cdot p)^2}{p^2} - 2k^2 - 6k \cdot p \right] \quad (6.5)$$

and the contribution of Γ_2^ν as:

$$\begin{aligned} \frac{g_0^2 T_F}{16\pi^4} \int \frac{d^4 k}{k^2 q^2} \frac{\mathcal{F}(q) - \mathcal{F}(k)}{k^2 - q^2} \frac{2}{3} \left[q^2 \left(\frac{8(k \cdot p)^2}{p^2} - 2k^2 - 3k \cdot p \right) \right. \\ \left. + k^2 \left(\frac{8(k \cdot p)^2}{p^2} - 2k^2 - 9k \cdot p + 3p^2 \right) \right] \quad (6.6) \end{aligned}$$

We can now use the $k \rightarrow -q$ $q \rightarrow -k$ symmetry of the integral to write Eq. 6.5 as:

$$\frac{g_0^2 T_F}{16\pi^4} \int \frac{d^4 k}{k^2 q^2} \frac{4}{3} \left(\frac{8(k \cdot p)^2}{p^2} - 2k^2 - 6k \cdot p \right) \quad (6.7)$$

and to write Eq. 6.6 as :

$$\frac{g_0^2 T_F}{16\pi^4} \int \frac{d^4 k}{k^2 q^2} \frac{\mathcal{F}(q) - \mathcal{F}(k)}{k^2 - q^2} \frac{4}{3} q^2 \left(\frac{8(k \cdot p)^2}{p^2} - 2k^2 - 3k \cdot p \right) \quad (6.8)$$

As in the preceding chapters we must, in general, evaluate the expressions in Eqs. 6.7 and 6.8 numerically. However, since the fermion equation remains explicitly unchanged, we will try to use the parameterisation in Eq. 5.45 for $\mathcal{F}(p)$, writing it as $f_1 p^2 / (p^2 + r_1^2)$. For this simple form for \mathcal{F} all the above integrals can be performed analytically. This only applies in the Landau gauge, because of the simple asymptotic form of \mathcal{F} . Of course, if we are unable to solve the equations with this form for \mathcal{F} , we would have to return to Eqs. 6.7 and 6.8, and perform a numerical integration with a more complicated parameterisation for $\mathcal{F}(p)$.

We first deal with Eq. 6.7. Using the integrals given in Appendix A, we can evaluate this as:

$$\begin{aligned} \frac{g_0^2 T_F}{16\pi^4} \frac{8\pi^2}{3} \left[\int_0^{p^2} dk^2 \mathcal{F}(k) \left(\frac{8(p^2 + k^2)k^2}{8p^4} - \frac{2k^2}{2p^2} - \frac{6k^2 p}{4p^3} \right) \right. \\ \left. + \int_{p^2}^{\kappa^2} dk^2 \mathcal{F}(k) \left(\frac{8(p^2 + k^2)k^2}{8k^4} - \frac{2k^2}{2k^2} - \frac{6kp^2}{4k^3} \right) \right] \end{aligned} \quad (6.9)$$

where we have introduced an ultraviolet cutoff κ . This simplifies to:

$$\begin{aligned} \frac{g_0^2 T_F}{16\pi^4} \frac{8\pi^2}{3} \left[\int_0^{p^2} dk^2 \mathcal{F}(k) \left(\frac{k^4}{p^4} - \frac{3k^2}{2p^2} \right) \right. \\ \left. + \int_{p^2}^{\kappa^2} dk^2 \mathcal{F}(k) \left(-\frac{p^2}{2k^2} \right) \right] \end{aligned} \quad (6.10)$$

Using the form $\mathcal{F}(k) = f_1 k^2 / (k^2 + r_1^2)$ we obtain:

$$\begin{aligned} \frac{g_0^2 T_F f_1}{6\pi^2} \left[\int_0^{p^2} dk^2 \frac{k^2}{k^2 + r_1^2} \left(\frac{k^4}{p^4} - \frac{3k^2}{p^2} \right) \right. \\ \left. + \int_{p^2}^{\kappa^2} dk^2 \frac{k^2}{k^2 + r_1^2} \left(-\frac{p^2}{2k^2} \right) \right] \end{aligned} \quad (6.11)$$

Transforming variables to $w^2 = k^2 + r_1^2$ gives:

$$\begin{aligned} \frac{g_0^2 T_F f_1}{6\pi^2} \left[\int_{r_1^2}^{p^2+r_1^2} dw^2 \left(\frac{(w^2 - r_1^2)^3}{p^4 w^2} - \frac{3(w^2 - r_1^2)^2}{2 p^2 w^2} \right) \right. \\ \left. + \int_{p^2+r_1^2}^{\kappa^2+r_1^2} \left(-\frac{p^2}{2w^2} \right) \right] \end{aligned} \quad (6.12)$$

giving us the contribution of the Γ_1' term as:

$$\begin{aligned} \frac{g_0^2 T_F f_1}{6\pi^2} \left[\left(-\frac{r_1^6}{p^4} - \frac{3r_1^4}{p^2} \right) \ln \left(\frac{p^2 + r_1^2}{r_1^2} \right) + \frac{r_1^4}{p^2} \ln \left(\frac{p^2 + r_1^2}{r_1^2} \right) - \frac{5p^2}{12} \right. \\ \left. + r_1^2 + \frac{r_1^4}{p^2} - \frac{p^2}{2} \ln \left(\frac{\kappa^2 + r_1^2}{p^2 + r_1^2} \right) \right] \end{aligned} \quad (6.13)$$

The contribution of Eq. 6.8 is more complicated. First of all we use our specific form for $\mathcal{F}(p)$ to obtain:

$$\begin{aligned}\frac{\mathcal{F}(q) - \mathcal{F}(k)}{k^2 - q^2} &= \frac{f_1(q^2 r_1^2 - k^2 r_1^2)}{(k^2 - q^2)(k^2 + r_1^2)(q^2 - r_1^2)} \\ &= \frac{-f_1 r_1^2}{(k^2 + r_1^2)(q^2 + r_1^2)}\end{aligned}\quad (6.14)$$

There are three integrals to evaluate:

$$\begin{aligned}I_1 &= \frac{1}{2\pi^2} \int d^4 k \frac{k^2}{(k^2 + r_1^2)(q^2 + r_1^2)} \\ I_2 &= \frac{1}{2\pi^2} \int d^4 k \frac{1}{(k^2 + r_1^2)(q^2 + r_1^2)} \frac{(k \cdot p)^2}{p^2} \\ I_3 &= \frac{1}{2\pi^2} \int d^4 k \frac{k \cdot p}{(k^2 + r_1^2)(q^2 + r_1^2)}\end{aligned}\quad (6.15)$$

Using the results of Appendix A, two of the angular integrals are trivial and give a factor of 4π . The remaining angular integral can be performed using Eq. A.21, with $a = p^2 + k^2 + r_1^2$, $b = 2pk$, to give:

$$\begin{aligned}I_1 &= \int_0^{\kappa^2} \frac{dk^2}{k^2 + r_1^2} \frac{1}{4p^2} \left(p^2 + k^2 + r_1^2 - \sqrt{(p^2 + k^2 + r_1^2)^2 - 4p^2 k^2} \right) \\ I_2 &= \int_0^{\kappa^2} \frac{dk^2}{k^2 + r_1^2} \left(\frac{(p^2 + k^2 + r_1^2)^2}{16p^4 k^2} \left(p^2 + k^2 + r_1^2 - \sqrt{(p^2 + k^2 + r_1^2)^2 - 4p^2 k^2} \right) \right. \\ &\quad \left. - \frac{p^2 + k^2 + r_1^2}{8p^2} \right) \\ I_3 &= \int_0^{\kappa^2} \frac{dk^2}{k^2 + r_1^2} \left(\frac{p^2 + k^2 + r_1^2}{8p^2 k^2} \left(p^2 + k^2 + r_1^2 - \sqrt{(p^2 + k^2 + r_1^2)^2 - 4p^2 k^2} \right) \right. \\ &\quad \left. - \frac{1}{4} \right)\end{aligned}\quad (6.16)$$

Although the momentum integral left is tractable, it is difficult and messy (see ref. 6.2), and it is best performed using an algebraic manipulations program, such as MACSYMA, which gives the results below:

$$\begin{aligned}
 I_1 &= \frac{1}{4p^2} \left(- (4p^2 r_1^2 + p^4)^{\frac{1}{2}} \ln \left[\frac{(p^2 + r_1^2)(4r_1^2 + p^2)^{\frac{1}{2}} + (p^2)^{\frac{1}{2}}(3r_1^2 + p^2)}{((4r_1^2 + p^2)^{\frac{1}{2}} - (p^2)^{\frac{1}{2}})r_1^2} \right] \right. \\
 &\quad \left. + 2p^2 + 2p^2 \ln \left(\frac{\kappa^2}{r_1^2} \right) \right) \\
 I_2 &= \frac{1}{16p^4 r_1^2} \left(p^4 (4p^2 r_1^2 + p^4)^{\frac{1}{2}} \ln \left[\frac{(p^2 + r_1^2)(4r_1^2 + p^2)^{\frac{1}{2}} + (p^2)^{\frac{1}{2}}(3r_1^2 + p^2)}{((4r_1^2 + p^2)^{\frac{1}{2}} - (p^2)^{\frac{1}{2}})r_1^2} \right] \right. \\
 &\quad \left. + 2(p^2 + r_1^2)^3 \ln \left(\frac{r_1^2}{p^2 + r_1^2} \right) + 3p^4 r_1^2 + 2p^2 r_1^4 + 2p^4 r_1^2 \ln \left(\frac{\kappa^2}{r_1^2} \right) \right) \\
 I_3 &= \frac{1}{8p^2 r_1^2} \left(p^2 (4p^2 r_1^2 + p^4)^{\frac{1}{2}} \ln \left[\frac{(p^2 + r_1^2)(4r_1^2 + p^2)^{\frac{1}{2}} + (p^2)^{\frac{1}{2}}(3r_1^2 + p^2)}{((4r_1^2 + p^2)^{\frac{1}{2}} - (p^2)^{\frac{1}{2}})r_1^2} \right] \right. \\
 &\quad \left. + 2(p^2 + r_1^2)^2 \ln \left(\frac{r_1^2}{p^2 + r_1^2} \right) + 2p^2 r_1^2 \right)
 \end{aligned} \tag{6.17}$$

Where we have ignored terms of $O(1/\kappa^2)$. This gives the contribution of Eq. 6.8 as:

$$\begin{aligned}
 &\frac{-g_0^2 T_F f_1 r_1^2}{6\pi^2} \left((4p^2 r_1^2 + p^4)^{\frac{1}{2}} \ln \left[\frac{(p^2 + r_1^2)(4r_1^2 + p^2)^{\frac{1}{2}} + (p^2)^{\frac{1}{2}}(3r_1^2 + p^2)}{((4r_1^2 + p^2)^{\frac{1}{2}} - (p^2)^{\frac{1}{2}})r_1^2} \right] \times \right. \\
 &\quad \times \left(\frac{1}{8r_1^2} + \frac{1}{2p^2} \right) + \left(\frac{(p^2 + r_1^2)^3}{p^4 r_1^2} - \frac{3(p^2 + r_1^2)^2}{4 p^2 r_1^2} \right) \ln \left(\frac{r_1^2}{r_1^2 + p^2} \right) \\
 &\quad \left. - \frac{1}{4} + \frac{r_1^2}{p^2} \right)
 \end{aligned} \tag{6.18}$$

Note that because of the factor $\mathcal{F}(k) - \mathcal{F}(q)$, the fact that $\mathcal{F}(k), \mathcal{F}(q) \rightarrow f_1$ as $k^2 \rightarrow \infty$, makes this term ultraviolet finite which is explicitly demonstrated in Eq. 6.18.

Putting together Eqs. 6.13 and 6.18 and dividing by p^2 gives the contribution of the fermion loop diagram as:

$$\begin{aligned}
 \Pi_F = & \frac{f_1 g_0^2 T_F}{12\pi^2 p^2} \left[\ln\left(\frac{p^2 + r_1^2}{r_1^2}\right) \frac{3}{2} \frac{(p^2 + r_1^2)^2}{p^2} - \frac{5}{6} p^2 + \frac{5}{2} r_1^2 - \left(\frac{1}{4} + \frac{r_1^2}{p^2}\right) \times \right. \\
 & \left. \times (4r_1^2 p^2 + p^4)^{\frac{1}{2}} \ln \left[\frac{(p^2 + r_1^2)(4r_1^2 + p^2)^{\frac{1}{2}} + (p^2)^{\frac{1}{2}}(3r_1^2 + p^2)}{((4r_1^2 + p^2)^{\frac{1}{2}} - (p^2)^{\frac{1}{2}}) r_1^2} \right] \right] \\
 & - \frac{f_1 g_0^2 T_F}{12\pi^2} \ln\left(\frac{\kappa^2}{r_1^2}\right)
 \end{aligned} \tag{6.19}$$

For convenience we write Eq. 6.18 as:

$$\Pi_F = \frac{f_1 g_0^2 T_F}{12\pi^2} [Q(p^2, r_1^2) - \ln\left(\frac{\kappa^2}{r_1^2}\right)] \tag{6.20}$$

where $Q(p^2, r_1^2)$ is simply read off. Note that Π_F is well behaved in the limits $p^2 \rightarrow 0$, $r_1^2 \rightarrow 0$, as it should be from its integral definition. This term also makes no contribution to the gluon mass (see sections 3.3 and 4.2), as it vanishes when we multiply by p^2 and take the limit $p^2 \rightarrow 0$. Note that Eq. 6.19 has the correct one-loop perturbative logarithmic divergence.

6.3 The Gluon Equation with Quarks

We now return to the gluon equation derived in chapter four, where we used the Mandelstam approximation for the triple gluon vertex. The unrenormalised equation (Eq. 4.7) can be written as:

$$\frac{1}{\mathcal{G}(p)} = 1 + \frac{g_0^2 C_A}{16\pi^2} \Sigma(p) \tag{6.21}$$

where $\Sigma(p)$ is simply read off from Eq. 4.7. The inclusion of quark loops means that the gluon equation becomes:

$$\begin{aligned}
 \frac{1}{\mathcal{G}(p)} &= 1 + \frac{g_0^2 C_A}{16\pi^2} \Sigma(p) - n_f \Pi_F \\
 &= 1 + \frac{g_0^2 C_A}{16\pi^2} \Sigma(p) - n_f \frac{f_1 g_0^2 T_F}{12\pi^2} \left[Q(p^2, r_1^2) - \ln\left(\frac{\kappa^2}{r_1^2}\right) \right]
 \end{aligned} \tag{6.22}$$

where we have included n_f flavours of massless quarks. As usual this really only defines $\mathcal{G}(p, \kappa)$ and $\mathcal{F}(p, \lambda, \kappa)$, and we define the renormalised functions (see Eqs. 4.8, 5.21 and 5.39) as:

$$\begin{aligned} Z_G(\kappa/\mu)\mathcal{G}_R(p) &= \mathcal{G}(p, \kappa) \\ Z_F(\kappa/\mu, \lambda/\mu)Z_{IR}(\lambda/\mu)\mathcal{F}_R(p) &= \mathcal{F}(p, \lambda, \kappa) \end{aligned} \quad (6.23)$$

As in section 4.2, we subtract Eq. 6.22 evaluated at $p^2 = \mu^2$ from itself, and, using the definitions in Eq. 6.23, we obtain the renormalised equation which includes quark loops as:

$$\begin{aligned} \frac{1}{\mathcal{G}_R(p)} &= \frac{1}{\mathcal{G}_R(\mu)} + \frac{C_A\alpha_1(\mu)}{4\pi} \left(\Sigma(p) - \Sigma(\mu) \right) \\ &\quad - n_f \frac{T_F f_1 \alpha_3(\mu)}{3\pi} \left(Q(p^2, r_1^2) - Q(\mu^2, r_1^2) \right) \end{aligned} \quad (6.24)$$

As in chapter four, $\alpha_1(\mu) = Z_G^2(\kappa/\mu)g_0^2/4\pi$, and here the new coupling $\alpha_3(\mu)$ is defined by $\alpha_3(\mu) = Z_G(\kappa/\mu)Z_F(\kappa/\mu, \lambda/\mu)Z_{IR}(\lambda/\mu)g_0^2/4\pi$. These couplings are different from each other and from the coupling $\alpha_2(\mu)$ defined in chapter five. These differences are discussed in chapter seven. To solve our coupled set of equations we choose to set $\alpha_1(\mu) = \alpha_2(\mu) = \alpha_3(\mu) = \alpha(\mu)$.

We have two non-linear coupled integral equations involving the two unknown functions $\mathcal{G}_R(p)$, $\mathcal{F}_R(p)$, with all other quantities being specified. Dealing with both equations simultaneously is a cumbersome numerical exercise, and so we choose to adopt an iterative approach. Firstly, with $n_f = 0$ the gluon equation decouples, and the solutions obtained in chapter four for the gluon function, and chapter five for the fermion function satisfy the coupled system identically. For non-zero n_f we take our solution for $\mathcal{F}_R(p)$ with $n_f = 0$ and substitute the values of the parameters obtained into Eq. 6.24. Keeping these fermion parameters fixed, we then re-solve the gluon equation until we once again obtain consistent numerical agreement over our range of p^2 . This new solution for

$\mathcal{G}_R(p)$ is then substituted into the fermion equation Eq. 5.41, and this too is resolved until we find a new solution for $\mathcal{F}_R(p)$. This procedure is repeated until the solutions we obtain remain reasonably stable. Having found these iterative solutions for $\mathcal{F}_R(p)$ and $\mathcal{G}_R(p)$, we now solve the equations as a simultaneous pair allowing all the parameters to vary. This final step was not found to change the iterative solutions very much, but did allow some ‘fine-tuning’. Since the iterative solutions were numerically close to the solutions which solve the coupled set, the potentially difficult numerical exercise was much simplified.

So long as n_f , the number of massless quark flavours was varied in small steps, this iterative procedure was found to converge relatively quickly. Using this method we obtain solutions for the coupled system for $\alpha(\mu) = 0.15, 0.2, 0.25, 0.3$ as before. We varied the number of flavours through $n_f = 0, 2, 4, 6$ over the usual range of p^2 , $0.01 < p^2 < 100 \text{ GeV}^2$. We plot the solutions in figs. 6.2-6.9, and table the parameters in tables 6.1-6.4.

As in chapter four, we obtain solutions for the gluon renormalisation function $\mathcal{G}_R(p)$ which have the power-law infra-red enhancement term $A\mu^2/p^2$. This in turn is reflected in the suppression of the fermion renormalisation function $\mathcal{F}_R(p)$, to the extent that the particle pole at $p^2 = 0$ is removed. The effect of closed quark loops, however, is to dampen both these effects by quite a large amount, as can be seen from figs. 6.2-6.9. Thus it is suspected that with more than seven flavours of massless quarks, the enhancement of the gluon propagator would no longer occur. This in turn would remove the suppression of the fermion propagator, and we can see this as an aspect of ‘deconfinement’. We discuss this further in the next chapter.

Finally, in the same spirit of the discussion of the static colour potential in section 4.5, we plot this for $\alpha(\mu) = 0.25$ with $n_f = 0, 2$ in fig. 6.10. Again, this is not to be taken too seriously, but merely demonstrates the ‘deconfining’ effect of even a small number of massless quarks.

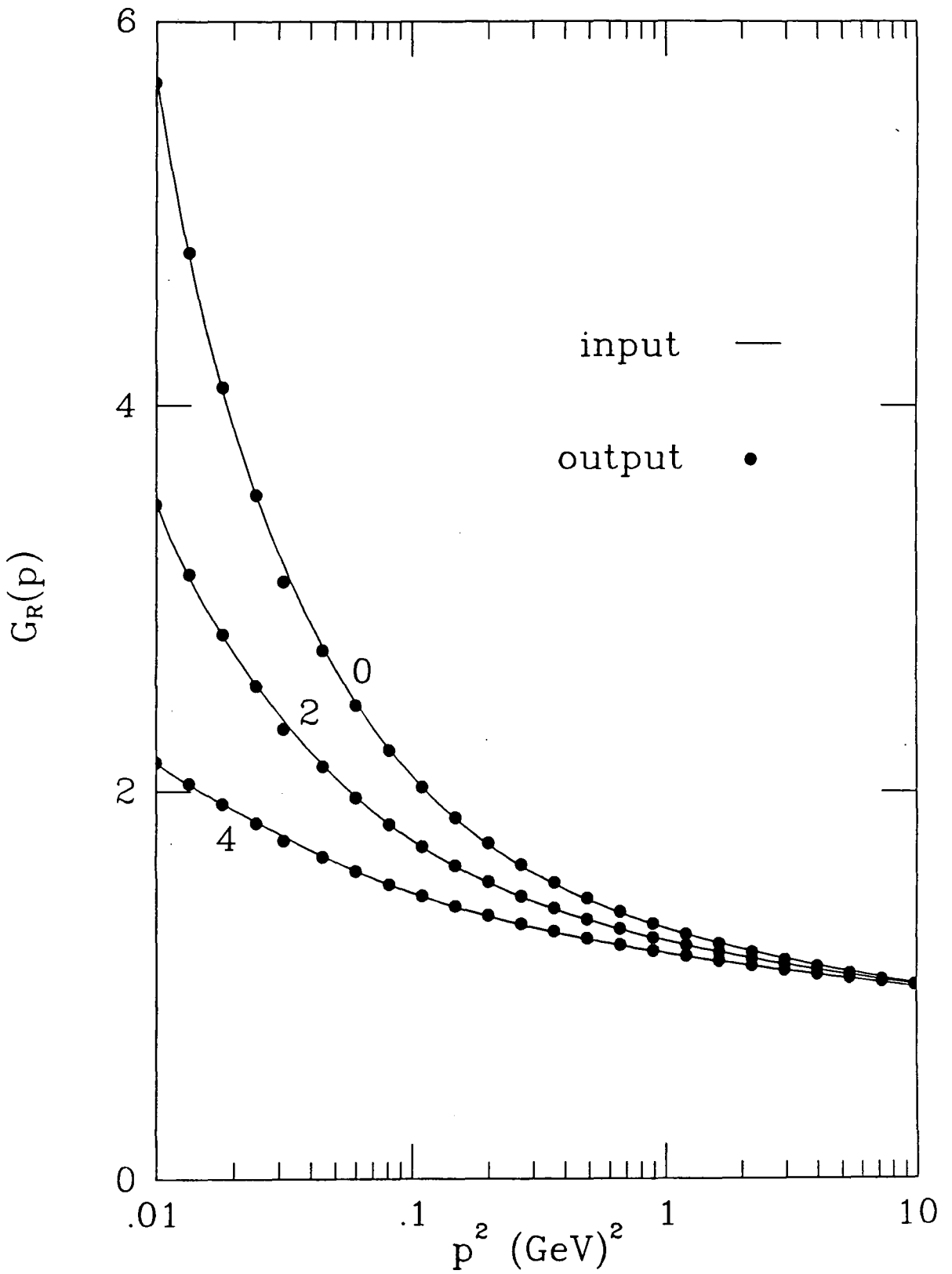


fig. 6.2: The gluon renormalisation function $\mathcal{G}_R(p)$ as a function of p^2 for $\alpha(\mu) = 0.15$, with $n_f = 0, 2, 4$.

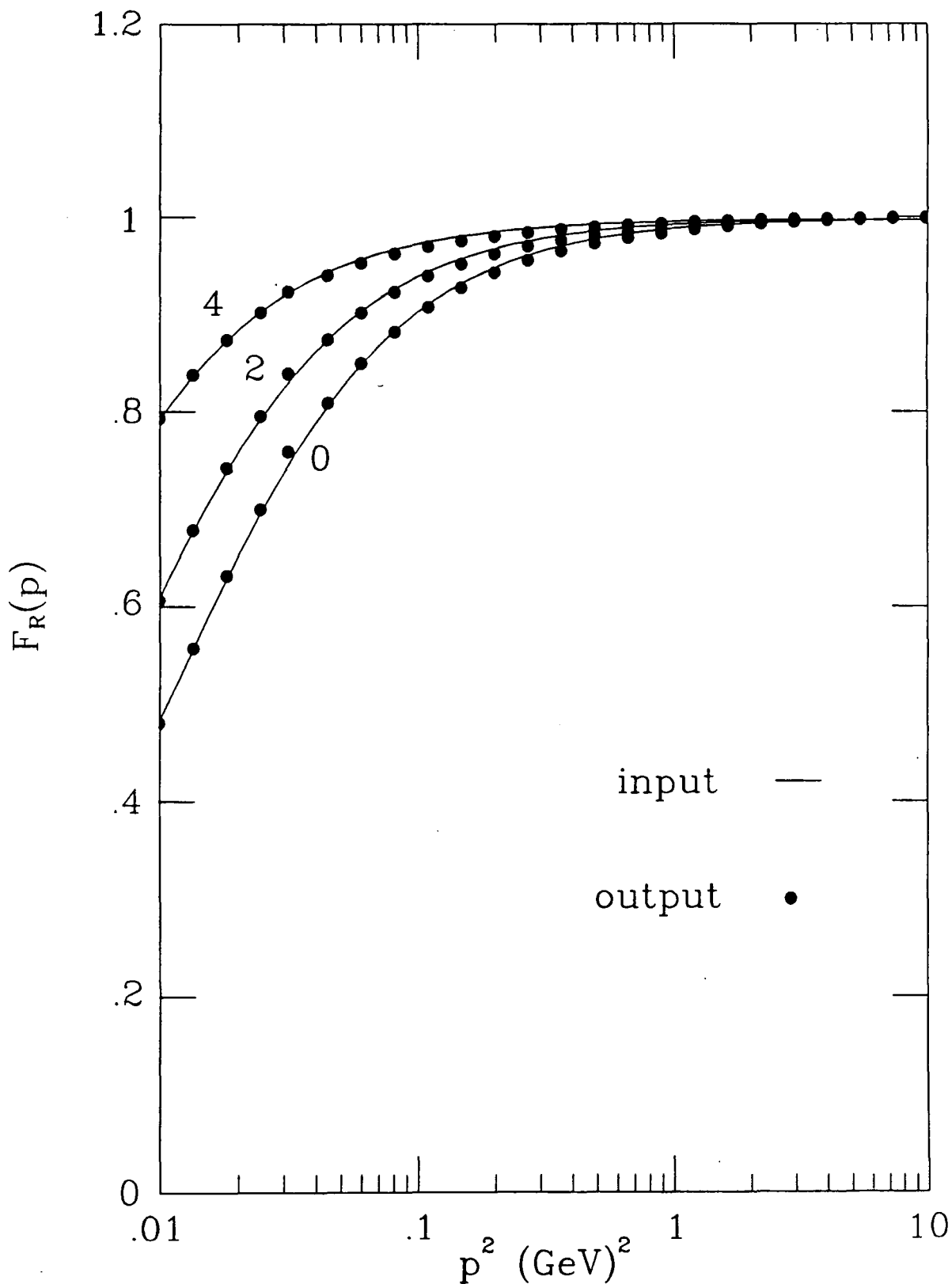


fig. 6.3: The quark renormalisation function $\mathcal{F}_R(p)$ as a function of p^2 for $\alpha(\mu) = 0.15$, with $n_f = 0, 2, 4$.

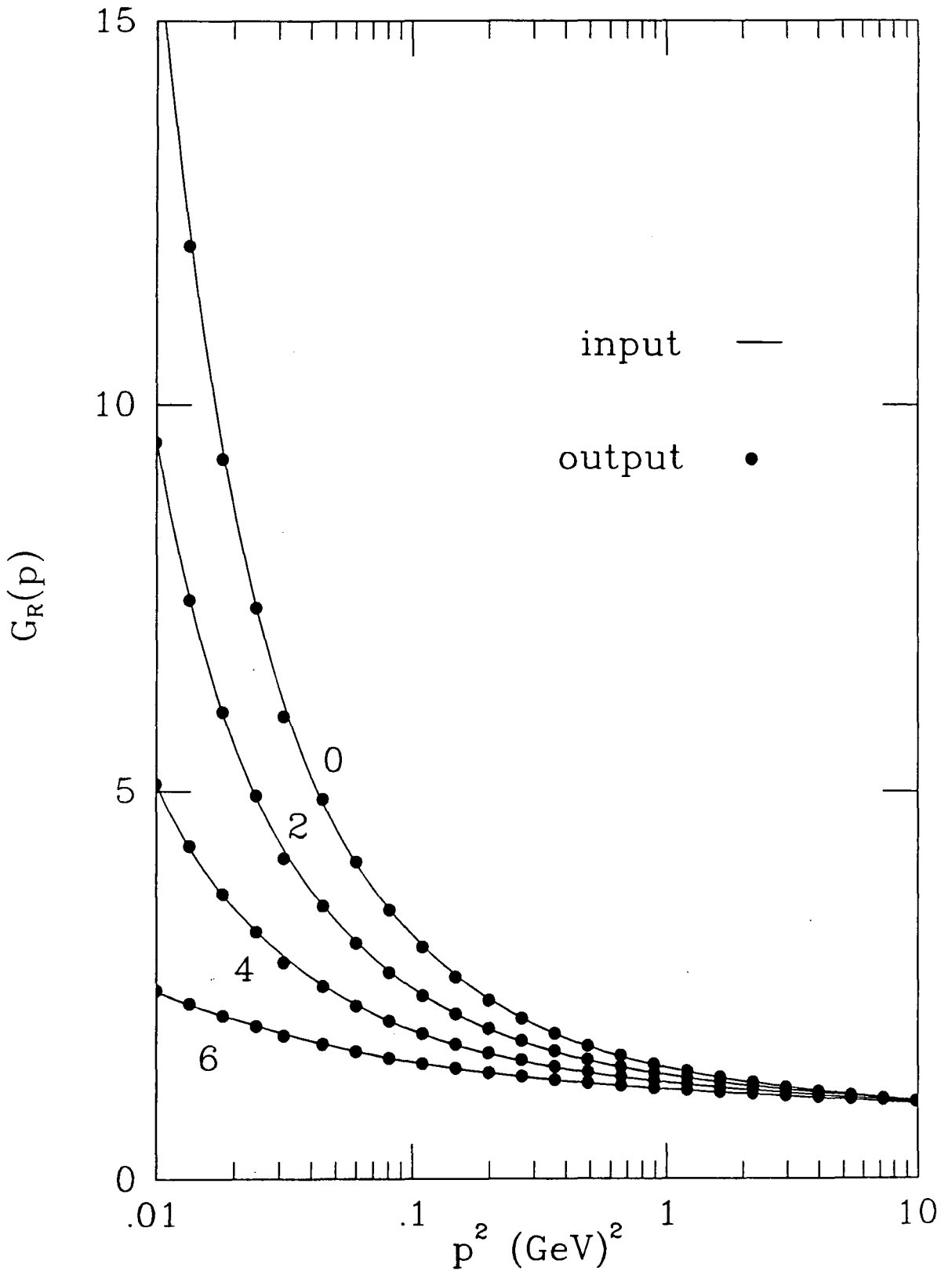


fig. 6.4: The gluon renormalisation function $\mathcal{G}_R(p)$ as a function of p^2 for $\alpha(\mu) = 0.2$, with $n_f = 0, 2, 4, 6$.

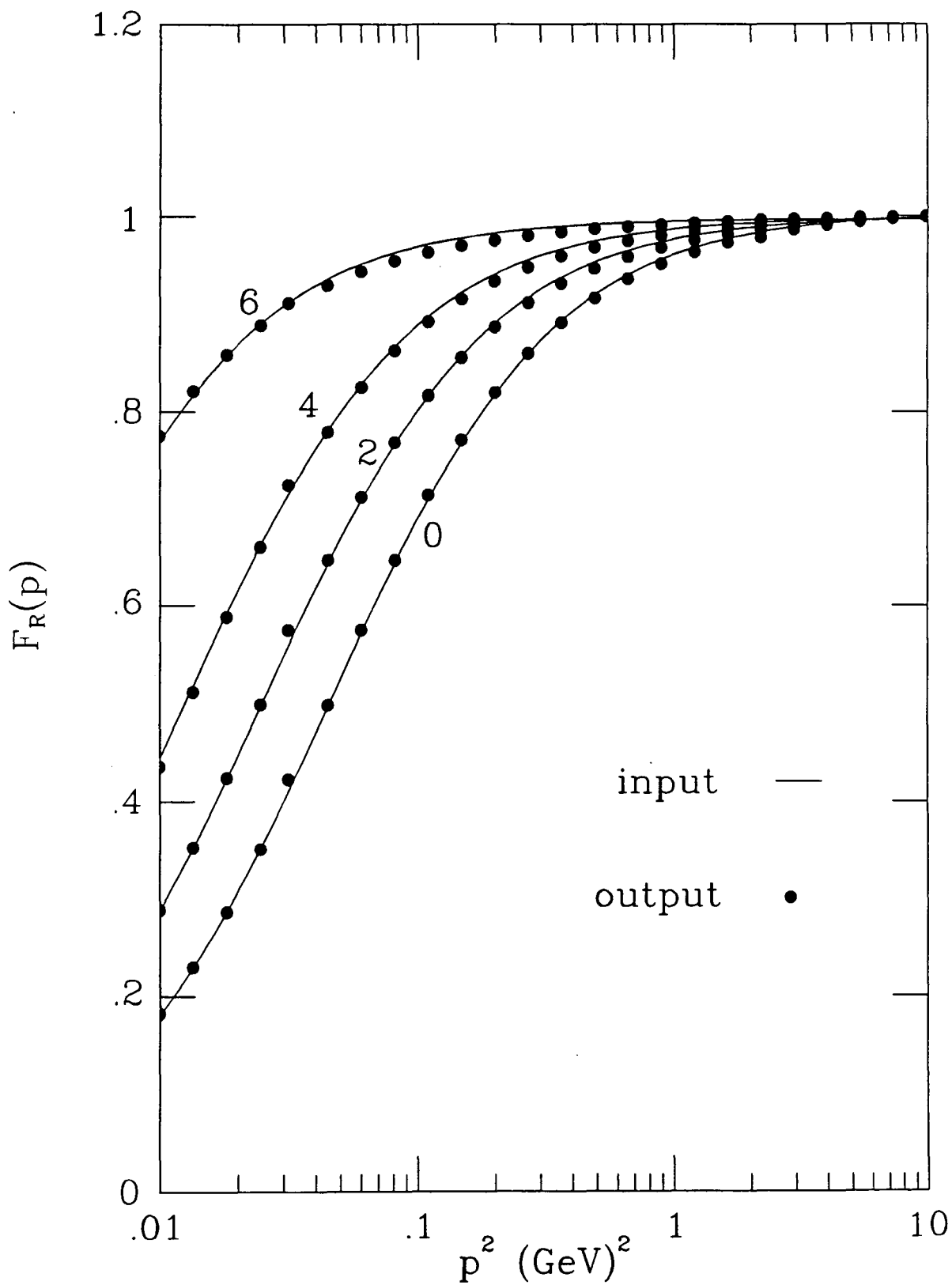


fig. 6.5: The quark renormalisation function $\mathcal{F}_R(p)$ as a function of p^2 for $\alpha(\mu) = 0.2$, with $n_f = 0, 2, 4, 6$.

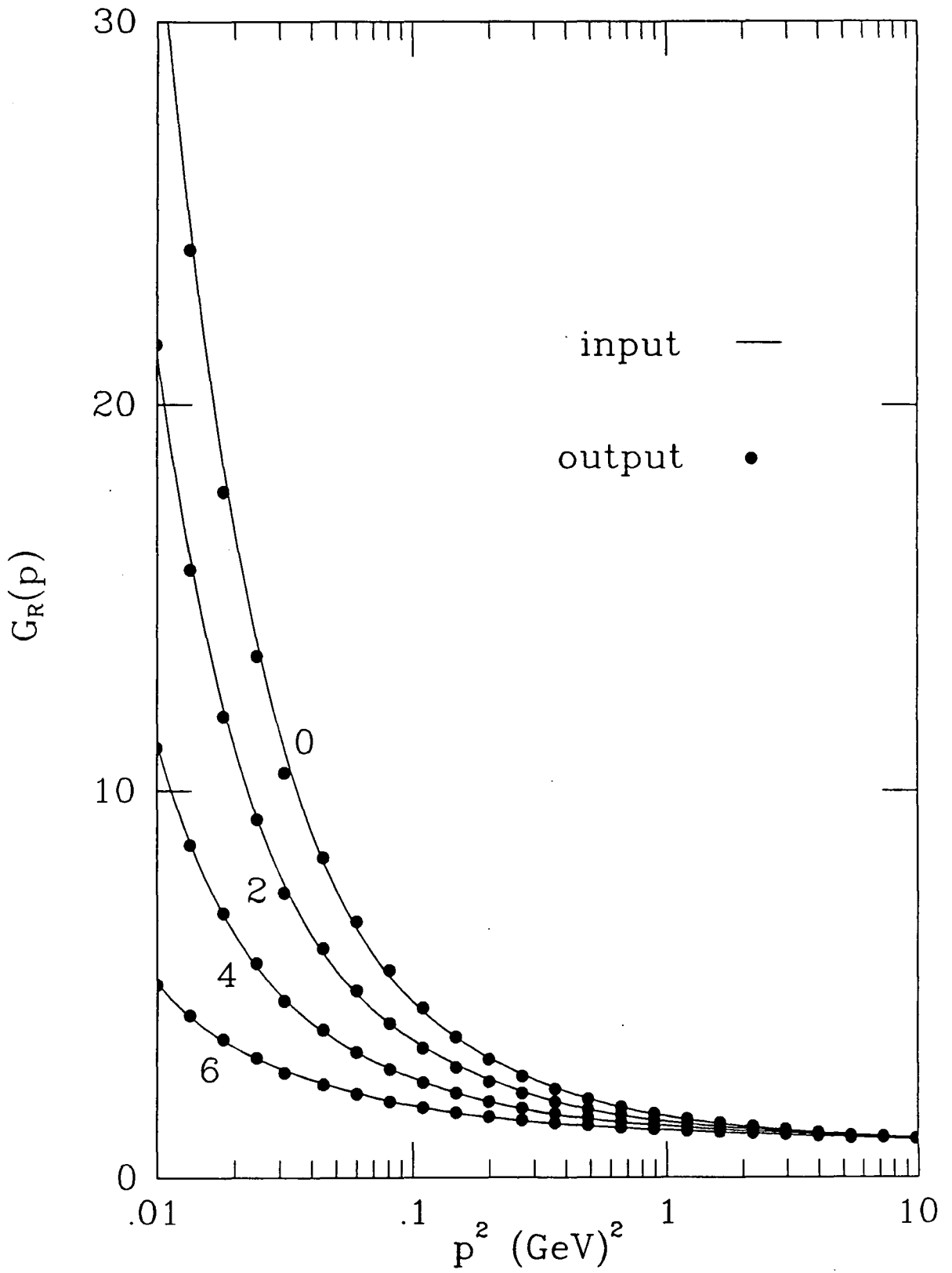


fig. 6.6: The gluon renormalisation function $\mathcal{G}_R(p)$ as a function of p^2 for $\alpha(\mu) = 0.25$, with $n_f = 0, 2, 4, 6$.

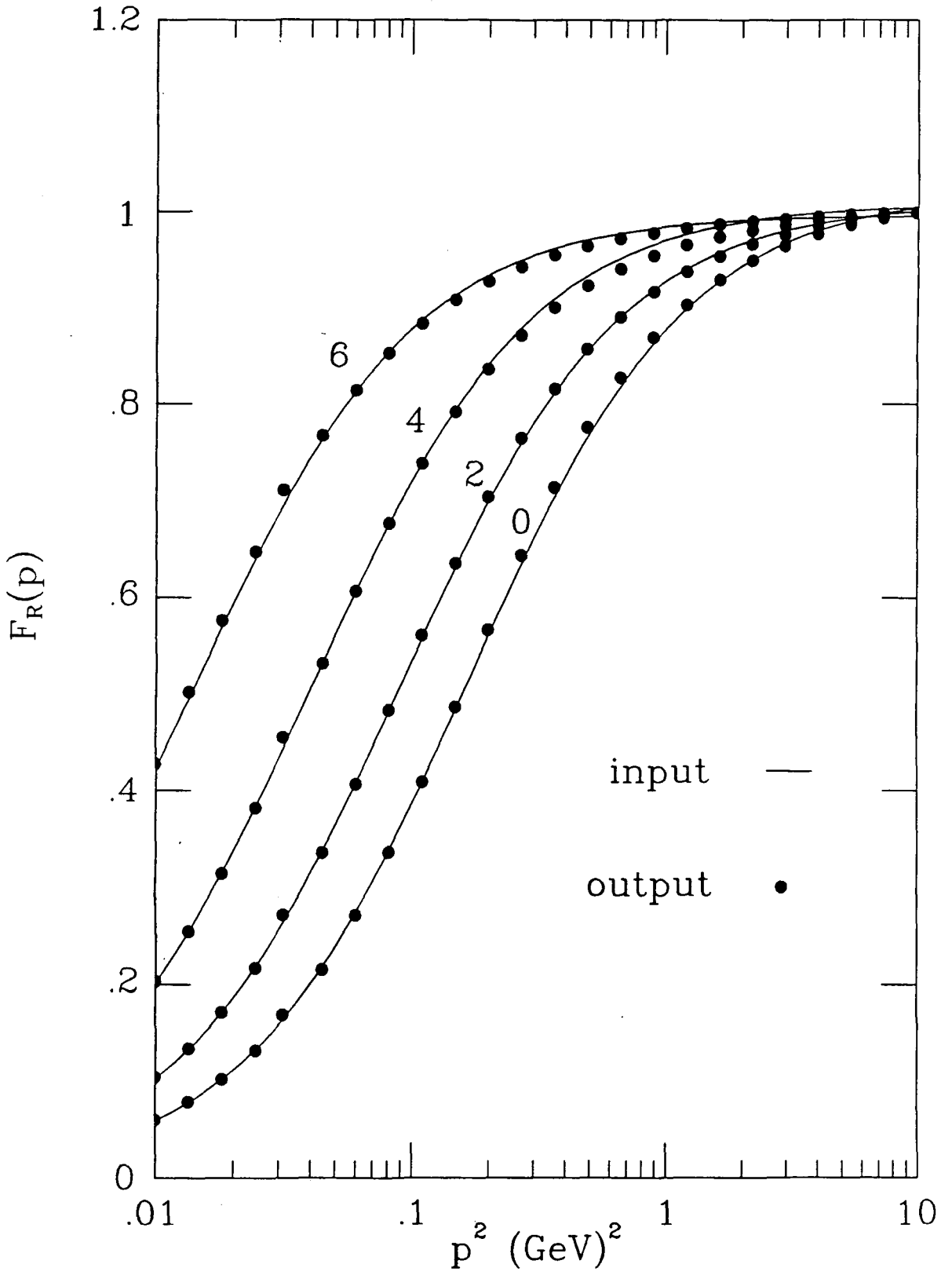


fig. 6.7: The quark renormalisation function $\mathcal{F}_R(p)$ as a function of p^2 for $\alpha(\mu) = 0.25$, with $n_f = 0, 2, 4, 6$.

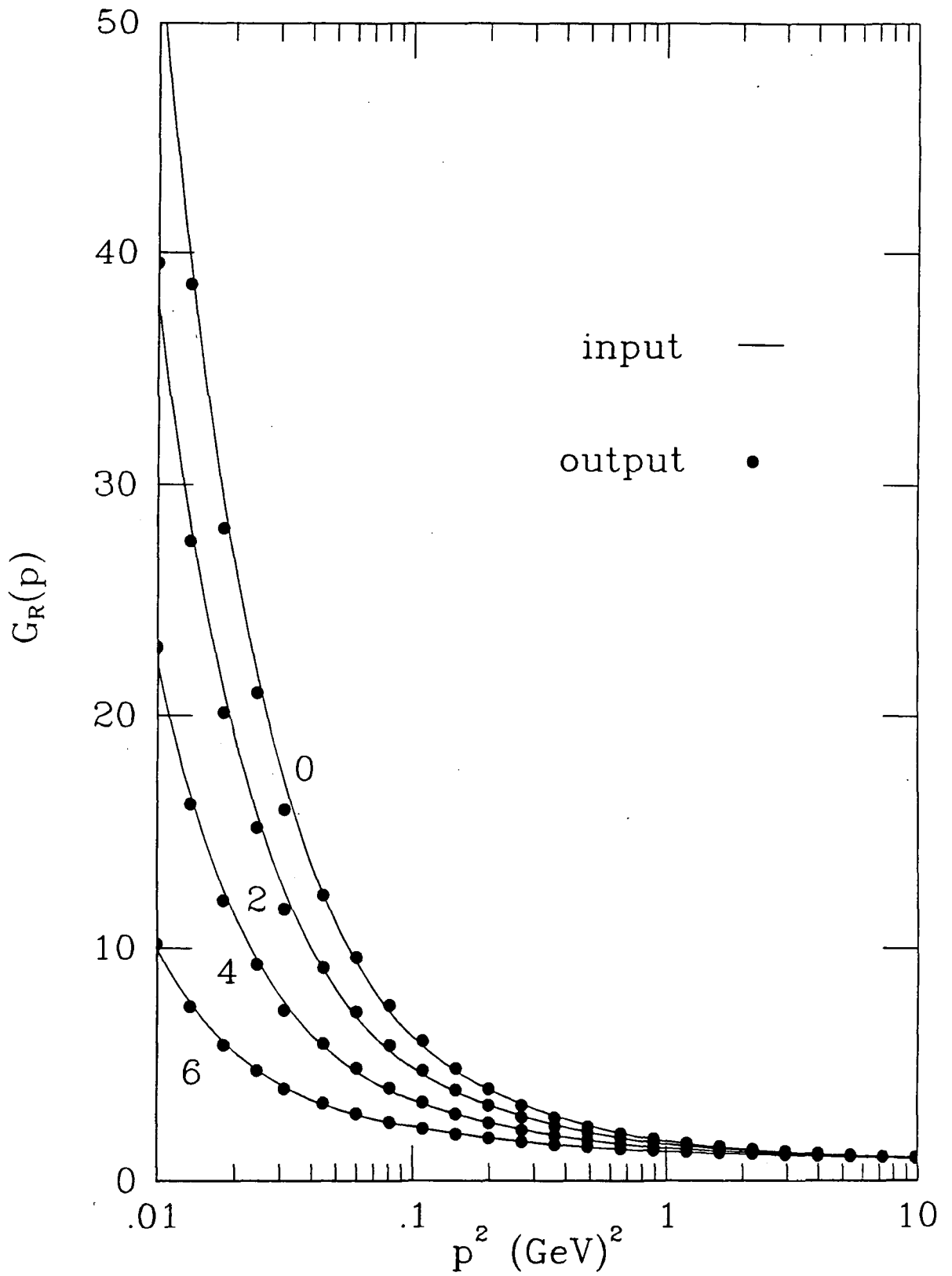


fig. 6.8: The gluon renormalisation function $\mathcal{G}_R(p)$ as a function of p^2 for $\alpha(\mu) = 0.3$, with $n_f = 0, 2, 4, 6$.

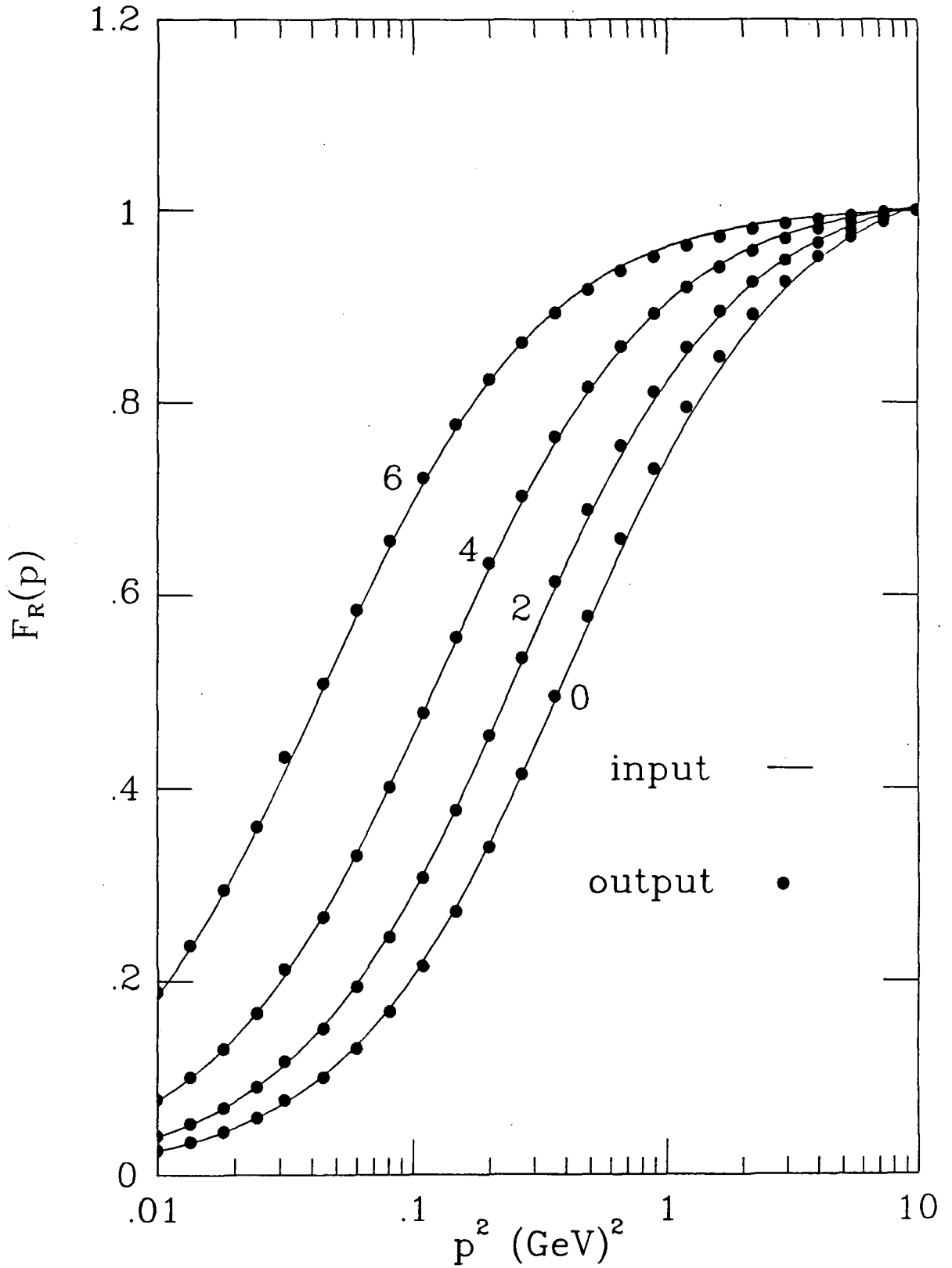


fig. 6.9: The quark renormalisation function $\mathcal{F}_R(p)$ as a function of p^2 for $\alpha(\mu) = 0.3$, with $n_f = 0, 2, 4, 6$.

| n_f | 0 | 2 | 4 |
|----------------|----------|----------|-----------|
| A | 0.004207 | 0.001881 | 0.0007524 |
| a_1 | 0.9313 | 0.9426 | 0.9544 |
| p_0 (GeV) | 0.1794 | 0.1873 | 0.1874 |
| b_1 | 1.055 | 0.6509 | 0.4534 |
| c_1 | 0.1308 | 0.1091 | 0.08631 |
| q_0 (GeV) | 0.1443 | 0.1252 | 0.1224 |
| d_1 | 0.4379 | 0.4311 | 0.4117 |
| f_1 | 0.9985 | 0.9982 | 0.9976 |
| r_1 | 0.1034 | 0.07986 | 0.0509 |
| δ (MeV) | 4.422 | 1.006 | 0.4539 |

Table 6.1: Parameters for $\mathcal{F}_R(p)$ and $\mathcal{G}_R(p)$ with $\alpha(\mu) = 0.15$, for solutions shown in figs. 6.2 and 6.3.

| n_f | 0 | 2 | 4 | 6 |
|----------------|---------|----------|----------|-----------|
| A | 0.01533 | 0.008523 | 0.003716 | 0.0009881 |
| a_1 | 0.9352 | 0.9315 | 0.9470 | 0.9610 |
| p_0 (GeV) | 0.3037 | 0.2611 | 0.2116 | 0.1927 |
| b_1 | 0.9394 | 0.8415 | 0.7944 | 0.4447 |
| c_1 | 0.1386 | 0.1361 | 0.1063 | 0.07684 |
| q_0 (GeV) | 0.2636 | 0.1986 | 0.1436 | 0.1217 |
| d_1 | 0.4918 | 0.4482 | 0.4514 | 0.4375 |
| f_1 | 1.004 | 1.000 | 0.9985 | 0.9971 |
| r_1 | 0.2130 | 0.1572 | 0.1115 | 0.05446 |
| δ (MeV) | 13.22 | 10.98 | 4.895 | 4.002 |

Table 6.2: Parameters for $\mathcal{F}_R(p)$ and $\mathcal{G}_R(p)$ with $\alpha(\mu) = 0.2$, for solutions shown in figs. 6.4 and 6.5.

| n_f | 0 | 2 | 4 | 6 |
|----------------|---------|--------|---------|----------|
| A | 0.03254 | 0.0208 | 0.01046 | 0.003833 |
| a_1 | 0.9744 | 0.9761 | 0.9467 | 0.9454 |
| p_0 (GeV) | 0.4501 | 0.4524 | 0.3935 | 0.4120 |
| b_1 | 1.198 | 1.296 | 1.128 | 0.4215 |
| c_1 | 0.1079 | 0.1155 | 0.1299 | 0.1054 |
| q_0 (GeV) | 0.3870 | 0.3250 | 0.2441 | 0.1696 |
| d_1 | 0.6605 | 0.6195 | 0.5188 | 0.4620 |
| f_1 | 1.021 | 1.010 | 1.001 | 0.9972 |
| r_1 | 0.4049 | 0.2980 | 0.1998 | 0.1167 |
| δ (MeV) | 8.861 | 12.44 | 12.39 | 10.27 |

Table 6.3: Parameters for $\mathcal{F}_R(p)$ and $\mathcal{G}_R(p)$ with $\alpha(\mu) = 0.25$, for solutions shown in figs. 6.6 and 6.7.

| n_f | 0 | 2 | 4 | 6 |
|----------------|---------|---------|---------|----------|
| A | 0.05263 | 0.03758 | 0.02173 | 0.009141 |
| a_1 | 1.006 | 0.9778 | 0.9605 | 0.9843 |
| p_0 (GeV) | 0.6121 | 0.6046 | 0.8482 | 0.6095 |
| b_1 | 1.527 | 1.432 | 0.5433 | 0.1634 |
| c_1 | 0.09592 | 0.1226 | 0.1269 | 0.06521 |
| q_0 (GeV) | 0.4867 | 0.4498 | 0.3827 | 0.3066 |
| d_1 | 0.8051 | 0.7034 | 0.5990 | 0.5852 |
| f_1 | 1.046 | 1.029 | 1.015 | 1.001 |
| r_1 | 0.6410 | 0.5035 | 0.3512 | 0.2103 |
| δ (MeV) | 5.087 | 7.769 | 10.90 | 12.47 |

Table 6.4: Parameters for $\mathcal{F}_R(p)$ and $\mathcal{G}_R(p)$ with $\alpha(\mu) = 0.3$, for solutions shown in figs. 6.8 and 6.9.

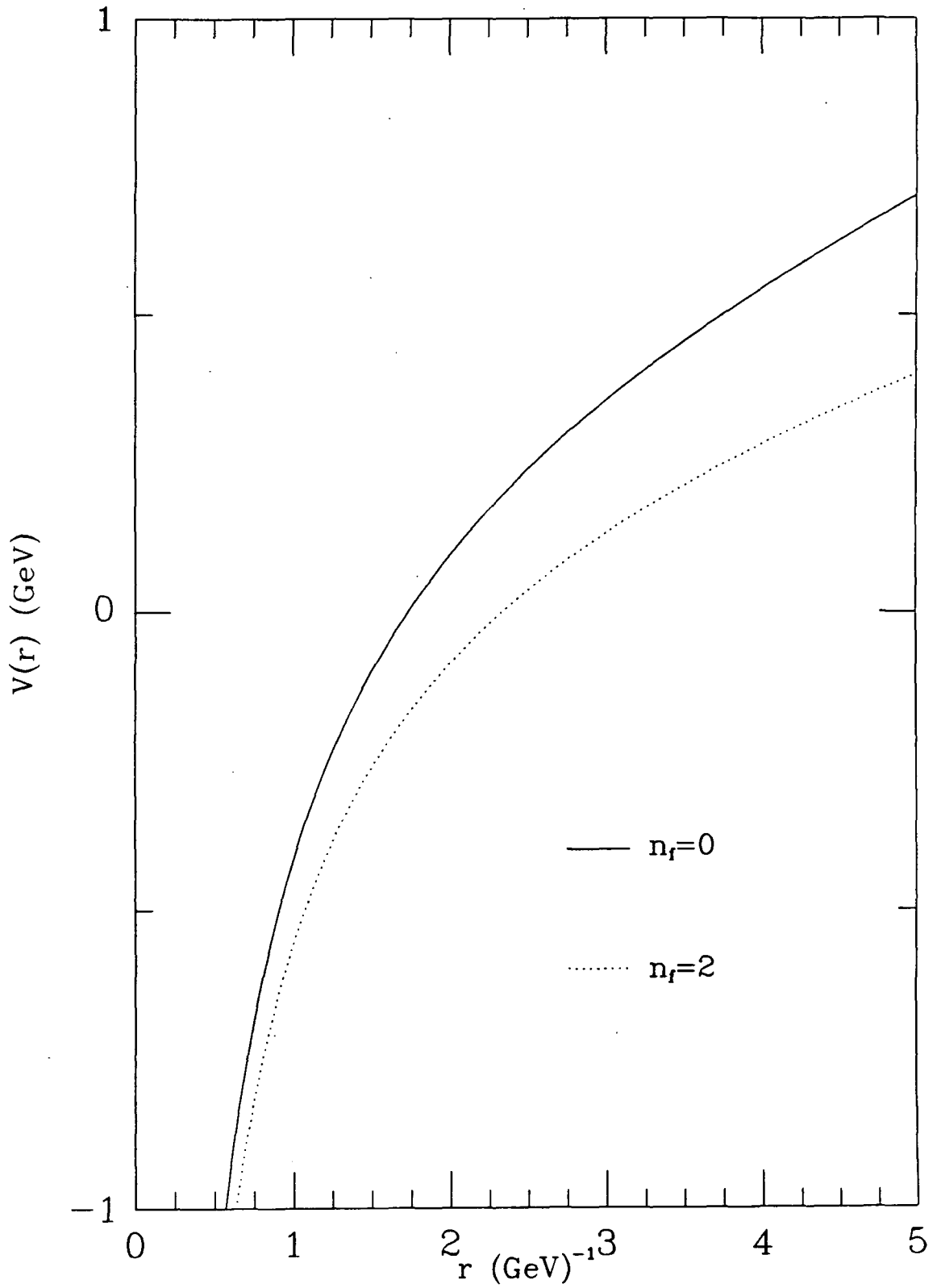


fig. 6.10: The static colour potential $V(r)$ as a function of r , derived from our gluon renormalisation function $\mathcal{G}_R(p)$ for $\alpha(\mu) = 0.25$, with $n_f = 0, 2$.

CHAPTER SEVEN

A NON-PERTURBATIVE STUDY OF QCD

7.1 Propagation of Quarks and Gluons

In the preceding chapters we have used a truncation of the Schwinger-Dyson equations to investigate the infra-red behaviour of the quark and gluon propagators in QCD. Our numerical analysis of the gluon and quark renormalisation functions $\mathcal{G}_R(p)$, $\mathcal{F}_R(p)$ reveal a striking low momentum behaviour. In the two different approximations we have used for the gluon equation in chapters three and four, we have obtained a consistent solution for $\mathcal{G}_R(p)$ which is as singular as $1/p^2$ as $p^2 \rightarrow 0$. This means that in this infra-red limit the gluon propagator itself is as singular as $1/p^4$. As discussed in section 4.5, there is very good reason to suppose that this enhanced infra-red behaviour is an indication of confinement. This can be demonstrated in a gauge invariant way by the fact that the Wilson loop operator obeys an area law. More naively, the Fourier transform of the propagator, which will contribute to the potential between static colour charges, gives rise to a linear term which should be sufficient to confine colour. We also have a simple intuitive interpretation of this confinement mechanism, it being related to a 'dual' Meissner effect with respect to colour charge.

We then proceeded to investigate the effect that this infra-red enhancement of the gluon has on the propagation of the coloured quarks. Corresponding to the low momentum enhancement of the gluon we find a suppression in the fermion function $\mathcal{F}_R(p)$, such that it vanishes at $p^2 \rightarrow 0$. Indeed it vanishes sufficiently fast that there is no physical particle pole on the quark mass-shell at $p^2 = 0$. Physically we can say that a quark cannot propagate on, or near mass shell, because of the vanishing of its propagator. At high momentum, however, the propagator is found to behave as if it were almost free. This offers us an explanation perhaps, of the experimental observation of almost free quarks in

high energy collisions over small distances, before the confining mechanism sets in as the quarks separate to larger distances. This high energy behaviour is also found for the gluon propagator. This is exactly what we would expect from the successes of perturbative QCD at high energies, and in particular the property of ‘asymptotic freedom’.

As was also mentioned in section 4.5, we have chosen to work in a covariant gauge as opposed to an axial gauge which has been studied before. This was a necessary step, as this infra-red enhancement which seems so intimately related to confinement can be shown to be absent in an axial gauge, and we cannot therefore hope to demonstrate confinement by using the Wilson loop operator in such axial gauges. Since this particular argument relies on gauge invariant quantities it remains the most important way of extracting information about the theory from the non gauge invariant propagator.

We have managed to demonstrate the validity of the simple ‘Mandelstam approximation’, used in chapter four, by comparing the qualitative features of the results obtained, to the more exact approximation used in chapter three, based on solving the Slavnov-Taylor identity for the full triple gluon vertex. Because of its relative simplicity, the use of the Mandelstam approximation has allowed us to study the inclusion of massless quarks into the theory. Numerical simplicity was essential in studying the coupled equations for both the quark and gluon propagators in chapter six, which is the first study of a dynamically coupled quark-gluon system within the context of the Schwinger-Dyson equations.

The infra-red enhancement of the gluon propagator, and the corresponding suppression of that of the quark, was first studied using the ‘quenched’ approximation, in which the effect of closed quark loops was neglected in the equation for the gluon. This infra-red behaviour was found to survive the inclusion of dynamical quarks, and the subsequent coupling of the equations. We do

find, however, that the effects are damped, and that as we include more flavours of fermions the gluon propagator has much less enhancement, and as a result of this, the suppression of the quark propagator is diminished. Indeed, as can be seen from the graphs in figs. 6.2-6.9, it seems that for about eight flavours of massless quarks the enhancement of the gluon propagator, and therefore maybe confinement, will disappear. We might well expect this, for the inclusion of quarks affects the one-loop beta function in perturbation theory (see Eqs. 1.17 to 1.23) to the extent that for more than sixteen flavours of quarks the sign of β_0 will change. This will mean that to leading order in perturbation theory the coupling strength will behave like that of QED, and grow as we go to larger momentum, becoming smaller as we go to low momentum. The effect that we find, however, suggests that non-perturbatively quarks have a bigger effect than we might naively expect from perturbation theory. Although it is only the qualitative features of our study which are likely to be reliable, this conclusion does support other evidence[6.2,6.3] that quarks play an important role in non-perturbative physics.

7.2 Ultraviolet Problems

In order to solve the equations generated for the quark and gluon propagators, it was necessary to remove the ultraviolet divergences which occurred, and to introduce the running couplings $\alpha_1(\mu), \alpha_2(\mu), \alpha_3(\mu)$ from Eqs. 4.12,5.26 and 6.23, which for completeness we give here:

$$\begin{aligned} \frac{1}{\alpha_1(p)} &= \frac{1}{\alpha_1(\mu)} \left(\frac{\mathcal{G}_R(\mu)}{\mathcal{G}_R(p)} \right)^2 \\ \frac{1}{\alpha_2(p)} &= \frac{\mathcal{G}_R(\mu)}{\mathcal{G}_R(p)} \left(\frac{1}{\alpha_2(\mu)} - \frac{C_F}{4\pi^3} \int d^4k \mathcal{G}_R(k) [\mathcal{K}(k,p) - \mathcal{K}(k,\mu)] \right) \\ \frac{1}{\alpha_3(p)} &= \frac{1}{\alpha_3(\mu)} \frac{\mathcal{G}_R(\mu) \mathcal{F}_R(\mu)}{\mathcal{G}_R(p) \mathcal{F}_R(p)} \end{aligned} \quad (7.1)$$

The last of these is derived in an analogous way to the first two using the definition of $\alpha_3(\mu)$ following Eq. 6.22. The consistent renormalisation of the Schwinger-Dyson equations is as yet an unsolved problem. Exact gauge invariance, as expressed in the content of the Slavnov-Taylor identities demands that these three couplings should be the same[1.6,2.1]. This is patently not so, as we can see from Eq. 7.1, but we would expect this, as the truncation detailed in chapter two, used to derive the equations we have studied, ignores the Schwinger-Dyson equations for the three-point functions. It is these that determine the behaviour of the couplings in the theory.

In our equations it is only the explicit $\alpha_i(\mu)$ that appear, although of course the full running coupling does enter implicitly through Eq. 7.1, and the equations for $\mathcal{G}_R(p)$ and $\mathcal{F}_R(p)$.

We can expand Eq. 7.1 in powers of the α_i to obtain:

$$\frac{1}{\alpha_i(p)} = \frac{1}{\alpha_i(p)} + \frac{\beta_0^{(i)}}{4\pi} \ln\left(\frac{p^2}{\mu^2}\right) = \frac{\beta_0^{(i)}}{4\pi} \ln\left(\frac{p^2}{\Lambda_i^2}\right) \quad (7.2)$$

where we have distinguished the three Λ_i (see sections 1.4 and 3.4). The coefficients $\beta_0^{(i)}$ are equal to :

$$\begin{aligned} \beta_0^{(1)} &= 2\left(\frac{7}{3}C_A - \frac{4}{3}n_f T_F\right) = 2\gamma_0 \\ \beta_0^{(2)} &= \frac{7}{3}C_A + \frac{3}{4}C_F \\ \beta_0^{(3)} &= \frac{7}{3}C_A \end{aligned} \quad (7.3)$$

where we have included the effects of fermions in $\alpha_1(\mu)$, and used the fact that $\mathcal{F}_R(p)$ is finite to one-loop in the Landau gauge. The lowest order perturbative results in the Landau gauge: $\beta_0 = (11/3)C_A - (4/3)n_f T_F$, which is independent of the gauge, and $\gamma_0 = (13/6)C_A - (4/3)n_f T_F$ are both independent of the Casimir C_F as a result of gauge invariance. Eq. 7.3 highlights the differences between our three couplings. We note in passing that all three couplings have

the correct sign for β_0 , as they better had do if we are to control the asymptotics.

For completeness we plot the three running couplings in fig. 7.1, over the range of p^2 for which we solved the Schwinger-Dyson equations for $\mathcal{G}_R(p)$ and $\mathcal{F}_R(p)$. Outside this range we cannot consistently determine them from Eq. 7.1 because of the dependence on these quark and gluon renormalisation functions. In the light of this it should be mentioned that for small enough p^2 , the $\alpha_2(p)$ coupling develops a pole. This arises from the bracketed term in the second equation of Eq. 7.1. The enhanced term $A\mu^2/k^2$ from $\mathcal{G}_R(k)$ inside the integral does not generate any infra-red singularities (see section 5.3). Nevertheless, it generates a term proportional to μ^2/p^2 by dimensional counting, which for sufficiently small p^2 (outside our range) is large enough to cancel the term $1/\alpha_2(\mu)$. Hence $1/\alpha_2(p)$ is zero and the coupling has a pole. This behaviour though, is entirely due to the form of our renormalisation, and to the approximations we have used. A totally consistent renormalisation of the equations which properly treats the couplings should rectify this problem. The other two couplings are well behaved for all momenta. In our study we make the simple ansatz that $\alpha_1(\mu) = \alpha_2(\mu) = \alpha_3(\mu)$.

In previous investigations of the Schwinger-Dyson equations, there has been little or no discussion of the problems of a consistent renormalisation. This remains one of the outstanding problems in using these equations to investigate non-perturbative physics. Hopefully by highlighting the difficulties as we have done here, it will be possible to reach a greater understanding of the problems involved, and eventually to solve them.

On a practical level, we note that not only do the ultraviolet renormalisations we have employed serve to make our equations finite, but they have done so *independently* of any form of parameterisation we might choose for the functions $\mathcal{G}_R(p)$ and $\mathcal{F}_R(p)$. Since our study has been largely a numerical one, the particular solutions we obtain should hopefully be *numerically* similar to the

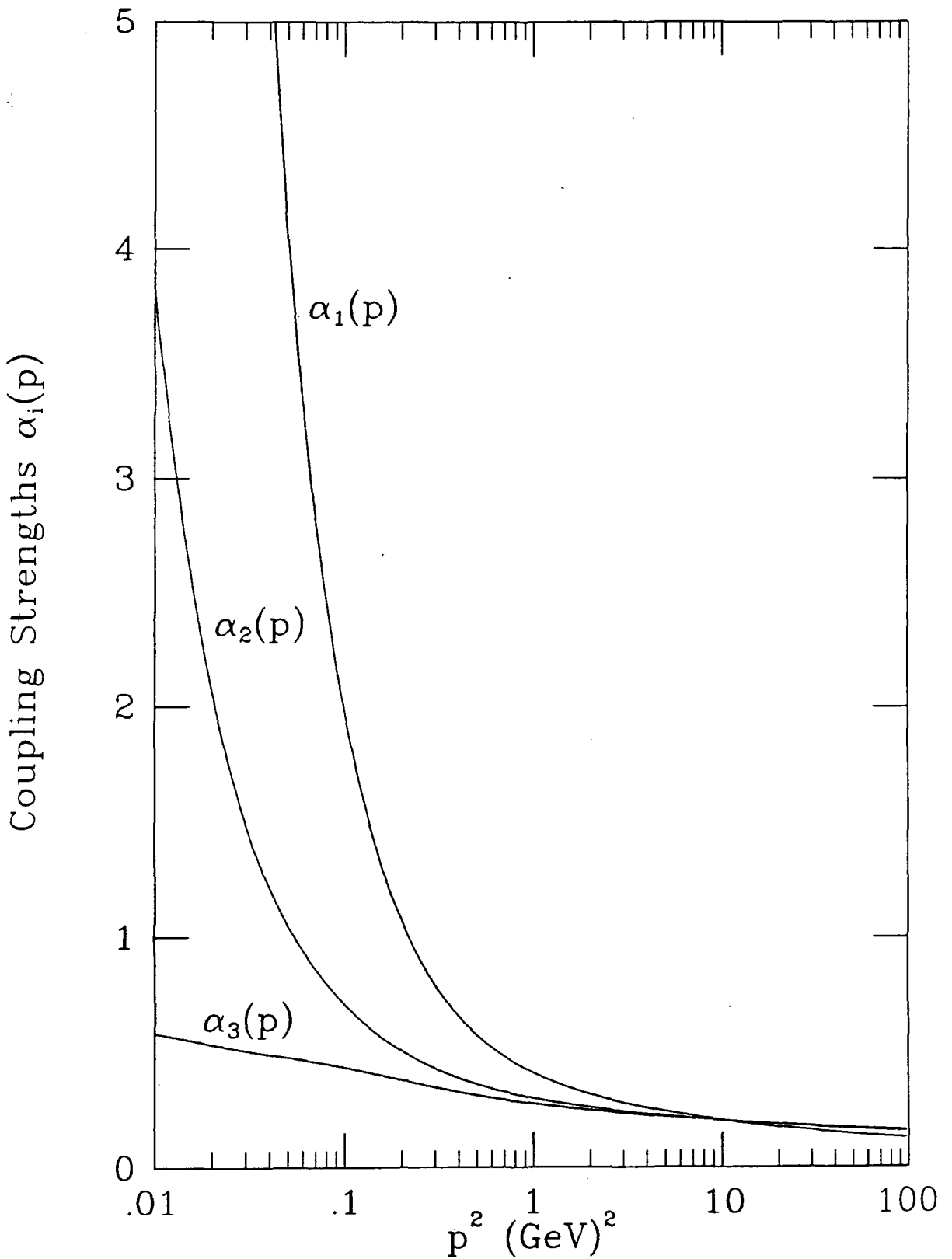


fig. 7.1: The three running couplings $\alpha_i(\mu)$, with $i = 1, 2, 3$, as a function of p^2 , with $\alpha_i(\mu) = 0.2$, $i = 1, 2, 3$.

exact solutions, although the analytic form will certainly be different.

Finally it is of interest to ask how the solutions depend on the renormalisation scale μ^2 . Were our renormalisations entirely consistent, we would expect them to be invariant under the transformations of the renormalisation group (see section 1.4). Since our renormalisations are not totally consistent we might expect some discrepancy. Nevertheless, it is possible to show that our solutions are at least approximately renormalisation group invariant. To demonstrate this we return to the Mandelstam equation of chapter four, with no quarks for simplicity. We start from Eq. 4.12, which we cast into the form:

$$\mathcal{G}_R(p, \mu) = \mathcal{G}_R(\mu, \mu) \left(\frac{\alpha_1(p)}{\alpha_1(\mu)} \right)^{1/2} \quad (7.4)$$

where here we use the notation $\mathcal{G}_R(p, \mu)$ to denote the gluon renormalisation function evaluated at p^2 , with renormalisation scale μ^2 . We can evaluate this equation at a different renormalisation scale $\bar{\mu}^2$. Since we must have $\mathcal{G}_R(\mu, \mu) = \mathcal{G}_R(\bar{\mu}, \bar{\mu})$ (which we usually choose equal to 1), we can easily derive:

$$\begin{aligned} \mathcal{G}_R(p, \bar{\mu}) &= \mathcal{G}_R(p, \mu) \left(\frac{\alpha_1(\mu)}{\alpha_1(\bar{\mu})} \right)^{1/2} \\ &= \frac{\mathcal{G}_R(p, \mu)}{\mathcal{G}_R(\bar{\mu}, \mu)} \end{aligned} \quad (7.5)$$

We can re-solve our Schwinger-Dyson equation, but this time choosing a renormalisation scale $\bar{\mu}^2$. The equation now depends explicitly on $\alpha_1(\bar{\mu})$, which we can evaluate from the first equation in Eq. 7.1 (see fig. 7.1), using our previous solution for the Schwinger-Dyson equation plotted in fig. 4.3. Having done this, we can check to what extent Eq. 7.5 holds. We solve the equation for three scales: $\mu^2 = 4, 10, 25 \text{ GeV}^2$, where we choose $\alpha_1(10) = 0.2$, which gives us $\alpha(4) = 0.2558$ and $\alpha(25) = 0.1650$ (see fig. 7.1). Here we use an obvious notation, in that $\alpha_1(4)$ denotes the value of the running coupling $\alpha_1(p)$ at $p^2 = 4$. From the solution of chapter four (parameters in table 4.1), we

have $\mathcal{G}_R(4, 10) = 1.131$, $\mathcal{G}_R(10, 10) = 1$ and $\mathcal{G}_R(25, 10) = 0.9083$. The curves $\mathcal{G}_R(p, \mu) \times \mathcal{G}_R(\mu, 10)$ are plotted for our three different values of μ^2 in fig. 7.2. We see that Eq. 7.5 does indeed hold to within a satisfactory degree.

This completes our discussion of the ultraviolet renormalisation of the equations we have studied. It is evident that problems of consistency remain and that further research is required. However, in the spirit of this study as a *model* for the true behaviour of these equations, it is hoped that what we have achieved does shed some light upon the non-perturbative region of QCD, as well as highlighting the problems which further study must face.

7.3 Infra-red Problems

Central to the results obtained throughout this study, is the conclusion that as the momentum $p^2 \rightarrow 0$, the gluon renormalisation function $\mathcal{G}_R(p) \sim A\mu^2/p^2$, and hence the gluon propagator behaves like $1/p^4$ in this limit. The size of this enhancement $A\mu^2$ carries the dimensions of mass-squared, and is presumably related to some intrinsic scale of the theory Λ . This enhancement of the gluon leads to a suppression of the quark function $\mathcal{F}_R(p)$, which using the parameterisation of Eq. 5.44 is characterised by a momentum scale r_1^2/f_1 . This too should be related to some intrinsic scale.

Such a scale naturally arises in renormalisation, but because of the difficulties of consistently renormalising the equations, it is not clear which of the three scales in Eq. 7.2 we might take. For definiteness, we consider the scale Λ_1 from the gluon equation, as it is the coupling α_1 which plays the most central role in this study, the others vanishing when we do not have quarks. Indeed it is this coupling which leads to the infra-red enhancement of $\mathcal{G}_R(p)$, which as stated is our central result.

In fig. 7.3, we plot the scale of the gluons infra-red enhancement $A\mu^2$, and that of the quarks suppression r_1^2/f_1 against Λ_1^2 , for $n_f = 0$. Essentially

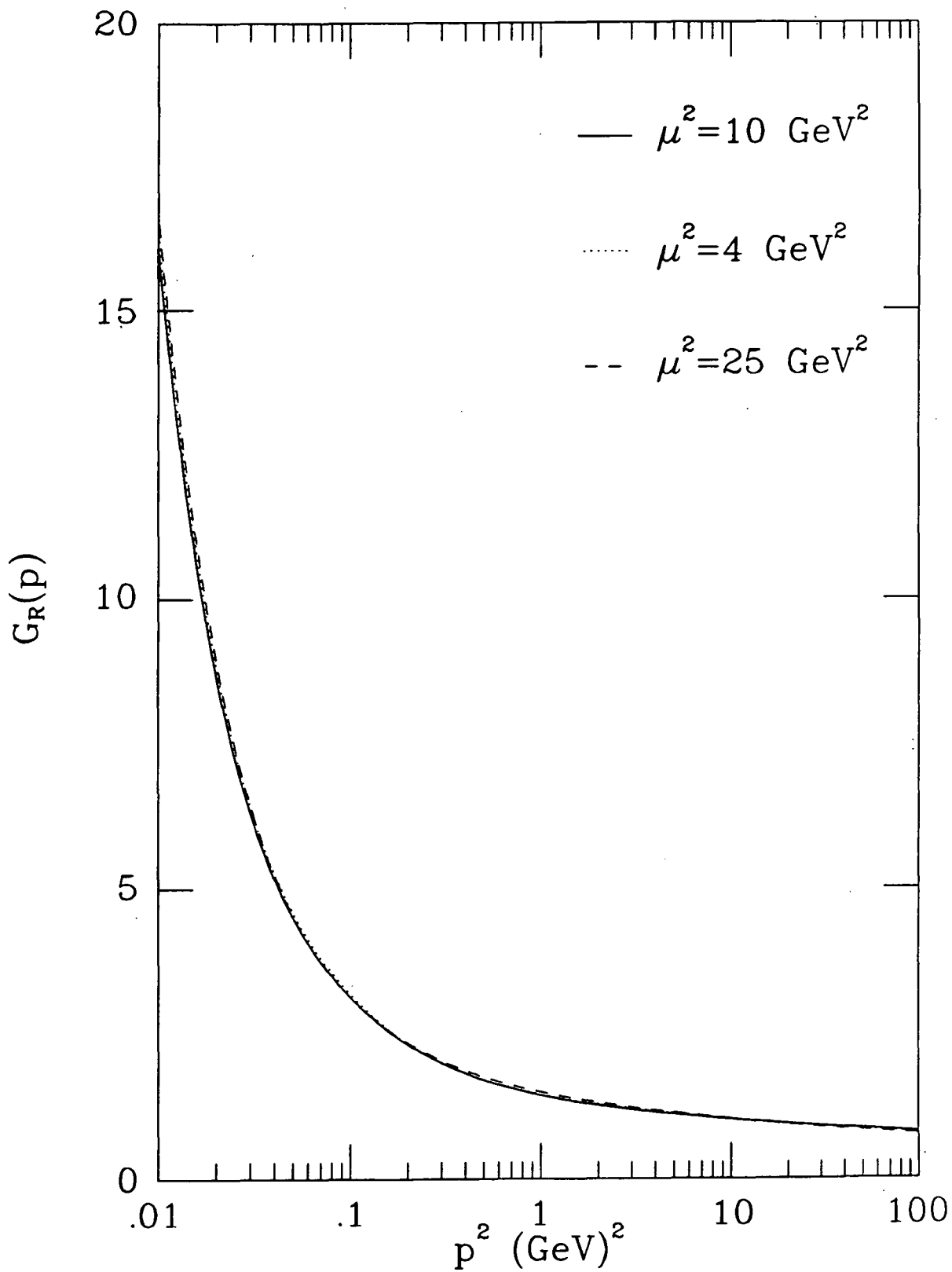


fig. 7.2: The curves $\mathcal{G}_R(p, \mu) \times \mathcal{G}_R(\mu, 10)$ as a function of p^2 , with $\mu^2 = 4, 10, 25 \text{ GeV}^2$.

this corresponds to solutions for different $\alpha_1(\mu)$, where as usual $\mu^2 = 10 \text{ GeV}^2$. We can represent both these scales as being proportional to Λ_1^2 modified by logarithms. In fig. 7.3 we have also plotted the curves

$$\begin{aligned} A\mu^2 &= 0.497\Lambda_1^2 \left(\ln\mu^2/\Lambda_1^2 \right)^{0.673} \\ r_1^2/f_1 &= \Lambda_1^2 \left(0.36 + 107 \left(\ln\mu^2/\Lambda_1^2 \right)^{-5} \right) \end{aligned} \quad (7.6)$$

These are more to guide the eye, than meant as serious analytic expressions. The error bars were determined using an analysis of the input/output agreement of our solutions. This modification by logarithms, however, may well be due to the fact that although the power of the infra-red enhancement of $\mathcal{G}_R(p)$ is given by $1/p^2$, the exact analytic form of this enhancement will have logarithmic modifications in p^2 . In a numerical study such as ours, it would be extremely difficult to determine such behaviour, and indeed the important fact is the existence of a power-law infra-red enhancement, irrespective of any logarithmic deviations. In general, the scale in our equations, and in perturbation theory, is introduced by choosing μ^2 and a value for $\alpha(\mu)$. The scale μ^2 is arbitrary, and can be eliminated leaving the theory dependent on a scale parameter Λ , which is intrinsic to the theory. Λ is to be determined by experiment. Perturbative quantities such as the running coupling at large momenta, have in general, a logarithmic dependence on Λ . We have seen that in the non-perturbative regime that this can become a power law dependence, with its important consequences for confinement.

The other infra-red momentum scale δ , introduced in chapter five to make the quark equation infra-red finite, seems to have no obvious dependence on the scale Λ_2 . We plot this variation for the $n_f = 0$ solutions in fig. 7.4. The error bars here are large, because the quark equation determines the quantity $\ln\mu/\delta$, for which the error is relatively small, but we need to exponentiate this to obtain δ . The value for δ mostly seems to be between 1 and 13MeV. As

mentioned in section 5.3, a priori δ could have taken any value, and the values obtained of a few MeV may well have physical significance. Firstly though, since these values are an order of magnitude less than any momentum for which we solve the quark and gluon equations, it may be hoped that the exact details of the infra-red regularisation employed do not significantly alter the qualitative nature of the solutions. Secondly, and perhaps more interestingly, such a value for δ is not widely different from the masses of the lightest flavours of quarks in the real world. This may bode well for solutions to the quark equation which break chiral symmetry and develop a dynamical mass for the quarks.

Finally, and related to this, we note that δ was introduced to remove the infra-red divergences in the fermion equation, arising from the $A\mu^2/p^2$ enhancement of $\mathcal{G}_R(p)$. In the completely separate study of the gluon equation in chapter three, we used a ‘plus’ prescription in order to define our integrals. In many respects this is less satisfactory than the introduction of an infra-red cut-off δ , since at least this latter procedure does have some physical interpretation, as well as being performed entirely within the context of the equations studied, since the non-linearity of the resulting equation should then determine this scale δ too. The plus prescription on the other hand is introduced somewhat arbitrarily, the main advantage being the relatively simple numerical implementation, without the somewhat contorted manipulations of section 5.3. However, this plus prescription as implemented through Eq. 3.41 does mean that we subtract a different finite amount at each value of p^2 , in addition to removing the infinity. This now seems rather unsatisfactory and so it would be nice to repeat the calculation of chapter three introducing such an infra-red cut-off δ , despite the increased complexity of the calculation.

Of course, there is some arbitrariness in any way of introducing an infra-red regularisation, although as far as our solutions are concerned it is arguments based on dimensionality which really matter. Since the functions $\mathcal{G}_R(p), \mathcal{F}_R(p)$

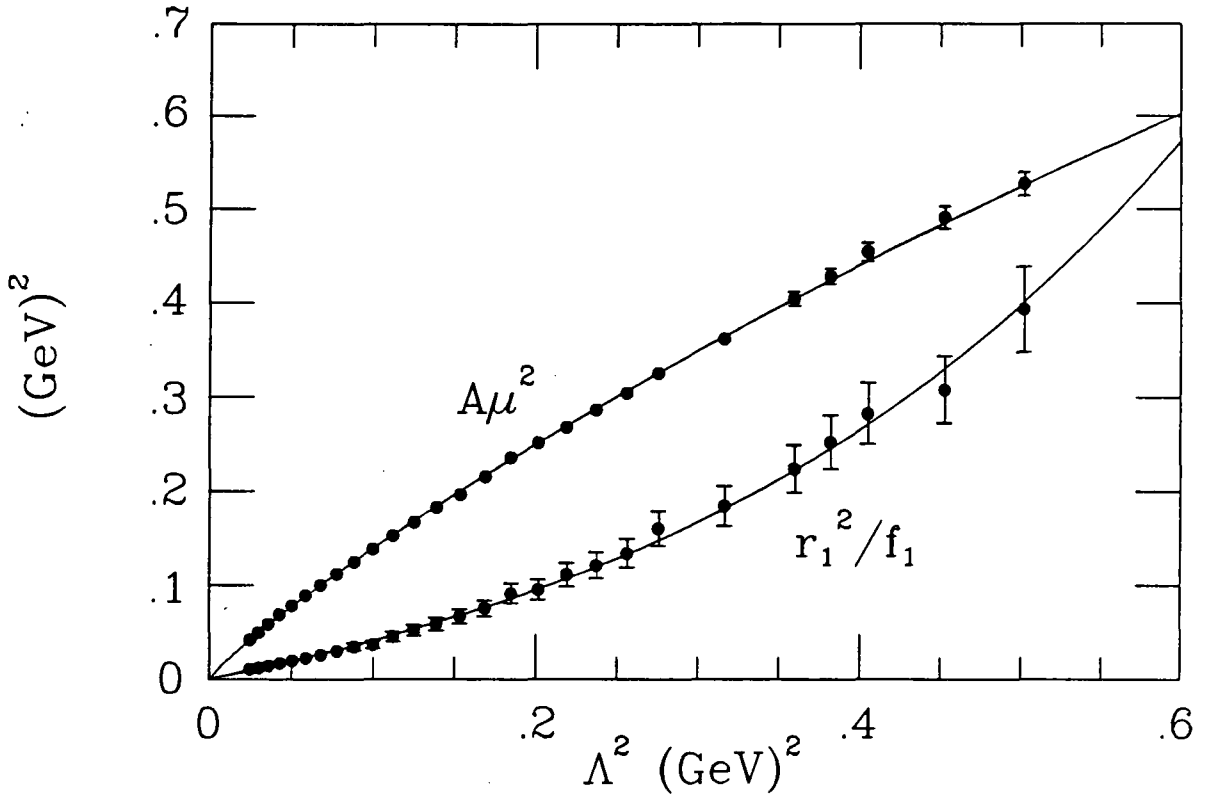


fig. 7.3: The gluon enhancement scale $A\mu^2$, and the quark suppression scale r_1^2/f_1 , as a function of Λ_1^2 . Also plotted are the curves described in Eq. 7.6. The error bars were determined from an input-output analysis of our solutions to the Schwinger-Dyson equations.

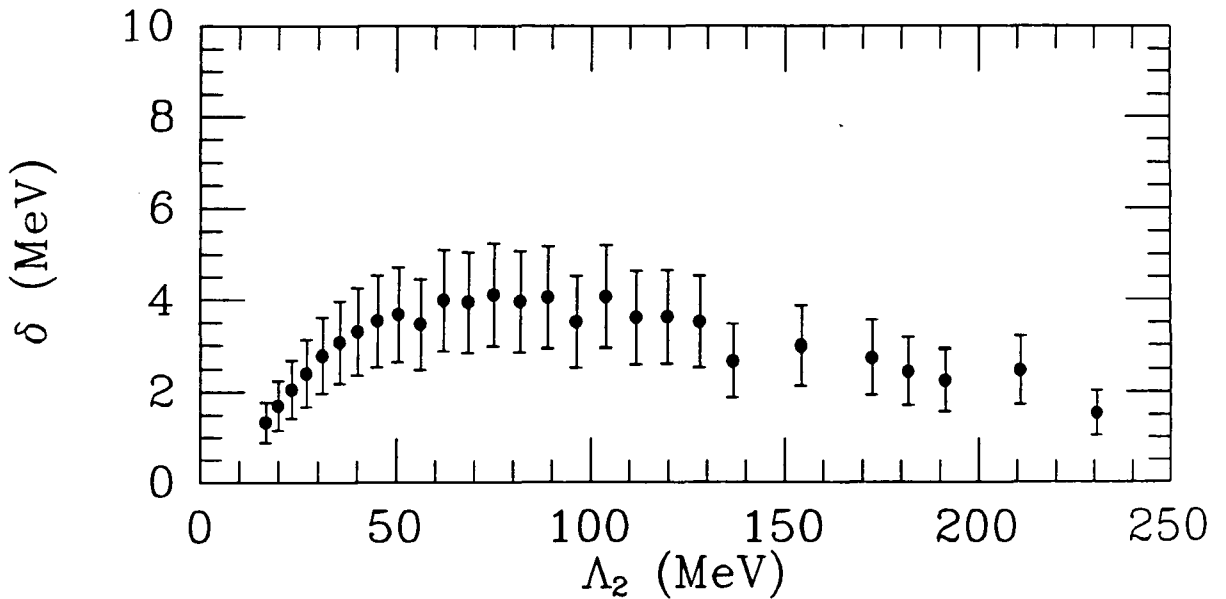


fig. 7.4: The infra-red cutoff δ as a function of Λ_2 .

are dimensionless, when we integrate a term proportional to $A\mu^2/k^2$, the answer too must be dimensionless. Thus the momentum μ^2 in the numerator must be balanced, and the only available quantity is the external momentum p^2 . Thus the result of such an integration must be proportional to μ^2/p^2 although of course for the divergent integrals the coefficient of this term will be infinite. Different methods of dealing with these divergences will only generate different coefficients for such a term, and not affect its existence. Thus the derivation of the infra-red enhanced solutions for $\mathcal{G}_R(p)$ in the different studies of refs. [3.1-3.3,4.1,4.2,6.1] encourages us to believe that this behaviour is indeed that of the complete theory, where presumably such problems might not arise.

7.4 Approximations and Improvements

Our entire program of analysis of the Schwinger-Dyson equations for QCD rests on the truncations and approximations, used to generate closed and finite equations. These approximations are obviously essential, as it is impossible to attack the entire infinite hierarchy of equations at once. Nevertheless, if we are to retain some hope of modelling the physics of the real world, we must try to justify these approximations, and to understand what they entail.

One of the main approximations we make in this study is the retention of only the longitudinal part of the vertices or three-point functions. As was shown in section 2.5, the neglected transverse part of these vertices will vanish when the external momenta go to zero, and as it is the low momentum behaviour we wish to investigate, this approximation is to a large extent justified. This is borne out by the study of ref. [3.2], where it is argued that inclusion of the transverse part of the vertex will not affect the existence of the infra-red enhanced solutions obtained, but they will affect its coefficient. It is likely, therefore, that retention of only the longitudinal part will accurately model the qualitative behaviour of the small momentum limit of the theory[7.1]. It should

also be noted that to leading order in $\alpha(\mu)$ the longitudinal part of the vertex gives the leading perturbative behaviour, although this can be affected in other ways, for example by our neglecting ghost contributions. Thus this particular approximation of neglecting the transverse part of the vertices seems to be well motivated.

In the light of our comments on axial gauges in section 4.5, it is desirable to perform calculations in other gauges. The immediate disadvantage of a covariant gauge is the inclusion of ghost contributions. If we work in the Landau gauge, however, then many of the ghost contributions will vanish at low momentum (see section 2.5), considerably simplifying the Slavnov-Taylor identities. We can also demonstrate that in perturbation theory the ghost contributions to the gluon propagator are numerically small (see section 2.6), and so we neglect the ghost loop in the Schwinger-Dyson equation.

The elimination of ghost contributions, however, is probably the least satisfactory part of the study. To demonstrate its validity we should study the Schwinger-Dyson equation for the ghost propagator, which is identical in form to the equation for the fermion. Unfortunately, we have no way of making a satisfactory ansatz for the ghost-gluon vertex, and so must rely on the argument that it is equal to the bare ghost-gluon vertex for small momentum in the Landau gauge. Indeed, it is the presence of ghosts in the spectrum which enables the covariant gauge propagator to escape the no-go theorem of West (see chapter 4.6), and which therefore allows the covariant gauge gluon propagator to have an infra-red enhanced behaviour.

Many of the problems may be related to the problem of gauge invariance. Although by demanding that our vertices satisfy the Slavnov-Taylor identities we do retain some form of gauge invariance, our truncation which neglects the Schwinger-Dyson equations for the three-point and higher Green's functions means that we cannot consistently treat the coupling strength of the theory.

The neglecting of the ghost contributions further compounds this.

In further studies, where the problems of renormalisation, and a more complete treatment of the ghost contributions should be addressed, it may well be that the guiding light of gauge invariance will play a crucial role. Indeed, were we able to treat the equations in a gauge invariant way, then not only could we really begin to believe our solutions, but we would have also developed a calculational tool to rival lattice gauge theory as a means of going beyond perturbation theory.

7.5 Comments on the Solutions

Although we have only solved the equations for the quark and gluon propagators over a finite range of momenta, we have built in the asymptotic behaviour of the solutions in the limits $p^2 \rightarrow 0$, $p^2 \rightarrow \infty$. In the light of this it is likely that our numerical solutions are indeed close to the exact solutions of the equations we have derived. An obvious question to ask is whether these solutions are unique. For the simple parameterisations we have chosen for $\mathcal{G}_R(p)$ and $\mathcal{F}_R(p)$ we have not found any other solutions. Indeed, it is difficult to see what a different solution would look like, given that we have built in the correct infra-red and ultraviolet behaviour of the solution.

The equations also depend explicitly on the various colour factors that arise. For all our solutions we have chosen $C_A = N_c = 3$ as in ‘real’ QCD. However, we have solved for a range of $\alpha(\mu)$ which suggests that the qualitative form of our solutions remain valid as we change the number of colours. It is the explicit combinations $\alpha(\mu)C_A$ and $\alpha(\mu)n_f$ which appear in the gluon equation, multiplying the gluon loop and the quark loop diagrams respectively. Since $C_A = N_c$, where the gauge group is $SU(N)$, our equation is invariant under the replacements:

$$\begin{aligned}
N_c &\rightarrow N'_c \\
\alpha &\rightarrow 3\alpha/N'_c \\
n_f &\rightarrow n_f N'_c/3
\end{aligned}
\tag{7.7}$$

For example, the solution with $N_c = 3$, $\alpha(\mu) = 0.3$ and $n_f = 0, 2, 4, 6$ can equally well be regarded as the solution for $N_c = 6$, $\alpha(\mu) = 0.15$ and $n_f = 0, 4, 8, 12$ respectively. The important conclusion is that for a gauge theory based on $SU(6)$ for example, we could accommodate many more flavours of massless fermions than for $SU(3)$, and we therefore expect that the solutions with $N = 6$, $\alpha(\mu) = 0.3$ will have a much larger infra-red enhancement. This is in keeping with the philosophy of the $1/N$ expansions, where in the limit that $N \rightarrow \infty$ we can neglect the dynamical effect of fermions. It is clear from our solutions, however, that $N = 3$ is a long way from this large N limit, at least as far as the effect of fermion flavours is concerned. A heuristic criterion for neglecting the effect of fermions would appear to be simply that $n_f/N_c < 1$. At high momentum, the one-loop beta function would tell us that this should be $(2n_f)/(11N_c) < 1$. Once again this demonstrates that at low momentum quarks play an important role.

7.5 Conclusions

In the preceding chapters we have carried out an extensive study of the Schwinger-Dyson equations for QCD. This infinite hierarchy of equations are in a sense the field equations of a quantum field theory, relating the different Green's functions to which all scattering amplitudes are related.

To date, however, most calculations in field theory are carried out using perturbation theory, expanding the Green's functions in powers of the coupling constant α . This allows a consistent and gauge invariant renormalisation of the ultraviolet infinities which appear. For a non-Abelian theory it is found that the renormalised coupling decreases as we go to larger momenta, making high

energy perturbative calculations reliable, and agreeing with the experimental observation of the coloured quarks behaving as if they were almost free within hadrons.

For small momenta, however, the coupling strength grows, and perturbation theory breaks down. If QCD really is the theory of strong interactions, as seems to be the case, then it must contain the dynamics whereby the coloured quarks and gluons are not seen as free particles at low momenta, but are permanently confined within hadrons. It is desirable, qualitatively at least, that we understand the mechanism by which this confinement occurs.

Perturbation theory itself is no more than a truncation of the Schwinger-Dyson equations to some power in the coupling strength. Here we have employed an entirely different truncation, including contributions from all orders in α . This will hopefully contain some information about the non-perturbative behaviour of QCD, and in particular confinement.

We have derived equations for the quark and gluon propagators. Studies of these have revealed a power law infra-red enhancement for the gluon propagator, which we have been able to relate to confinement through an area law for the Wilson loop operator. This enhancement gives rise to a linearly rising potential, strong enough to confine colour. This enhancement in turn suppresses the quark propagator at small momenta, so that physical massless quarks cannot propagate on their mass-shell. At large momenta, both the full quark and gluon propagators are equal to their bare counterparts, with logarithmic modifications. This is exactly what we expect from perturbation theory, and corresponds to the quarks and gluons behaving like almost free particles at these high momenta.

Our study has in no way been exhaustive, and as we have highlighted in this chapter, significant problems remain in making this non-perturbative treatment entirely consistent. Nevertheless, the qualitative nature of the solutions we have obtained are physically believable, and may give us a deeper insight

into the nature of confinement. Perhaps more importantly, we believe we have demonstrated that the Schwinger-Dyson equations are an important tool for examining the long distance behaviour of a continuum non-Abelian gauge theory, a region hitherto out of our calculational reach, yet of fundamental importance in our understanding of strong interactions. Indeed since non-Abelian gauge theories appear to play a vital role in physics as a whole, the study of these equations may well be of even more fundamental importance.

APPENDIX A INTEGRALS

In this appendix we detail the analytic integrations we have performed throughout this study. All our integrals have been of a ‘one-loop’ type, involving a four dimensional integral over some loop momentum k . The answer depends on some external momentum such as p or μ . As we mentioned in section 2.5 our calculations are performed in Euclidean space. We choose a frame of reference in which the external momentum is defined to be:

$$p^\mu = (p, 0, 0, 0) \quad (\text{A.1})$$

and we parameterise the loop momentum in terms of the following variables:

$$k^\mu = (k \cos \psi, k \sin \psi \sin \theta \cos \phi, k \sin \psi \sin \theta \sin \phi, k \sin \psi \cos \theta) \quad (\text{A.2})$$

where $0 \leq k \leq \infty$, $0 \leq \theta, \psi \leq \pi$ and $0 \leq \phi \leq 2\pi$. In terms of these variables the four dimensional integration measure is given by:

$$d^4 k = k^3 dk \sin^2 \psi d\psi \sin \theta d\theta d\phi \quad (\text{A.3})$$

All functions in the integrand depend only on the quantities $k^2, q^2, k \cdot p$, where $q = p - k$. from Eqs. A.1 and A.2 all these are independent of θ and ϕ . Thus these two angular integrals can be performed trivially giving a factor of 4π . In many cases this is as much as we can do analytically, for example, in the calculation of chapter three, many of the terms contain the factor $\mathcal{G}(k)\mathcal{G}(q)$ in the integrand, which necessitates a numerical integration over k and ψ . However many of the integrals contain no dependence on ψ , except for powers of q^2 in the denominator from propagator factors, and powers of $k \cdot p$ in the numerator. In these cases the ψ integral can be performed, and the main work of this appendix is to detail this.

In general we must calculate an angular integral of the form:

$$\int_0^\pi \sin^2 \psi d\psi \frac{(k \cdot p)^n}{(q^2)^m} \quad (\text{A.4})$$

since $k \cdot p = kpcos\psi$, so we must evaluate:

$$I_{n,m} = \int_0^\pi \sin^2 \psi d\psi \frac{\cos^n \psi}{(a - b\cos\psi)^m} \quad (\text{A.5})$$

where the integral in Eq. A.4 for example, has $a = k^2 + p^2$, $b = 2pk$.

The simplest of these is:

$$I_{0,1} = \int_0^\pi \frac{\sin^2 \psi}{a - b\cos\psi} d\psi = \int_{-1}^1 \frac{\sqrt{1-z^2}}{a-bz} dz \quad (\text{A.6})$$

where we have substituted $z = \cos\psi$ to obtain the second integral. Putting $y = a - bz$, we obtain:

$$I_{0,1} = \frac{1}{b^2} \int_{a-b}^{a+b} \frac{\sqrt{b^2 - (a-y)^2}}{y} dy \quad (\text{A.7})$$

We set $R = b^2 - (a-y)^2 = b^2 - a^2 + 2ay - y^2$, and rewrite Eq. A.7 to get:

$$I_{0,1} = \frac{1}{b^2} \int_{a-b}^{a+b} \frac{\sqrt{R}}{y} dy = \frac{1}{b^2} \int_{a-b}^{a+b} \frac{R}{y\sqrt{R}} dy \quad (\text{A.8})$$

Using the explicit form of R in the numerator gives:

$$I_{0,1} = \frac{b^2 - a^2}{b^2} \int_{a-b}^{a+b} \frac{dy}{y\sqrt{R}} + \frac{a}{b^2} \int_{a-b}^{a+b} \frac{dy}{\sqrt{R}} + \frac{1}{b^2} \int_{a-b}^{a+b} \frac{a-y}{\sqrt{R}} dy \quad (\text{A.9})$$

The last of these three integrals is zero, as can be explicitly seen by writing $w = y - a$, giving:

$$- \int_{-b}^b \frac{w}{\sqrt{b^2 - w^2}} dw = 0 \quad (\text{A.10})$$

which vanishes by symmetry. The second of the integrals in Eq. A.9 is easily evaluated by writing $w = y - a$, giving:

$$\int_{-b}^b \frac{dw}{\sqrt{b^2 - w^2}} = \int_{-\pi/2}^{\pi/2} d\theta = \pi \quad (\text{A.11})$$

where we have used $w = b\sin\theta$. Finally, in the first integral of Eq. A.9 we put $t = 1/y$ to obtain:

$$\begin{aligned} \int_{a-b}^{a+b} \frac{dy}{y\sqrt{R}} &= - \int_{\frac{1}{a+b}}^{\frac{1}{a-b}} \frac{dt}{t\sqrt{b^2 - (a - \frac{1}{t})^2}} \\ &= \int_{\frac{1}{a+b}}^{\frac{1}{a-b}} \frac{dt}{\sqrt{b^2 t^2 - a^2 t^2 + 2at - 1}} \\ &= \frac{1}{\sqrt{a^2 - b^2}} \int_{\frac{1}{a+b}}^{\frac{1}{a-b}} dt \left[\frac{b^2}{(a^2 - b^2)^2} - \left(\frac{a}{a^2 - b^2} - t \right)^2 \right]^{-\frac{1}{2}} \end{aligned} \quad (\text{A.12})$$

where we have completed the square. Now with $v = t - a/(a^2 - b^2)$ we obtain:

$$\frac{1}{\sqrt{a^2 - b^2}} \int_{\frac{-b}{a^2 - b^2}}^{\frac{b}{a^2 - b^2}} dv \left[\frac{b^2}{(a^2 - b^2)^2} - v^2 \right]^{-\frac{1}{2}} = \frac{1}{\sqrt{a^2 - b^2}} \int_{-\pi/2}^{\pi/2} d\theta = \frac{\pi}{\sqrt{a^2 - b^2}} \quad (\text{A.13})$$

where we have used $y = b\sin\theta/(a^2 - b^2)$. Putting Eqs. A.11 and A.12 together with A.9 gives us:

$$I_{0,1} = \frac{\pi}{b^2} (a - \sqrt{a^2 - b^2}) \quad (\text{A.14})$$

We have calculated this integral in some detail, as all the other integrals are easily obtained from Eq. A.14 by differentiation and simple algebraic rearranging. In order to calculate these we also need to know the form of $I_{r,0}$. We have:

$$I_{r,0} = \int_0^\pi d\psi \sin^2\psi \cos^r\psi = \int_{-1}^1 dz z^r \sqrt{1 - z^2} = \int_0^1 dw w^{\frac{r-1}{2}} \sqrt{1 - w} \quad (\text{A.15})$$

where we have used the substitutions $z = \cos\psi$ and then $w = z^2$. The final integral in Eq. A.15 is equal to $B(\frac{r+1}{2}, \frac{3}{2})$, where $B(a, b)$ is the well known Beta function which can be written in terms of the Gamma function as:

$$B(a, b) = \frac{\Gamma(a)\Gamma(b)}{\Gamma(a+b)} \quad (\text{A.16})$$

Using the property of the Gamma function $\Gamma(n) = (n-1)\Gamma(n-1)$, we obtain:

$$I_{r,0} = \frac{\Gamma(\frac{r+1}{2})\Gamma(\frac{3}{2})}{\Gamma(\frac{r+4}{2})} = \frac{(\frac{r-1}{2})\Gamma(\frac{r-1}{2})\Gamma(\frac{3}{2})}{(\frac{r+1}{2})\Gamma(\frac{r+2}{2})} = \left(\frac{r-1}{r+2}\right)I_{r-2,0} \quad (\text{A.17})$$

For r odd the $I_{r,0}$ vanish by symmetry. Using the fact that $\Gamma(\frac{1}{2}) = \sqrt{\pi}$ we have:

$$\begin{aligned} I_{0,0} &= \frac{\pi}{2} \\ I_{2,0} &= \frac{\pi}{8} \\ I_{4,0} &= \frac{\pi}{16} \end{aligned} \quad (\text{A.18})$$

Any others needed can be calculated using Eq. A.17.

To calculate $I_{n,1}$ we write:

$$\begin{aligned} I_{n,1} &= \int_0^\pi d\psi \frac{\sin^2\psi \cos^n\psi}{a - b\cos\psi} \\ &= -\frac{1}{b} \int_0^\pi d\psi \sin^2\psi \cos^{n-1}\psi + \frac{a}{b} \int_0^\pi d\psi \frac{\sin^2\psi \cos^{n-1}\psi}{a - b\cos\psi} \end{aligned} \quad (\text{A.19})$$

and this allows us to derive the relationship:

$$I_{n,1} = -\frac{1}{b}I_{n-1,0} + \frac{a}{b}I_{n-1,1} \quad (\text{A.20})$$

Using this, together with Eqs. A.14 and A.18 we obtain:

$$\begin{aligned} I_{0,1} &= \frac{\pi}{b^2}(a - \sqrt{a^2 - b^2}) \\ I_{1,1} &= \frac{\pi a}{b^3}(a - \sqrt{a^2 - b^2}) - \frac{\pi}{2b} \\ I_{2,1} &= \frac{\pi a^2}{b^4}(a - \sqrt{a^2 - b^2}) - \frac{\pi a}{2b^2} \\ I_{3,1} &= \frac{\pi a^3}{b^5}(a - \sqrt{a^2 - b^2}) - \frac{\pi a^2}{2b^3} - \frac{\pi}{8b} \end{aligned} \quad (\text{A.21})$$

Finally we have:

$$\frac{\partial}{\partial a} I_{n,1} = \frac{\partial}{\partial a} \int_0^\pi d\psi \frac{\sin^2 \psi \cos^n \psi}{a - b \cos \psi} = - \int_0^\pi d\psi \frac{\sin^2 \psi \cos^n \psi}{(a - b \cos \psi)^2} = -I_{n,2} \quad (\text{A.22})$$

From Eq. A.21 we compute:

$$\begin{aligned} I_{0,2} &= - \frac{\partial}{\partial a} I_{0,1} = - \frac{\pi}{b^2} \left(1 - \frac{a}{\sqrt{a^2 - b^2}} \right) \\ I_{1,2} &= - \frac{\partial}{\partial a} I_{1,1} = - \frac{\pi}{b^3} (a - \sqrt{a^2 - b^2}) - \frac{\pi a}{b^3} \left(1 - \frac{a}{\sqrt{a^2 - b^2}} \right) \\ I_{2,2} &= - \frac{\partial}{\partial a} I_{2,1} = - \frac{2\pi a}{b^4} (a - \sqrt{a^2 - b^2}) - \frac{\pi a}{b^4} \left(1 - \frac{a}{\sqrt{a^2 - b^2}} \right) + \frac{\pi}{2b^2} \end{aligned} \quad (\text{A.23})$$

which after some tidying up gives:

$$\begin{aligned} I_{0,2} &= \frac{\pi}{b^2} \left(\frac{a}{\sqrt{a^2 - b^2}} - 1 \right) \\ I_{1,2} &= \frac{\pi}{b^3} \left(\frac{a^2}{\sqrt{a^2 - b^2}} - 2a + \sqrt{a^2 - b^2} \right) \\ I_{2,2} &= \frac{\pi}{b^4} \left(\frac{a^3}{\sqrt{a^2 - b^2}} - 3a^2 + \frac{1}{2}b^2 + 2a\sqrt{a^2 - b^2} \right) \end{aligned} \quad (\text{A.24})$$

It is obviously easy to generalise this to calculate any $I_{n,m}$. The integrals we have calculated, however, suffice for the calculations of this study. Eqs. A.19 and A.21 are the general form of these integrals for any a and b . Usually we have $a = p^2 + k^2$ and $b = 2pk$. In the calculations of chapter six, however, where we use the expression $f_1 q^2 / (q^2 + r_1^2)$ for the fermion function $\mathcal{F}(q)$, we again obtain angular integrals of this form, but this time with $a = p^2 + k^2 + r_1^2$ and $b = 2pk$. For this last choice of a and b the remaining momentum integral is difficult and we performed it using an algebraic manipulations program. However, if $a = p^2 + k^2$, and no other functions appear in the integrand except for simple powers of k and p , then the momentum integral can be explicitly performed analytically. This is the case, for example, when we are calculating the asymptotic leading behaviour

of an integral by setting $\mathcal{F}, \mathcal{G} = 1 + O(\alpha(\mu))$. Since this was an important part of our analysis, we give this in some detail. We start by noting:

$$\sqrt{a^2 - b^2} = \left((p^2 + k^2)^2 - 4p^2k^2 \right)^{\frac{1}{2}} = (p^4 + k^4 + 2p^2k^2 - 4p^2k^2)^{\frac{1}{2}} = |p^2 - k^2| \quad (\text{A.25})$$

We define a function $h(x)$ such that:

$$h(x) = \begin{cases} x & \text{for } x < 1 \\ 1 & \text{for } x \geq 1 \end{cases} \quad (\text{A.26})$$

An important way of writing $h(x)$ is:

$$h(x) = \frac{1}{2}(1 + x - |1 - x|) \quad (\text{A.27})$$

From Eqs. A.19 and A.24 we can compute:

$$\begin{aligned} I_{0,1} &= \frac{\pi}{4p^2k^2}(p^2 + k^2 - |p^2 - k^2|) = \frac{\pi}{2k^2} \frac{1}{2} \left(1 + \frac{k^2}{p^2} - \left| 1 - \frac{k^2}{p^2} \right| \right) \\ &= \frac{\pi}{2k^2} h\left(\frac{k^2}{p^2}\right) \end{aligned}$$

$$\begin{aligned} I_{1,1} &= \frac{\pi(p^2 + k^2)}{8p^3k^3}(p^2 + k^2 - |p^2 - k^2|) - \frac{\pi}{4pk} \\ &= \frac{\pi}{8p^3k^3}((p^2 + k^2)^2 - 2p^2k^2 - (p^2 + k^2)|p^2 - k^2|) \\ &= \frac{\pi p}{4k^3} \frac{1}{2} \left(1 + \frac{k^4}{p^4} - \left| 1 - \frac{k^4}{p^4} \right| \right) \\ &= \frac{\pi}{4k^2} \frac{p}{k} h\left(\frac{k^4}{p^4}\right) \end{aligned}$$

$$\begin{aligned} I_{2,1} &= \frac{a}{b} I_{1,1} = \frac{p^2 + k^2}{2pk} \frac{\pi}{4k^2} \frac{p}{k} h\left(\frac{k^4}{p^4}\right) \\ &= \frac{\pi}{8k^4} (p^2 + k^2) h\left(\frac{k^4}{p^4}\right) \end{aligned}$$

$$\begin{aligned}
 I_{3,1} &= \frac{\pi}{32p^5k^5} (-2p^4k^4 + (p^2 + k^2)^4 - (p^2 + k^2)^3 |p^2 - k^2| - 2(p^2 + k^2)^2 p^2 k^2) \\
 &= \frac{\pi}{32p^5k^5} (p^8 + k^8 + 2p^6k^2 + 2k^6p^2 - (p^6 + p^4k^2 + p^2k^4 + k^6) |p^2 - k^2| \\
 &\quad - 2k^2p^2(p^2 + k^2) |p^2 - k^2|) \\
 &= \frac{\pi}{32p^5k^5} (p^8 + k^8 - |p^8 - k^8| + 2k^2p^2(p^4 + k^4 - |p^4 - k^4|)) \\
 &= \frac{\pi}{16k^4} \frac{p^3}{k} h\left(\frac{k^8}{p^8}\right) + \frac{\pi}{8k^2} \frac{p}{k} h\left(\frac{k^4}{p^4}\right) \\
 I_{0,2} &= \frac{\pi}{4p^2k^2} \left(\frac{p^2 + k^2}{|p^2 - k^2|} - 1 \right) \\
 &= \frac{\pi}{2k^2} \frac{1}{|p^2 - k^2|} h\left(\frac{k^2}{p^2}\right) \\
 I_{1,2} &= \frac{\pi}{8p^3k^3} \left(\frac{(p^2 + k^2)^2}{|p^2 - k^2|} - 2(p^2 + k^2) + |p^2 - k^2| \right) \\
 &= \frac{\pi}{8p^3k^3} \frac{1}{|p^2 - k^2|} \left(p^4 + k^4 - |p^4 - k^4| \right) \\
 &= \frac{\pi}{2k^2} \frac{1}{|p^2 - k^2|} h\left(\frac{k^4}{p^4}\right) \\
 I_{2,2} &= \frac{\pi}{16p^4k^4} \left(\frac{(p^2 + k^2)^3}{|p^2 - k^2|} - 3(p^2 + k^2)^2 + 2p^2k^2 + 2(p^2 + k^2) |p^2 - k^2| \right) \\
 &= \frac{\pi}{16p^4k^4} \frac{1}{|p^2 - k^2|} \left(3(p^6 + k^6) - 3(p^4 + p^2k^2 + k^4) |p^2 - k^2| \right. \\
 &\quad \left. + p^2k^2(p^2 + k^2) - k^2p^2 |p^2 - k^2| \right) \\
 &= \frac{3\pi p^2}{8k^4} \frac{1}{|p^2 - k^2|} h\left(\frac{k^6}{p^6}\right) + \frac{\pi}{8k^2} \frac{1}{|p^2 - k^2|} h\left(\frac{k^2}{p^2}\right)
 \end{aligned} \tag{A.28}$$

First a comment on the factor $|p^2 - k^2|$ which appears in the denominator of the integrals of the type $I_{n,2}$, and which would appear to have a pole at $p^2 = k^2$. In fact when all the factors of this type are added in any calculation they will be finite, coming as they do from a $q^\mu q^\nu / q^2$ term in a propagator, which does not have a pole at $k^2 = p^2$. The pole appears because we expand

$q = p - k$ in the numerator. An example of this is:

$$\int_0^\pi d\psi \sin^2 \psi \frac{p^2 k^2 - (k \cdot p)^2}{k^2 q^4} = p^2 (I_{0,2} - I_{2,2}) \quad (\text{A.29})$$

The denominator has a doublepole at $q^2 = 0$, in other words when $k = p$ and $\cos\psi = 1$. The numerator has a factor $\sin^2\psi = (1 - \cos\psi)(1 + \cos\psi)$ from the measure, and another from the integrand. Thus the integral does not diverge at $k^2 = p^2$ and should exist. Using Eq. A.28 this integral equals:

$$\begin{aligned} & \begin{cases} \frac{\pi}{p^2 - k^2} \left(\frac{1}{2p^2} - \frac{3k^2}{8p^4} - \frac{1}{8p^2} \right) & \text{for } 0 \leq k \leq p \\ \frac{\pi}{k^2 - p^2} \left(\frac{1}{2k^2} - \frac{3p^2}{8k^4} - \frac{1}{8p^2} \right) & \text{for } p < k \end{cases} \\ & = \begin{cases} \frac{3\pi}{8p^4} & \text{for } 0 \leq k \leq p \\ \frac{3\pi}{8k^4} & \text{for } p < k \end{cases} \end{aligned} \quad (\text{A.29})$$

To extract the leading logarithmic behaviour of the ultraviolet divergent integrals is now trivial. For example:

$$\begin{aligned} \int \frac{d^4 k}{k^2 q^2} &= 2\pi \int_0^{\kappa^2} dk^2 \int_0^\pi \frac{\sin^2 \psi}{2} d\psi = 2\pi \int_0^{\kappa^2} I_{0,1} dk^2 \\ &= 2\pi^2 \int_0^{p^2} \frac{dk^2}{2p^2} + 2\pi^2 \int_{p^2}^{\kappa^2} \frac{dk^2}{2k^2} \\ &= \pi^2 + \pi^2 \ln\left(\frac{\kappa^2}{p^2}\right) \end{aligned} \quad (\text{A.30})$$

After renormalisation this will simply become $\ln(\mu^2/p^2)$. Another way of doing this is to expand the integrand in powers of $1/k^2$, and read off the divergent terms. To do this we write:

$$\frac{1}{(q^2)^n} = \frac{1}{(k^2 + p^2 - 2k \cdot p)^n} = \frac{1}{k^2} \left(1 + \frac{p^2 - 2 \cdot p}{k^2} \right)^{-n} = \frac{1}{k^2} + O\left(\frac{1}{k^3}\right) \quad (\text{A.31})$$

Since the denominator is now ψ independent, all the angular integrals are of the form $I_{r,0}$, listed in Eq. A.18, with $I_{r,0} = 0$ for r odd. We can therefore calculate

the logarithmic divergence of the following integrals where we use \approx to denote that terms have the same ultraviolet divergence. For some of the terms we have to keep higher orders in this expansion of the q^2 terms in the denominator.

$$\begin{aligned}
 \int \frac{d^4 k}{k^2 q^2} &\approx 2\pi \int_{p^2}^{\kappa^2} \frac{dk^2}{k^2} I_{0,0} \approx \pi^2 \ln\left(\frac{\kappa^2}{p^2}\right) \\
 \int d^4 k \frac{k \cdot p}{p^2 k^2 q^2} &\approx 2\pi \int_{p^2}^{\kappa^2} \frac{dk^2}{k^2} 2I_{2,0} \approx \frac{\pi^2}{2} \ln\left(\frac{\kappa^2}{p^2}\right) \\
 \int d^4 k \frac{k \cdot p}{q^4 p^2} &\approx 2\pi \int_{p^2}^{\kappa^2} \frac{dk^2}{k^2} 4I_{2,0} \approx \pi^2 \ln\left(\frac{\kappa^2}{p^2}\right) \\
 \int d^4 k \frac{(k \cdot p)^2}{k^4 p^2 q^2} &\approx 2\pi \int_{p^2}^{\kappa^2} \frac{dk^2}{k^2} I_{2,0} \approx \frac{\pi^2}{4} \ln\left(\frac{\kappa^2}{p^2}\right) \\
 \int d^4 k \frac{(k \cdot p)^2}{k^2 p^2 q^4} &\approx 2\pi \int_{p^2}^{\kappa^2} \frac{dk^2}{k^2} I_{2,0} \approx \frac{\pi^2}{4} \ln\left(\frac{\kappa^2}{p^2}\right) \\
 \int d^4 k \frac{(k \cdot p)^3}{k^4 q^2 p^2} &\approx 2\pi \int_{p^2}^{\kappa^2} \frac{dk^2}{k^2} 2I_{4,0} \approx \frac{\pi^2}{4} \ln\left(\frac{\kappa^2}{p^2}\right) \\
 \int d^4 k \frac{(k \cdot p)^3}{q^4 k^2 p^2} &\approx 2\pi \int_{p^2}^{\kappa^2} \frac{dk^2}{k^2} 4I_{4,0} \approx \frac{\pi^2}{2} \ln\left(\frac{\kappa^2}{p^2}\right)
 \end{aligned} \tag{A.32}$$

On renormalisation, κ^2 gets replaced by μ^2 . Note that this analysis equally works if instead of q^2 in the denominator we had $q^2 + \mu^2$. Finally we must also extract the leading behaviour of:

$$\int d^4 k \frac{4(k \cdot p)^2 - k^2 p^2}{k^2 q^2 p^4} \tag{A.33}$$

Here both of the terms in Eq. A.33 are quadratically divergent, but this cancels by using the expansion above. To see this, we again expand q^2 , but this time to a higher power in $1/k^2$:

$$\frac{1}{q^2} = \frac{1}{k^2} \left(1 - \frac{p^2 - 2k \cdot p}{k^2} + \left(\frac{p^2 - 2k \cdot p}{k^2} \right)^2 \right) \tag{A.34}$$

Giving us for the leading behaviour of Eq. A.33:

$$\begin{aligned}
 & \int d^4k \frac{1}{k^4 p^4} \left(4(k \cdot p)^2 - k^2 p^2 \right) \left(1 - \frac{p^2}{k^2} + \frac{4(k \cdot p)^2}{k^4} \right) \\
 & \approx 2\pi \int_{p^2}^{\kappa^2} \frac{dk^2}{k^2} \left(\frac{k^2}{p^2} (4I_{2,0} - I_{0,0}) + (-4I_{2,0} + 16I_{4,0} + I_{0,0} - 4I_{2,0}) \right) \\
 & \approx \pi^2 \ln \left(\frac{\kappa^2}{p^2} \right)
 \end{aligned} \tag{A.35}$$

where the quadratic divergence has cancelled between the two terms, and the logarithmic divergence can be read off too.

REFERENCES

CHAPTER ONE STRONG INTERACTIONS

- [1.1] M. Banner, *et al* Phys. Lett. **122B** (1983) 476
G. Arnison, *et al* Phys. Lett. **122B** (1983) 103
- [1.2] E. Rutherford, Phil. Mag. **37** (1919) 581
- [1.3] A. Pais, *Inward Bound*, Oxford university Press, (1986)
- [1.4] G. Rochester and C.C. Butler, Nature **160** (1947) 885
- [1.5] M. Gell-Mann and Y. Ne'eman, *The Eightfold Way*, Benjamin New York, (1964)
S. Okubo, Progr. Theor. Phys. **27** (1962) 949
- [1.6] For reviews of QCD see, for example:
W. Marciano and H. Pagels, Phys. Rep. **36** (1978) 137
M.R. Pennington, Rep. Progr. Phys. **46** (1983) 393
- [1.7] For a review of possible confinement mechanisms see:
M. Bander, Phys. Rep. **75** (1981) 207
- [1.8] F. Bloch and A. Nordsieck Phys. Rev. **52** (1937) 54
T. Kinoshita, J. Math. Phys. **3** (1964) 650
T.D. Lee and M. Nauenberg, Phys. Rev. **133** (1964) 1549
For infra-red divergences in QCD see:
J. Frenkel, M-L. Frenkel and J.C. Taylor, Nucl. Phys. **B124** (1977) 268
T. Appelquist, J. Carrazone, H. Kluberg-Stern and M. Roth, Phys. Rev. Lett. **36** (1976) 768
- [1.9] J. Cornwall and G. Tiktopoulos Phys. Rev. **D13** (1976) 3370
- [1.10] K.G. Wilson Phys. Rev. **D10** (1974) 2445
For reviews see:
C. Rebbi, Phys. Rep. **67** (1980) 55
J.B. Kogut Phys. Rep. **67** (1980) 67

CHAPTER TWO THE SCHWINGER-DYSON EQUATIONS

[2.1] For a general account of quantum field theory see:

C. Itzykson and J.B. Zuber, *Quantum Field Theory*, McGraw-Hill, (1980); in particular see chapter nine on 'functional methods'.

More details on functional methods are given in:

P. Ramond, *Field Theory, a Modern Primer*, Benjamin Cummings, (1981)

C. Nash, *Relativistic Quantum Fields*, Academic press, (1978)

[2.2] See the first reference of [2.1] as well as:

H. Lehmann, K. Symanzik and W. Zimmermann, *Nuovo Cim.* 1 (1955) 205

[2.3] L.D. Fadeev and V.N. Popov, *Phys. Lett.* 25B (1967) 29

see also:

T.P. Cheng and L.F. Li, *Gauge Theory of Elementary Particle Physics*, Clarendon press, Oxford, (1984)

[2.4] E.J. Eichten and F.L. Feinberg, *Phys. Rev.* D15 (1977) 2201

[2.5] A.A. Slavnov, *Theor. and Math. Phys.* 10 (1972) 99

J.C. Taylor, *Nucl. Phys.* B33 (1971) 436

[2.6] J.C. Ward, *Phys. Rev.* 78 (1950) 1824

Y. Takahashi, *Nuovo Cim.* 6 (1957) 370

[2.7] J.S. Ball and T.W. Chui, *Phys. Rev.* D22 (1980) 2542 and 2550

S.K. Kim and M. Baker, *Nucl. Phys.* B164 (1980) 152

[2.8] H. Pagels, *Phys. Rev.* D14 (1976) 2747

H. Pagels, *Phys. Rev.* D15 (1977) 2991

[2.9] U. Bar-Gadda, *Nucl. Phys.* B163 (1980) 812

see also ref. [1.6]

CHAPTER THREE THE GLUON EQUATION

- [3.1] N. Brown and M.R. Pennington *Phys. Lett.* **106B** (1988) 133
- [3.2] M. Baker, J.S. Ball and F. Zachariasen, *Nucl. Phys.* **B186** (1981) 531
and 560
- [3.3] A.D. Worrall, Ph. D. Thesis submitted to the University of Durham,
unpublished (1985)
M.R. Pennington and A.D. Worrall, unpublished, (1983)

CHAPTER FOUR THE MANDELSTAM APPROXIMATION

- [4.1] S. Mandelstam, *Phys. Rev.* **D20** (1979) 3223
- [4.2] J.S. Ball and F. Zachariasen, *Nucl. Phys.* **B143** (1978) 148
C. Nash and R.L. Stuller, *Proc. Roy. Irish Acad.* **78** (1978) 217
R. Anishetty, M.Baker, S.K. Kim, J.S. Ball and F. Zachariasen, *Phys.*
Lett. **86B** (1979) 52
M. Baker, J.S. Ball, P. Lucht and F. Zachariasen, *Phys. Lett.* **89B**
(1980) 211
A.I. Alekseev, *Yad. Fiz.* **33** (1981) 561
W.J. Schoenmaker, *Nucl. Phys.* **B194** (1982) 535
B.A. Arbuzov, *Phys. Lett.* **125B** (1983) 497
E.J. Gardner, *J. Phys. G*, **9** (1983) 139
D. Atkinson, P.W. Johnson, W.J. Schoenmaker and H.A. Slim, *Nuovo*
Cim. **A77** (1983) 197
- [4.3] T. Appelquist, M.Dine and I.J. Muzinich, *Phys. Lett.* **69B** (1977) 231
F. Feinberg, *Phys. Rev. Lett.* **39** (1977) 316
W. Fischler, *Nucl. Phys.* **B129** (1977) 157
- [4.4] C. Quigg and J.L. Rosner, *Phys. Rep.* **56** (1980) 167
- [4.5] G.B. West, *Phys. Lett.* **115B** (1982) 468
- [4.6] B. Humpert and W.L. Van Neerven, *Phys. Lett.* **101B** (1981) 101

G. Leibbrandt, Rev. Mod. Phys. **59** (1987) 1067

[4.7] G.B. West, Phys. Rev. **D27** (1983) 1878

[4.8] M. Creutz, Phys. Rev. **D10** (1974) 2696

V.P. Nair and C. Rosenzweig, Phys. Lett. **135B** (1984) 450

[4.9] G. 't Hooft, Nucl. Phys. **B190** (1981) 455

[4.10] M. Baker, J.S. Ball and F. Zachariasen, Phys. Rev. **D37** (1988) 1036

M. Baker, J.S. Ball and F. Zachariasen, Phys. Rev. **D31** (1985) 2575

CHAPTER FIVE THE FERMION EQUATION

[5.1] R.L. Stuller, Phys. Rev. **D13** (1976) 513

J.S. Ball and F. Zachariasen, Phys. Lett. **106B** (1981) 133

H.J. Munczek Phys. Lett. **175B** (1986) 215

[5.2] T. Appelquist, M. Bowick, D. Karabali and L.C.R. Wijewardhana,
Phys. Rev. **D33** (1986) 3704

D. Atkinson and P.W. Johnson, J. Math. Phys. **28** (1987) 2488

D. Atkinson, P.W. Johnson and M. Koopmans, Z. Phys. **C34** (1987)
99

D. Atkinson, P.W. Johnson and K. Stam, Phys. Lett. **201B** (1988) 105

[5.3] J.M. Cornwall, Phys. Rev. **D22** (1980) 1452

V.S. Gogokhia and B.A. Magradze, Tbilisi report KFKI-1987-01/A

CHAPTER SIX QUARK LOOPS

[6.1] N. Brown and M.R. Pennington, Brookhaven preprint BNL-41101, to
be published in Phys. Rev. D (1988)

[6.2] M.R. pennington, Phys. Rev. Lett. **60** (1988) 267

CHAPTER SEVEN A NON-PERTURBATIVE STUDY OF QCD

[7.1] P. Rambiessa, Phys. Rev. **D33** (1986) 2333

